UNIVERSITY OF CALGARY

SELECTIVE TRANSCRIPTIONAL DOWN-REGULATION OF HUMAN RHINOVIRUS-INDUCED PRODUCTION OF CXCL10 IN AIRWAY EPITHELIAL CELLS VIA MEK1 PATHWAY EFFECTS ON INTERFERON REGULATORY FACTOR-1

by

Raza Syed Zaheer

A THESIS

SUBMITTED TO THE FACULTY OF GRADUATE STUDIES

IN PARTIAL FULFILMENT OF THE REQUIREMENTS FOR THE

DEGREE OF DOCTOR OF PHILOSOPHY

DEPARTMENT OF CARDIOVASCULAR AND RESPIRATORY SCIENCES

CALGARY, ALBERTA

MARCH, 2010

UNIVERSITY OF
CALGARY

Abstract

Human rhinovirus (HRV) infections can trigger exacerbations of lower airway diseases. Infection of airway epithelial cells induces production of a number of pro-inflammatory chemokines that may exacerbate airway inflammation, including interferonγ-inducible protein of 10kDa (CXCL10), a chemoattractant for type 1 lymphocytes and Natural Killer cells. Primary human bronchial epithelial (HBE) cells and the BEAS-2B human bronchial epithelial cell line were used to examine the role of the mitogen-activated protein kinase (MAPK) pathways in HRV-16-induced production of CXCL10. Infection with HRV-16 induced the activation of the major MAPK pathways, including chronic activation of ERK1/2. Inhibitors of the MEK1/2 pathway, PD98059 and U0126, significantly enhanced HRV-16, but not interferon (IFN)-β, induced production of CXCL10 mRNA and protein. Inhibitor effects were not due to changes in cell viability or viral replication. Studies using siRNA revealed that knockdown of MEK1 was primarily associated with the enhancement of HRV-16-induced CXCL10 production. Promoter construct studies revealed that PD98059 and U0126 enhanced HRV-16-induced transcriptional activation of CXCL10. Inhibitors of the MEK1/2 pathway did not alter NF-κB translocation and/or binding to the CXCL10 promoter. In contrast, inhibitors of the MEK1/2 pathway and siRNA knockdown of MEK1 enhanced translocation and/or binding of HRV-16-induced IFN regulatory factor (IRF)-1 to the CXCL10 promoter. Further examination revealed that HRV-16 induced the expression of both IRF-1 mRNA and protein in a time-dependent manner. Both PD98059 and U0126 significantly enhanced HRV-16-induced IRF-1 mRNA levels in BEAS-2B and HBE, although IRF-1 protein expression was only enhanced in HBE. Using siRNA targeting IRF-1, both

HRV-16-induced IRF-1 expression and nuclear translocation and/or binding of IRF-1 to the CXCL10 promoter was substantially reduced. Knockdown of IRF-1 also led to a significant reduction in HRV-16-induced CXCL10 production, confirming that IRF-1 is directly involved in HRV-16-induced CXCL10 expression. Moreover, pronounced IRF-1 knockdown abrogated the enhancement of CXCL10 normally induced by the loss of MEK1 function. Phosphatase experiments indicate that IRF-1 binding to the CXCL10 promoter may not be dependent upon its phosphorylation state. In conclusion, these studies demonstrate that activation of MEK1 selectively down-regulates HRV-16-induced expression of CXCL10 by modulating IRF-1 interactions with the gene promoter in human airway epithelial cells.

Acknowledgements

This thesis is the culmination of over 6 years of work and its completion would not have been possible without the contributions of many people.

I would like to acknowledge my Ph.D. supervisor, Dr. David Proud, who has guided me through this highly enlightening process. David has provided an excellent environment for learning and experimentation. His calm demeanor and "open door" policy only encouraged me to succeed during times of failure. For better or worse, I am certainly not the same person that first walked into the lab one summer day. I was also fortunate to have a second mentor, Dr. Richard Leigh, whose guidance and support has been indispensable throughout this degree. Richard provided a second voice and opinion of all matters regarding my degree and future aspirations. I am grateful to have had a basic scientist and clinician providing great counsel and setting examples of great achievement.

Even though I am responsible for the work in this thesis, everyone in the lab, past or present, contributed to this thesis in his or her own way. I would especially like to thank Shahina for training me in the ways of the pipette, Wale for his incredible friendship, and Claire for being an extraordinary fellow grad student and friend. We all shared some great laughs that I will always remember. I am also indebted to my friends and fellow Ph.D. candidates, Chris, Laura, and Peter. Whether it was going to a hockey game, talking science, or just hanging out, thanks for the great times!

I also need to acknowledge Dr. Brent Winston who took a chance on an average undergraduate student and helped start my journey into scientific research.

I would also like to thank my thesis committee for their invaluable guidance. The Alberta Lung Association has been a great financial supporter of my studies. Funding from CIHR, Province of Alberta, and the University of Calgary also supported this thesis.

Music helped me get through the monotony of running experiments and long walks to my car. So thank you Gomez, Groove Armada, Alice Russell, and The Roots!

Finally, I want to thank my family. I am nothing without their love and support. I love you.

Table of Contents

List of Tables

List of Figures and Illustrations

List of Symbols, Abbreviations and Nomenclature

α - alpha

β - beta

γ - gamma

δ - theta

ε - epsilon

κ - kappa

ABTS - 2,2'-azino-bis(3-ethylbenzthiazoline-6-sulphonic acid)

ANOVA - analysis of variance

AP-1 - activator protein-1

ATP - adenosine triphosphate

BAL - bronchoalveolar lavage

BEAS-2B - immortalized bronchial epithelial cell line

BEBM - bronchial epithelial basal medium

BMK - Big MAPK

BSA - bovine serum albumin

CARD - caspase recruiting domain

CBP – CREB binding protein

CCL22 - macrophage-derived chemokine; MDC

CCL17 - thymus and activation-regulated chemokine; TARC

CCL5 - regulated on activation normal T cell expressed and secreted; RANTES

CCL2 - monocyte chemotactic protein 1; MCP-1

CD - cluster of differentiation

cDNA - complementary deoxyribonucleic acid

CIP - calf intestinal phosphatase

COPD - chronic obstructive pulmonary disease

CREB – cAMP response element binding protein

CT - cycle threshold

CXCL11 - interferon-inducible T cell alpha chemoattractant

CXCL10 - interferon-inducible protein of 10kDa; IP-10

CXCL9 - monokine inducible by IFN-gamma; Mig

CXCL8 - interleukin-8; IL-8

CXCL1 – growth-related oncogene

DMEM - Dulbecco's modified Eagle medium

DMSO - dimethyl sulfoxide

DNA - deoxyribonucleic acid

dNTP - deoxyribonucleotide triphosphate

dsRNA - double-stranded RNA

DTT - dithiothreitol

ECL - enhanced chemiluminscent

ECMV - encephalomyocarditis virus

EGF - epidermal growth factor

eIF4G – eukaryotic translational initiation factor 4G

ELISA - enzyme-linked immunosorbent assay

Elk-1 - E-26 like protein-1

ELR - glutamic acid-leucine-arginine

EMEM - Eagle's minimal essential medium

EMSA - electrophoretic mobility shift assay

EMTU - epithelial-mesenchymal trophic unit

ERK - extracellular signal-regulated kinase

FBS - fetal bovine serum

GAPDH - glyceraldehyde-3-phosphate-dehydrogenase

GINA – Global Initiative for Asthma

GOLD - Global Initiative for Chronic Obstructive Lung Disease

HAE - human adenoid epithelial cell

HBE - human bronchial epithelial cell

HBSS - Hanks' balanced salt solution

HC - hydrocortisone

HDAC – histone deacetylase

HEPES - 4-(2-hydroxyethyl)-1-piperazineethanesulfonic acid

HRP - horseradish peroxidase

HRV - human rhinovirus

IAD – interferon regulatory factor association domain

ICAM-1 - intracellular adhesion molecule-1

ICSBP – interferon consensus sequence binding protein

IFN - interferon

IkB-alpha - inhibitor of kappa B alpha

IKK - inhibitor of kappa B kinase

IL - interleukin

iNKT - invariant natural killer T cell

IPS-1 - IFN-beta promoter stimulator-1

IRES - internal ribosomal entry site

IRF - interferon regulatory factor

ISGF - interferon-stimulated gene factor

ISRE - interferon-stimulated response element

JNK - c-Jun amino terminal kinase

LB - Luria-Bertani

LDH - lactate dehydrogenase

LDLR - low-density lipoprotein receptor

LFA-1 - lymphocyte-function associated antigen-1

MAPK - mitogen-activated protein kinase

MAPKAPK - MAPK-activated protein kinase

MDA-5 - melanoma differentiation-associated gene 5

MEK (or MAP2K) - mitogen-activated protein kinase kinase

MHC - major histocompatibility complex

miRNA - microRNA

MOI - multiplicity of infection

mRNA - messenger RNA

NALP - nacht Domain-, Leucine-Rich Repeat-, and PYD-Containing Protein

NF-kB - nuclear factor kappa-light-chain-enhancer of activated B cells

NGF – nerve growth factor

NK – natural killer

NOD - nucleotide oligodimerization domain

PAMP - pathogen activated molecular pattern

PBS - phosphate buffered saline

PCR - polymerase chain reaction

PI3K – phosphoinositide 3-kinase

PKR - protein kinase R

PMSF - phenylmethanesulphonylfluoride

PRR - pattern recognition receptor

RIG-I - retinoic acid-inducible gene I

RNA - ribonucleic acid

RSV – respiratory syncytial virus

RT-PCR - real time polymerase chain reaction

SAPK - stress-activated protein kinase

SDS - sodium dodecyl sulfate

SEM - standard error of the mean

Ser - serine

siRNA - short interfering RNA

Src – sarcoma

Syk – spleen tyrosine kinase

TBK-1 - TRAF family member-associated NF-kB activator-binding kinase 1

TBS - Tris-buffered saline

$TCID_{50}$ - 50% tissue culture-infective dose

TFBII – basal transcription factor

T_H1 - type 1 T helper lymphocyte

T_H17 - IL-17 producing T helper lymphocyte

T_H2 - type 2 T helper lymphocyte

Thr - threonine

TIR - Toll/IL-1 receptor domain

TLR - Toll-like receptor

TNF - tumor necrosis factor

T_{REG} - regulatory T lymphocyte

TRIF - Toll/IL-1 receptor domain contaning adaptor inducing IFN-beta

TSLP - thymic stromal lymphopoeitin

TTBS - Tris-buffered saline with Tween-20

Tyr - tyrosine

URI - upper respiratory tract viral infection

UTR – untranslated region

VP - viral protein

Epigraph

The human mind, once stretched by a new idea, never regains its original dimensions.

-Dr. Oliver Wendell Holmes

Chapter One: Introduction

Normal body function requires the constant uptake of oxygen from the environment, thus it is necessary that the lungs inhale thousands of litres of air each day. In addition to oxygen, inhaled air may contain allergens, pathogens, and pollutants. Normally, these agents are cleared by a highly regulated immune response in the lungs. In contrast, both environmental and genetic factors may predispose certain individuals to respond to specific insults in an over-exuberant manner resulting in markedly reduced lung function characterized by chronic inflammation and structural changes. This dysregulated immune response contributes, in part, to the pathogenesis of airway diseases, such as asthma and chronic obstructive pulmonary disease (COPD)[1]. Thus, the ability to control inflammatory status in response to these agents is paramount for normal lung function, and impairment of this ability may predispose an individual to future infections and subsequent disease.

1.1 Airway epithelium

The human lung contains a series of conducting airways starting at the trachea and continually branching to the alveoli, which serves as the site of gas exchange for blood oxygenation (Figure 1.1). There are three main regions of the airways, including the cartilaginous proximal airway (trachea, bronchi, and submucosal glands), non-cartilaginous distal bronchioles (bronchioles, terminal bronchioles, respiratory bronchioles) and the alveolar gas exchange region (alveolar ducts and sacs)[2,3].

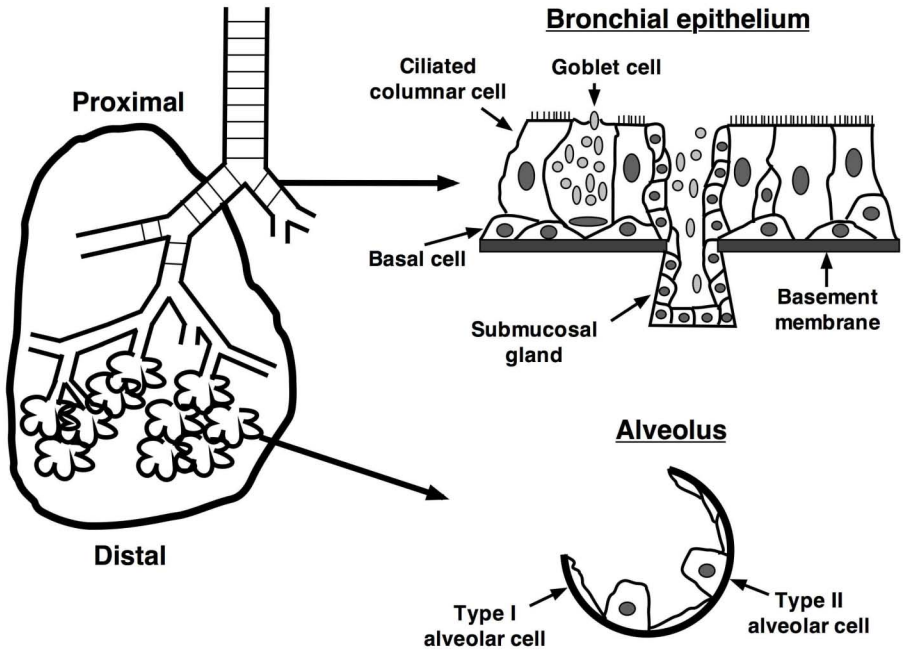

Figure 1.1 – Human airway epithelium structure. The human lung contains a series of branching airways lined with epithelial cells of various function. Proximal airways contain mainly pseudostratified columnar ciliated cells interspersed with mucus-producing Goblet cells and submucousal glands. Basal cells anchor overlying epithelial cells to the basement membrane through hemi-desmosomal linkages. The distal airways end at alveoli, which serve as the site of gas exchange and blood oxygenation. They are composed of flattened type I and cuboidal type II alveolar epithelial cells.

The airways are lined with numerous morphologically and functionally distinct types of epithelial cells[4]. Starting approximately 1 cm into the nose, the upper airway is lined with pseudostratified, columnar epithelium comprised of basal cells, which support ciliated epithelial cells. This morphology continues well into the lower airways beginning at the larynx and continuing into the trachea. Interspersed within the ciliated epithelial cells are mucus-producing Goblet cells and lactoferrin-producing serous cells. The large airways also contain secretory submucosal glands[5]. Epithelial cells become more non-ciliated and cuboidal as the lower airways become < 2 mm in diameter as seen in the more distal bronchioles[5]. There is also an increased presence of secretory Clara

cells, which act as progenitor cells for the bronchial epithelium[6]. The respiratory tract ends at small sac-like structures known as alveoli, composed of flattened type I and cuboidal type II alveolar cells. Type I cells mainly function to enable efficient gas exchange with pulmonary capilliaries. Type II cells secrete surfactant to prevent the collapse of the small airways and also serve as progenitor cells for the alveolar epithelium[3,7].

The airway epithelium serves as a physical barrier between the environment and underlying tissue, but also engages in various dynamic activities to maintain normal lung function. These activities include regulation of ion transport, mucociliary clearance of particulate matter, secretion of substances (surfactant, mucus, antimicrobial peptides) for protection of the airway surface, repair and regeneration of the epithelium, and modulation of the inflammatory response to injury or infection[8]. It is now recognized that the airway epithelium plays an active role in host defense and immunoregulation through contributions to both innate and adaptive immune responses. Activation of the innate immune response induces the release of various epithelium-derived pro-inflammatory molecules, including cytokines, chemokines, lipid, and peptide mediators[8]. Given that the epithelium lies at the interface between the external environment and underlying tissue, it is not surprising that it may play a key role in the inception and/or amplification of inflammatory airway diseases, such as asthma and COPD[9,10].

1.2 Asthma

1.2.1 Definition

Asthma is a complex, heterogeneous disease with major characteristics, including variable degree of airflow obstruction, bronchial hyperresponsiveness, and airway inflammation[11]. The Global Initiative for Asthma (GINA)[12] provides a working definition that:

> Asthma is a chronic inflammatory disorder of the airways in which many cells and cellular elements play a role. The chronic inflammation is associated with airway hyperresponsiveness that leads to recurrent episodes of wheezing, breathlessness, chest tightness, and coughing, particularly at night or in the early morning. These episodes are usually associated with widespread, but variable, airflow obstruction within the lung that is often reversible either spontaneously or with treatment.

Asthma is classified into four categories depending on severity: intermittent, mild persistent, moderate persistent, and severe persistent[12].

1.2.2 Burden of disease

Asthma is a major healthcare problem with an estimated 300 million affected individuals worldwide. Rates of asthma incidence and prevalence are increasing in Canada and the rest of the world[13,14]. If current trends continue, it is estimated that there will be a 100 million additional asthmatics by 2025[12]. In 1997, total healthcare costs for asthma in the United States was $12 billion[15]. Given that Canada has one-tenth the population of the United States, it is reasonable to extrapolate that total costs are in excess of $1 billion dollars. Of these total costs, one-half are linked to acute exacerbations[16], which includes drugs and illness-related disability[17].

1.2.3 Pathogenesis

Risk factors for the development of asthma include both host and environmental factors, including genes pre-disposing individuals to allergy (atopy) or airway hyperresponsiveness, viral infections, allergens, and occupational sensitizers[11,12]. To date, the strongest risk factor associated with the development of asthma is a family history of atopic disease. Increases in allergen-specific immunoglobulin E (IgE) antibodies correlates with increased risk of developing asthma[18]. More recently, it has been shown that children who have human rhinovirus (HRV)-induced wheezing in the first 3 years of life are at a significantly higher risk for the development of asthma at 6 years of age[19].

The allergic inflammation seen in asthma results in characteristic pathological changes through the release of inflammatory mediators from both infiltrating and structural cells[11]. Asthma is typified by an increased presence of type 2 (T_H2) lymphocytes and release of the cytokines interleukin (IL)-4, IL-5, IL-9, and IL-13, which, together, modulate B-cell IgE production and eosinophilic inflammation[20]. Numbers of eosinophils are increased in the airways of asthmatics[21] and release of eosinophil basic proteins, such as major basic protein, may damage the airway epithelium[21,22]. Mast cells, activated by IgE cross-linking of the high-affinity FcεRI receptor, release bronchoconstrictors, such as histamine, cysteinyl leukotrienes, and prostaglandin D_2[11]. Airway epithelium-derived chemokines, such as CXCL8 (IL-8), interferonγ-inducible protein of 10kDa (CXCL10; IP-10), thymus and activation-regulated chemokine (CCL17; TARC), and macrophage-derived chemokine (CCL22; MDC) are increased in asthmatic airways and are involved in the recruitment of lymphocytes and leukocytes[23].

Furthermore, regulatory T (T_{REG}) cell function, which normally suppress T cell responses, is impaired in asthmatics[24,25]. Although invariant natural killer T (iNKT) cells have been shown to play a role in the pathogenesis of a mouse model of allergic airway inflammation[26], their role in humans is less clear[27,28]. The role of IL-17 producing T_H17 cells in asthma is currently unknown, but may play a role in severe, neutrophilic asthma[29].

Structural changes, also known as airway remodelling, occur in asthmatic airways and represent improper repair processes[30]. Characteristic changes include loss of epithelial cell integrity resulting in shedding of clumps of epithelial cells into the airway lumen called Creola bodies[31,32]. Furthermore, Goblet cell metaplasia, hyperplasia and the enlargement of submucousal glands results in increased mucus secretion into the airway lumen[11]. Loss of the epithelial layer mainly occurs between columnar and basal epithelial cells, but desquamation to the basement membrane layer has been observed in severe asthmatics[33]. This loss is thought to occur, in part, as a result of neutrophil and eosinophil-derived proteases[22,34] and also due to the cytotoxic effects of viral infection[35]. Although it has been argued that loss of the epithelium is a sampling artifact[36], such epithelial fragility is not observed in other airway inflammatory diseases such as COPD[9]. There is also a thickening of the reticular basement membrane (*lamina reticularis*) through an increase in the deposition of fibroblast-derived collagen and proteoglycan products[37,38]. This increased thickening has been proposed to occur, in part, through reactivation of the epithelial-mesenchymal trophic unit (EMTU), whereby epithelium-derived growth factors, such as transforming growth factor (TGF)-β, induce myofibroblast proliferation that further contribute to the remodelling seen in asthma[39,40].

Other characteristic changes include hypertrophy and hyperplasia of airway smooth muscle and increased angiogenesis[11].

1.3 Chronic obstructive pulmonary disease

1.3.1 Definition

Chronic obstructive pulmonary disease (COPD) is a growing global health concern in both the industrialized and developing world[41]. It is a heterogeneous disease characterized by a slow and progressive decline in lung function. The definition put forth by The Global Initiative on Obstructive Lung Disease (GOLD)[42] is:

> COPD is a preventable and treatable disease with some significant extrapulmonary effects that may contribute to the severity in individual patients. Its pulmonary component is characterized by airflow limitation that is not fully reversible. The airflow limitation is usually progressive and associated with an abnormal inflammatory response of the lung to noxious particles or gases.

Based on the current definition, COPD is classified into 4 separate stages: Stage I (mild), Stage II (moderate), Stage III (severe), and Stage IV (very severe). Causes of death in patients with COPD include cardiovascular disease, lung cancer, and respiratory failure[42,43].

1.3.2 Burden of disease

The World Health Organization (WHO) predicts that COPD will become the fifth most common cause of disability and third most common cause of death in the world by 2020[44]. COPD affects 10% of the general population, though this may be largely underestimated through underrecognition and underdiagnosis. Women and men suffer

from COPD equally, though it is believed that women are more susceptible to impairment of lung function[45]. Furthermore, the death rate of men and women with COPD in Canada has been increasing since 1997 and the death rate of women has now surpassed men[46]. In addition, COPD is a costly disease encompassing both direct and indirect costs. In the United States, total costs were in excess of $30 billion with a similar financial burden in the European Union[42].

1.3.3 Pathogenesis

Smoking is the most common risk factor associated with the development of COPD in the Western world, though not all smokers develop COPD, implying that other factors contribute to an individual's risk[47,48]. These include genetic risk factors[49-51] and environmental pollution[52,53]. The characteristic airflow limitation found in COPD is associated with chronic, steroid-resistant lung inflammation. It has been suggested that alveolar damage is due to excess production of proteinases and oxidative stress[54]. Various hypotheses have been put forth to explain susceptibility to COPD, including polymorphisms in pro- and anti-inflammatory genes[55], latent adenoviral infection[56], impaired activity of histone deacetylases (HDACs)[57,58], and autoimmunity[59,60].

Structural changes seen in COPD patients are induced through the disruption of normal repair processes. The resulting pathological changes occur in the proximal airways, peripheral airways, lung parenchyma, and pulmonary vasculature[61]. This includes fibrosis and obstruction of the small airways (chronic bronchiolitis), enlargement of airspaces and destruction of alveoli, loss of lung elasticity, and closure of

airways (emphysema)[54,62]. Mucus hypersecretion (chronic bronchitis) is also found, but is not necessarily associated with airflow limitation[62].

The inflammation in COPD is characterized by increased infiltration of various inflammatory cells and release of pro-inflammatory mediators[54]. Compared to normal smokers, numbers of neutrophils are increased in the airways of patients with COPD and relate to disease severity[63,64]. The secretion of neutrophil-derived proteases, such as elastase, may contribute to both alveolar destruction and mucus hypersecretion[65]. Increased numbers of macrophages are localized to sites of alveolar destruction in patients with emphysema and correlate with disease severity[66-68]. Furthermore, levels of the macrophage-derived pro-inflammatory cytokines tumour necrosis factor (TNF)-α and IL-6 are increased, and contribute to chronic inflammation[64,69]. There is also an increase in measurable levels of reactive oxygen and nitrogen species, including hydrogen peroxide and peroxynitrite, which may also contribute to the pathological changes seen in COPD[70,71]. Epithelium and macrophage-derived chemokines that attract leukocytes and lymphocytes, are increased in COPD. These include CXCL10[72], CXCL8[64], growth-related oncogene-α (CXCL1; GRO-α) and monocyte chemotactic protein 1 (CCL2; MCP-1)[73]. Increased numbers of CD8+ cytotoxic T cells of the T_C1 subset may contribute to emphysema by inducing apoptosis of alveolar epithelial cells[74]. The role of T_{REG} cells remains unclear, though the numbers of CD4+CD25+FOXP3+ T_{REG} cells are reduced both in patients with COPD and in smokers without airflow obstruction[75]. B cells are only increased in the peripheral airways of severe COPD patients within lymphoid follicles and may be a response to chronic bacterial colonization[62]. The roles of

T_H17, invariant natural killer T (iNKT), and dendritic cells in COPD are currently uncertain[29,76].

1.4 Viral-associated exacerbations of asthma and COPD

Acute exacerbations of asthma and COPD are defined as "a worsening of the patient's condition, beyond day-to-day variability associated with the disease, that is sufficient enough to require change in management, or to seek emergency medical intervention"[77,78]. Exacerbations of asthma and COPD account for 50% and 70% of all healthcare costs associated with each disease, respectively[16,79]. Furthermore, frequent COPD exacerbations have a marked effect on the quality of life in patients and lead to a more rapid decline of health status[80].

Various risk factors are associated with exacerbations of asthma and COPD, including allergens, pollutants, and bacterial infections, but a major risk factor for both diseases is upper respiratory tract viral infection (URI)[78]. URIs are associated with up to 80-85% of asthma exacerbations in children and adolescents[81-84], and between 40-60% of exacerbations in adults[83,85]. There is a clear temporal link between outbreaks of URIs and rates of hospitalization for asthma exacerbations[86,87]. Furthermore, HRV is detected in 60% of viral-induced asthma exacerbations in both children and adults[85,88]. Other viruses also associated with asthma exacerbations include coronavirus, respiratory syncytial virus (RSV), and parainfluenza[88]. In addition, about half of all COPD exacerbations are associated with viral infections[89,90]. During viral-associated exacerbations, HRV is the most commonly (~ 50%) detected virus[89]. A lower percentage of exacerbations are associated with RSV, coronavirus, influenza virus, and

metapneumovirus[89,91]. Taken together, these studies indicate that HRV is a major pathogen associated with exacerbations of asthma and COPD, but the mechanisms underlying HRV-induced exacerbations have not been fully elucidated and warrant further investigation.

1.5 Human rhinovirus

1.5.1 Prevalence and Incidence

Human rhinovirus (Greek *rhin-*, "nose") is the main etiological agent of the common cold[92,93]. Interestingly, over 90% of children by 2 years of age will have detectable HRV antibodies demonstrating its high prevalence in the general population[94]. Complications as a result of HRV infection include otitis media[95], sinusitis[96] and exacerbations of asthma and COPD[85,89]. In the Northern hemisphere, increased incidence of HRV infection occurs in the spring (April-May)[97] and fall (September-November)[98]. Coincidentally, peaks in the incidence of asthma and COPD exacerbations occur in September[99] and November[100], respectively. To date, there are no marketed drugs that specifically prevent or reduce HRV infections[101].

1.5.2 Classification

HRV belongs to the family *Picornaviridae* (Spanish *Pico-*, “small”; *rna-*, ribonucleic acid genome) and genera *enterovirus*, which also includes hepatitis A, foot and mouth, and polio viruses. According to the Picornaviridae Study Group (www.picornastudygroup.com), there are currently 2 defined HRV species, HRV-A and HRV-B, based on genomic sequences. More recently, however, genetic analysis has

discovered a third new species, HRV-C[102], and potentially fourth species, HRV-D[103]. There are more than 100 serotypes of HRV based on four surface neutralizing antibody immunogenic regions[104].

1.5.3 Receptor usage and cell entry

Serotypes are also split into 2 main groups based on cell-surface receptor usage. Major group HRV (> 90 serotypes) utilize intracellular adhesion molecule-1 (ICAM-1; CD54)[105] and minor group HRV (10 serotypes) utilize members of the low-density lipoprotein (LDL) receptor family[106]. Furthermore, other receptors for cell entry have been demonstrated, including heparan sulphate proteoglycan (HRV-89, HRV-54)[107-109].

ICAM-1 contains 5 tandem extracellular domains and was originally shown to be the ligand for lymphocyte-function associated antigen-1 (LFA-1), found on neutrophils[110]. Only domains 1 and 2 are required for HRV binding, and the internalization of HRV does not require ICAM-1 cytoplasmic or transmembrane domains[111,112]. The surface of HRV contains a star-shaped plateau at a five-fold axis of symmetry that surrounds a canyon containing a hydrophobic pocket[101,113]. ICAM-1 binding within this pocket results in the dislodgement of a fatty acid, termed the fatty pocket factor, which is found in all but two HRV strains (HRV-3, HRV-14). This decreases the stability of the capsid leading to release of viral RNA[101]. In contrast, minor group binding to LDLR occurs near the tip of the five-fold axis[114]. The mechanism of viral entry after receptor binding has yet to be fully elucidated. Minor group HRV-2 is internalized through clathrin-mediated, pH-dependent endocytosis[115,116]. Studies with major group HRV-14, however, demonstrate that uncoating can occur in early

endosomes, but is unaffected by changes in pH[117]. In addition to receptor binding, HRV infection requires the formation of membrane microdomains, also known as lipid rafts, for cellular entry[118].

1.5.4 Capsid and genome structure

All HRVs are non-enveloped and consist of an icosahedral capsid comprising 60 separate protein units, known as protomers, and a single-stranded positive sense RNA[119]. The 60 protomers are formed from 4 separate viral proteins (VP) that make up the capsid[120]. The outer capsid consists of VP1, VP2, and VP3. VP4 is buried inside the capsid and binds the single RNA strand. The positive sense RNA strand is composed of a single open-reading frame of approximately 7.4 kilobases flanked by 5' and 3' untranslated regions (UTRs) (Figure 1.2). The viral protein (VPg) is covalently attached to the 5' end and serves as primer to initiate viral RNA synthesis. The 3' end is polyadenylated similar to host mRNAs[119]. The viral genome encodes all of the proteins required for viral replication and formation of infectious virions within the cytoplasm of the host cell.

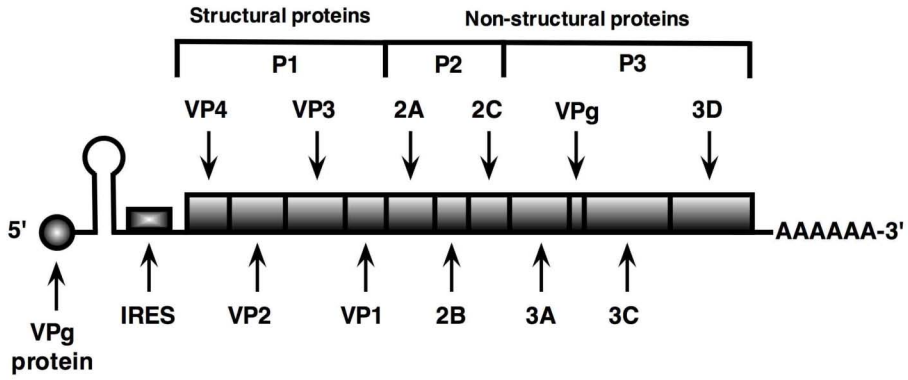

Figure 1.2 – HRV genome structure. A 7.4 kb single-strand positive sense RNA is packaged within a viral capsid and encodes all of the proteins necessary for replication and virion formation. The open reading frame is flanked by a 5' UTR, including highly conserved hairpin loop and internal ribosomal entry site **(**IRES) sequences, and a 3' polyadenylated tail. Structural viral proteins (VPs) necessary for capsid formation are contained within the P1 region. Non-structural enzymes necessary for cleavage of the translated protein (2A & 3C) and replication of viral RNA (3D & VPg) are contained within the P2 and P3 regions.

1.5.5 Viral replication

After uncoating, host ribosomes translate the viral RNA through a 5' cap-independent mechanism, utilizing the highly conserved internal ribosomal entry site (IRES). This results in a polyprotein that is cleaved by the viral proteases 2A and 3C into 11 final protein products (4 structural and 7 non-structural)[103,121,122]. The 2A and 3C proteases also markedly decrease host RNA transcription and translation through degradation of the transcription factors TFIID[123] and OCT-1[124] and host translation-initiation factor 4G (eIF4G)[125]. Also encoded is an RNA-dependent RNA polymerase (3D) for the synthesis of viral genomic RNA. The newly synthesized positive sense RNAs, generated from negative strand template RNA, are packaged into empty capsids to produce non-infectious provirions[119]. Infectious particles are formed through a maturation cleavage resulting in the formation of mature VP2 and VP4 subunits[126]. The

exact mechanism behind the release of newly synthesized HRV is yet to be determined, though reported mechanisms include apoptosis[127] and subversion of autophagosome function[128]

1.6 HRV infection of the airway epithelium

The airway epithelial cell is the principal site of HRV infection *in vivo* in humans[129,130]. Infection of healthy human volunteers results in a productive HRV infection of the upper airways and requires as little as 10^1 $TCID_{50}$ units, but does not infect the entire nasal epithelial lining at peak symptoms[131]. Furthermore, infectious virus can be detected in nasal secretions 8-10 h post-infection with peak shedding at 2 days post-infection and detectable virus and viral RNA for up to 3 weeks[131,132]. HRV replication in the airways is optimal between 33-35^{o}C although replication does occur at 37^{o}C[119,133].

In addition to infection of the upper airways[134], studies using *in situ* hybridization, immunohistochemistry, and RT-PCR techniques have also demonstrated HRV infection can spread to the lower airways[135-138]. In fact, infection of epithelial cells in the upper and lower airways occurs at a similar frequency resulting in a patchy infection with 5-10% cells infected[137,139]. An unidentified subepithelial cell in bronchial tissue is also infected by HRV[137].

In contrast to other respiratory viruses, such as influenza and adenovirus[35], HRV infection *in vivo* does not cause overt cytopathic effects in the epithelium[129,140]. These results suggest that alteration of lower airway epithelial cell biology, rather than cytoxicity, may be responsible for the inflammatory responses seen in HRV-induced

exacerbations of asthma and COPD. As such, airway epithelial cell models were developed to further understand the contribution of the epithelium to HRV-induced changes during exacerbations. Using human tissue fragments isolated from the nasal passage and adenoids, *Winther et al.*, grew an epithelial monolayer *in vitro* that was successfully infected with HRV[35]. Infection of these epithelial cells with HRV did not result in an increase of cytopathic effects compared with other respiratory viruses, including influenza and adenovirus. In addition, using the transformed bronchial epithelial cell line, BEAS-2B, *Subauste et al.*, were the first to demonstrate routine HRV infection of a pure population of airway epithelial cells[141]. HRV is capable of non-cytopathic replication and also induces the release of the pro-inflammatory cytokine (IL-6) and chemokines (CXCL8, CXCL10) similarly seen during *in vivo* infections[136,141-143]. These studies further supported the notion that symptoms after HRV infection are due to changes in epithelial cell biology rather than cytotoxicity.

Although some studies demonstrate that HRV infection *in vitro* induces an increase in cytopathic effects, these results appear to depend on the airway epithelial cell model, low cell density, and seem to be specific to certain HRV strains[144,145]. Differentiated bronchial epithelial cells are also susceptible to HRV infection, but require higher amounts of virus for infecton than undifferentiated basal cells[146,147] or even *in vivo* infections[131].

Overall, the development of *in vitro* models of primary and transformed airway cells has allowed the study of the mechanisms of HRV-induced pro-inflammatory gene expression in the context of asthma and COPD exacerbations.

1.7 Airway epithelium and the pro-inflammatory response

Once thought to primarily serve as a physical barrier to the external environment, the airway epithelium is now widely recognized to be actively involved in modulating the the innate and adaptive immune response[8]. Given its proximity to the external environment, the epithelium is the first cell to encounter invading pathogens, and recognition of these pathogens is crucial in regulating the immune response through the production of a wide variety of epithelium-derived inflammatory mediators (Table 1.1). Given that the airway epithelial cell is the primary site of HRV infection, and that infection does not result in overt cytotoxicity, production of epithelium-derived pro-inflammatory mediators is thought to contribute to the HRV-induced increase in airway inflammation seen in asthma and COPD exacerbations.

HRV infection of airway epithelial cells *in vitro* results in the expression and release of various pro-inflammatory cytokines and chemokines, including IL-1[148], IL-6[141,149], CXCL8[141,149,150], CXCL10[143], CXCL5[151], GM-CSF[141], and CCL11[152] (Table 1.1). Experimental HRV infection of human volunteers also results in an increase of these mediators in airway secretions, and is characterized by a predominant influx of neutrophils and lymphocytes. This suggests that epithelium-derived chemokines contribute to inflammatory cell infiltration during an exacerbation.

Table 1.1 – List of airway epithelium-derived inflammatory mediators

Chemokines	**Pleiotropic cytokines**	**Anti-microbial**
CXC;α CXCL8 (IL-8)* CXCL5 (ENA-78)* CXCL1 (Gro-α)* CXCL3 (Gro-γ) CXCL10 (IP-10)* CXCL9 (Mig) CXCL11 (I-TAC)	IL-6* IL-11* IL-1* IFN-β* IFN-λ* TSLP IL-10	Lysozyme Lactoferrin SLPI Elafin Surfactant (SP-A/SP-D) β-defensins* LL-37 iNOS*
CC;β CCL11 (Eotaxin)* CCL5 (RANTES)* CCL2 (MCP-1) CCL13 (MCP-4) CCL3 (MIP-1α) CCL20 (MIP-3α) CCL17 (TARC) CCL22 (MDC)	**Colony-stimulating factors** GM-CSF* G-CSF* CSF-1 M-CSF	**Lipid mediators** Lipoxin A 15-lipoxygenase PGE_2 $PGF_{2\alpha}$
CX_3C;δ CX_3CL1 (Fractalkine)	**Growth factors** TGF-β TGF-α EGF Activin A Amphiregulin* SCF VEGF*	**Anti-viral** iNOS* Viperin*

*shown to be HRV-inducible *in vitro*. Adapted from *Proud, D.* (ref. 8). EGF, epidermal growth factor; GM-SCF, granulocyte macrophage colony-stimulating factor; G-CSF, granulocyte colony-stimulating factor; HB-EGF, heparin-binding EGF-like growth factor; iNOS, inducible nitric oxide synthase; LL-37, human cathelicidin anti-microbial protein; PG, prostaglandin; SLPI, secretory leukocyte protease inhibitor; TGF, transforming growth factor; VEGF, vascular endothelial growth factor.

Illness due to an uncomplicated HRV infection is maximal at 2-3 days post-infection and the median duration is 7 days[153]. Following HRV infection, neutralizing antibody in serum and nasal secretions are first detected 14-21 days post-infection[154] and reach maximal levels by 5 weeks post-infection[155]. The kinetics of virus-specific T lymphocyte infiltration into the airways after HRV infection is less certain[156], although non-specific T lymphocyte infiltration into nasal passages has been shown to peak 2 days post-infection[143]. Previous studies have also shown that HRV-specific responses are predominately mediated by type 1 CD4+ cells[157,158], although the role of CD8+ cells has yet to be fully elucidated[156]. Interestingly, HRV is believed to dampen the adaptive response via alteration of DC function[159,160]. Taken together, this suggests that HRV-induced symptoms are primarily mediated through innate responses. It should be noted that the airway epithelium is capable of modulating the adaptive response via several mechanisms[161]. These include the production of the dendritic cell maturation factor thymic stromal lympopoietin (TSLP)[162-164] and expression of immunomodulatory receptors, including major histocompatibility complexes (MHC)-I, MHC II and B7 family T-cell co-stimulatory molecules[165-167]. Finally, the epithelium has also been shown to internalize and present antigen[168,169].

1.7.1 Innate immune response

The innate immune response provides the first line of host defense against viral infection, such as HRV[156]. This response occurs in a non-specific manner and does not confer long-lasting protective immunity, although it plays a key role in the activation of the adaptive immune system. Since the airway epithelium is the primary site of HRV

infection, it plays an important role in the initiation of the innate immune response after infection through the release of various pro-inflammatory mediators, including cytokines and chemokines[8]. Expression of some epithelium-derived pro-inflammatory cytokines and chemokines, such as CXCL10, are not induced for hours after infection and absolutely require HRV replication[143]. As such, increased expression of these chemokines requires the recognition of replication intermediates of HRV by a set of cellular receptors known as pattern-recognition receptors (PRRs). The PRRs recognize and bind a double-stranded RNA (dsRNA) intermediate, known as a pathogen-associated molecular pattern (PAMP), generated during HRV replication in airway epithelial cells.

Currently, there are three main classes of PRRs involved in the detection of viruses[170,171]. These include the Toll-like receptors (TLRs), retinoic acid-inducible gene-I (RIG-I)-like receptors (RLRs), and nucleotide oligomerization domain (NOD)-like receptors (NLRs). The mRNA for ten human TLRs are expressed in human airway epithelial cells[172], but only TLR3 detects dsRNA and can be in found in airway epithelial cells predominately on the surface of intracellular endosomes[173,174]. The RLRs, RIG-I and melanoma differentiation-associated gene 5 (MDA-5) are also found in airway epithelial cells[175,176] and bind cytoplasmic dsRNA through their C-terminal DExD/H-Box RNA helicase domain[177]. Considered more of a DNA sensor, the NLR, Nacht domain-, leucine-rich repeat-, and PYD-containing protein 3 (NALP3) induces IL-1β production after introduction of adenoviral DNA[178]. Its role during RNA virus infection of the airway epithelium has not been characterized[179]. Protein kinase R (PKR) is another dsRNA receptor found within the airway epithelium whose role in anti-viral responses is uncertain as PKR knockout mice maintain normal anti-viral responses[180], thus it is oft

neglected during anti-viral studies. However, *in vitro* studies using human cells, including airway epithelial cells, demonstrate PKR-dependent pro-inflammatory gene expression in response to virus and synthetic dsRNA[176,181-183].

Although TLR3, RIG-I, and MDA-5 recognize dsRNA, each PRR has a specific set of dsRNA binding characteristics. TLR3 binding is highly dependent on pH and requires a minimum of ~45 bp to bind both the C- and N-terminal ends[184,185]. RIG-I-induced responses are thought to be a result of the recognition of dsRNA < 1 kb in length, in contrast with MDA-5 that recognizes dsRNA > 1 kB in length[186]. Furthermore, RIG-I can also recognize 5' triphosphate modified single-stranded RNA (ssRNA), not normally found on host RNA transcripts[187]. More recently, it has been shown that dsRNA length directly influences the transcriptional mechanisms of pro-inflammatory cytokine and chemokine expression[188].

In addition to selective binding characteristics, dsRNA recognition and subsequent responses are also thought to be dependent on cell type. This is exemplified by the picornavirus, encephalomyocarditis (ECMV), which requires MDA-5 recognition in mouse fibroblasts and conventional DCs, but the TLR system is used in plasmacytoid DCs[189]. Although TLR3, RIG-I, and MDA-5 have been shown to mediate responses in airway epithelial cells, their specific roles are dependent on the infecting virus and model system used for study[173,190,191]. In fact, mice deficient in RIG-I have been shown to recognize the hepatitis C, Sendai, influenza, rabies, and Newcastle disease viruses, while MDA-5 has been shown to selectively recognize ECMV and synthetic dsRNA[192,193]. In human airway epithelial cells, chemokine expression after HRV infection has been shown to be mediated through either MDA-5 or TLR3, but not RIG-I[175,194].

As shown in Figure 1.3, TLR3-induced responses are mediated through the specific adaptor protein, Toll/IL-1 receptor (TIR) domain containing adaptor inducing IFN-β (TRIF)[195] and RIG-I/MDA-5 responses require the adaptor protein IFN-β promoter stimulator 1 (IPS-1/MAVS/VISA/Cardif)[196-199]. The interactions of TLR3/TRIF and RIG-I/MDA-5/IPS-1 are mediated through TIR and caspase recruitment domains (CARDs), respectively[171]. TLR/TRIF and RIG-I/MDA-5/IPS-1 complexes further activate downstream signalling proteins subsequently leading to the activation of the kinase complexes, inhibitor of kappa B kinase (IKK-α/IKK-β/IKK-γ)[200,201] and IKK-γ/IKK-ε/TRAF family member-associated NF-κB activator-binding kinase 1 (TBK-1) [202,203]. Activation of these complexes are responsible for the phosphorylation and nuclear translocation of the transcription factors nuclear factor kappa-light-chain-enhancer of activated B cells (NF-κB) and interferon-regulatory factor 3 (IRF-3)[201]. Binding of these proteins to specific DNA sequences near the transcriptional start sites of viral replication-dependent pro-inflammatory genes, including the chemokines CXCL10[175,204] and regulated on activation normal T cell expressed and secreted (CCL5; RANTES)[205], results in the up-regulation of gene expression and subsequent protein release. Although much work is still required to elucidate the exact mechanisms of HRV recognition, it is clear that recognition by any of the aforementioned PRRs is sufficient to induce pro-inflammatory chemokine production that can contribute to inflammation that is seen during asthma and COPD exacerbations.

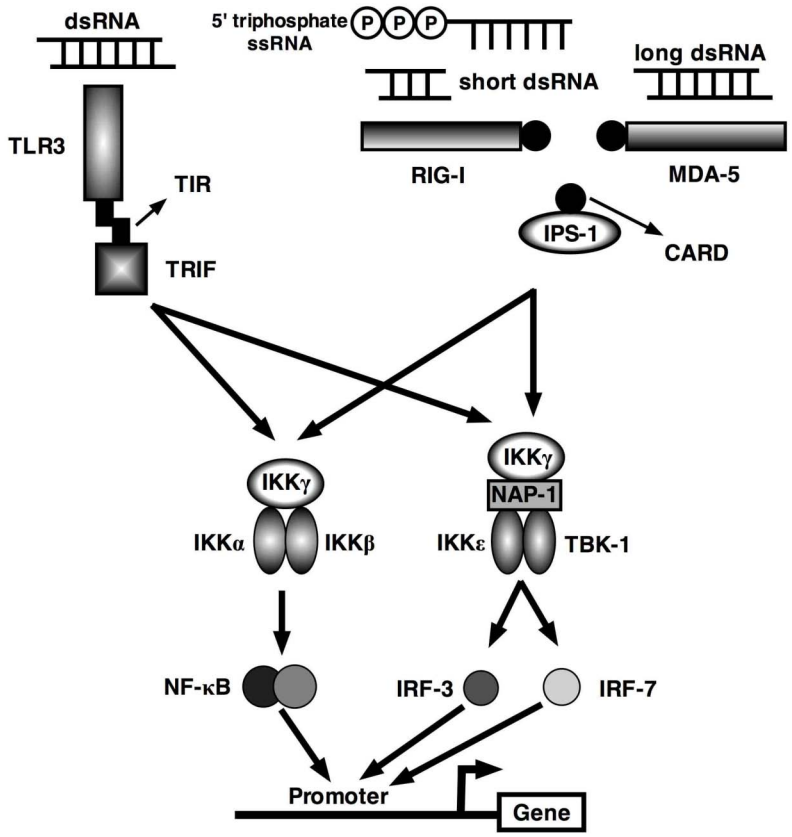

Figure 1.3 – Viral double stranded RNA (dsRNA) recognition pathways. Following viral infection, RNA virus replication results in the formation of a dsRNA intermediate. The dsRNA is recognized by pathogen-recognition receptors (PRRs), including Toll-like receptor (TLR)-3, retinoic acid-inducible gene (RIG)-I, and melanoma differentiation antigen (MDA)-5. Each PRR recognizes specific nucleic acid characteristics, such as dsRNA length or 5' phoshorylation. Interaction with endosomal TLR3 leads to interaction with Toll/IL-1 receptor (TIR) domain-containing adaptor inducing IFN-β (TRIF), which is mediated by the presence of TIR domains. Engagement of cytosolic RIG-I and MDA-5 leads to interaction with IFN-β promoter stimulator 1 (IPS-1) through caspase-recruiting domains (CARDs). All three PRR pathways converge on the classical NF-κB pathway complex composed inhibitor of kappa B kinase (IKK-α/IKK-β/IKK-γ) . In addition, activation of the IKK-γ/IKK-ε/TRAF family member-associated NF-κB activator-binding kinase 1 (TBK-1) complex leads to IRF-3 and IRF-7 phosphorylation. Association of IKK-γ to IKK-ε/TBK-1 is mediated by NAK1-associated protein (NAP)-1. Phosphorylation and nuclear translocation of NF-κB and IRF3/7 mediate transcription of pro-inflammatory cytokines, chemokines, and interferon-inducible genes.

1.8 Chemokines

1.8.1 Classification and function

An effective inflammatory response requires the trafficking of leukocytes and lymphocytes to sites of infection through the production of navigational cues known as chemokines. Abnormal inflammatory responses, as seen in asthma and COPD, are due, in part, to increased production of these chemokines and contribute not only to disease pathogenesis[206,207], but also to virus-induced exacerbations of asthma and COPD[78,208].

Chemokines, or chemoattractant cytokines, are 8-15 kDa, positively-charged proteins that play a crucial role in the recruitment of inflammatory cells to sites of inflammation, but also in homeostasis, T-cell differentiation, and embryogenesis[209]. The chemotactic function of chemokines is mediated through seven-transmembrane domain, pertussis toxin-sensitive, G-protein-coupled receptors (GPCR) with G protein subunits ($G_{\alpha i}$ & $G\beta\gamma$). There are currently 47 chemokines and 19 chemokine receptors identified[209]. The four chemokine families are classified by the arrangement of two N-terminal cysteine residues within their amino acid sequence and include the CXC (α) family, CC (β) family, C (γ) family, and the CX_3C (δ) famliy. The CXC family, with a single amino acid between the cysteine residues, can be further sub-divided into two groups based on the presence of an N-terminal glutamic acid-leucine-arginine (ELR) sequence. Members of the CXC (ELR+) family include CXCL8[210] and epithelial neutrophil-activating protein 78 (CXCL5; ENA-78)[211], which are primarily chemotactic for neutrophils and have angiogenic properties. CXC (ELR-) chemokines, including CXCL10[212], monokine-induced by IFN-γ (CXCL9; Mig)[213], and interferon-inducible T cell α-chemoattractant (CXCL11; I-TAC)[214] are chemotactic for several cell types,

including T_H1 lymphocytes and display angiostatic properties. The CC chemokines, including CCL5[215], CCL17[216], and CCL11[217] are chemotactic for monocytes, T_H2 lymphocytes, and eosinophils. The C chemokine family includes one member, XCL1 (lympotactin)[218] and its splice variant single cysteine motif (SCM)-1β[219]. Finally, CX_3CL1 (fractalkine) is the only member of the CX_3C and found predominately as a cell membrane protein[220]. Chemokines are produced by various cell types, including infiltrating cells (leukocytes), tissue resident cells (fibroblasts), and structural cells (epithelial cells)[209].

1.8.2 CXCL10

As mentioned previously, the airway epithelium is capable of producing a plethora of chemokines including those induced after HRV infection[8] (Table 1.1). This includes the increased expression of the HRV-inducible CXC chemokine, CXCL10[143], whose levels are increased in both stable and acute asthma and COPD[72,221-223].

First cloned in 1985, CXCL10 was initially designated pIFNγ-31 because of its expression in IFN-γ-stimulated U937 cells (histiocytic lymphoma cell line with monocytic characteristics) and characterized as a cyclohexamide-insensitive, primary response gene[212,224]. As a member of the CXC (ELR-) chemokine family, it displays additional biological functions including angiostatic[225], anti-tumour[226], and anti-microbial activity[227]. It is expressed by many cell types, including airway epithelial cells[228], endothelial cells[229], fibroblasts[230], activated T cells[231], monocytes[232], and neutrophils[233]. Expression of CXCL10 is induced by a variety of stimuli, including, but not limited to, types I and II interferon[212,234], IL-1β[230], IL-12[235], synthetic dsRNA[236], hypoxia[237], and

viral infection[143,238]. CXCL10 is viewed as a T_H1 chemokine because of its increased expression by IFN-γ and also the ability of IL-4 to down-regulate IFN-γ-induced CXCL10 expression[239].

CXCR3 serves as the receptor for CXCL10 as well as the related chemokines, CXCL9 and CXCL11[209]. This receptor is found on many cell types, including NK cells[240], activated T_H1 lymphocytes[241,242], NKT cells[243], dendritic cells[244], monocytes[242], eosinophils[245], mast cells[246], endothelial cells[244], and airway epithelial cells[247]. Interestingly, T_H1 lymphocytes preferentially express CXCR3 compared with T_H2 lymphocytes[248,249]. In contrast, CXCR3 is not found on resting T cells, B cells or neutrophils and, thus, these cell types are not responsive to CXCL10-induced chemotaxis[241,250]. In addition to the classical CXCR3 isoform, a splice variant termed CXCR3B serves as the receptor for the classical CXCR3 ligands and CXCL4 (platelet factor; PF4) and is also expressed on airway epithelial cells[247,251]. Autocrine or paracrine binding of CXCR3 ligands on airway epithelial cells has been suggested to mediate epithelial cell migration via actin cytoskeleton reorganization[247].

Expression of CXCL10 is increased in various inflammatory diseases such as atherosclerosis, multiple sclerosis, and inflammatory bowel disease[209]. Of note, CXCL10 protein levels are increased in the airways of patients with asthma and COPD[72,221]. Similarly, CXCL9 and CXCL11 protein levels in the sputum of COPD patients are also increased[252]. Interestingly, CXCL10 has been recently shown to be a novel serum biomarker for HRV-induced exacerbations of both asthma and COPD[222,223]. Evidence exists for a contribution of CXCL10 to airway hyperresponsiveness and inflammation in a murine model of allergen-induced T_H2-type inflammation typically seen in

asthma[253,254]. Moreover, segmental allergen challenge results in an increase of CXCR3 ligands in the bronchoalveolar lavage (BAL) of asthmatics[255]. Finally, a functional CXCL10 knockout mouse model displays impaired T cell responses, proliferation, generation of CD8+ effector function, and overall ability to control viral infections[256].

There is a marked increase of nasal epithelial expression of CXCL10 mRNA in experimentally HRV-16-infected versus sham-infected control subjects[257]. Furthermore, it has also been shown that HRV-16-induced nasal secretion of CXCL10 protein *in vivo* correlates with symptom score, viral titre, and lymphocyte count[143]. Using the same serotype to correlate the findings *in vitro*, infection of human airway epithelial cells with HRV-16 induces the expression of the CXCL10 mRNA and protein in a time- and replication-dependent manner. Therefore, it is reasonable to suggest that epithelial cell production of CXCL10 contributes to the pathogenesis of HRV-induced exacerbations of these airway diseases. Although airway epithelial cells have the capability to produce CXCL9 and CXCL11[228], their roles in the context of HRV infection have not been studied. As such, CXCL10 was chosen as an appropriate model to study chemokine production after HRV-16 infection of airway epithelial cells.

1.9 Signal transduction

Signal transduction is the process through which changes in cellular behaviour are induced in response to extra- or intracellular stimuli[258]. These inducible changes include, transcriptional regulation, cell proliferation, differentiation, and apoptosis. Transmission of an HRV-induced signal is initiated after capsid binding to ICAM-1/LDLR or during viral replication where dsRNA binds the intracellular receptors, TLR3 or MDA-5 (Figure

1.3). Regardless of the receptor used, ligand binding results in the activation of a complex set of intracellular pathways that amplify the signal through a cascade of interacting proteins. This amplification is controlled through changes in conformation and/or enzymatic activities resulting in the modulation of downstream targets[258]. Furthermore, feedback control of these pathways is crucial to prevent excessive stimulation that may lead to certain pathologies[259]. As such, research has focused on how these signaling pathways can be manipulated to reduce inflammation observed in asthma and COPD[260,261].

Given that the airway epithelium can produce a plethora of pro-inflammatory mediators, including CXCL10[143], it is without surprise that numerous signalling pathways can be found within the airway epithelium[8]. However, surprisingly little is known about the signaling pathways involved in the production of chemokines from HRV-infected epithelial cells. As mentioned in section 1.7.1, the binding of dsRNA to the intracellular PRRs, TLR-3, RIG-I, and MDA-5, results in the activation of a specific set of signalling pathways leading to increased gene transcription of pro-inflammatory and anti-viral genes, including CXCL10[143,175]. In addition to these pathways, the binding of major group HRV capsid to ICAM-1 certainly induces the activation of other signalling pathways that may contribute to the an increase in HRV-induced, replication-dependent expression of CXCL10. Although the pathways involved in CXCL10 expression after HRV infection are not well characterized, they could include pathways activated during HRV-induced CXCL8 expression, such as spleen tyrosine kinase (Syk)[262,263], sarcoma (Src) tyrosine kinase[264], phosphatidylinositol-3-kinase (PI3K)[265], and p38 mitogen-activated protein kinase (MAPK)[266,267]. Interestingly, Syk is activated early after

infection and mediates the activation of downstream PI3K and p38 MAPK[262,263]. HRV infection of airway epithelial cells has also been shown to activate p38 MAPK-related pathways[262,267,268], which together constitute a well characterized family of signalling molecules known as the MAPK pathways. Importantly, the MAPK pathways have the ability to affect targets directly involved in the up-regulation of chemokine expression[269]. Therefore, the MAPK pathways were chosen as the focus of study in the regulation of HRV-induced expression of CXCL10 in human airway epithelial cells.

1.9.1 Mitogen-activated protein kinases

First characterized in yeast, the mitogen-activated protein kinase (MAPK) pathways are a family of evolutionarily conserved protein kinase cascasdes[270,271]. These cascades serve to mediate important cellular functions, including proliferation, differentiation, development, transcription, stress response, and apoptosis[271]. Currently, four major MAPK pathways have been elucidated, including extracellular signal-regulated kinase 1/2 (ERK1/2), also known as p44/p42; c-Jun amino terminal kinase (JNK) also known as stress-activated protein kinase 1 (SAPK1); p38 MAPK, also known as SAPK2-4; and Big MAPK (BMK), also known as ERK5 (Figure 1.4). Although the ERK pathways have been generally implicated in cell proliferation and differentiation, and the p38 and JNK pathways seem to be involved in the stress response, it must be noted that the function of each individual pathway is dependent on cell type and stimulus[269].

MAPK pathway activation is usually initiated by a small G protein (e.g. Ras, cdc42) that is located near the cell membrane and can act on downstream kinases[269]. This

signal is subsequently transmitted through a cascade of enzymes located at three main tiers, which are referred to as MAPK kinase kinases (MAPKKK or MEKK), MAPK kinases (MAPKK, MEK, or MKK), and MAPK[271]. Although the regulation of MAPK pathway activation is very complex, most studies focus at the level of MAPK. Activation of each tier is mediated by site-specific phosphorylation by an upstream kinase on either serine (Ser), threonine (Thr), or tyrosine (Tyr) residues in an area known as the activation loop of each substrate[271]. At the level of MAPK, each protein is activated by their respective upstream MAPKK resulting in the phosphorylation of Thr and Tyr residues. Specificity of recognition is further enhanced by amino acid sequences that surround the phospho-acceptor sites and the presence of distinct docking domains[272]. For simplicity, each MAPK pathway is usually described as a linear pathway, but the ability of the MAPKs to transmit different signals within the same cell suggests a more complex regulation. In this regard, signal specificity is dictated by various factors, including the duration and length of signal, interaction with scaffold proteins, subcellular localization, cross-talk, and the presence of multiple components at each tier[273].

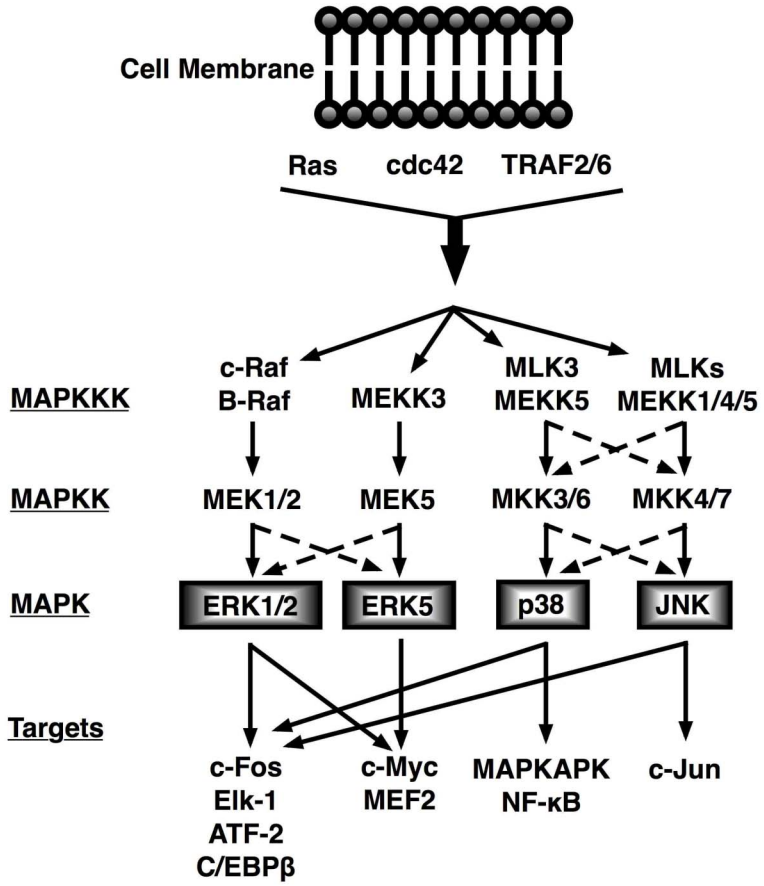

Figure 1.4 – Schematic diagram of the mitogen-activated protein kinase (MAPK) pathways. There are four major MAPK pathways, including extracellular signal-regulated kinase 1/2 (ERK1/2), ERK5 (BMK1), p38 MAPK, and c-Jun amino terminal kinase (JNK). Each MAPK pathway is composed of at least three main tiers, including MAPKKK, MAPKK, and MAPK. Each signaling cascade can be induced by various stimuli, such as stress, growth factors, cytokines, and HRV. Pathway activity is initiated by small G proteins (e.g. Ras) located at the cell membrane, although viral dsRNA binding to intracellular pathogen recognition receptors (PRRs) may induce MAPK activity via the TNF receptor-associated factor (TRAF) family of proteins. Following activation, site-specific phosphorylation of Ser, Thr, or Tyr residues on kinases at each tier results in signal amplification. This leads to the phosphorylation of transcription factors or other kinases that have direct roles in mediating cell proliferation, differentiation, apoptosis, and transcription. Although mechanisms exist to maintain signal specificity, the dashed arrows indicate the complexity of these pathways as crosstalk at various MAPK levels can occur depending on stimulus and cell type.

1.9.2 p38 MAPK pathway

The p38 MAPK pathway is activated by various stimuli, such as pro-inflammatory cytokines, HRV, lipopolysaccharide (LPS), and stress such as osmotic shock and ionizing radiation[267,271]. This pathway is composed of four isoforms, including p38α, p38β, p38γ, and p38δ. The α and β isoforms are ubiquitously expressed and are sensitive to pharmacological inhibitors, hence are primarily studied during release of pro-inflammatory mediators[271,274]. Upstream MKK3 and MKK6 are responsible for the phosphorylation of p38[275,276]. Downstream targets of p38 include MAPK activated protein kinases (MAPKAPKs) and the transcription factors ATF2, Elk-1, and MEF2C[277,278].

Interestingly, airway biopsies of severe asthmatic subjects have increased levels of p38 phosphorylation in the airway epithelium compared to mild asthmatics and healthy controls[279]. Futhermore, the p38 pathway is implicated in many processes involved in the pathogenesis of asthma and COPD, including T_H1 differentiation and IFN-γ production[280], epithelial cell apoptosis[281], eosinophil degranulation[282], and the production of pro-inflammatory cytokines and chemokines[283,284].

1.9.3 JNK pathway

Similar to the p38 pathway, the JNK pathway is activated by stress, but also pro-inflammatory cytokines and HRV[267,268,271]. It is composed of 3 isoforms, including JNK1, JNK2, and JNK3[271]. While JNK1 and JNK2 are ubiquitously expressed, JNK3 is mainly expressed in neuronal cells[285]. The upstream activators responsible for JNK phosphorylation are MKK4 and MKK7[271]. Downstream targets of JNK include c-Jun,

Elk-1, and ATF-2[286]. Examination of airway biopsies revealed increased levels of JNK phosphorylation in airway smooth muscle and not the epithelium, although phosphorylation intensity is decreased in severe and mild asthmatics compared to healthy controls[279]. The JNK pathway has also been shown to negatively regulate T_H2 differentiation[287], modulate myofibroblast transformation[288], inflammatory cell infiltration[289], cytokine release[289], and airway smooth muscle proliferation[290].

1.9.4 ERK5 pathway

The ERK5 pathway is readily activated by stress-related stimuli and growth factors, including nerve growth factor (NGF) and epidermal growth factor (EGF)[291]. The activation loop and kinase domain of ERK5 is similar to ERK1/2, although it retains a unique C-terminal domain that acts as a transcriptional activator and is not found in ERK1/2[291,292]. The upstream kinase for ERK5 has been identified as MEK5[293], but the ERK1/2 kinases, MEK1/2, have been shown to phosphorylate ERK5[294,295]. Downstream targets include the transcription factors MEF2C and Sap1[269], although ERK5 itself can serve as a transcription factor[296]. The role of ERK5 in asthma and COPD has yet to be elucidated, but ERK5 has been implicated in angiogenesis and T lymphocyte function[291].

1.9.5 ERK1/2 pathway

The ERK1/2 pathway is composed of two main proteins at the MAPK level, including ERK1 (p44; MAPK3) and ERK2 (p42; MAPK1)[297,298]. These proteins share 70% overall homology, with > 90% homology in their kinase domains[299]. ERK2 is the predominant form found in most cells[273]. Alternatively spliced forms of ERK1

(ERK1b)[300] and ERK2 (ERK2b)[301] have been identified, though their functions have yet to be fully elucidated. The ERK1/2 pathway is readily activated by growth factors and serum, although stress, cytokines, and HRV can also activate this pathway[262,267,268,271]. Both ERK1 and ERK2 are activated by dual phosphorylation of their Thr-X-Tyr motif by the upstream dual-specificity MAPKKs, MEK1 and MEK2[302,303]. Upon activation the ERKs translocate to the nucleus via dimerization[304] or direct interaction with nuclear pore proteins (NUPs)[305], and phosphorylate downstream targets on Pro-X-Ser/Thr-X-Pro consensus sites. Downstream targets include the transcription factors Elk-1[306], c-Fos[307], p53[308], Ets1/2[309], STAT[310], and MAPKAPKs such as ribosomal S6 kinase (RSKs)[311]. Inactivation of ERK1/2 activity is accomplished by the removal of phosphate on Thr and Tyr residues[259]. This removal is mediated by phosphatases, including Ser/Thr protein phosphatase 2A (PP2A)[312], protein Tyr phosphatases[313], and dual specificity phosphatases known as MAPK phosphatases (MKPs)[314].

Both ERK1 and ERK2 share similar activation kinetics, cellular localization, and substrates[269]. However, differences between ERK1 and ERK2 functions exist[315-317]. ERK1-deficient mice are viable[318], while ERK2-deficient mice are embryonic lethal[319], thus demonstrating that ERK1 may not always compensate for the loss of ERK2 activity.

Airway biopsy samples show increased levels of phosphorylated ERK1/2 in the airway epithelium and smooth muscle of severe and mild asthmatics compared with healthy controls, although levels of phosphorylated ERK1/2 are substantially higher in severe patients[279]. The ERK1/2 pathway is also important in the differentiation of naïve T lymphocytes into a T_H2 phenotype[320]. In addition, ERK2 is involved in eosinophil chemotaxis and degranulation[282]. Hyperplasia of airway smooth muscle has also been

found to be mostly dependent on the ERK1/2 pathway[321,322]. Furthermore, the ERK1/2 pathway is involved in the expression of cytokines and chemokines, such as CXCL8, CCL5, IL-1β, IL-6 and GM-CSF from mast cells, epithelial cells and smooth muscle in the airway[283]. Cigarette smoke-induced damage and cytokine expression in bronchial epithelial cells is mediated, in part, through an ERK1/2-dependent manner[323,324]. In a rat model, ERK1/2 activity was required for increased airway epithelium permeability to allow leukocyte transmigration into the airway lumen[325]. Also of note, the ERK1/2 pathway has been shown to positively regulate the replication of various RNA viruses, including influenza and coronavirus[326].

1.9.6 MEK1 and MEK2

MEK1 and MEK2 serve as the upstream kinases for ERK1 and ERK2, which are believed to be their only physiological substrates[273,303]. The MEKs share ~85% overall homology and are nearly identical in their kinase domains[327,328]. They are mainly activated by the Raf kinase family through the phosphorylation of two Ser residues in the Ser-X-Ala-X-Ser/Thr motif[329]. In addition, the MEKs are also phosphorylated by the ERKs, which can either inhibit or enhance MEK activity[330,331]. In this regard, it was recently shown that a novel feedback loop exists whereby ERK phosphorylation of MEK1 prevents inhibition of MEK2-dependent phosphorylation of ERK1/2[332]. Downregulation of MEK1/2 activity involves dephosphorylation by various phosphatases, including PP2A[259,333].

In addition to serving as ERK kinases, MEK1/2 sequester ERK1/2 in the cytoplasm through scaffolding proteins including kinase repressor of Raf-1 (KSR-1)[334],

β-arrestin[335], and MEK partner 1 (MP1)[336]. Although MEK1/2 can translocate to the nucleus, they are rapidly shuttled back to the cytoplasm due to the presence of a nuclear export signal (NES) sequence[337]. Similar to the ERKs, MEK1 and MEK2 have similar and divergent functions[273]. MEK1-deficient mice are embryonic lethal[338], but MEK2-deficient mice are normal[339]. Both Ras and Raf-1 have been shown to preferentially bind MEK1 and not MEK2[340], although c-Raf will activate both MEK1 and MEK2[341].

Given their ability to directly activate ERK1/2, the role of MEK1 and MEK2 in asthma and COPD has not been studied in depth, but potential therapies to modulate ERK1/2-mediated airway inflammation currently rely on pharmacologic inhibitors that target MEK1 and MEK2[342]. In this regard, pharmacologic inhibition of MEK1 and MEK2 inhibits expression of pro-inflammatory mediators, eosinophil counts, and airway hyperresponsiveness in a mouse model of asthma[343].

1.10 Transcriptional regulation

Conversion of virus-induced signals into changes in gene expression is mediated, in part, at the level of transcription and requires the actions of DNA-binding protein known as transcription factors[344]. Once activated by signaling kinases via post-translational modifications, such as phosphorylation, transcription factors bind to specific DNA sequences found in the promoter region upstream of the transcriptional start site of a gene. This initiates a series of events to increase transcription, including histone modifications, chromatin remodelling, and binding of transcription-initation factors and RNA polymerase II[345]. As seen in asthma and COPD, transcriptional dsyregulation leads

to enhanced levels of pro-inflammatory cytokines, chemokines, and adhesion molecules that contribute to exacerbations of both diseases[346].

1.10.1 NF-κB

The mammalian transcription factor nuclear factor kappa-light-chain-enhancer of activated B cells (NF-κB) is a crucial activator of genes associated with the pathogenesis of airway diseases, such as asthma and COPD[346,347]. In fact, NF-κB is activated in alveolar macrophages, airway epithelial cells and bronchial mucosal biopsies from asthmatics[348,349]. Similar to asthma, bronchial biopsies of patients with mild to moderate COPD and smokers without COPD demonstrate increased epithelial expression of NF-κB compared to non-smokers[350]. Downstream targets of NF-κB implicated in asthma and COPD include cytokines, such as IL-1β[351], IL-4[352], TNF-α[353]; chemokines, such as CXCL10[143], CCL5[354], CXCL8[150], and CCL10[355]; adhesion molecules, including ICAM-1[356] and IgE[357]; and enzymes, such as inducible nitric oxide synthase (iNOS)[358] and matrix metalloproteinase-9 (MMP-9)[359].

Mammalian NF-κB can be formed from a group of related proteins of the Rel family, which includes p65 (RelA), p50 (NF-κB1), p52 (NF-κB2), cRel, and RelB[347]. These proteins can exist as hetero- or homodimers. NF-κB is maintained in an inactive state in the cytoplasm by the binding of inhibitory proteins, such as inhibitor of κB (IκB)[360]. After stimulation, phosphorylation of IκB by IKK-β results in ubiquitination and subsequent degradation by the 26S proteosome[361,362]. The canonical NF-κB pathway IKK complex is composed of the catalytic subunits IKK-α/IKK-β[363] and the regulatory subunit IKK-γ or NEMO[364]. The IKK-related kinases, IKKε and TBK-1, directly

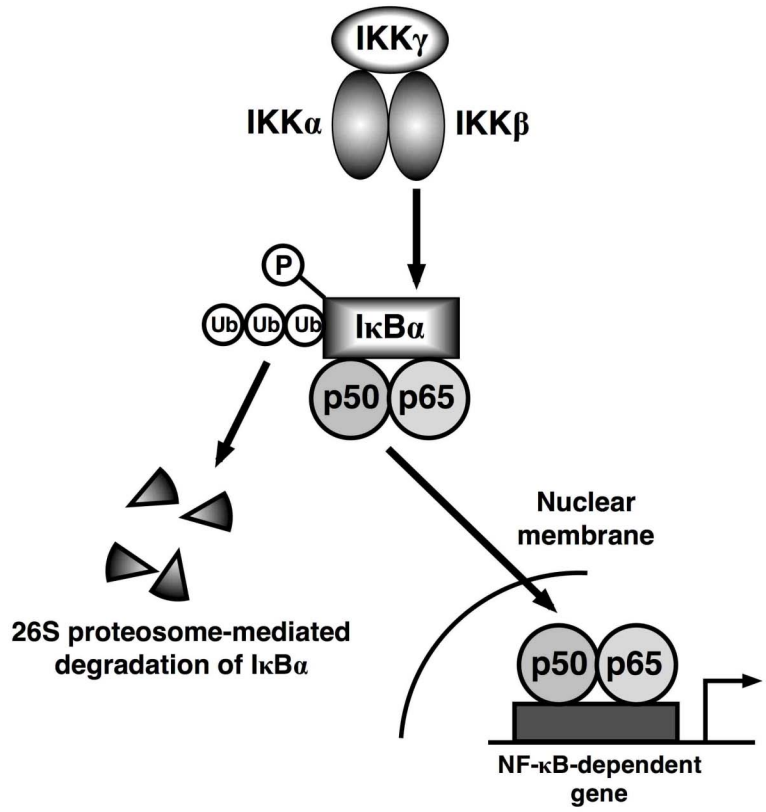

Figure 1.5 – Schematic diagram of the canonical NF-κB pathway. The transcription factor nuclear factor-kappa-light-chain-enhancer of activated B cells (NF-κB) is sequestered in the cytoplasm by inhibitor of κB-α (IκB-α) in non-infected cells. Upon viral infection, IκBα is phosphorylated by an upstream kinase, inhibitor of κB kinase-β (IKK-β), which targets IκBα for ubiquitin-mediated degradation by the 26S proteosome. The unbound Rel family proteins, p50 and p65, are now able to translocate to the nucleus and bind to specific DNA sequences found within the promoters of various genes, including CXCL10. This DNA binding is, in part, essential to initiate gene transcription.

phosphorylate RelA and c-Rel [365,366], in addition to phosphorylation of IRF-3 and IRF-7, to regulate transactivation potential[191]. Both of these pathways are activated after viral infection to induce pro-inflammatory gene expression[367]. IKK inhibitor studies have shown that HRV-induced CXCL10 and CXCL8 expression in airway epithelial cells is dependent on IKKβ-mediated activation of p50 and p65[182,368]. Also, previous studies

have shown that the p38 and ERK1/2 MAPK pathways may directly or indirectly alter NF-κB activity[369-375].

1.10.2 Interferon regulatory factors

Interferon regulatory factors (IRFs) are a family of transcription factors involved in a wide variety of biological processes including pro-inflammatory and anti-viral gene expression, development of immune cells, cell growth regulation, and apoptosis (Table 1.2)[376-380]. There are currently 9 identified human IRF proteins including IRFs 1-3, IRF-4 (Pip, PU.1-interacting factor; ICSAT, IFN consensus sequence-binding protein in adult T-cell leukemia cell line or activation T cells; LSIRF, lymphoid-specific member of IRF family), IRFs 5-7, IRF-8 (ICSBP, IFN consensus sequence binding protein), and IRF-9 (p48)[377]. IRF-10 has been identified in chickens, but is either not found or rendered non-functional in human cells[381]. The IRFs have been subdivided into four large groups: IRF1-G (IRF-1, IRF-2), IRF-3G (IRF-3, IRF-7), IRF-4G (IRF-4, IRF-8, IRF-9) and IRF-5G (IRF-5, IRF-6)[381]. In addition to those encoded by the human genome, viral forms of IRFs have been discovered including vIRF1, vIRF2, and VIRF3/LANA2, but function to either dampen or evade the immune response[378].

IRF family members all share a conserved N-terminal DNA binding domain (DBD) with a winged-typed helix-loop-helix structure and a characteristic repeat of five tryptophan residues[382]. Due to the similarity of the secondary structures of the DBD of all IRFs, it has been suggested that these proteins recognize similar core binding sequences, specifically 5'-GAAA-3' and 5'-AANNGAAA-3' as determined by the crystal structure of IRF-1 and 2[383]. The regulatory C-terminal portion of the IRFs, which

Table 1.2 – IRF family member functions

IRF	Expression	Target genes	Role in immune cell development
IRF-1	- Both constitutive and inducible in many cell types - Mainly nuclear	- iNOS, caspase-1, COX-2, CIITA, TAP1, LMP2, IFN-β, IL-12	-NK cell development -Promote T_H1 differentiation -Suppress T_H2 differentiation
IRF-2	- Both constitutive and inducible in many cell types	- Mainly antagonizes IRF-1 and IRF-9-dependent gene expression	-NK cell development -Promote T_H1 differentiation -Suppress T_H2 differentiation
IRF-3	- Both constitutive and inducible in many cell types - Mainly cytoplasmic	- type I interferons, CXCL10, CCL5	Unknown
IRF-4	- Constitutive in B cells, macrophages, DCs, and T cells - Mainly nuclear	- Negative regulation of TLR-dependent pro-inflammatory gene expression	-Differentiation of DCs -Plasma cell differentiation - Promote T_H2 differentiation
IRF-5	- Constitutive in B cells and DCs - Mainly cytoplasmic	- type I interferons, IL-12, IL-6, TNF-α	Unknown
IRF-6	- Constitutive in skin	Unknown	-Keratinocyte differentiation
IRF-7	- Constitutive in B cells, DCs, and monocytes - Induced in many cells types	- type I interferons	-Unknown
IRF-8	- Constitutive in B cells, macrophages, DCs, and T cells	- type I interferons, IL-12, iNOS	- Differentiation of DCs - Promote T_H1 differentiation
IRF-9	- Constitutive and inducible in many cells types	- OAS, PKR, IRF-7	Unknown

Adapted from *Tamura, T. et al.* (ref. 377); CIITA, class II transactivator; COX, cyclooxygenase: OAS, oligoadenlyate synthetase; TAP1, antigen peptide transporter 1; LMP2, low molecular mass poylpeptide 2

contain IRF assocation domains 1 and 2 (IAD1 and IAD2), is responsible for transactivation potential, homo- or heterodimeric interactions and post-translational modifications[377]. The IAD2 is only found in IRF-1 and IRF-2, while the remaining IRFs contain IAD1[378].

In addition to interactions with each other[384-387], IRFs and NF-κB have been shown to function in a co-operative manner to induce chemokine expression, including CXCL10[205,368,388]. In fact, it has even been suggested that both protein families co-evolved based on their roles in host defense, diversification in vertebrates, and similar core binding sequences[367,389-393]. In addition to other transcription factors, IRF proteins bind transcriptional co-factors such as CREB binding protein (CBP)/p300 proteins and basal transcription proteins (TFBII) to facilitate transcriptional activity as IRFs are thought be weak transcriptional activators alone[394-397].

There are only a few studies demonstrating the role of IRF proteins in HRV infected epithelial cells. A recent study demonstrated that HRV infection results in IRF-3 activation and is required in TLR3 and MDA-5-mediated regulation of CXCL10 mRNA expression in human airway epithelial cells[175]. In contrast, two other studies demonstrate the attenuation of IRF-3 activation in HRV-infected cells, in part, through the degradation of the adaptor molecule IPS-1[398,399]. Furthermore, binding of IRF-1 to the promoter of CXCL10 is increased in HRV-16 infected airway epithelial cells and is dependent on IKK-β activity[368]. Interestingly, knockout of IRF-1 selectively impairs the clearance of picornaviruses, such as ECMV and coxsackievirus B3, but not vesicular stomatitis virus[400]. The role of IRFs in asthma and COPD is unclear at this time.

1.11 Objective of thesis

This thesis seeks to delineate specific aspects of the cellular and molecular mechanisms by which HRV-16 infection of human airway epithelial cells regulates CXCL10 expression.

1.12 General hypothesis

HRV-16-induced CXCL10 expression in human airway epithelial cells occurs, in part, via MAPK pathway-mediated effects on transcription.

1.13 Aims of thesis

Aim #1 – Delineate the role of the MAPK pathways in HRV-16-induced CXCL10 mRNA expression and protein production

Aim #2 – Investigate the role of transcriptional regulation and identify the transcription factors involved in MEK1 pathway mediated down-regulation of CXCL10 expression

Aim #3 – Investigate the role of IRF-1 in HRV-16-induced CXCL10 expression and its modulation by the MEK1 pathway

Chapter Two: Materials and Methods

2.1 Materials

Materials and suppliers used:

AbD Serotec (Raleigh, NC, USA): glyceraldehyde-3-phosphate-dehydrogenase (GAPDH) antibody

Ambion (Austin, TX, USA): DNA-*free* DNase I kit

American Type Culture Collection (Manassas, VA, USA): WI-38 fetal lung fibroblasts and human rhinovirus type 16 (HRV-16)

Applied Biosystems (Foster City, CA, USA): 20X GAPDH master mix, MicroAmp optical 96-well reaction plate, MultiScribe reverse transcriptase, RNase inhibitor, Taqman master mix, custom CXCL10 primers and probes (see section 2.2.13.4 for sequences), Taqman CCL5 gene expression assay (ID# Hs00174575), and Taqman IRF-1 gene expression assay (ID# Hs00971960)

Biorad Laboratories (Mississauga, ON, Canada): ammonium persulfate ($(NH_4)_2S_2O_8$), nitrocellulose membrane, 30% acrylamide and bis-acrylamide solution (37.5:1), glycine, sodium dodecyl sulfate (SDS), dithiothreitol (DTT), Mini-PROTEAN gel electrophoresis equipment, Mini Trans-blot electrophorectic transfer cell, DC protein

assay kit (modified Lowry assay), modified Bradford protein assay reagent, Precision Plus pre-stained protein standard, Benchmark 96-well microplate reader, Model 583 gel dryer, and Hydrotech vacuum pump

Calbiochem EMD Biosciences (Gibbstown, NJ, USA): ERK Inhibitor, [3-(2-Aminoethyl)-5-((4-ethoxyphenyl)methylene)-2,4-thiazolidinedione, HCl]; FR180204 (ERK Inhibitor II), [5-(2-Phenyl-pyrazolo[1,5-a]pyridin-3-yl)-1H-pyrazolo[3,4-c]pyridazin-3-ylamine]; PD98059, [2′-Amino-3′-methoxyflavone]; U0126, [1,4-Diamino-2,3-dicyano-1,4-*bis*(2-aminophenylthio)butadiene]; SB203580, [4-(4-Fluorophenyl)-2-(4-methylsulfinylphenyl)-5-(4-pyridyl)1H-imidazole]; SP600125, [Anthra(1,9-cd)pyrazol-6(2H)-one 1,9-Pyrazoloanthrone], methanol, Tween-20, and isopropyl alcohol (C_3H_7OH)

Cell Signaling Technology (Beverly, MA, USA): antibodies against phospho-Elk-1 (#9181), phospho-ERK1/2 (#9101), total ERK1/2 (#9102), phospho-ERK5 (#3371), total ERK5 (#3372), phospho-IκBα (#9246), total MEK1 (#9124), total MEK2 (#9125), phospho-p38 (#9211), and total p38 (#9212)

Corning Life Sciences (Lowell, MA, USA): T-75cm^2 flasks, T-175cm^2 flasks, 6-well plates, 96-well flat-bottom plates

Dako (Mississauga, ON, Canada): horseradish peroxidase (HRP)-conjugated anti-mouse Ig antibody

Fujifilm Medical Systems (Stamford, CT, USA): SuperRX X-ray film

GE Healthcare Bio-Sciences (Piscataway, NJ, USA): HRP-conjugated anti-rabbit Ig antibody, enhanced chemiluminescent (ECL) substrate reagent, [γ-^{32}P]-adenosine triphosphate (ATP), and G25 Sephadex spin chromatography columns

Hoefer (Holliston, MA, USA): SE 600 Chroma vertical gel electrophoresis unit

Invitrogen (Burlington, ON, Canada): Dulbecco's modified Eagle medium (DMEM) Eagle's minimal essential medium (EMEM), Ham's F12 medium, OptiMEM serum-free medium, Hanks balanced salt solution (HBSS), DH5α competent *E. coli*, penicillin-streptomycin-amphotericin-B (PSF), L-glutamine, sodium pyruvate ($C_3H_3NaO_3$), non-essential amino acids, HEPES (4-(2-hydroxyethyl)-1-piperazineethanesulfonic acid), gentamicin, fetal bovine serum (FBS), TRIzol reagent, TrypLE Select recombinant enzyme, Superscript III, oligo d(T), dNTPs, dithiothreitol (DTT), 5x First Strand Buffer, RNAiMAX lipid transfection reagent, MediumGC control siRNA, MEK1 and MEK2 specific siRNA (sequences below)

Lonza (Walkersville, MD, USA): 10x Accugene TBE buffer, bronchial epithelial cell basal medium (BEBM), additives to create serum-free bronchial epithelial cell growth medium (BEGM) including: bovine pituitary extract, human epidermal growth factor, epinephrine, gentamicin/amphotericin, hydrocortisone, insulin, trans-retinoic acid, transferrin, and triiodothyronine

Mirius Bio (Madison, WI, USA): TransIT lipid transfection reagent

New England Biolabs (Ipswich, MA, USA): calf intestinal alkaline phosphatase, T4 polynucleotide kinase, T4 kinase buffer, *KpnI* and *NheI* restriction enzymes, and restriction enzyme buffer 1

Qiagen (Mississauga, ON, Canada): QIAprep spin miniprep and maxiprep plasmid isolation kits, QIAquick gel extraction kit, ERK1 and ERK2 specific siRNA (sequences below)

Pall Corporation (East Hills, NY, USA): 0.45μm and 0.2μm sterile filters

Promega (Madison, WI, USA): pGL3 basic firefly luciferase reporter plasmid, pRL-null *Renilla* luciferase plasmid, 5x passive lysis buffer, dual-luciferase reporter assay reagents, and Cyto96™ lactate dehydrogenase (LDH) assay

R&D Systems (Minneapolis, MN, USA): recombinant human IFN-β/CXCL10/CCL5 proteins, CXCL10 and CCL5 matched antibody pairs

Roche (Mississauga, ON, Canada): Fugene6 lipid transfection reagent, Pronase protease powder, protease inhibitor cocktail tablets, Rapid DNA Ligation Kit, and ABTS (2,2'-azino-bis(3-ethylbenzthiazoline-6-sulphonic acid))

Santa Cruz Biotechnology (Santa Cruz, CA, USA): Supershift Abs for p50 (sc-114), p65 (sc-109), p52 (sc-848), c-Rel (sc-70), IRF-1 (sc-497), IRF-2 (sc-498), IRF-3 (sc-9082), IRF-7 (sc-9083), and interferon-stimulated gene factor (ISGF)-3γ/p48 (sc-496). Immunoblot primary antibody for IκBα (sc-371).

Sigma-Aldrich (Oakville, ON, Canada): dimethyl sulfoxide (DMSO; C_2H_6SO), poly[deoxyinosinic-deoxycytidylic] (Poly dI:dC), Triton X-100, PMSF (phenylmethylsulphonyl fluoride; $C_7H_7FO_2S$), citric acid ($C_6H_8O_7$), MES (2-(*N*-morpholino)ethanesulfonic acid; $C_6H_{13}NO_4S$), EDTA (ethylenediaminetetraacetic acid; $C_{10}H_{16}N_2O_8$), potassium phosphate monobasic (KH_2PO_4), sodium orthovanadate (Na_3VO_4), sodium pyrophosphate ($Na_4P_2O_7$), sodium fluoride (NaF), sodium chloride (NaCl), sodium azide (NaN_3), sodium phosphate dibasic (Na_2HPO_4), magnesium chloride ($MgCl_2$), Tris-HCl (2-Amino-2-(hydroxymethyl)-1,3-propanediol, hydrochloride; $C_4H_{11}NO_3ClH$), and Tris-base (2-Amino-2-(hydroxymethyl)-1,3-propanediol; $NH_2C(CH_2OH)_3$)

2.2 Methods

2.2.1 Virus propagation and purification

HRV-16 stocks were generated through infection of confluent WI-38 lung fibroblast monolayers in T-175cm^2 flasks. Viral supernatants from previous propogations were diluted in WI-38 medium (Dulbecco's modified Eagle medium [DMEM], 10% (v/v) Fetal bovine serum [FBS], 5% (v/v) L-glutamine, and 5% (v/v) non-

essential amino acids) and incubated for 24-28 h at 34°C in 5% CO_2 until obvious signs of cytotoxicity were observed. At this point, medium was removed from infected cells and 8 mL of fresh medium was added. Cells were scraped, sonicated (15 sec, 50% amplitude), and centrifuged (425 x g, 15 min, 4°C). Supernatant was collected for purification. HRV-16 was purified by sucrose density centrifugation to remove ribosomes and soluble factors. Viral supernatants in WI-38 medium were underlayed with a 30% (w/v) sucrose solution and centrifuged (28,000 rpm, 5 h, 16°C). WI-38 medium supernatant was aspirated and virus-containing sucrose supernatants were combined in 1:1 ratio with F12/50mM HEPES (pH 7.4) solution, sterile filtered through a 0.45 μM filter, and frozen in aliquots at -80°C. This viral stock was used for infection of BEAS-2B cells. Pellets were resuspended in F12/50 mM HEPES, sterile filtered, and frozen in aliquots at -80°C. This viral stock was used for infection of primary human airway epithelial cells. As previously described, cell responses were determined to be directly a result of viral infection and not due to residual soluble components of WI-38 origin[149].

2.2.2 HRV-16 detection and titration

HRV-16 was detected by infection of confluent WI-38 monolayers with serial half-log dilutions (1/100-1/3000000) of purified HRV-16 in 96-well plates containing WI-38 medium. Cells were incubated for 5 days at 34°C in 5% CO_2 and then washed with HBSS followed by fixing cells with methanol for 1 min. Cells were stained with 0.1% (w/v) crystal violet solution for 20 min and washed 3 times in double distilled H_20 (ddH_20). After drying for 24 h, absorbances were read at 570 nm using a Biorad

Benchmark microplate reader. The tissue culture infective dose $(TCID)_{50}$/mL was calculated using the Reed-Muensch method[401].

2.2.3 BEAS-2B cell line

The BEAS-2B bronchial epithelial cell line was a gift from Dr. Curtis Harris (National Cancer Institute, Bethesda, MD, USA). This non-tumorigenic cell line was derived from infection of normal primary bronchial epithelial cells with adenovirus (Ad) type 12-simian virus (SV) 40 hybrid virus (Ad12-SV40). These cells retained a bronchial epithelial morphology with characteristic cytokeratin staining[402]. BEAS-2B cells were cultured in serum-free bronchial epithelial medium (BEGM) supplemented with growth additives (bovine pituitary extract, human epidermal growth factor, epinephrine, gentamicin/amphotericin, hydrocortisone, insulin, trans-retinoic acid, transferrin, and triiodothyronine) and antibiotics (0.5% penicillin-stretomycin-amphotericin-B [PSF]) in T-75cm^2 flasks and passaged weekly with a recombinant enzyme (TrypLE Select) in lieu of trypsin. Experiments were performed on BEAS-2B cells between passages 35-55 on 6-well plates and were incubated at 37^oC in 5% CO_2.

2.2.4 Primary human bronchial epithelial cells

Primary human bronchial epithelial cells (HBE) were obtained from normal human lungs not used for transplantation (International Institute for the Advancement of Medicine, Jessup, PA). Sections of trachea, main stem bronchi, and terminal bronchioles were dissected from lung tissue and used as the source of epithelial cells. Airway sections were placed in sterile filtered F12 medium containing 10% (w/v) pronase

protease and 0.1% (v/v) gentamicin for 30-40 h at 4^{o}C. Airway segments were dissected longitudinally and epithelial cells were removed from tissue by continuous and forceful application of F12 medium supplemented with 20% (v/v) FBS (F12/FBS) with a 5mL syringe. Cells were centrifuged at 153 x g for 8 min at room temperature (RT) and resuspended in F12/FBS. Total number of cells was determined by staining cells with erythrosin B and cell counts were carried out on a hemocytometer. Cells were centrifuged again and resuspended in a 1:1 solution of 2X PSF and 2X DMSO to create aliquots of $0.5x10^{6}$ cells/vial. Cells were frozen at -80^{o}C for 24 h and then transferred to liquid nitrogen (N_2) until use. This procedure has been shown to produce primary cell cultures of >98% epithelial cells using cytokeratin staining[403].

For experiments, HBE were thawed and immediately placed in F12/FBS followed by centrifugation at 153 x g for 8 min at RT. Cells were resuspended in BEGM supplemented with 5% sterile FBS and incubated for 72 h at 37^{o}C in 5% CO_2. After 72 h, cells were washed with HBSS and fed with BEGM for 14 days with medium changed every two days. After 14 days, the cells were used for experiments. HBE were used at a confluence of >85% for most experiments procedures, except for transfections (70-80%).

2.2.5 Primary human adenoid epithelial cells

Upper airway epithelial cells (HAE) were isolated from adenoid tissue removed during tonsillectomy in children. Similar to bronchial tissue, adenoids were cut into small pieces and placed in F12 medium supplemented with 10% (w/v) pronase and 0.1% (v/v) gentamicin for 24-36 h at 4^{o}C. Epithelial cells were removed from tissue by repeated and forceful application of F12/FBS with a 5mL syringe. Cells were centrifuged

at 153 x g for 8 min at RT and resuspended in F12/FBS. Total number of cells was determined by staining cells with erythrosin B and counting cells with a hemocytometer. In contrast to bronchial tissue, adenoid tissue did not generate large numbers of epithelial cells, thus cells were directly plated onto 6-well plates and not frozen down. The day after plating, HAE were vigourously washed with HBSS to remove any contaminating non-adherent cells. HAE were grown to 60-70% confluence in BEGM at 37^{o}C in 5% CO_2 before use in experiments.

2.2.6 HRV-16 infection of airway epithelial cells

BEAS-2B cells were infected with $10^{4.5}$ $TCID_{50}$/mL units or multiplicity of infection (MOI) of ~0.1 HRV-16. Alternatively, HBE and HAE required $10^{5.5}$ $TCID_{50}$/mL units or MOI of ~1.0 HRV-16 for infection. The higher dose was required to induce robust responses, as it has been shown that only ~10% of primary airway epithelial cells are infected, even with high doses of HRV[139]. For most experiments, cells were cultured overnight in BEGM from which hydrocortisone had been removed prior to stimulation.

2.2.7 IFN-β stimulation of airway epithelial cells

BEAS-2B or HBE cells were stimulated with IFN-β (3 ng/mL) to induce responses comparable to HRV-16 infection. As with viral infection, cells were cultured overnight in BEGM without hydrocortisone after washing with HBSS.

2.2.8 MAPK pathway inhibitors

Pharmacologic MAPK pathway inhibitors were used to determine any effect on HRV-16 or IFN-β modulation of airway epithelial cell responses. The specific MAPK targets and the respective inhibitor(s) included:

MEK1/2 – PD98059[404] (MEK1, IC_{50} = 4 μM; MEK2 IC_{50} = 50 μM) and U0126[342] (MEK1, IC_{50} = 0.07 μM; MEK2 IC_{50} = 0.06 μM)

p38 – SB203580[405] (IC_{50} = 0.6 μM)

JNK – SP600125[406] (JNK1, IC_{50} = 0.04 μM; JNK2 IC_{50} = 0.04 μM)

ERK2 – ERK Inhibitor[407] (ERK2, IC_{50} = ≤ 25 μM)

ERK1/2 - FR180204[408] (ERK1, IC_{50} = 0.51 μM; ERK2, IC_{50} = 0.33 μM)

All inhibitors were dissolved in DMSO at a working stock concentration of 10 mM. Dilutions were made in appropriate medium per experimental protocol and DMSO vehicle control did not exceed 0.1% (v/v). Cells were pre-incubated with inhibitors for 1 h prior to stimulation to ensure maximal inhibition.

2.2.9 Lactate dehydrogenase assay

To assess cell viability after MAPK inhibitor treatment, the release of lactate dehydrogenase (LDH) was measured using the Cyto96 colourmetric assay (Promega). This assay measures LDH release through the conversion of tetrazolium salt into red formazan product. HBE or HAE cells in 6-well plates were infected with HRV-16 in BEGM without hydrocortisone for 1 h (37^{o}C, 5% CO_2) and washed with HBSS twice

followed by the addition of appropriate concentrations of MAPK inhibitors or DMSO (0.1% v/v) in BEGM without hydrocortisone. After 21 h, 60 µL of supernantant was collected from control well and 90 µL of 5x Passive Lysis Buffer (Promega) was added to the same control well. Cells were further incubated at 34^{o}C for 30 min. Lysate from control well and supernatants from all other wells were collected. In a 96-well plate, control lysate and supernatants from treated cells were incubated with tetrazolium salt substrate for 30 min in the dark. The reaction was stopped and absorbance (optical density units) was measured at 490 nm. Calculation of cell viability was determined with the following equation:

$$\% \text{ cell death} = \frac{\text{Absorbance of sample}}{\text{Absorbance of control well supernatant} + (\text{control well lysate}) \times 10} \times 100$$

2.2.10 Western blotting

2.2.10.1 Whole cell lysate preparation

BEAS-2B or HBE were cultured on 6-well plates and stimulated according to specific experimental protocol. Supernatants were aspirated, cells were washed with HBSS and subsequently lysed with 500µL/well of ice-cold lysis buffer (1% (v/v) Triton X-100 in 1x MES buffered saline, 5 mM EDTA pH 7.4, anti-protease tablets, 1 mM phenylmethylsulphonyl fluoride [PMSF], 2 mM Na_3VO_4, 20 mM $Na_4P_2O_7$, and 50 mM NaF). Cells were scraped on ice, sonicated, and centrifuged at 20,000 x g for 10 min at 4^{o}C. Supernatants (triton-soluble fraction) were transferred to a fresh tube and stored at -80^{o}C. Small aliquots were taken for protein quantification.

2.2.10.2 Protein quantification

Protein was quantified in a 96-well plate using the modified Lowry DC protein assay (Biorad). Human serum albumin (HSA) standard (4 μg/mL-0.125 μg/mL) was diluted in 1x PBS and 5 μL was added to duplicate wells. Similarly, 5 μL of sample was added to duplicate wells followed by the addition of 25 μL reagent A' and 200 μL of reagent B. The samples were incubated in the dark for 15 min at room temperature to allow for colour development. Absorbances were read at 750 nm and protein quantity was determined through interpolation of the standard curve.

2.2.10.3 SDS polyacrylamide gel electrophoresis and protein transfer

Samples were run using the Biorad Mini-PROTEAN gel electrophoresis system. Samples (10-15 μg) were prepared by diluting in 1x PBS to ensure equal loading of protein. To each diluted sample, 5x Laemmli sample buffer (50% glycerol (v/v), 10% SDS (w/v), 250 mM Tris-HCl pH 6.8, 1 mg/mL bromophenol blue, and 0.5 M DTT) was added and boiled for 4 min. Samples were loaded onto a 10% SDS polyacrylamide gel and electrophoresed at 150 V in 1x Running buffer (25 mM Tris-base, 0.1% SDS (w/v), and 192 mM glycine). A protein standard ladder was also added to confirm the sizes of proteins being investigated. Following electrophoresis, proteins were transferred to a nitrocellulose membrane using a wet transfer system (Biorad) in 1x transfer buffer (20% methanol (v/v), 2.5 mM Tris-base, and 19.2 mM glycine) for 1 h at 100 V.

2.2.10.4 Immunoblotting

Following protein transfer, nitrocellulose membranes were blocked with 5% (w/v) skim milk powder in 1x TBS (0.5 M Tris-base, 1.5 M NaCl, pH 7.4) supplemented with 0.05% (v/v) Tween-20 (TTBS) for 1 h with gentle shaking. Membranes were washed 3 x 5 min in TTBS and incubated with specific primary antibody (Table 2.1) in 5% BSA/TTBS solution overnight at 4^{o}C with gentle shaking. Membranes were washed 3 x 5 min in TTBS followed by incubation with either rabbit or mouse HRP-conjugated Ig Ab for 1 h at room temperture with gentle shaking. Membranes were washed 2 x 15 min and placed in ECL substrate reagent (GE Healthcare Bio-Sciences) for 1 min. Membranes were exposed to film (Fujifilm Medical Systems) for various times and placed in an automated developer.

Table 2.1 – Primary antibodies used in SDS/PAGE immunoblotting

Target	**Species**	**Dilution**	**Company**	**Epitope**
phosho-Elk-1	Rabbit	1/750	Cell Signaling	Ser383
phospho ERK1/2	Rabbit	1/1000	Cell Signaling	Thr202/Tyr204
ERK1/2	Rabbit	1/1000	Cell Signaling	C-terminus
phospho ERK5	Rabbit	1/200	Cell Signaling	Thr218/Tyr220
ERK5	Rabbit	1/200	Cell Signaling	N/A
phospho p38	Rabbit	1/750	Cell Signaling	Thr180/Tyr182
p38	Rabbit	1/750	Cell Signaling	N/A
MEK1	Rabbit	1/1000	Cell Signaling	N/A
MEK2	Rabbit	1/1000	Cell Signaling	N/A

phospho-IκBα	Mouse	1/1000	Cell Signaling	Ser32/36
IκBα	Rabbit	1/1000	Santa Cruz	C-terminus
IRF-1	Rabbit	1/4000	Santa Cruz	C-terminus
GAPDH	Mouse	1/40000	AbD Serotec	N/A

2.2.10.5 Immunoblot stripping protocol

To ensure equal loading, immunoblots were stripped and re-probed with appropriate antibody (Table 2.1). Immunoblot stripping solution (70 mM Tris-HCl pH 6.8, 2% (v/v) SDS) was heated to 80^{o}C and 0.01% β-mercaptoethanol (β-ME) was added. Blots were incubated in the stripping solution for 5 min with gentle shaking. Blots were washed 4 x 15 min in TTBS (0.05% Tween-20) and probed with appropriate primary and secondary (anti-mouse or anti-rabbit) antibodies.

2.2.10.6 Assessment of GAPDH levels

Equal loading was determined by stripping each membrane and reprobing with antibody to glyceraldehyde 3-phosphate dehydrogenase (GAPDH). After stripping, blots were blocked in 5% skim milk in TTBS for 30 min at room temperature with gentle shaking. Blots were washed 3 x 5 min and incubated with anti-GAPDH (1/40000) in TTBS for 20 min at room temperature. After primary antibody incubation blots were washed 3 x 5 min and incubated with anti-mouse Ig-HRP antibody (1/10000) in TTBS for 20 min at room temperature and visualized with ECL substrate reagent.

2.2.11 Electrophorectic mobility shift assay (EMSA)

2.2.11.1 Nuclear protein extraction

BEAS-2B cells or HBE were cultured on 6-well plates and stimulated according to the specific experimental protocol. All centrifugations were carried out a 4^{o}C. After stimulation, cells were scraped on ice and centrifuged at 5,000 x g for 5 min. Supernatant was removed and the pellet was re-suspended in 50 µL Gough buffer (0.01 M Tris-HCl, 0.15 M NaCl, 1.5 mM $MgCl_2$, 0.65% Nonidet P-40, 0.5 mM PMSF, and 0.01 M DTT), vortexed for 15 s, left on ice for 10 min, and centrifuged at 12,000 x g for 2 min. The pellet was re-suspended in 15µL of buffer C (0.02 M HEPES pH 7.9, 25% glycerol, 0.4 M NaCl, 1.5 mM $MgCl_2$, 0.5 mM PMSF, and 0.01 M DTT), subjected to agitation every 15 min for 2 h, and centrifuged at 12,000 x g for 10 min. The supernatant (nuclear extract) was transferred to a fresh tube containing 35µL of buffer D (0.02 M HEPES pH 7.9, 20% glycerol, 0.05 M KCl, 0.2 mM EDTA pH 8.0, 0.5 mM PMSF, and 0.01 M DTT). A 5 µL aliquot was taken for protein quantification and the remaining nuclear extract was stored at -80^{o}C.

2.2.11.2 Nuclear extract protein quantification

Protein concentration of nuclear extract was determined using a modified Bradford assay (BioRad). In a 96-well plate, 2 µL of sample in duplicate wells was added to 200 µL 1x protein assay dye reagent. HSA standards diluted in buffer D (4 µg/mL to 0.125 µg/mL) were also added to enable quantification through interpolation of the standard curve. Samples were incubated for 10 min at room temperature and absorbances were read at 570 nm.

2.2.11.3 Oligonucleotides

All CXCL10-specific oligonucleotides were generated by The University of Calgary DNA Services. The forward nucleotide sequences for CXCL10-specific NF-κB and interferon-stimulated response element (ISRE) recognition sequences were as follows (mutations in lowercase bold letters):

NF-κB1, 5'-TGCAACATGGGACTTCCCCAGGAAC-3'

ΔNF-κB1, 5'-TGCAACATG**t**GACTTC**a**CCAGGAAC-3'

NF-κB2, 5'-GGAGCAGAGGGAAATTCCGTAACTT-3'

ΔNF-κB2, 5'-GGAGCAGAG**t**GAAATT**a**CGTAACTT-3'

ISRE, 5'- TGTTTTGGAAAGTGAAACCTAATTC-3'

ΔISRE, 5'- TGTTTTGGA**c**AGTGA**c**ACCTAATTC-3'

Oligonucleotides were annealed in a 100 μL reaction containing 25 μL sense and anti-sense oligonucleotide (100 μM each), 10 μL 10x Oligo Annealing buffer (100 mM Tris-HCl pH 7.5, 1 M NaCl, 10 mM EDTA pH 7.4) and 40 μL RNase/DNase-free H_20. Annealing was carried out in a Techne Flexigene thermocycler with the following parameters: 95^oC for 2 min, A* for 5 min (A*= 5^oC over oligo T_m), A*-37^oC (-1^oC/cycle) over 90 min, and 37^oC for 2 min. Annealed oligonucleotides were stored at -20^oC until use.

2.2.11.4 EMSA probe labelling

Annealed CXCL10-specific oligonucleotides were 5' end-labeled with T4

polynucleotide kinase (New England Biolabs). In a 20 μL reaction mixture, 1.75 μM CXCL10-specific annealed oligonucleotide was incubated with 10 units T4 polynucleotide kinase in 1x T4 kinase buffer (70 mM Tris-HCl, 10 mM $MgCl_2$, 5 mM DTT) and 40 μCi [γ-^{32}P]ATP at 37^{o}C for 30 min. Radiolabeled oligonucleotides were mixed with 180 μL TE buffer (10 mM Tris-HCl pH 7.4, 1 mM EDTA) and excess [γ-^{32}P]ATP was removed using G25 Sephadex spin columns (GE Healthcare Bio-Sciences).

2.2.11.5 EMSA binding reaction

The binding reactions included the incubation of 2.5-5 μg of nuclear extract with 4 μL of binding buffer (20% glycerol, 5 mM $MgCl_2$, 2.5 mM EDTA, 1 μg poly(dI:dC), 250 mM NaCl, 50 mM Tris-HCl pH 7.4, and 0.01 M DTT). Buffer D was used to bring the volume up to 14 μL and incubated at 4^{o}C for 20 min. As a non-specific binding control, one binding reaction sample contained 2 μL 100x non-radiolabeled annealed CXCL10-specific oligonucleotide. Labeled probe (2 μL) was added to the binding reaction and incubated at 4^{o}C for 1 h.

2.2.11.6 Non-SDS PAGE and autoradiography

The binding reaction was stopped by the addition of 3 μL of EMSA loading buffer (50% (v/v) glycerol and 0.05% (w/v) bromophenol blue). Samples were loaded onto a 6% non-SDS polyacrylamide gel and electrophoresed for 1.5-2 h in 0.25 X TBE buffer (890 mM Tris-borate, 20 nM EDTA, pH 8.3). Gels were dried, exposed to film at -80^{o}C, and analyzed with autoradiography.

2.2.11.7 Antibody supershift assay

For supershift assays, 2 μL of appropriate purified IgG antibody (2 μg/μL) was added to binding reaction 2 h prior to addition of radiolabeled oligonucleotide.

2.2.11.8 Calf intestinal alkaline phosphatase treatment of nuclear extracts

Nuclear extracts were prepared as described above, but using buffers C and D without EDTA. Nuclear protein (2.5 μg) was incubated with 6.5 U of calf intestinal alkaline phosphatase (New England Biolabs) in buffer D without EDTA for 15 min at 37^{o}C. Phosphatase activity was inhibited with 50 mM EDTA and further incubated for 15 min at 37^{o}C. Radiolabeled CXCL10-specific ISRE probe was added and EMSA was performed.

2.2.12 Enzyme-linked immunosorbent assay (ELISA)

2.2.12.1 Measurement of CXCL10 and CCL5 protein release

Supernatants from treated cells were assayed on 96-well Immulon 4 plates using matched antibody pairs and recombinant protein for human CXCL10 and CCL5 (R&D Systems). Plates were coated overnight at RT with monoclonal anti-human CXCL10 (3 μg/mL) or CCL5 (2 μg/mL) antibody diluted in 1x PBS. Following primary Ab incubation, plates were washed 4x with ELISA wash buffer (0.05% Tween-20 (v/v), 137 mM NaCl, 1.5 mM potassium phosphate monobasic, 8.1 mM sodium phosphate dibasic, 2.7 mM potassium chloride, pH 7.4) followed by incubation in ELISA blocking buffer (1x PBS, 1% BSA (w/v), 5% sucrose (w/v)) for 1 h at RT. Recombinant protein standard was serially diluted in ELISA diluent (1x TBS, BSA 0.1% (w/v), 0.05% Tween-20 (v/v))

using 1:1 dilutions for CXCL10 (3000 pg/mL-23.44 pg/mL) or CCL5 (2000 pg/mL-31.25 pg/mL) and added to duplicate wells (100 µL/well). Samples were prepared with three serial dilutions (e.g. 1/2, 1/4, 1/8) in ELISA diluent to ensure that sample readings were within the linear range of the standard curve. Samples were added to duplicate wells (100 µL/well) and incubated for 2 h at room temperature. Plates were washed 4x with ELISA wash buffer and incubated with 100 µL/well biotinylated anti-human CXCL10 (300 ng/mL) or CCL5 (10 ng/mL) antibody for 2 h at room temperature. Following biotinylated anti-human antibody incubation, plates were washed 4x with ELISA wash buffer and incubated with 100 µL/well streptavidin peroxidase (1 µg/mL) diluted in ELISA diluent for 30 min at room temperature. Plates were developed by the addition of 100 µL/well H_2O_2/ABTS in citrate phosphate buffer (29.4 mM citric acid, 41.7 mM sodium phosphate pH 4.3) and incubation at 37^{o}C in the dark. The development reaction was stopped with 2 mM sodium azide (100 µL/well) and absorbances were read at 405 nm. Protein concentrations were determined through interpolation of a linear standard curve (Bio-Rad Microplate Manager II ver. 2.248). The sensitivity of the assay was 30 pg/mL.

2.2.12.2 Measurement of CXCL8 protein release

Supernatants from treated cells were assayed on 96-well Immulon 4 plates coated with 100 µL/well of 1:1200 dilution of polyclonal rabbit anti-human CXCL8 antibody in 0.1 M carbonate buffer (pH 9.6). The plate was covered and incubated at 4^{o}C overnight. Following primary antibody incubation, wells were washed 4X with ELISA wash buffer and non-specific binding sites were blocked with 100 µL/well of a 1:100 sheep serum

diluted in sample buffer (1x PBS pH 7.4, 0.05% Tween-80, 1% BSA) and incubated for 30 min at RT. The plate was washed 4X with ELISA wash buffer and recombinant CXCL8 protein standard was serially diluted in sample buffer using 1:1 dilutions (15 ng/mL-0.059 ng/mL) and added to duplicate wells (100 µL/well). Samples were prepared with three serial dilutions (e.g. 1/2, 1/4, 1/8) in sample buffer to ensure that sample readings were within the linear range of the standard curve. Samples were added to duplicate wells (100 µL/well) and incubated for 90 min at 37^{o}C. After incubation, the plate was washed 4X in ELISA wash buffer and 100 µL/well biotinylated polyclonal rabbit anti-human CXCL8 antibody diluted 1:1300 in sample buffer was added and incubated for 90 min at 37^{o}C. Following secondary antibody incubation, plates were washed 4x with ELISA wash buffer and incubated with 100 µL/well streptavidin peroxidase (1 µg/mL) diluted in ELISA diluent for 30 min at room temperature. Plates were developed by the addition of 100 µL/well H_2O_2/ABTS in citrate phosphate buffer (29.4 mM citric acid, 41.7 mM sodium phosphate pH 4.3) and incubation at 37^{o}C in the dark. The development reaction was stopped with 2 mM sodium azide (100 µL/well) and absorbances were read at 405 nm. Protein concentrations were determined through interpolation of a 4-parameter standard curve (Bio-Rad Microplate Manager II ver. 2.248) The sensitivity of the assay was 30 pg/mL. The assay has no cross-reactivity with various chemokines or structurally unrelated cytokines[141].

2.2.13 Real-time polymerase chain reaction (Real time PCR)

2.2.13.1 RNA isolation

RNA was isolated using TRIzol reagent following manufacturer's instructions (Invitrogen). After cell stimulation, cells were washed with HBSS and 500 μL/well of TRIzol reagent was added. Cells were lysed with TRIzol by pipetting several times and placed in RNase/DNase-free tubes. All centrifugation steps were carried out at 4^{o}C. TRIzol lysates were applied to Phase Lock Gel tubes (Eppendorf) after which chloroform (0.2 mL/1 mL TRIzol reagent) was added, mixed vigourously for 15 sec, and centrifuged at 12,000 x g for 10 min. The resulting aqueous phase was carefully transferred to a fresh tube to prevent transfer of DNA or protein. RNA was precipitated with the addition of isopropyl alcohol (0.5 mL/1 mL TRIzol reagent), incubated for 10 min at RT and centrifugation at 12,000 x g for 10 min. The RNA pellet was washed with 1 mL of 75% ethanol and centrifuged at 7,500 x g for 5 min. Ethanol was carefully removed and RNA pellet was air dried for 8-10 min and re-suspended in 20 μL of RNase/DNase-free H_20. RNA concentrations were measured at 260 nm and sample purity was determined with 260 nm/280 nm ratio readings. RNA was stored at -80^{o}C until use.

2.2.13.2 DNase treatment

To ensure no genomic DNA contamination was present, RNA samples were treated with DNA-*free* DNase I (Ambion). Briefly, 10 μg of RNA was incubated with DNase I (2 units) and 10X DNase buffer for 25 min at 37^{o}C. DNase activity was inhibited with the addition of 5 μL DNase Inactivation reagent, incubated for 2 min at room temperature, and centrifuged at 10,000 x g for 1 min. Treated RNA was transferred

to a fresh tube, RNA concentration was measured at 260 nm, and stored at -80^{o}C until use.

2.2.13.3 Assessment of CCL5 and IRF-1 mRNA expression

Analysis of CCL5 and IRF-1 mRNA expression required the generation of cDNA. Input RNA (1 μg) was reverse transcribed into cDNA in a 20 μL reaction mixture containing 0.5 μg Oligo(dT)12-18 primer, and 0.5 mM dNTP each [dATP, dCTP, dTTP, dGTP]. Samples were heated to 65^{o}C for 5 min and incubated on ice for 1 min before addition of 1x First Strand Buffer, 5 mM DTT, and 200 units Superscript 3 reverse transcriptase (Invitrogen). The subsequent PCR parameters were 4^{o}C for 3 min, 50^{o}C for 1 h, and 70^{o}C for 15 min. Samples were stored at -80^{o}C until further use. CCL5 and IRF-1 cDNA were amplified in a real-time PCR reaction using the Applied Biosystems Model 7900 sequence detector and a Taqman CCL5 and IRF-1 gene expression kit including primers and probes (sequences not available from Applied Biosystems). In an optical 96-well plate 1 μL of cDNA was added to 24 μL of CCL5 or IRF-1 reaction mix containing 12.5 μL 2x Taqman Master mix, 1.25 μL 20x gene expression kit, and 10.25 μL H_20. GAPDH was also amplified from the same samples using a 20X GAPDH Master mix (Applied Biosystems). Real-time PCR parameters were 50^{o}C for 2 min, 95^{o}C for 10 min, and 40 cycles of 95^{o}C for 15 sec and 60^{o}C for 1 min. All samples were run in triplicate wells. To ensure specificity of amplification, a negative control was used where input RNA was withheld from the PCR reaction. Data was expressed as fold increase using the comparative $\Delta\Delta C_T$ as described previously[409].

2.2.13.4 Assessment of CXCL10 mRNA expression

Expression of CXCL10 mRNA was assessed using the above mentioned sequence detector in an optical 96-well plate using triplicate wells for each sample. Input RNA (400 ng) was reverse transcribed into cDNA at 48^{o}C for 30 min followed by PCR amplification at 95^{o}C for 10 min, 40 cycles of 95^{o}C for 15 sec and 60^{o}C for 1 min. The 25 μL reaction mixture contained the following: 400 nM specific forward (5'-GAAATTATTCCTGCAAGCCAATTT-3') primer, 400 nM specific reverse (5'-TCACCCTTCTTTTTCATTGTAGCA-3') primer, 400 nM specific (5'-FAM-TCCACGTGTTGAGATCA-MGB-3') probe, 10 units RNase Inhibitor, 18.8 units MultiScribe reverse transcriptase, Taqman Master mix, and RNase/DNase-free H_20. GAPDH was also assessed from the same samples using a 20X GAPDH Master mix containing specific primers and probes.

2.2.13.5 Absolute quantification

To permit absolute quantification, a first strand cDNA oligonucleotide (5'-AACTTGAAATTATTCCTGCAAGCCAATTTTGTCCACGTGTTGAGATCATTGCT ACAATGAAAAAGAAGGGTGAGAAGA-3') was synthesized (University of Calgary DNA Services). The CXCL10 standard was run with each real-time PCR reaction using the same reaction mixture and cycling parameters mentioned above. CXCL10 standard was log-diluted (100 fg-0.0001 fg) in RNase/DNase-free H_20 supplemented with transfer RNA (100 ng/mL). Data were expressed as attograms calculated from the standard curve after corrections for variation in GAPDH levels.

2.2.14 Promoter-luciferase constructs

2.2.14.1 CXCL10 promoter

A 972-bp human CXCL10 full length promoter corresponding to the sequence from -875 to +97 (relative to the transcriptional start site) of the 5' flanking region was generated. The promoter was amplified from genomic human DNA using forward 5'GCGTAGGTACCTAGAACCCCATCGTAAATC-3' and reverse 5'-GCGTAGCTAGCTAGCAGCAAATCAGAATGG-3' primers incorporating restriction sites for *KpnI* and *NheI*, respectively[143]. The amplicon was resolved using agarose gel electrophoresis and the resulting band was excised and gel purified with the QIAquick gel extraction kit (Qiagen). The CXCL10 promoter amplicon was cloned into a pGL3 basic vector containing an inducible firefly luciferase gene. The CXCL10 promoter amplicon and 0.25-0.5 μg pGL3 basic vector were incubated with *KpnI* (10 units) and *NheI* (10 units) restriction enzymes (New England Biolabs) for 2 h at 37^{o}C. The double cut pGL3 vector was treated with calf intestinal alkaline phosphatase (10 units) to prevent re-ligation, resolved on a 1% agarose gel and appropriate bands were gel purified. The CXCL10 promoter amplicon was ligated into the pGL3 basic vector using the Rapid DNA Ligation Kit (Roche). The resulting CXCL10 promoter-luciferase construct was transformed into DH5α competent *Escherichia coli* (Invitrogen) using heat shock techniques (1 h on ice, 45 sec at 42^{o}C, 2 min on ice). The transformed bacteria were grown on Luria-Bertani (LB) agar plates supplemented with ampicillin (50 μg/mL) overnight at 37^{o}C. Individual colonies were picked and grown in LB broth supplemented with ampicillin (100 μg/mL) overnight at 37^{o}C with vigorous shaking. Plasmids were purified with the QIAquick spin miniprep kit according to manufacturer's instructions

(Qiagen) and 0.25-0.5 μg plasmid was incubated with the restriction enzymes *KpnI* (10 units) and *NheI* (10 units) for 2 h at 37^{o}C to confirm the presence of the CXCL10 promoter insert in the pGL3 basic vector. Correct sequencing of the CXCL10 promoter insert was also confirmed (University of Calgary DNA Services). Large quantities of plasmid were prepared using the QIAGEN plasmid maxi prep kit according to manufacturer's instructions (Qiagen).

2.2.14.2 CXCL10 truncated promoter

A 376-bp truncated promoter construct (sequence from -279 to +97 relative to the transcriptional start site of the 5' flanking region of the CXCL10 gene) was generated with the 972-bp CXCL10 construct as a template through amplification using a forward 5'-GCGTAGGTACCTAGAGAATGGATTGCAACC-3' primer with an incorporated *KpnI* restriction site and the same full length reverse primer mentioned above. The resulting amplicon was cloned into a pGL3 basic vector similarly to the 972-bp construct.

2.2.14.3 CXCL10 mutant constructs

Potential transcription factor binding sites were determined using Genomatix MatInspector program as previously described[143]. Point mutations were introduced in either the 972-bp or 376-bp CXCL10 promoter-luciferase construct using site-directed mutagenesis techniques. Mutations were created in the putative activator protein-1 (AP-1), NF-κB1 (κB1), NF-κB2 (κB2), and ISRE sites.

Table 2.2 – CXCL10 promoter point mutation primer sequences

Promoter site	**5'-3' Forward sequence (mutations in lowercase bold letters)**
AP-1	CCAGCAGGTTTTGCTAAG**at**AACTGTAATGC
κB1	GCAACATG**t**GACTTC**a**CCAGG
κB2	GCAGAG**t**GAAATT**a**CGTAACTTGG
ISRE	GTTTTGGA**c**AGTGA**c**ACCTAATTC

2.2.14.4 CXCL10-specific tandem repeat constructs

Promoter-luciferase constructs containing 5 tandem copies of CXCL10-specific κB1 recognition sequence (forward; 5'-TGGGACTTCCCCA-3'), κB2 (forward; 5'-GGGAAATTCCGT-3'), or ISRE (forward; 5'-GGAAAGTGAAACCTA-3') were synthesized incorporating restriction sites for *KpnI* and *NheI* and cloned into a pGL3 basic construct containing a TATA box (gift from Dr. Rob Newton). As described earlier, plasmids were purified and incubated with the restriction enzymes *KpnI* and *NheI* for 2 h at 37^{o}C to confirm the presence of the CXCL10 tandem repeat insert in the pGL3.TATA basic vector. Correct CXCL10 tandem repeat sequences were confirmed by DNA sequencing (University of Calgary DNA Services).

2.2.15 Luciferase assay

2.2.15.1 Transfection

Sub-confluent (40-50%) monolayers of BEAS-2B cells in 6-well plates were transfected with the lipid reagents Fugene6 (Roche) or TransIT (Mirius) in an optimal 3:1 ratio of lipid:DNA. In separate tubes, 3 μL/well of lipid reagent was added to 100 μL

BEBM/well and incubated for 20 min at room temperature. After incubation, 1 μg/well of CXCL10 promoter-luciferase construct and 0.1 μg/well of Renilla luciferase plasmid without promoter or enhancer elements (pRL-null) was added and incubated for a further 20 min at room temperature. The constitutively driven pRL-null plasmid was used as a transfection efficiency control. During incubation, cells were washed with HBSS followed by the addition of 600 μL/well of BEBM. Lipid/DNA mixture was added to cells and incubated for 5 h at 37^{o}C followed by aspiration, washing with HBSS, and addition of 5% sterile FBS/BEGM without hydrocortisone overnight at 37^{o}C. Cells were then treated according to specific experimental protocol. Of note, cells transfected with CXCL10 promoter-luciferase constructs were infected with $10^{5.0}$ $TCID_{50}$/mL units of purified HRV-16 to ensure maximal promoter activity.

2.2.15.2 Lysate isolation

After stimulation, cells were washed with HBSS followed by the addition of 700 μL/well of 1x Passive Lysis Buffer (Promega). Plates were gently agitated for 15 min at room temperature followed by scraping on ice, sonication on ice, and centrifugation (10,621 x g, 5 min, 4^{o}C). Supernatants from lysates were assayed for luciferase activity using the Dual-Luciferase Reporter Assay System (Promega). Firefly activity was normalized to Renilla activity and data was expressed as fold increase of stimulated cells over control. Results were averaged from triplicate wells.

2.2.16 Short interfering RNA (siRNA)

2.2.16.1 siRNA sequences

The specific siRNA sequences used were:

Table 2.3 - Specific siRNA sequences

Target Name	**Sequence (5'-3' forward)**	**Supplier**
ERK1 duplex A	CCCGTCTAATATATAAATATA	Qiagen
ERK1 duplex B	CTCCCTGACCCGTCTAATATA	Qiagen
ERK2 duplex A	AAGTTCGAGTAGCTATCAAGA	Qiagen
ERK2 duplex B	AATGACATTATTCGAGCACCA	Qiagen
MEK1 duplex A	GCCUUGAGGCCUUUCUUACCCAGAA	Invitrogen
MEK1 duplex B	CCCGCAAUCCGGAACCAGAUCAUAA	Invitrogen
MEK2 duplex A	CCAUCUUUGAACUCCUGGACUAUAU	Invitrogen
MEK2 duplex B	GAACUCAAAGACGAUGACUUCGAAA	Invitrogen
IRF-1 duplex A	GGGACAUCAACAAGGAUGCCUGUUU	Invitrogen
IRF-1 duplex B	UCCCAAGACGUGGAAGGCCAACUUU	Invitrogen
IRF-1 duplex C	CGGACAGCACCAGUGAUCUGUACAA	Invitrogen

Negative control siRNA (MedGC duplex 1) sequence was not available from the supplier (Invitrogen).

2.2.16.2 Transfection

Sub-confluent monolayers of BEAS-2B (40-50%) or HBE (70-80%) in 6-well plates were used for transient siRNA transfection. Individual siRNA were diluted to appropriate concentrations in 125 μL/well of serum-free OptiMEM (Invitrogen). RNAiMAX Lipofectamine (Invitrogen) was diluted 1/50 in a volume of 125 μL/well with OptiMEM. The lipid and siRNA mixtures were combined (250 μL/well) and incubated for 20 min at room temperature. For wells containing only lipid reagent, 125 μL/well of OptiMEM was added in place of siRNA. During incubation, cells were washed with HBSS and 750 μL/well of BEGM without antibiotics (no PSF or gentamicin/amphotericin) was added. The lipid/siRNA mixture (250 μL/well) was added gently to appropriate wells and incubated for 6 h at 37^{o}C in 5% CO_2. For mock transfected cells, 250 μL/well of OptiMEM without lipid reagent or siRNA was added. After 6 h, media was aspirated and replaced with fresh BEGM without antibiotics. Transfected cells were incubated for 72 h for desired siRNA effect, with media changed to BEGM without hydrocortisone after 48 h. Cells were stimulated according to specific experimental protocol.

2.2.17 Densitometry

Densitometric analysis of gels was carried out using ImageJ software version 1.41 (NIH). To assess the percentage “knockdown” of proteins in the presence of specific siRNA compared to control siRNA, levels of GAPDH was used to correct any minor variation in loading.

2.2.18 Statistical analysis

All data presented are mean ± SEM. For normally distributed data, between group comparisons were made by one-way ANOVA, with appropriate post hoc analysis using Fisher's least significant difference test. To assess difference between two groups, a paired *t*-test was used. For non-parametric data, Kruskal-Wallis ANOVA was used, followed by Wilcoxon matched-pairs signed-rank test. Alternatively, Mann-Whitney U test was performed. For all statistical tests, a p value of ≤ 0.05 was assumed to be significant.

Chapter Three: The effect of MAPK pathway inhibition on HRV-16-induced CXCL10 expression in human airway epithelial cells

3.1 Introduction

This thesis specifically focuses on selected signalling events involved in the expression of HRV-16-induced CXCL10. HRV infection of airway epithelial cells has been shown to induce the activation of the MAPK signalling pathways, including p38, JNK1/2, and ERK1/2[262,266-268]. Though related to ERK1/2, no studies have examined the activation of the ERK5 pathway by HRV-16[291]. Both the p38 and ERK1/2 pathways have been implicated in the adenoviral induction of CXCL10 expression in kidney epithelial cells, and the ERK1/2 pathway has also been shown to mediate the expression of CXCL10 in murine macrophages in response to rabies virus infection[410,411].

In this chapter, the roles of the p38, JNK, ERK5 and ERK1/2 MAPK pathways in HRV-16-induced expression of CXCL10 were evaluated in human airway epithelial cells. It was hypothesized that HRV-16 infection of human airway epithelial cells would activate the major MAPK pathways and that pharmacological inhibition of these pathways would alter the expression of CXCL10 after viral infection.

3.2 Materials and Methods

3.2.1 HRV-16-induced MAPK pathway activation

Sub-confluent monolayers (70-80%) of BEAS-2B cells were pre-incubated in 500 μL BEBM for 1 h to decrease basal MAPK activity prior to HRV-16 infection. Purified HRV-16 for infection was diluted in BEGM without bovine pituitary extract,

hydrocortisone, epidermal growth factor, and epinephrine (BEGM -4). These additives were removed as they were most likely to activate basal MAPK activity in the absence of HRV. The additives that remained in BEGM -4 included gentamicin/amphotericin, PSF, insulin, trans-retinoic acid, transferrin, and triiodothyronine. After BEBM pre-incubation, 500 μL of HRV-16 diluted in BEGM -4, or BEGM -4 alone, was carefully added to appropriate wells and whole cell lysates were collected at various time points (see section 2.2.10 for further details).

Effects of MEK1/2 pathway inhibition on HRV-16-induced phosphorylation of ERK1/2, ERK5, JNK1/2 and p38 were performed using a similar protocol, but the MEK1/2 pathway inhibitors, PD98059 (10 μM) and U0126 (3 μM), were pre-incubated for 1 h in BEGM -4 before the direct addition of HRV-16 for 1 h and whole cell lysate extraction.

3.2.2 Effect of MAPK pathway inhibitors on chemokine expression

To assess the effect of MAPK pathway inhibition on HRV-16 or IFN-β induced chemokine expression, airway epithelial cells were pre-incubated with MAPK inhibitors dissolved in DMSO (0.1% v/v) for 1 h at 37^{o}C, 5% CO_2. Inhibitor dilutions were made in BEGM no HC and 1 mL of each dilution was added to duplicate wells. The MAPK inhibitor vehicle control, DMSO, was also used and did not exceed 0.1% v/v. After pre-incubation, HRV-16 was added directly to wells and samples were incubated for 24 h at 34^{o}C, 5% CO_2. Supernatants were assessed for chemokine production using ELISA techniques (see section 1.2.12 for further details). RNA was isolated using the TRIzol

method and RNA levels were assessed using real-time PCR techniques (see section 1.2.13 for further details).

3.2.3 Effect of MAPK pathway inhibitors on HRV-16 replication

To assess any effects of the MAPK pathway inhibitors on HRV-16 replication, cells were infected with HRV-16 for 3 h followed by washing of unadsorbed virus with HBSS three times and addition of MAPK inhibitor or DMSO vehicle control in fresh BEGM no HC. Supernatants were collected after 24 h and levels of infectious HRV-16 were determined using a WI-38 viral titre assay (see section 2.2.2 for further details).

3.3 Results

3.3.1 HRV-16 activates the major MAPK signalling pathways

In order to study the role of the MAPK pathways during HRV-16-induced CXCL10 expression in human airway epithelial cells, it was necessary to demonstrate that HRV-16 was capable of inducing activation through site-specific phosphorylation. In the current study, HRV-16 infection of BEAS-2B cells induced variable, time-dependent phosphorylation of ERK1/2, ERK5, p38, and JNK1/2 (Figure 3.1A-D). Phosphorylation of the JNK2 isoform (lower band) was evident at 15 min post-infection with increased phosphorylation through 1 h, but diminished by 3 h post-infection (Figure 3.1D). In contrast, phosphorylation of JNK1 (upper band) was weakly evident at 30 min post-infection, peaked at 1 h, and was diminished by 3 h post-infection. Similar to the transient nature of JNK1/2 phosphorylation, p38 phosphorylation was evident at 15 min post-infection with peak phosphorylation between 30 min and 1 h (Figure 3.1C). The

activation of p38 was clearly diminshed by 9 h post-infection, though a secondary increase in the level of phosphorylation was apparent at 24 h post-infection. Phosphorylation of ERK5 was apparent at 15 min post-infection with peak activation at 1 h and subsequently diminished by 9 h (Figure 3.1B). Similar to JNK1/2, phosphorylation was not evident at 9 and 24 h post-infection. ERK1/2 phosphorylation was evident 15 min post-infection with a decrease, but not complete loss of phosphorylation by 6 h (Figure 3.1A). The chronic phosophorylation of ERK1/2 increased at 9 h with continued activation evident at 24 h. These results demonstrate that HRV-16 infection initiates early activation of 4 major MAPK pathways (ERK1/2, ERK5, p38, and JNK1/2). Activation of the p38 pathway occurs in two distinct early and late waves, but ERK1/2 is chronically active with varying levels of phosphorylation.

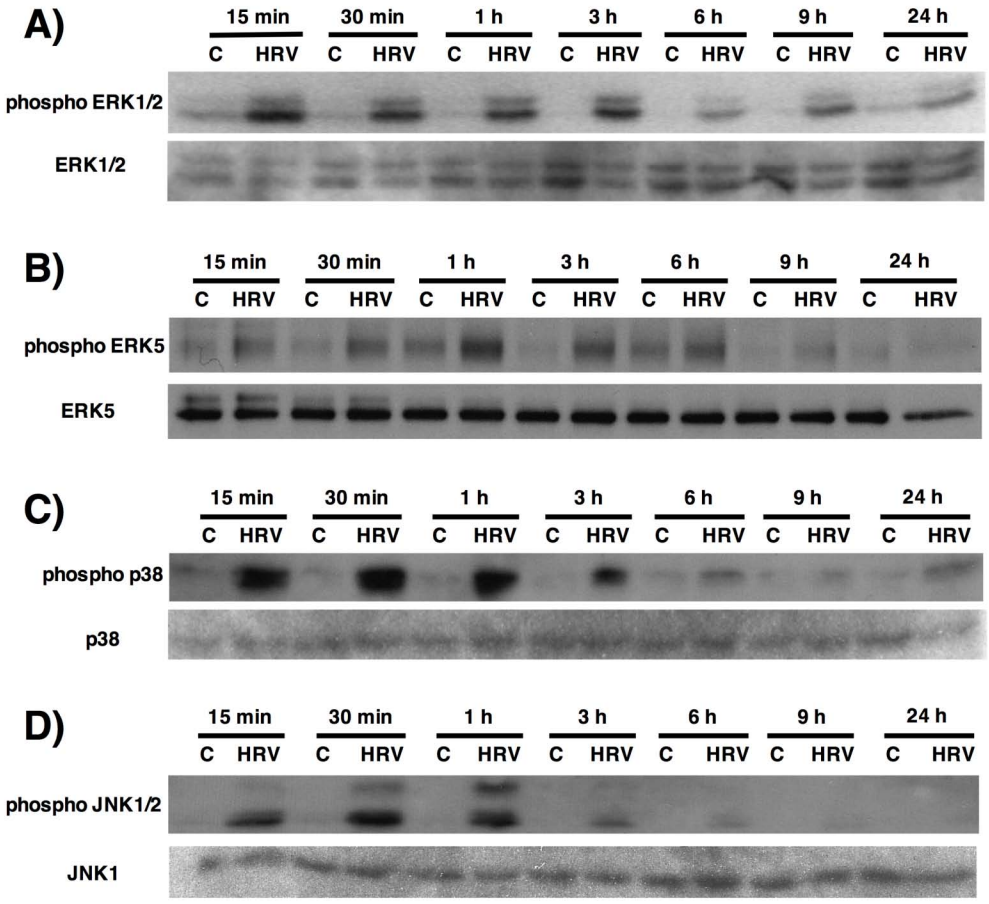

Figure 3.1 - HRV-16 infection induces the activation of the major MAPK pathways. BEAS-2B cells were infected with HRV-16 for the indicated time points. At each time point, whole cell lysates were collected, resolved using SDS/PAGE, and immunoblotted with phospho-specific antibodies for each major MAPK including: **A)** ERK1 (upper band) & ERK2 (lower band), **B)** ERK5, **C)** p38, and **D)** JNK1 (upper band) & JNK 2 (lower band). Each immunoblot is representative of three separate experiments.

3.3.2 Effect of MAPK pathway pharmacological inhibitors on HRV-16-induced CXCL10 expression

Having demonstrated the activation of the major MAPK pathways after HRV-16 infection, widely used pharmacological inhibitors that selectively target each respective MAPK pathway were employed to investigate the role of these pathways in HRV-16-induced CXCL10 mRNA and protein expression. Concentration curves were carried out initially in the BEAS-2B cell line. A single optimal concentration determined in BEAS-

2B cells was used in primary human epithelial cells from the both upper (HAE) and lower (HBE) airways to confirm major findings in a physiological relevant and non-transformed model. In BEAS-2B cells, an ATP-competitive inhibitor of the p38 MAPK pathway, SB203580 (10-1 μM), inhibited CXCL10 mRNA in a seemingly concentration-dependent manner compared to HRV-16 plus DMSO (0.1% v/v) (Figure 3.2A), but this did not reach overall significance by one way ANOVA. Significance (p <0.05) was reached when CXCL10 mRNA levels of HRV-16 plus DMSO are compared with HRV-16 plus SB203580 (10 μM) using a paired t-test test. The lack of significance may have been due to the overall variation of the standard error of the mean. In contrast to mRNA data, HRV-16-induced CXCL10 protein production was significantly (p <0.05) inhibited in a concentration-dependent manner in the presence of SB203580 (10-1 μM), displaying an almost identical pattern to that of CXCL10 mRNA (Figure 3.2B). In contrast to the p38 pathway, inhibition of the JNK pathway in BEAS-2B cells with SP600125 (10-1 μM), an ATP-competitive inhibitor, did not significantly change HRV-16-induced CXCL10 mRNA and protein expression (Figures 3.2A & B). Surprisingly, inhibition of the MEK1/2 pathway with non-ATP competitive inhibitors, PD98059 (10-1 μM) or U0126 (3-0.3 μM), significantly (p <0.001 in all cases) enhanced HRV-16-induced CXCL10 mRNA and protein in a concentration-dependent manner (Figures 3.2C & D).

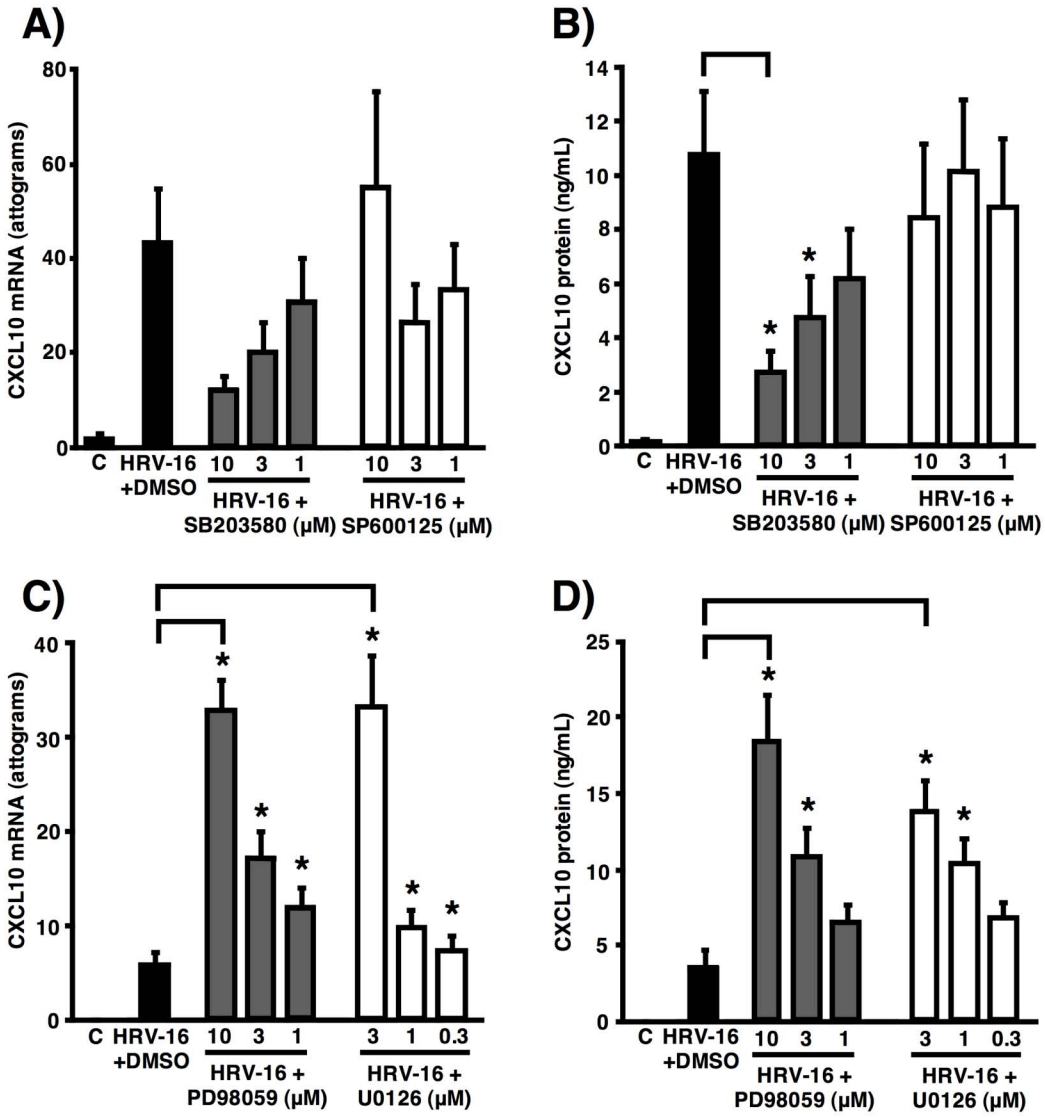

Figure 3.2 – Effect of MAPK pathway inhibitors on HRV-16-induced CXCL10 mRNA and protein in BEAS-2B cells. BEAS-2B were pre-incubated with varying concentrations of the p38 inhibitor (SB203580, 10-1 μM), JNK inhibitor (SP600125, 10-1 μM), MEK1/2 inhibitors (PD98059, 10-1 μM; U0126, 3-0.3 μM), or vehicle control (DMSO 0.1% v/v) for 1 h followed by the addition of HRV-16. Samples were collected 24 h post-infection and assayed for CXCL10 mRNA expression **(A & C)** and protein release **(B & D)** using real time PCR and ELISA, respectively. Asterisks indicate significant differences compared with HRV-16 plus DMSO. Data are expressed as mean ± SEM (*n* = 7, SB203580 & SP600125; *n* = 6, PD98059 & U0126). Differences in CXCL10 mRNA expression assessed with Kruskal-Wallis ANOVA, followed by Wilcoxon matched-pairs signed-rank test. Differences in CXCL10 protein release assessed with one-way ANOVA followed by Fisher's least significant difference test.

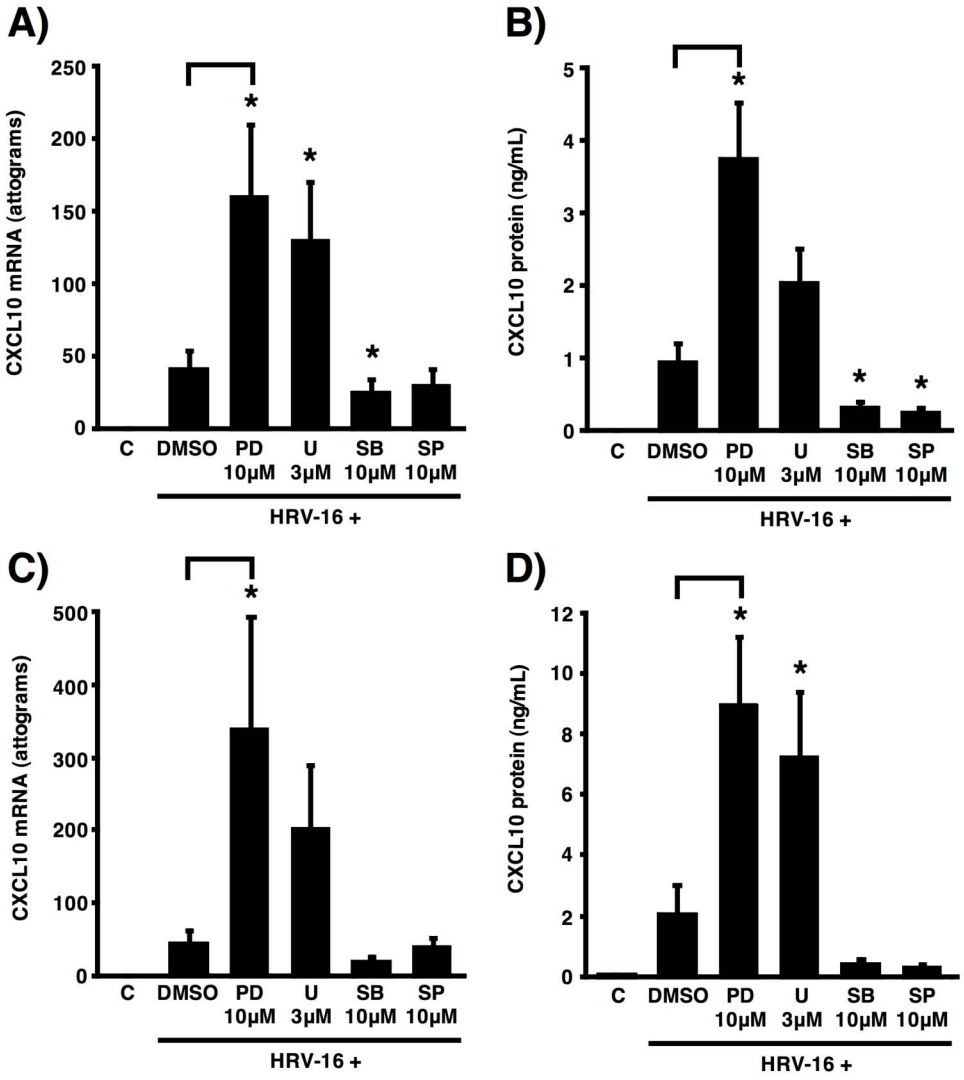

Figure 3.3 - Effect of MAPK pathway inhibitors on HRV-16-induced CXCL10 mRNA and protein in primary human airway epithelial cells. Primary human bronchial **(A & B)** or adenoid-derived **(C & D)** epithelial cells were pre-incubated with SB203580 (10 μM), SP600126 (10 μM), PD98059 (10 μM), U0126 (3 μM), or DMSO (0.1% v/v) for 1 h followed HRV-16 infection for 24 h. Samples were assayed for CXCL10 mRNA expression **(A & C)** and protein release **(B & D)** using real time PCR and ELISA, respectively. Asterisks indicate significant differences compared with HRV-16 plus DMSO. Data are expressed as mean ± SEM (n = 9, HBE; n = 5, HAE). Differences in CXCL10 mRNA and protein from HBE assessed with Kruskal-Wallis ANOVA, followed by Wilcoxon matched-pairs signed-rank test. Differences in CXCL10 mRNA and protein from HAE assessed with one-way ANOVA followed by Fisher's least significant difference test.

Using an optimal dose determined in BEAS-2B cells, SB203580 (10 μM) significantly (p <0.05) abrogated HRV-16-induced CXCL10 mRNA and protein in HBE (Figures 3.3A & B). Though there was a trend towards inhibition within each experiment in HAE, SB203580 treatment did not significantly abrogate HRV-16-induced CXCL10 mRNA and protein expression (Figures 3.3C & D). In both HBE and HAE, SP600125 (10 μM) did not inhibit HRV-16-induced CXCL10 mRNA expression (Figures 3.3A & C). HRV-16-induced CXCL10 protein was significantly (p <0.05) inhibited in HBE and though there was clear trend of inhibition in HAE within each experiment, this did not reach significance (Figures 3.3B & D). HRV-16-induced CXCL10 mRNA and protein expression with PD98059 treatment was significantly (p <0.05 in both cases) enhanced in HAE and HBE (Figures 3.3A-D). Though treatment with U0126 did not significantly enhance HRV-16-induced CXCL10 mRNA in HAE or protein in HBE, there was a clear trend of enhancement in each experiment (Figures 3.3B & C). This likely reflected the wide variability of the absolute magnitude of responses using cells from different donor tissue. Overall, these results suggested that the MEK1/2 pathway may negatively regulate HRV-16-induced CXCL10 expression in both BEAS-2B cells and primary airway epithelial cells.

3.3.3 Effect of MEK1/2 pathway inhibition on HRV-16-induced MAPK phosphorylation

Having demonstrated HRV-16 infection activated the major MAPK pathways and enhanced HRV-16-induced CXCL10 expression with MEK1/2 pathway inhibition, experiments were performed to validate the effect of these inhibitors. PD98059 and U0126 have been reported to inhibit the phosphorylation of both ERK1/2 and ERK5

through effects on their upstream kinases, MEK1/2 and MEK5, respectively[294,295]. Whole cell lysates from BEAS-2B cells infected for 1 h with HRV-16 in the presence of varying concentrations of PD98059 (30-1 μM) and U0126 (10-0.3 μM) were immunoblotted for the phosphorylated forms of ERK1/2, ERK5, and p38 (Figure 3.4). As expected, U0126, which equally inhibits both MEK1 and MEK2[342], inhibited the phosphorylation of both ERK1 and ERK2 in a concentration-dependent manner. In contrast, PD98059, which preferentially inhibits MEK1[342], inhibited the upper ERK1 band in a concentration-dependent manner. There was a much weaker effect on the lower ERK2 band compared with the effect of U0126.

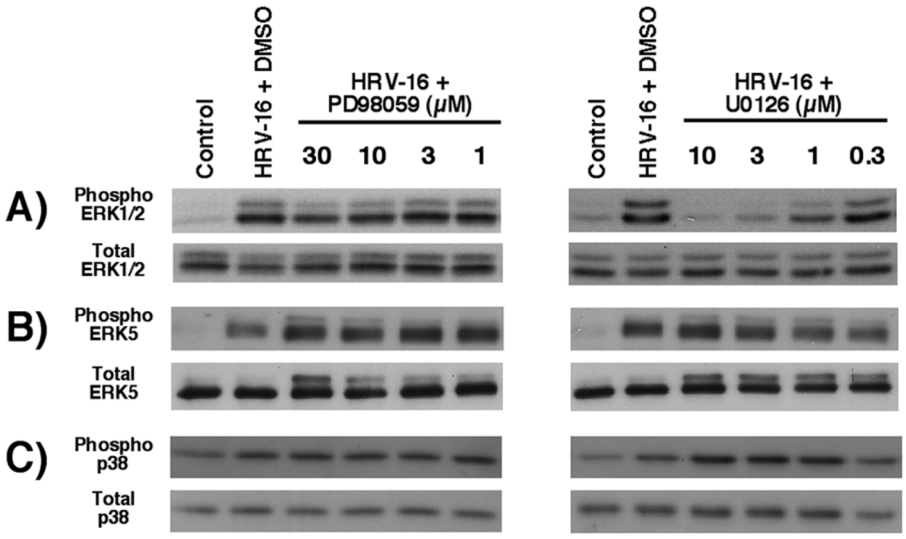

Figure 3.4 – Effect of MEK1/2 pathway inhibition on HRV-16-induced ERK1/2, ERK5, and p38 phosphorylation. BEAS-2B cells were pre-incubated with varying concentrations of PD98059 (30-1 μM), U0126 (10-0.3 μM), or vehicle control (DMSO 0.1% v/v) for 1 h followed by the addition of HRV-16 for 1 h. Whole cell lysates were collected, resolved using SDS/PAGE, and immunoblotted with phospho-specific antibodies for each major MAPK including: **A)** ERK1/2, **B)** ERK5, and **C)** p38. Each immunoblot is representative of three separate experiments.

At the concentration of optimal CXCL10 enhancement with PD98059 (10 μM) and U0126 (3 μM), the upper ERK1 band was clearly inhibited with both drugs, but there was a clear difference in the level of inhibition of the lower ERK2 band. HRV-16-induced ERK5 phosphorylation was modestly enhanced in the presence of PD98059, though this did not occur in a concentration-dependent manner. In contrast, U0126 did not have any marked effects on ERK5. At the optimal concentration of CXCL10 enhancement, while there was a modest enhancement of ERK5 with PD98059 (10 μM), there was no clear difference in the level of ERK5 phosphorylation in the presence of U0126 (3 μM). Cross-talk between the p38 and ERK pathways has been documented[270,371,412-414] and since p38 inhibition lowered HRV-16-induced CXCL10 expression, experiments were performed to evaluate if PD98059 or U0126 modulated CXCL10 expression via effects on p38 phosphorylation. PD98059 had no effect on HRV-16-induced p38 phosphorylation, but U0126 modestly enhanced p38 phosphorylation. Similar to the contradictory effects on ERK5 phosphorylation, this disparity in p38 phosphorylation cannot account for the enhancement of CXCL10 that is commonly induced by both PD98059 and U0126. These results demonstrate that inhibition of the MEK1/2 pathway and its effects on downstream ERK1 phosphorylation is consistent with HRV-16-induced enhancement of CXCL10 expression.

3.3.4 MEK1/2 pathway inhibition enhances HRV-16-induced CCL5 expression

Because of the surprising observation that inhibition of the MEK1/2 pathway with PD98059 or U0126 enhanced HRV-16-induced CXCL10 expression, further studies were undertaken to determine if this observation held true for other HRV-inducible chemokines. In HBE, both PD98059 (10 μM) and U0126 (3 μM) significantly (p <0.05) enhanced CCL5 mRNA and protein expression compared to HRV-16 plus DMSO (Figures 3.4A & B). Treatment with either PD98059 (10 μM) or U0126 (3 μM) also significantly (p <0.05) enhanced CCL5 protein in HAE (Figure 3.4C). In contrast to p38 inhibitor effects on CXCL10, SB203580 (10 μM) did not significantly alter HRV-16-induced CCL5 mRNA and protein in either HBE or HAE (Figures 3.4A-C). Inhibition of the JNK pathway with SP600125 (10 μM) significantly (p <0.05) inhibited HRV-16-induced CCL5 mRNA and protein in HBE and HAE. These data confirm that MEK1/2 pathway-mediated enhancement of HRV-inducible chemokine expression is not unique to CXCL10, but also occurs with CCL5.

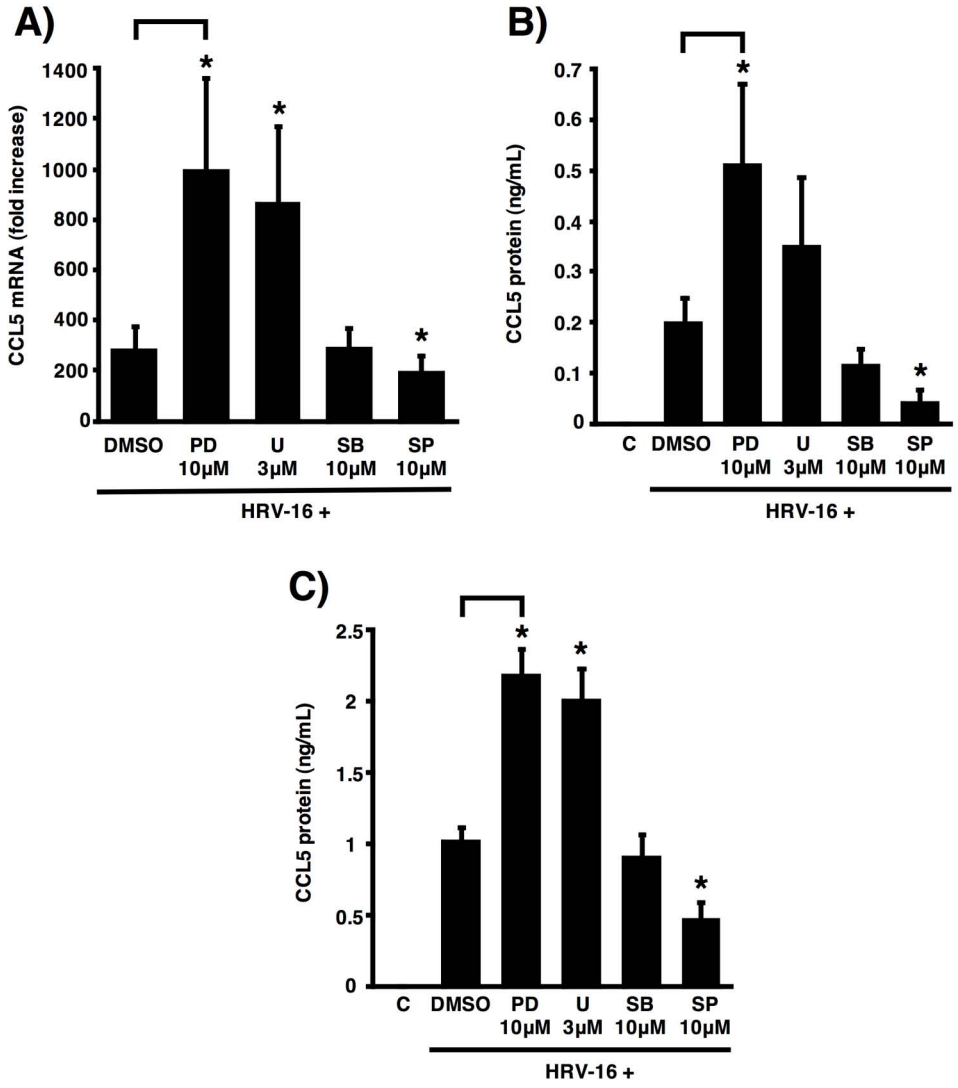

Figure 3.5 - Effect of MAPK pathway inhibitors on HRV-16-induced CCL5 mRNA and protein in primary human airway epithelial cells. Primary human bronchial **(A & B)** or adenoid-derived **(C)** epithelial cells were pre-incubated with SB203580 (10 μM), SP600126 (10 μM), PD98059 (10 μM), U0126 (3 μM), or DMSO (0.1% v/v) for 1 h followed by HRV-16 infection for 24 h. Samples were assayed for CCL5 mRNA expression **(B)** and protein release **(A & C)** using real time PCR and ELISA, respectively. Asterisks indicate significant differences compared with HRV-16 plus DMSO. Data are expressed as mean ± SEM (n = 7, HBE; n = 5, HAE). Differences in CCL5 mRNA and protein from HBE assessed with Kruskal-Wallis ANOVA, followed by Wilcoxon matched-pairs signed-rank test. Differences in CCL5 protein release from HAE assessed with one-way ANOVA followed by Fisher's least significant difference test.

3.3.5 MEK1/2 pathway inhibition does not enhance IFN-β-induced CXCL10 expression

Having shown that MEK1/2 pathway inhibition resulted in an enhancement of HRV-16-induced CXCL10 expression, studies were carried out to determine if the enhancement phenomenon was selective for HRV-16. Another known inducer of CXCL10 expression is IFN-β[143], thus the effect of these MEK1/2 pathway inhibitors on IFN-β-induced CXCL10 expression was assessed. A concentration of IFN-β (3 ng/mL) was selected to induce comparable levels of CXCL10 expression to those seen with HRV-16. In BEAS-2B cells, neither PD98059 (10-1 μM) nor U0126 (3-0.3 μM) significantly enhanced IFN-β-induced CXCL10 mRNA or protein production compared to IFN-β plus DMSO (Figures 3.5A & B). In HBE, PD98059 (10 μM) or U0126 (3 μM) also did not significantly enhance IFN-β-induced CXCL10 mRNA and protein production (Figures 3.5C & D). Additionally, IFN-β did not markedly induce the phosphorylation of ERK1/2 at various time points compared to HRV-16 (1 h post-infection) in BEAS-2B cells (Figure 3.6). These results suggest that CXCL10 expression is selectively enhanced by certain stimuli and is associated with the phosphorylation of ERK1/2.

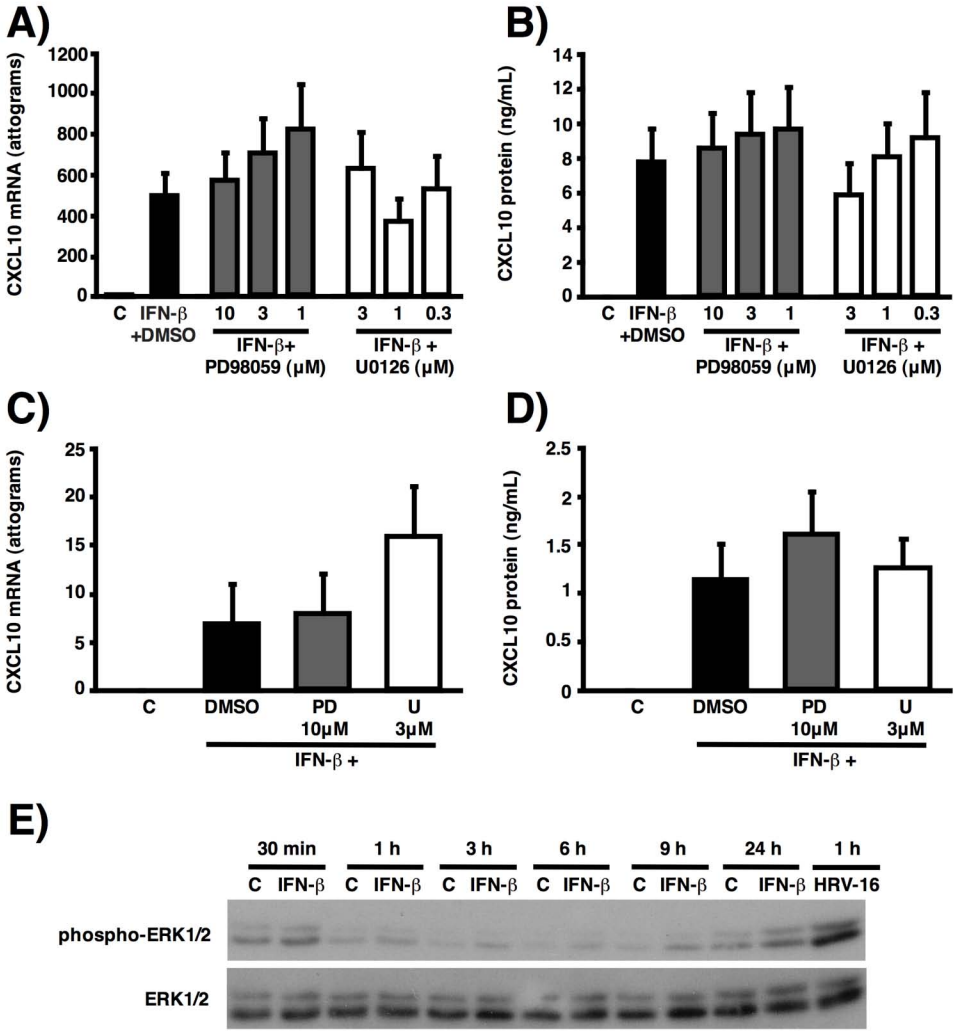

Figure 3.6 - MEK1/2 pathway inhibition does not enhance IFN-β-induced CXCL10 expression in airway epithelial cells. BEAS-2B cells **(A & B)** and HBE **(C & D)** were pre-incubated with DMSO (0.1% v/v) or the MEK1/2 inhibitors, PD98059 (10-1 μM) or U0126 (3-0.3 μM), for 1 h followed by IFN-β (3 ng/mL) stimulation for 24 h. Samples were assayed for CXCL10 mRNA expression **(A & C)** and protein release **(B & D)** using real time PCR and ELISA, respectively. **E)** BEAS-2B cells were stimulated with IFN-β (3 ng/mL) or HRV-16 for the indicated time points and whole cell lysates were collected, resolved using SDS/PAGE, and immunoblotted with phospho-specific antibody for ERK1/2. Asterisks indicate significant differences compared with HRV-16 plus DMSO. Data are expressed as mean ± SEM (n = 6, BEAS-2B; n = 6, HBE). Differences in CXCL10 mRNA (BEAS-2B) and protein (BEAS-2B & HBE) assessed with one-way ANOVA followed by Fisher's least significant difference test. Differences in CXCL10 mRNA and protein from HBE assessed with Kruskal-Wallis ANOVA, followed by Wilcoxon matched-pairs signed-rank test. Immunoblot is representative of three separate experiments.

3.3.6 Effect of MAPK inhibitors on HRV-16 replication and cell viability

Since the inhibition of various MAPK pathways had variable effects on HRV-16-induced CXCL10 mRNA and protein production, including a MEK1/2 pathway-mediated enhancement of CXCL10, it was necessary to confirm that inhibitor treatment did not alter cell viability or HRV-16 replication. Potential effects on cell viability were determined through the measurement of lactate dehydrogenase (LDH) release into supernatants from BEAS-2B cells and HBE. HRV-16 infection in the presence of DMSO modestly increased cell cytotoxicity to approximately 10% (BEAS-2B) or 3% (HBE) compared to control cells (4% and 1%, respectively). The addition of the MAPK inhibitors did not further alter cell viability in either cell type (Figures 3.7A & B).

To confirm that the MAPK inhibitors did not alter HRV-16 replication, viral titre assays were performed. Using the optimal concentration of PD98059 (10 μM) and U0126 (3 μM) determined earlier, HRV-16 replication in HBE and HAE was not altered compared to HRV-16 plus DMSO (Figures 3.8A & C). In addition, SB203580 (10 μM) and SP600126 (10 μM) did not alter viral replication in HBE (Figure 3.8A). Since viral titre assays require that unadsorbed virus be removed before the end of the first replication cycle (8-10 h post-infection)[143], cells were incubated with HRV-16 for 3 h, washed, and then incubated with inhibitors for a further 21 h. As such, it was necessary to determine that this protocol gave similar results to the experiments where inhibitors were added 1 h prior to HRV infection. HRV-16-induced CXCL10 protein production was consistently, but not significantly, enhanced using either inhibitor 3 h after HRV infection (Figure 3.8C). The levels of CXCL10 protein were consistently enhanced in each experiment using PD98059 or U0126 and again demonstrated the wide variability of

the absolute magnitude of responses from different donor tissue. Inhibition of the p38 and JNK pathways did not significantly alter HRV-16-induced CXCL10 protein production using this protocol. Overall, these data confirmed that enhancement of HRV-16-induced CXCL10 in the presence of PD98059 or U0126 was not due to alterations in cell viability or viral replication.

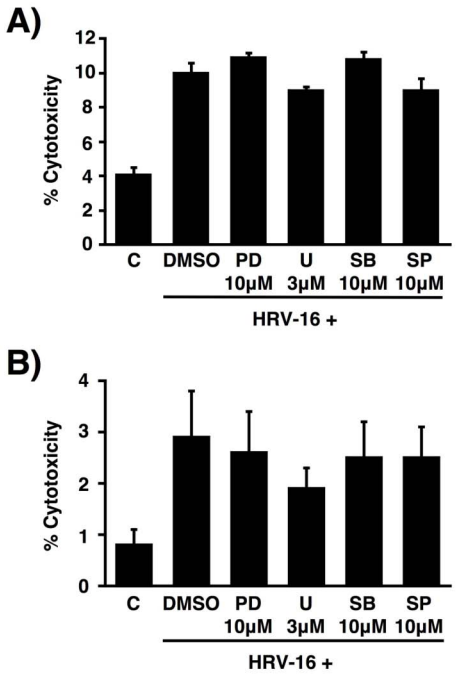

Figure 3.7 – MAPK inhibitors do not alter cell viability. BEAS-2B **(A)** or HBE **(B)** were pre-incubated with the MAPK inhibitors SB203580 (10 μM), SP600125 (10 μM), PD98059 (10μM), U0126 (3 μM), or vehicle control (DMSO 0.1% v/v) for 1 h followed by HRV-16 infection for 24 h. Lysate and supernatants were collected and assayed for lactate dehydrogenase (LDH) release. Data are expressed as mean ± SEM (BEAS-2B, *n* = 3; HBE, *n* = 3). Medium control is designated (C).

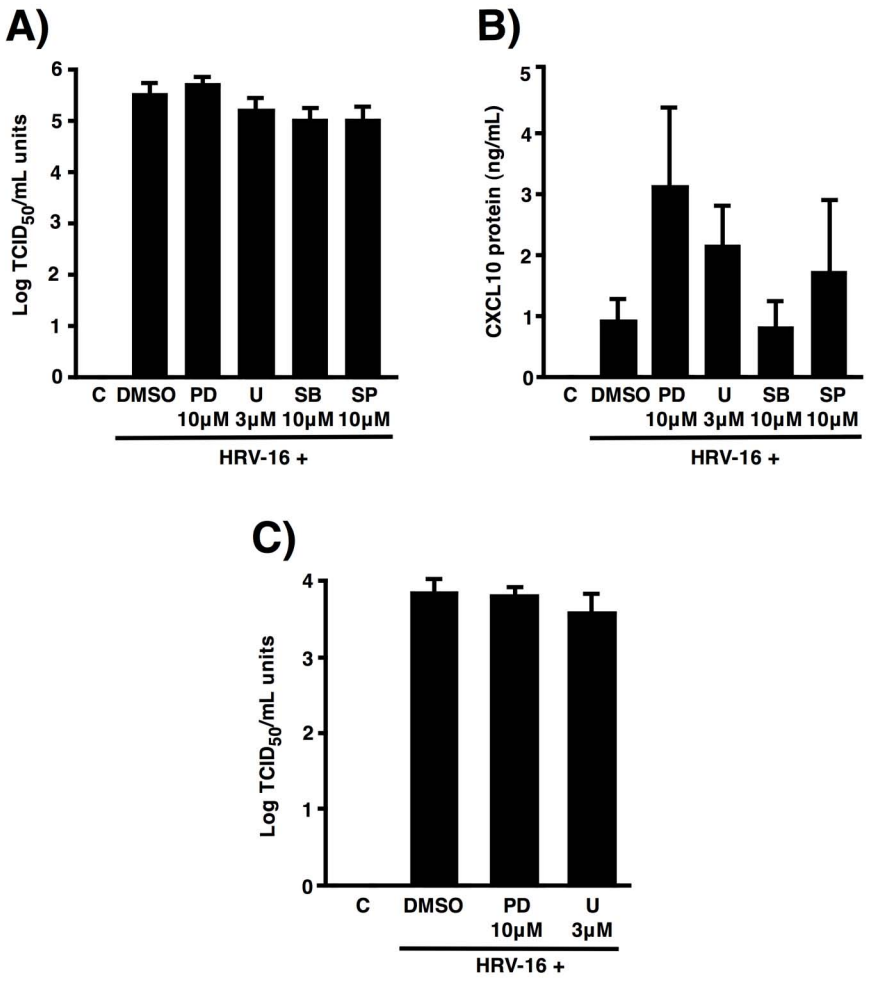

Figure 3.8 – MAPK inhibitors do not alter HRV-16 replication in airway epithelial cells. Primary airway epithelial cells were infected with HRV-16 for 3 h, washed with HBSS three times, and incubated with MAPK inhibitors SB203580 (10 μM), SP600125 (10 μM), PD98059 (10 μM), U0126 (3 μM), or vehicle control (DMSO 0.1% v/v) in fresh medium for 24 h. HRV-16 titres from HBE **(A)** and HAE **(C)** were measured from supernatants using WI-38 lung fibroblast viral titre assay. **B)** Supernatants from HBE were also assayed for HRV-16-induced CXCL10 protein release using ELISA techniques. Data are expressed as mean ± SEM (HBE, $n = 5$; HAE, $n = 5$). Differences in CXCL10 protein release assessed with one-way ANOVA followed by Fisher's least significant difference test.

3.4 Discussion

Our understanding of the signaling events regulating HRV-induced chemokine expression remains limited and there has been little focus on the signalling events involved in HRV-16-induced expression of chemokines, such as CXCL10, which absolutely require viral replication. In this chapter, experiments focused on the role of the major MAPK pathways, including p38, JNK, ERK5, and ERK1/2 during HRV-16-induced CXCL10 expression in human airway epithelial cells.

Initial studies confirmed previous observations, in that HRV-16 infection of BEAS-2B cells induced the phosphorylation of p38, JNK, and ERK1/2 in a time-dependent manner[267,268]. In contrast to previous studies where only acute activation (< 6 h) was studied, more time points were included to further study the kinetics of MAPK activation, as induction of CXCL10 does not occur for several hours after infection. HRV-16 infection induced the chronic phosphorylation of ERK1/2 with activation as early as 15 min post-infection and continued, albeit weaker, activation at 24 h post-infection. This chronic activation is in agreement with a previous study that found HRV-16-induced ERK1/2 phosphorylation at 17 h post-infection[262]. Also, this thesis provides the first demonstration of HRV-16-induced activation of ERK5 in airway epithelial cells. Peak ERK5 phosphorylation was evident at 1 h post-infection, but in contrast to ERK1/2, ERK5 activation was not maintained beyond 6 h. Similar to ERK5, both p38 and JNK1/2 phosphorylation are observed early after infection, but while JNK1/2 activation is diminished beyond 3 h, a second wave of p38 phosphorylation is apparent at 24 h post-infection. This late activation of p38 is in agreement with a previous study that also

found HRV-16 induces the phosphorylation of p38 as late as 17 h post-infection in BEAS-2B cells[262].

Pharmacological inhibitors were employed to assess the role of the MAPK pathways, as they are both widely used and have well-characterized selectivities for their respective targets[415]. Inhibition of the JNK pathway had no significant effect on HRV-16-induced CXCL10 mRNA and protein levels in BEAS-2B or HAE cells at any of the concentrations used. It did, however, significantly inhibit HRV-16-induced CXCL10 protein production, but not mRNA expression, in HBE. The lack of effect on CXCL10 mRNA expression in the presence of the JNK inhibitor is not easily explained, unless the JNK pathway exerts effects at the translational or post-translational level in primary cells, but not in the BEAS-2B cell line. In contrast, blockade of the p38 pathway significantly inhibited HRV-16-induced CXCL10 mRNA and protein in a concentration-dependent manner. Similarly, p38 pathway inhibition significantly reduced HRV-16-induced CXCL10 mRNA and protein in HBE. Though not significant in HAE, CXCL10 mRNA and protein showed a trend towards inhibition upon p38 pathway blockade. These results are consistent with the findings that the p38 pathway is involved in the up-regulation of the adenoviral induction of CXCL10[410].

In marked contrast to the inhibition of the p38 and JNK pathways, inhibition of MEK1/2 with either PD98059 or U0126, two structurally distinct inhibitors, significantly enhanced HRV-16-induced CXCL10 mRNA and protein in a concentration-dependent manner in BEAS-2B cells. Using the optimal concentration determined in BEAS-2B, similar effects were seen in both HBE and HAE. These results clearly demonstrate that HRV-16-induced CXCL10 production is negatively regulated through the MEK1/2

pathway and occurs in both a cell line and primary cells. Furthermore, the modulation of HRV-16-induced CXCL10 expression with MAPK pathway inhibition was not due to altered cell viability or HRV-16 replication. Of importance, the similar results in primary cells demonstrated that the enhancement phenomenon is not a cell line artifact and provided justification for the use of BEAS-2B cells as an appropriate and representative model for techniques (e.g. promoter construct studies) that are not possible in primary cells. Additionally, this negative regulation is common to both upper and lower airway epithelial cells, further indicating a conserved mechanism by which HRV-induced chemokine expression is regulated in airway epithelial cells. Given this commonality, experiments in subsequent chapters were carried out in either BEAS-2B cells and/or HBE, as appropriate.

Given their high level of homology, specifically in their kinase domains, MEK1 and MEK2 are assumed to phosphorylate ERK1/2 equally[327,328,416]. Interestingly, U0126, which has equal affinity for MEK1 and MEK2[342], inhibited the phosphorylation of both ERK1 and ERK2 at the concentration (3 μM) used for CXCL10 experiments. In contrast, PD98059 (10 μM), which has been shown to more selective for MEK1 over MEK2[404], was only effective at inhibiting ERK1 phosphorylation, while having little effect on ERK2. This discrepancy is difficult to explain other than to speculate that in BEAS-2B cells, MEK1 may preferentially phosphorylate ERK1 protein in response to HRV-16 infection. Since both PD98059 and U0126 enhanced HRV-16-induced CXCL10 expression to similar degrees, this implied that inhibition of ERK1 phosphorylation is associated with the enhancement of HRV-16-induced production of CXCL10.

Inhibition with PD98059 slightly enhanced HRV-16-induced ERK5 phosphorylation, but did not effect HRV-16-induced p38 phosphorylation. By contrast, U0126 slightly enhanced p38 phosphorylation, but was without effect on ERK5 phosphorylation. In either case, the enhancement of ERK5 and p38 phosphorylation was not concentration-dependent. Overall, this indicated that the enhancement of HRV-16-induced CXCL10 production was not due to redundant activation of the ERK5 or p38 MAPK pathways.

Similar to HRV-16-induced CXCL10, inhibition of the MEK1/2 pathway enhanced HRV-16-induced CCL5 mRNA and protein. By contrast, it has been previously reported that MEK1/2 pathway inhibition does not enhance HRV-16-induced CXCL8 expression in airway epithelial cells[267]. Though it remains speculative, the MEK1/2 pathway may exert its effects on a subset of HRV-inducible genes in airway epithelial cells, but the mechanisms underlying this regulation remain unclear. IFN-β-induced CXCL10 expression was not enhanced upon MEK1/2 pathway inhibition nor was ERK1/2 phosphorylation apparent after IFN-β treatment implying that the enhancement of CXCL10 expression demonstrates a stimulus-dependent selectivity and requires the activation of the ERK1/2 pathway.

In summary, the results demonstrate that HRV-16 induces the activation of the major MAPK signalling pathways in airway epithelial cells. Pharmacologic inhibition of the p38 pathway abrogates HRV-16-induced CXCL10 mRNA and protein production. In contrast, MEK1/2 pathway inhibition selectively enhances HRV-16, but not IFN-β-induced, CXCL10 mRNA and protein expression. Enhancement is also shown with HRV-inducible CCL5. In addition, the negative regulation of HRV-16-induced CXCL10

expression is associated with activation of ERK1/2 and specific modulation of ERK1 phosphorylation. These effects are not due to alterations in cell viability or viral replication. This is the first description of the negative regulation of an HRV-inducible chemokine in airway epithelial cells.

Chapter Four: Inhibition of the MEK1/2 pathway enhances HRV-16-induced CXCL10 expression through transcriptional effects

4.1 Introduction

In Chapter 3, a novel observation is described whereby pharmacologic inhibition of the MEK1/2 pathway with two structurally distinct inhibitors, PD98059 and U0126, selectively enhanced HRV-16, but not IFN-β, induced CXCL10 mRNA and protein expression in airway epithelial cells. Regulation of gene expression is mediated, in large part, by the rate of mRNA transcription and degradation (steady state mRNA), though they are not mutually exclusive[417-419]. HRV-16-induced CXCL10 expression is transcriptionally regulated, in an NF-κB-dependent manner, in airway epithelial cells[143]. As such, studies were undertaken to assess any effects on transcription during MEK1/2 pathway-mediated enhancement of HRV-16-induced CXCL10 expression. It was hypothesized that blockade of the MEK1/2 pathway would enhance CXCL10 expression through transcriptional effects.

4.2 Materials and Methods

4.2.1 Western blotting for IκBα activation

Subconfluent (60-70%) monolayers of BEAS-2B cells grown in 6-well plates were incubated in BEBM overnight and then pre-incubated with PD98059 (10 μM) or U0126 (3 μM) for 1 h followed by HRV-16 (1 x 10^4 $TCID_{50}$ U/mL) infection in BEBM for the designated time points. At each time point, supernatants were removed and cells were washed with HBSS and lysed in ice-cold lysis buffer. Triton-soluble samples were

separated using 10% SDS-PAGE, and proteins were transferred to a PVDF membrane. Membranes were blocked with 5% skim milk for 1 h and probed with either 1/1000 dilution of phospho-specific or total anti-IκBα antibody in TTBS (0.5% v/v Tween-20) overnight at 4°C with gentle shaking. Membranes were washed and then incubated for 1 h with 1/2000 dilution of HRP-conjugated anti-rabbit Ig antibody or anti-mouse HRP-conjugated Ig antibody in TTBS.

4.3 Results

4.3.1 Inhibition of the MEK1/2 pathway enhances HRV-16-induced CXCL10 transcription

Effects on transcription were studied using a 972-bp full length CXCL10 promoter luciferase construct containing the putative binding sites for various transcription factors that was transiently transfected into BEAS-2B cells (Figure 4.1A). In the presence of the MEK1/2 pathway inhibitors, PD98059 (10-1 μM) or U0126 (3-0.3 μM), HRV-16-induced CXCL10 promoter luciferase activity was significantly (p <0.05 in all cases) enhanced compared to HRV-16 plus DMSO at each inhibitor concentration (Figure 4.2). PD98059 (10 μM) and U0126 (3 μM) maximally enhanced promoter activity to 16.1 ± 2.6 and 23.1 ± 3.2 fold increase, respectively, compared to 7.7 ± 0.8 fold increase by HRV-16 + DMSO. The inhibitors alone did not have any effect on CXCL10 promoter activity.

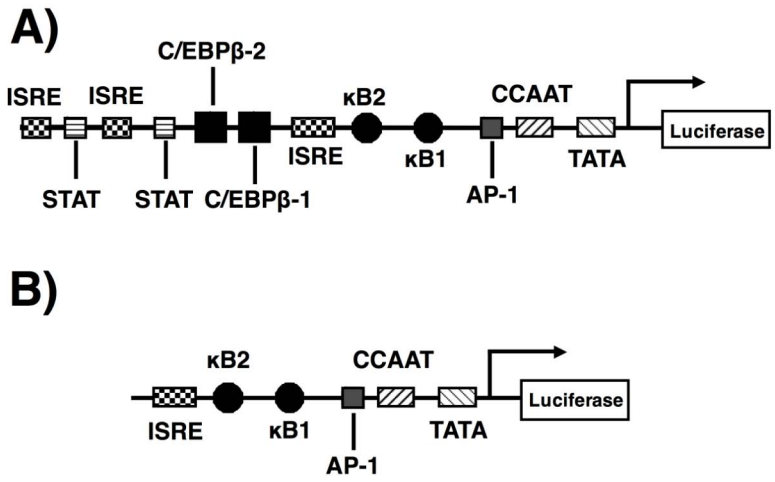

Figure 4.1 – Schematic diagram of the human CXCL10 promoter. Putative transcription factor binding sites in the **A)** full length (972 bp) and **B)** truncated (376 bp) human CXCL10 promoter-luciferase constructs. Binding sites include: activator protein-1 (AP-1), NF-κB binding sites 1 & 2 (κB1 & κB2), interferon-stimulated response element (ISRE), CCAAT enhancer binding protein-β 1 & 2 (C/EBPβ-1 & C/EBPβ-2), and signal transducer and activator of transcription (STAT).

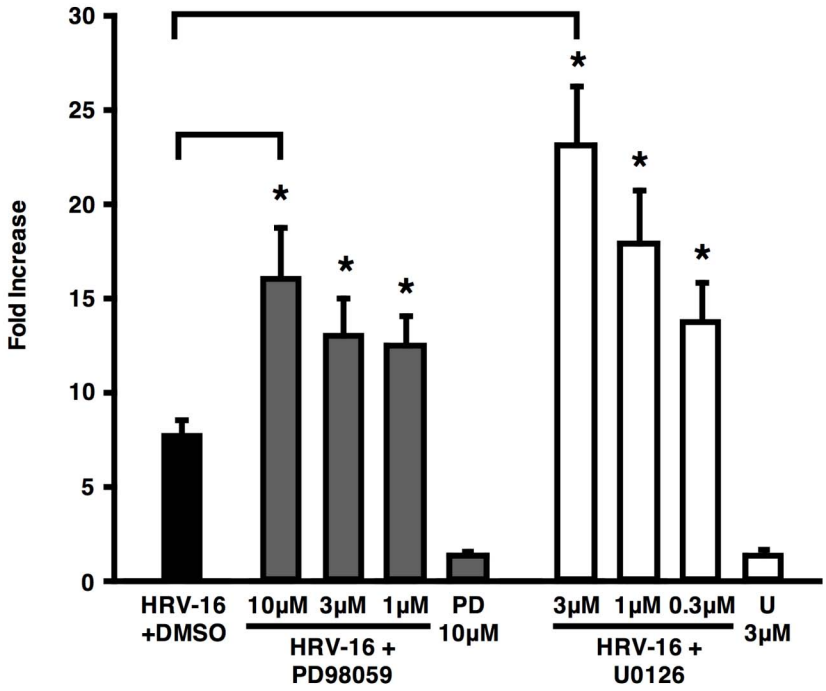

Figure 4.2 – Inhibitors of the MEK1/2 pathway enhance HRV-16-induced CXCL10 transcription. BEAS-2B cells were transiently transfected with 1.0 μg of full length CXCL10 promoter-luciferase plasmid and 0.1 μg of *Renilla* luciferase plasmid. Transfected cells were pre-incubated with DMSO (0.1% v/v), PD98059 (10-1 μM) or U0126 (3-0.3 μM) for 1 h followed by HRV-16 or mock infection for 24 h. Lysates from triplicate wells were assayed for firefly and *Renilla* luciferase activity and calculated as fold increase compared to control wells. Data are expressed as mean ± SEM (n = 6). Asterisks indicate significant differences compared with HRV-16 plus DMSO assessed with Kruskal-Wallis ANOVA, followed by Wilcoxon matched-pairs signed-rank test.

To determine the region(s) of the CXCL10 promoter that were involved for the enhancement phenomenon, a 376-bp truncated construct was generated that contained only four putative transcription factor binding sites (Figure 4.1B). These sites included the AP-1, NF-κB binding sites (κB1 and κB2), and an ISRE. The 376-bp truncated promoter has been reported to be inducible by HRV-16, but to a lesser extent than the 972-bp full length promoter[143]. In accord with this previous finding, HRV-16 induction of the 376-bp promoter was slightly, though significantly (p <0.05), reduced compared to

the 972-bp promoter (Figure 4.3A). In the presence of the optimal concentration of PD98059 (10 μM) or U0126 (3 μM) determined in Chapter 3, HRV-16-induced CXCL10 promoter drive was significantly (p <0.05 in all cases) enhanced using either the 972-bp or the 376-bp construct versus virus in the presence of DMSO (Figure 4.3A).

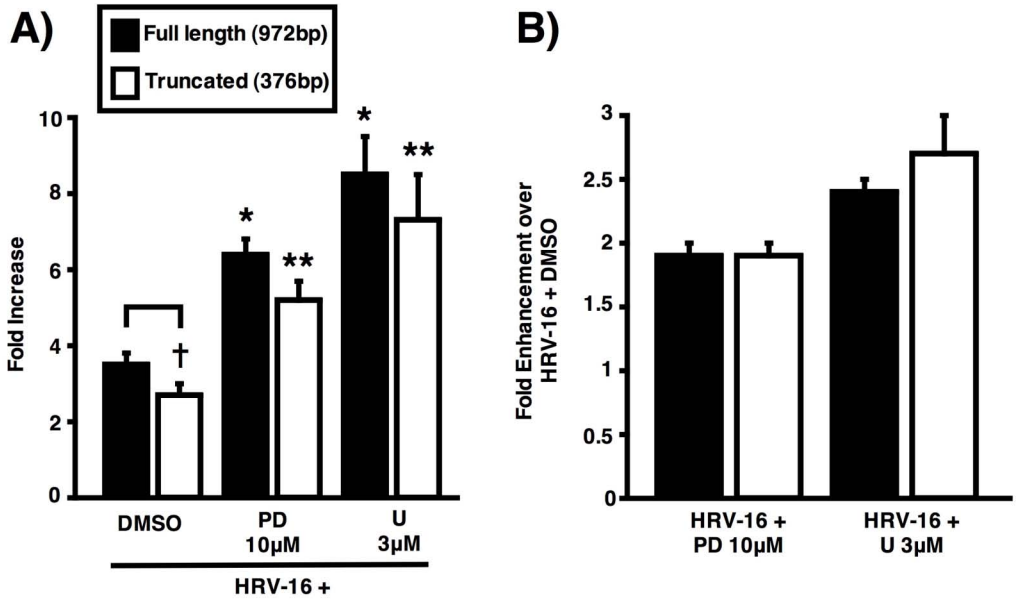

Figure 4.3 – CXCL10 promoter activity is similarly enhanced upon MEK1/2 pathway inhibition in both the full length and truncated promoters. BEAS-2B cells transiently transfected with 1.0 μg full length (black) or truncated (white) CXCL10 promoter-luciferase constructs and 0.1 μg *Renilla* luciferase plasmid were pre-incubated with DMSO (0.1% v/v), PD98059 (10 μM) or U0126 (3 μM) for 1 h followed by HRV-16 or mock infection for 24 h. Lysates from triplicate wells were assayed for firefly and *Renilla* luciferase activity and calculated as **(A)** fold increase compared to control wells or **(B)** fold enhancement over HRV-16 plus DMSO. Data are expressed as mean ± SEM (n = 6). Dagger indicates significant difference between full length and truncated promoter drive with HRV-16 plus DMSO. Asterisks indicate significant differences compared to HRV-16 plus DMSO using full length (*) or truncated (**) promoter constructs assessed with Kruskal-Wallis ANOVA, followed by Wilcoxon matched-pairs signed-rank test

Although there was a modest difference in HRV-16-induced CXCL10 promoter drive between the 376-bp and the 972-bp constructs, when the effects of MEK1/2 pathway inhibition were expressed as fold enhancement over virus alone for each construct, a virtually identical level of enhancement was observed for both the 972-bp and 376-bp constructs (Figure 4.3B). In addition, control studies were carried out with a promoter-luciferase construct containing only a TATA box. HRV-16 did not induce this promoter and neither PD98059 nor U0126 had any effect on the basal activity in the presence of virus (data not shown). These results indicated that the essential elements involved in mediating the enhancement of HRV-16-induced CXCL10 promoter drive by MEK1/2 pathway inhibition were within the 376-bp promoter construct. Thus, subsequent studies focused on the specific binding sites found within this promoter region (Figure 4.1B).

Using site-directed mutagenesis, point mutations were separately introduced into the transcription factor binding sites found within the 376-bp CXCL10 promoter construct (Table 2.2). Mutation of the AP-1 site did not alter HRV-16-induced promoter activity (2.8 ± 0.4 fold increase) compared with the wildtype promoter (2.7 ± 0.2 fold increase), or the level of enhancement in the presence of PD98059 (10 μM) or U0126 (3 μM) (Figure 4.4). Mutation of the κB1 or κB2 promoter sites have been shown to abrogate HRV-16-induced 972-bp promoter drive, with κB1 playing a more prominent role[143,236]. A similar pattern was observed using the 376-bp construct. Mutation of the κB1 site significantly (p <0.05) and almost completely abrogated HRV-16-induced promoter activity (1.1 ± 0.1 fold increase) compared to wildtype (2.7 ± 0.2 fold increase).

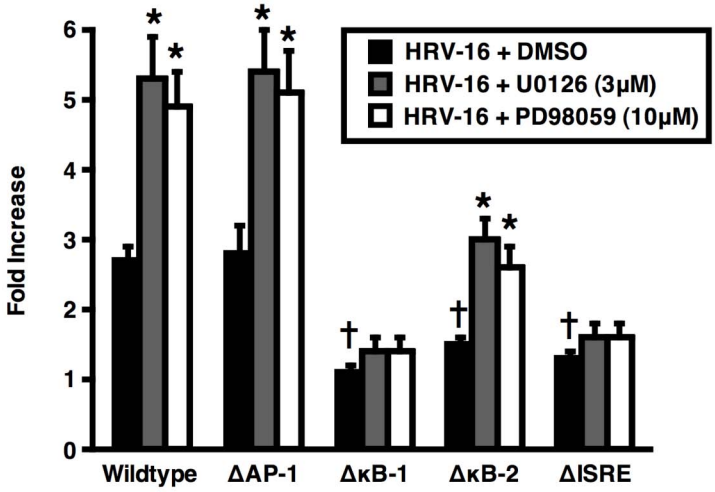

Figure 4.4 – Effects of MEK1/2 pathway inhibitors on HRV-16-induced activation of wild-type and point mutant versions of the truncated promoter. BEAS-2B cells were transiently transfected with 1.0 μg wild-type or mutant truncated CXCL10 promoter luciferase construct and 0.1 μg *Renilla* luciferase plasmid. Transfected cells were pre-incubated with 0.1% v/v DMSO (black), 10 μM PD98059 (grey) or 3 μM U0126 (white) for 1 h followed by HRV-16 or mock infection for 24 h. Lysates from triplicate wells were assayed for firefly and *Renilla* luciferase activity and calculated as fold increase compared to control wells. Data are expressed as mean ± SEM (n = 6). Dagger indicates significant abrogation of HRV-16-induced promoter activity between individual constructs. Single asterisk indicates significant enhancement of HRV-16-induced promoter activation in the presence of PD98059 or U0126 compared to HRV-16 plus DMSO. All significant differences were assessed with Kruskal-Wallis ANOVA, followed by Wilcoxon matched-pairs signed-rank test

Enhancement of this low level of promoter activity by PD98059 or U0126 was not observed (Figure 4.4). Mutation of κB2 also significantly (p <0.05) reduced HRV-16-induced promoter activity (1.5 ± 0.1 fold increase), though not to same extent as κB1. In the presence of PD98059 or U0126, the residual promoter activity found in the κB2 mutant construct was significantly (p <0.05 in both cases) enhanced (Figure 4.4). Similar to κB1, mutation of the ISRE significantly (p <0.05) abrogated HRV-16-induced promoter drive (1.3 ± 0.1 fold increase) and the residual promoter activity was not

enhanced in the presence of either PD98059 or U0126 (Figure 4.4). In all mutant constructs, PD98059 and U0126 alone did not have an effect on CXCL10 promoter activity (data not shown). These studies suggested that the NF-κB and ISRE binding sites required for viral activation of the promoter may also play a role in the MEK1/2 pathway-mediated enhancement of HRV-16-induced CXCL10 expression.

4.3.2 Evaluation of the role of NF-κB in MEK1/2 pathway-mediated modulation of HRV-16-induced CXCL10 expression

To further evaluate the role of NF-κB in the MEK1/2 pathway-mediated enhancement of HRV-16-induced CXCL10 expression, a luciferase construct was generated containing five tandem copies of CXCL10-specific κB1 or κB2 recognition sequences cloned into a pGL3.basic vector with a TATA box. HRV-16 induced promoter activity of both tandem repeat κB1 and κB2 constructs, but this activity was not enhanced in the presence of either PD98059 (10 μM) or U0126 (3 μM) (Figures 4.5A & B). Inhibitors alone had no effect on basal promoter drive (data not shown). To directly evaluate if HRV-16-induced NF-κB nuclear translocation and/or binding was altered by the MEK1/2 pathway inhibitors, EMSA analysis was performed using CXCL10-specific κB1 and κB2 radiolabeled oligonucleotides (see section 2.2.11.3 for details). First, HRV-16 infection was confirmed to induce the binding of nuclear proteins to the κB1 and κB2 radiolabeled probes. In BEAS-2B cells, HRV-16 infection resulted in a time-dependent induction of two complexes (bands 1 and 2) with the κB1 recognition sequence (Figure 4.6A). Binding was evident at 3 h post-infection and intensity of the

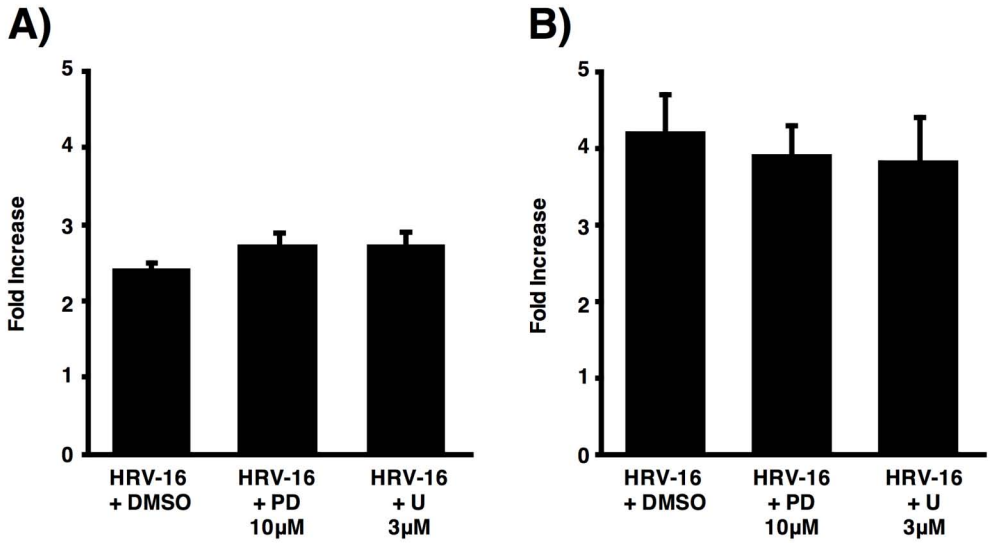

Figure 4.5 – MEK1/2 pathway inhibitors do not enhance HRV-16-induced activity of tandem repeat κB1 or κB2 promoter constructs. BEAS-2B cells were transiently transfected with 1.0 μg of a plasmid containing five copies of either the CXCL10-specific κB1 **(A)** or κB2 **(B)** recognition sequence cloned into pGL3.basic with a TATA box. Transfected cells were pre-incubated with DMSO (0.1% v/v), PD98059 (10 μM) or U0126 (3 μM) for 1 h followed by HRV-16 or mock infection for 24 h. Lysates from triplicate wells were assayed for firefly activity and calculated as fold increase compared to control wells. Data are expressed as mean ± SEM (*n* = 6, κB1; n = 4, κB2). Significant differences were assessed with Kruskal-Wallis ANOVA.

two bands increased from 6-9 h post-infection. In an analogous manner, HRV-16 infection induced the formation of two specific complexes with the κB2 oligonucleotide with peak band intensity at 3 h post-infection (Figure 4.6B). The intensity decreased after 3 h, but was still evident at 9 h post-infection. In HBE, HRV-16 induced the formation of two complexes (bands 1 and 2) with the κB1 oligonucleotide that were evident at 6 h post-infection. The intensity of binding subsequently decreased from 9-12 h post-infection (Figure 4.6C). A similar binding pattern was observed in HBE using the κB2 probe with an evident formation of two complexes (bands 1 and 2) at 3 h post-

infection (Figure 4.6D). Again, the intensity of binding peaked at 6 h with a gradual decrease between 9-12 h post-infection.

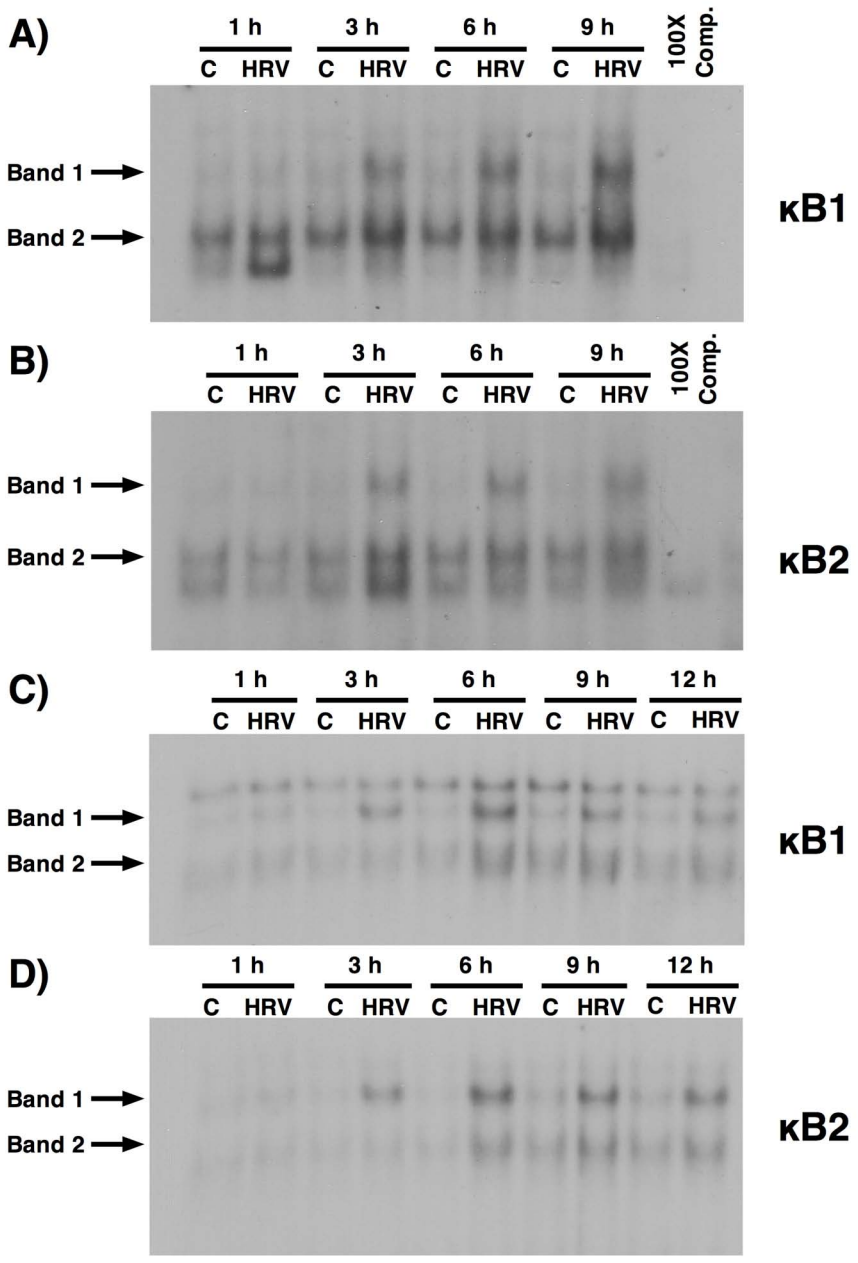

Figure 4.6 – HRV-16 induces time-dependent binding on the CXCL10 NF-κB recognition sequences. BEAS-2B **(A & B)** and HBE **(C & D)** were infected with HRV-16 for the indicated time points. Nuclear protein extracts were prepared and incubated with [γ-^{32}P]-labeled CXCL10-specific κB1 **(A & C)** or κB2 **(B & D)** probe. Samples were resolved using non-SDS/PAGE and analyzed by autoradiography. Each blot is

representative of three separate experiments. 100X Cold Comp. indicates the presence of 100-fold excess κB1 or κB2 cold probe. Specific complexes are indicated by arrows. Medium control is abbreviated as C.

Having shown HRV-16-induced time-dependent formation of complexes with both κB oligonucleotides, we next determined the effect of MEK1/2 pathway inhibition. In BEAS-2B cells, neither PD98059 (10 μM) nor U0126 (3 μM) enhanced the intensity of the complexes formed with the κB1 oligonucleotide at 3 h post-infection (Figure 4.7A). In fact, there was slight reduction in band intensity on κB1 of the lower complex (band 2) with pre-treatment with either inhibitor. Pre-treatment with either PD98059 or U0126 without the presence of virus slightly increased the intensity of the lower complex (band 2), but had no effect on the upper complex (band 1). Similarly in HBE, the intensity of two prominent complexes formed with κB1 oligonucleotide 6 h post-infection was not enhanced with PD98059, although there was a consistent and slight increase in the binding of the upper complex (band 1) in the presence of U0126 compared to virus alone (Figure 4.7C). Pre-treatment with the inhibitors alone slightly increased the intensity of the lower band (band 2) compared to control levels.

To determine the protein components comprising the HRV-16-induced complexes formed on κB1, supershift experiments were performed using antibodies to individual Rel family proteins. Addition of antibody to p50 clearly shifted both the upper and lower complexes in both BEAS-2B cells and HBE compared to virus alone (Figures 4.7B & D). Only the upper complex was shifted with antibody to p65 in both cell types, suggesting that the upper band comprised the canonical p50-p65 heterodimer, which we have

previously demonstrated to be induced in HRV-16 infected cells[143,236]. The addition of antibodies to p52 or c-Rel were without effect in either cell type.

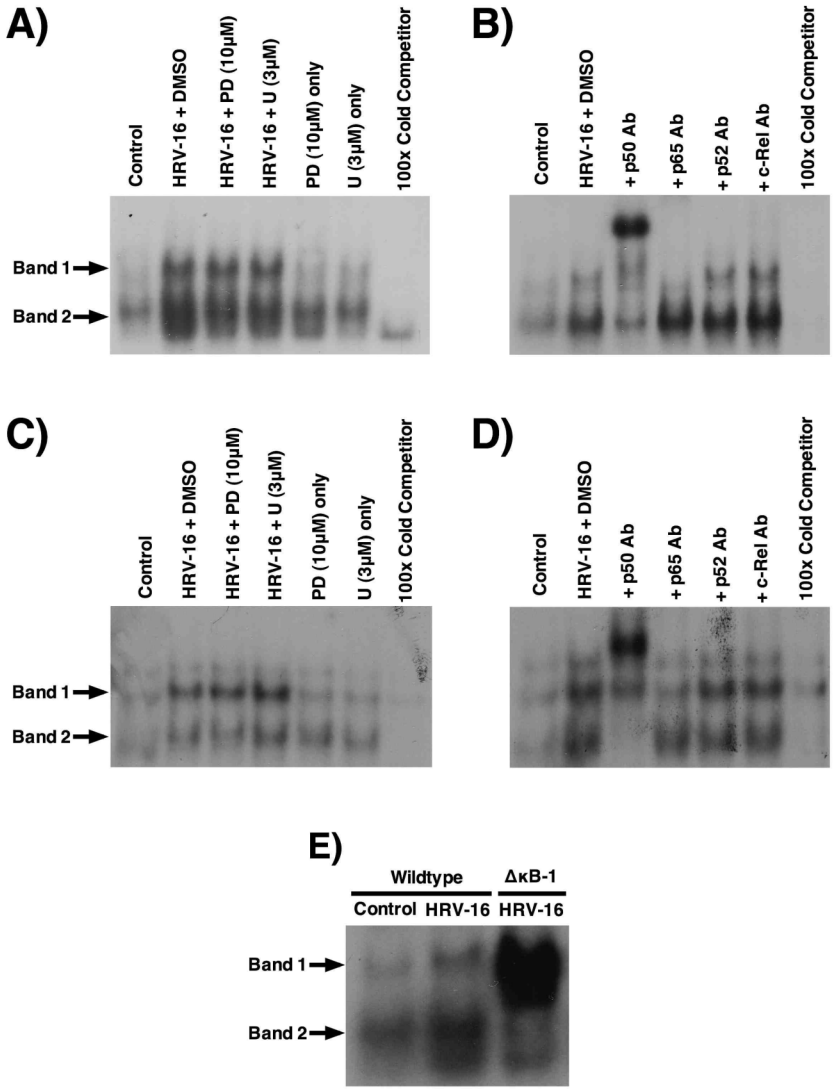

Figure 4.7 – Inhibition of the MEK1/2 pathway does not enhance HRV-16-induced NF-κB nuclear translocation and/or binding to the CXCL10 κB1 recognition sequence. BEAS-2B **(A)** or HBE **(C)** were pre-incubated with DMSO (0.1% v/v), PD98059 (10 μM), or U0126 (3 μM) for 1 h and infected with HRV-16 for 3 or 6 h, respectively. Nuclear protein extracts were prepared and incubated with [γ-^{32}P]-labeled CXCL10-specific κB1 probe. Samples were resolved using non-SDS/PAGE and analyzed by autoradiography. Supershift analysis was carried out using nuclear extracts from HRV-16 plus DMSO-infected BEAS-2B **(B)** or HBE **(D)** cells. Extracts were pre-

incubated with Rel family antibody 2 h before addition of probe. 100X Cold Comp. indicates the presence of 100-fold excess κB1 cold probe. **E)** Nuclear extracts from HRV-16 infected BEAS-2B cells were incubated with mutant κB1 probe. Blots are representative of three separate experiments.

A CXCL10-specific κB1 probe (see section 2.2.11.3 for details) was generated containing the same point mutations in the 376-bp ΔκB1 promoter luciferase construct to confirm the specificity of p50 and p65 binding and to also correlate this binding to CXCL10 promoter studies. In BEAS-2B cells, HRV-16-induced binding of p50 homodimers (band 2) 3 h post-infection was clearly diminished with the mutant oligonucleotide compared to wildtype (Figure 4.7E). Loss of p50/p65 heterodimer (band 1) binding was difficult to ascertain given the formation of a unidentified and prominent complex.

Similar to results with the κB1 recognition sequence, pre-incubation with either PD98059 (10 μM) or U0126 (3 μM) did not markedly enhance HRV-16-induced formation of either of the complexes formed with the κB2 recognition sequence, in either BEAS-2B cells or HBE (Figures 4.8A & C). In contrast to κB1, pre-treatment with either inhibitor without HRV-16 did not increase the binding intensity of the complexes compared to control levels in BEAS-2B cells or HBE. Supershift experiments in both cell types showed that addition of antibody to p50 clearly shifted both of the complexes, but p65 Ab only shifted the upper compex (band 1) compared to HRV-16 alone (Figures 4.8B & D). Addition of antibody to p52 or c-Rel did not affect the intensity of binding in either BEAS-2B cells or HBE. It must noted that the addition of antibodies prior to incubation with radiolabeled probe, in addition to supershifting the NF-κB complexes,

may have also prevented p50 and/or p65 binding to the radiolabeled oligonucleotide by blocking the epitope that specifically recognizes the κB1 or κB2 DNA binding sequence. Nonetheless, these results suggested that both κB1 and κB2 were bound by the same set of Rel proteins, specifically p50/p65 heterodimers and p50 homodimers, though inhibition of the MEK1/2 pathway did not markedly enhance the binding of these proteins to either NF-κB recognition sequence. HRV-16-induced binding of p50 and p65 3 h post-infection to mutant κB2 oligonucleotide was lost (Figure 4.7E). These data suggest that loss of p50 and p65 binding is associated with the loss of κB-dependent HRV-16-induced CXCL10 promoter activity, but do not play a role in the MEK1/2 pathway-mediated negative regulation of CXCL10.

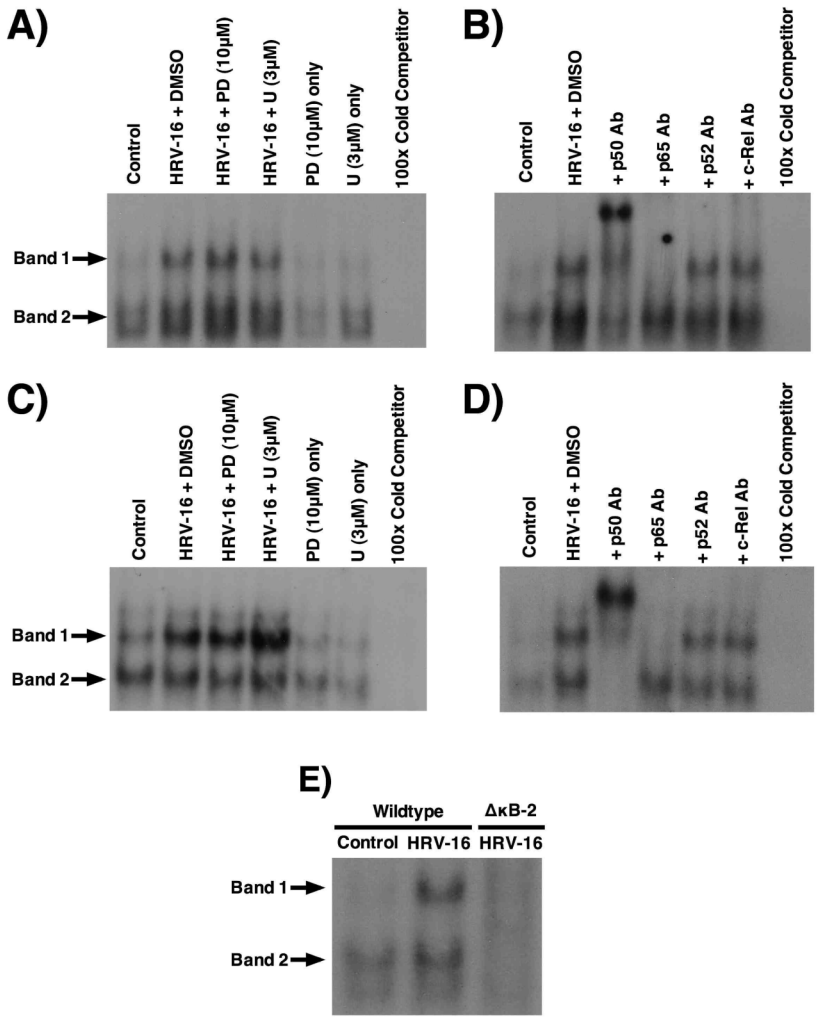

Figure 4.8 – Inhibition of the MEK1/2 pathway does not enhance HRV-16-induced NF-κB nuclear translocation and/or binding to the CXCL10 κB2 recognition sequence. BEAS-2B **(A)** or HBE **(C)** were pre-incubated with DMSO (0.1% v/v), PD98059 (10 μM), or U0126 (3 μM) for 1 h and infected with HRV-16 for 3 or 6 h, respectively. Nuclear protein extractions were prepared and incubated with [γ-^{32}P]-labeled CXCL10-specific κB2 probe. Samples were resolved using non-SDS/PAGE and analyzed by autoradiography. Supershift analysis was carried out using nuclear extracts from HRV-16 plus DMSO-infected BEAS-2B **(B)** or HBE **(D)** cells. Extracts were pre-incubated with Rel family antibody 2 h before addition of probe. 100X Cold Comp. indicates the presence of 100-fold excess κB2 cold probe. **E)** Nuclear extracts from HRV-16-infected BEAS-2B cells were incubated with mutant κB2 probe. Blots are representative of three separate experiments.

Thus far, we have shown that inhibition of the MEK1/2 pathway does not enhance HRV-16-induced κB1 or κB2 tandem repeat construct luciferase activity. In addition, MEK1/2 pathway inhibition does not enhance HRV-16-induced NF-κB nuclear translocation and/or binding to the recognition sequences in the CXCL10 promoter. Activation of the classical NF-κB pathway (p50 and p65) occurs through IKKβ-mediated phosphorylation, ubiquitination, and degradation of IκBα (Figure 1.5). Furthermore, HRV-16-induced CXCL10 expression in human airway epithelial cells is dependent on IKKβ, based on studies using selective small molecule inhibitors of this enzyme[368]. To further confirm that the MEK1/2 pathway does not modulate NF-κB signaling, the effect of PD98059 and U0126 on the phosphorylation and degradation of IκBα was assessed. HRV-16 infection of BEAS-2B cells resulted in a time-dependent phosphorylation of IκBα, starting as early as 1 h post-infection, with peak phosphorylation at 3 h post-infection and a subsequent decrease by 6 h (Figures 4.9A & B). HRV-16-induced degradation of total IκBα was evident at 2 h post-infection with a reversal of degradation by 6 h. Pre-treatment with either PD98059 (10 μM) or U0126 (3 μM) did not markedly alter HRV-16-induced IκBα phosphorylation or degradation at any of the time points (Figures 4.9A & B). Taken together, these data further support the concept that the MEK1/2 pathway does not modulate HRV-16-induced NF-κB activation or p50/p65 translocation/binding to the CXCL10-specific κB1 or κB2 recognition sequences.

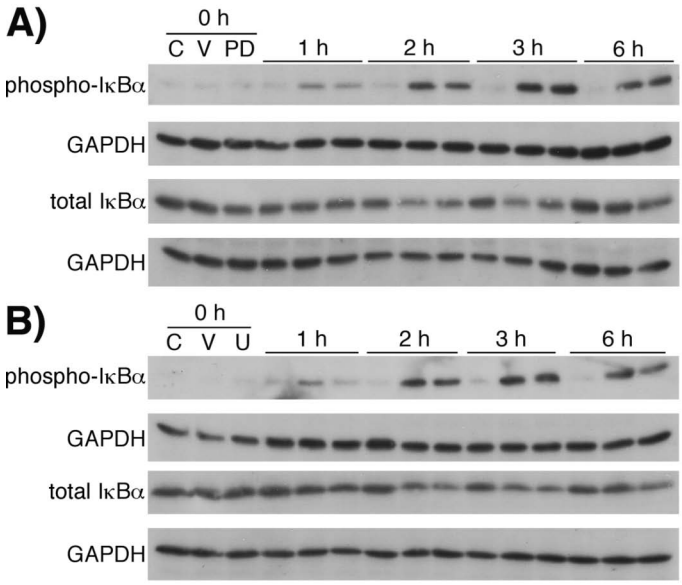

Figure 4.9 – Inhibitors of the MEK1/2 pathway do not affect HRV-16-induced phosphorylation or degradation of IκBα. A) BEAS-2B cells were pre-incubated with 0.1% v/v DMSO or 10 μM PD98059 (PD) for 1 h followed by HRV-16 (V) infection for the indicated time points. Whole cell lysates were collected and immunoblotted with phospho-specific or total IκBα antibody. **B)** Cells pre-treated with 3 μM U0126 (U) were also assessed for any effects on IκBα. Membranes were stripped and re-probed with antibody to GAPDH to ensure equal protein loading. Immunoblots are representative of three separate experiments. Medium control is abbreviated as C

4.3.3 Evaluation of the interactions at the ISRE site in MEK1/2 pathway-mediated modulation of HRV-16-induced CXCL10 expression

In order to study the role of the ISRE site in MEK1/2 pathway-mediated enhancement of HRV-16-induced CXCL10 expression, a promoter-luciferase construct was generated containing five tandem copies of the CXCL10-specific ISRE recognition sequence. Surprisingly, HRV-16 infection did not induce activation of this construct (data not shown). Previous reports have speculated that there is a cooperativity between the κB and ISRE sites within both the CXCL10 and CCL5 promoters during virus-induced gene expression[388,421]. Thus, it is possible that the ISRE site contributes to the activation of CXCL10 only when present in conjunction with an NF-κB site. Therefore,

a double mutant was generated in the 376-bp CXCL10 promoter construct where both the AP-1 and κB2 recognition sequences were mutated, leaving only functional κB1 and ISRE binding sites (Figure 4.1B). HRV-16 induced the activity of the double mutant (3.4 ± 0.5 fold increase) and wildtype construct (3.8 ± 0.9 fold increase) almost equally (Figure 4.10). Interestingly, the level of enhancement between the two promoter constructs after MEK1/2 inhibition with PD98059 (10 μM) or U0126 (3 μM) was nearly identical.

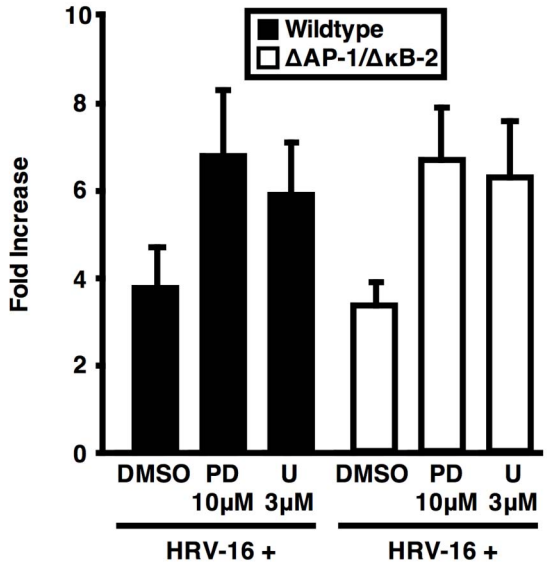

Figure 4.10 – CXCL10 promoter activity containing only functional κB1 and ISRE binding sites is enhanced upon MEK1/2 pathway inhibition. BEAS-2B cells were transiently transfected with 1.0 μg of either the 376 bp truncated wildtype CXCL10 promoter (black) or truncated CXCL10 promoter containing mutations in both AP-1 and κB2 sites (white). Transfected cells were pre-incubated with DMSO (0.1% v/v), PD98059 (10 μM) or U0126 (3 μM) for 1 h followed by HRV-16 or mock infection for 24 h. Lysates from triplicate wells were assayed for firefly activity and calculated as fold increase compared to control wells. Data are expressed as mean ± SEM (n = 4).

Experiments were then performed to determine the kinetics of HRV-16-induced transcription factor binding to a radiolabeled CXCL10-specific ISRE probe using EMSA analysis (see section 2.2.11.3 for details). In BEAS-2B cells, HRV-16 induced the formation of a complex (band 1) with weak intensity at 3 h post-infection and the appearance of additional complexes (bands 2 & 3) occurred at 6 and 9 h post-infection (Figure 4.11A). In HBE, HRV-16 induced the binding of various complexes at 6 h post-infection with peak intensity between 9 and 12 h post-infection (Figure 4.11B). Similar to time courses using κB1 or κB2 oligonucleotides, a difference in binding kinetics was apparent between BEAS-2B cells and HBE.

Based on the time course data, the effects of MEK1/2 pathway inhibition were examined using nuclear extracts from BEAS-2B cells (6 h post-infection) and HBE (9 h post-infection). In BEAS-2B cells (Figure 4.12A), both PD98059 (10 μM) and U0126 (3 μM) enhanced the intensity of the uppermost complex (band 1), with no consistent effects on the lower complexes (bands 2 and 3). Densitometric analysis revealed that both PD98059 and U0126 significantly (p <0.02 in both cases) increased the intensity of band 1 to 190% ± 20% and 190 ± 30% compared with HRV-16 alone (100% baseline intensity), respectively. The intensity of band 2 was not significantly increased by either PD98059 (91 ± 16%) or U0126 (126 ± 43%) compared to HRV-16 alone. Also, the intensity of band 3 was not significantly enhanced by PD98059 (120 ± 19%) or U0126 (84 ± 22%) compared to virus alone. In HBE, both PD98059 and U0126 enhanced the binding of band 1 compared to virus alone (Figure 4.12C). Densitometric analysis of band 1 revealed that PD98059 increased the intensity to 178 ± 18% while U0126

increased band intensity to 317 ± 100% compared to HRV-16 alone. Binding intensity of band 3 was enhanced by both PD98059 (280 ± 63%) and U0126 (383 ± 63%) compared to virus alone.

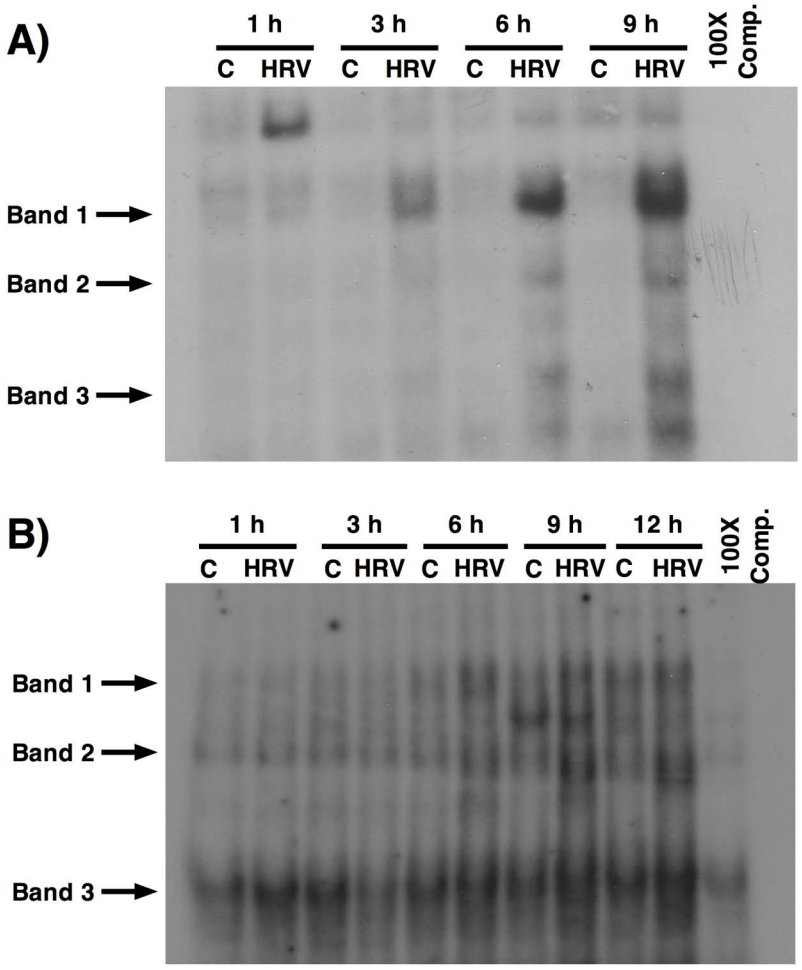

Figure 4.11 - HRV-16 induces time-dependent binding on the CXCL10 ISRE recognition sequence. BEAS-2B **(A)** and HBE **(B)** were infected with HRV-16 for the indicated time points. Nuclear protein extracts were prepared and incubated with [γ-^{32}P]-labeled CXCL10-specific ISRE probe. Samples were resolved using non-SDS/PAGE and analyzed by autoradiography. Each blot is representative of three separate experiments. 100X Cold Comp. indicates the presence of 100-fold excess ISRE cold probe. Specific complexes are indicated by arrows. Medium control is abbreviated as C.

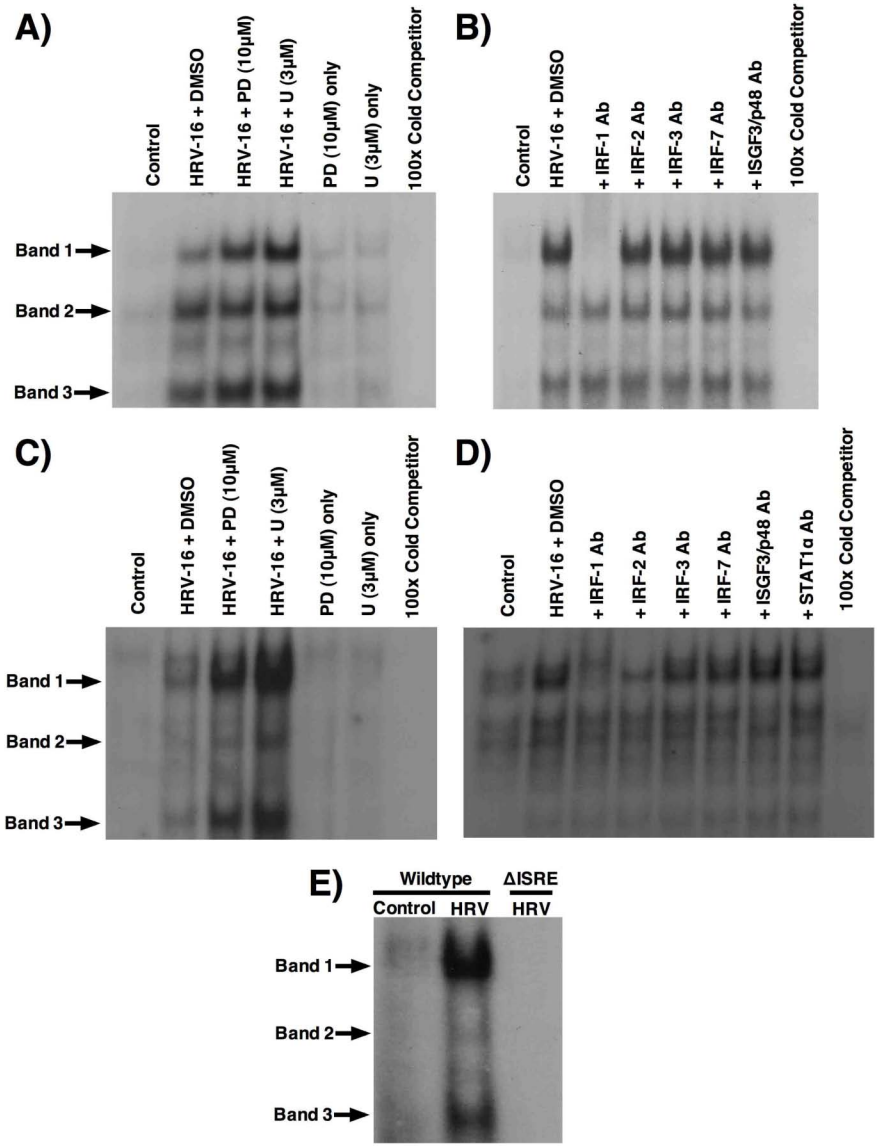

Figure 4.12 – Inhibition of the MEK1/2 pathway enhances HRV-16-induced IRF-1 nuclear translocation and/or binding to the CXCL10 ISRE recognition sequence. BEAS-2B **(A)** or HBE **(C)** were pre-incubated with DMSO (0.1% v/v), PD98059 (10 μM), or U0126 (3 μM) for 1 h and infected with HRV-16 for 6 or 9 h, respectively. Nuclear protein extractions were prepared and incubated with [γ-^{32}P]-labeled CXCL10-specific ISRE probe. Samples were resolved using non-SDS/PAGE and analyzed by autoradiography. Supershift analysis was carried out using nuclear extracts from HRV-16 plus DMSO-infected BEAS-2B **(B)** or HBE **(D)** cells. Extracts were pre-incubated with IRF or STAT family antibody 2 h before addition of probe. 100X Cold Comp. indicates the presence of 100-fold excess ISRE cold probe. **E)** Nuclear extracts from HRV-16-infected BEAS-2B cells were incubated with mutant ISRE probe. Blots are representative of three separate experiments.

Supershift analysis demonstrated that addition of antibody to IRF-1 completely shifted band 1 in BEAS-2B cell extracts (Figure 4.12B). Bands 2 and 3 remained unidentified as they were unaffected by the addition of antibodies to IRF-1, IRF-2, IRF-3, IRF-7, and interferon-stimulated gene factor-3 (ISGF3/p48). In HBE, addition of antibody to IRF-1 shifted the lower portion of band 1 that corresponds to one of the two enhanced bands with MEK1/2 pathway inhibition (Figure 4.12D). However, in HBE, the addition of antibody to IRF-2 clearly shifted all parts of band 1, suggesting that at least a portion of the band is an IRF-1/IRF-2 heterodimer. Band 2 was shifted with the addition of antibody to ISGF3/p48, but addition of antibodies to IRF-3, IRF-7, or STAT1α did not shift any of the bands. Band 3 was not shifted with the addition of any of the antibodies used, though it was clearly enhanced with PD98059 and U0126. Supershift analysis was performed to confirm the identity of the enhanced band (Figure 4.12) seen with PD98059 and U0126 treatment in both BEAS-2B cells and HBE. Antibody to IRF-1 was added to nuclear extracts pre-treated with PD98059 or U0126. In both BEAS-2B cells and HBE, antibody to IRF-1 shifted the enhanced band to a similar degree as the IRF-1 band in HRV-16 alone extracts (Figures 4.13A & B).

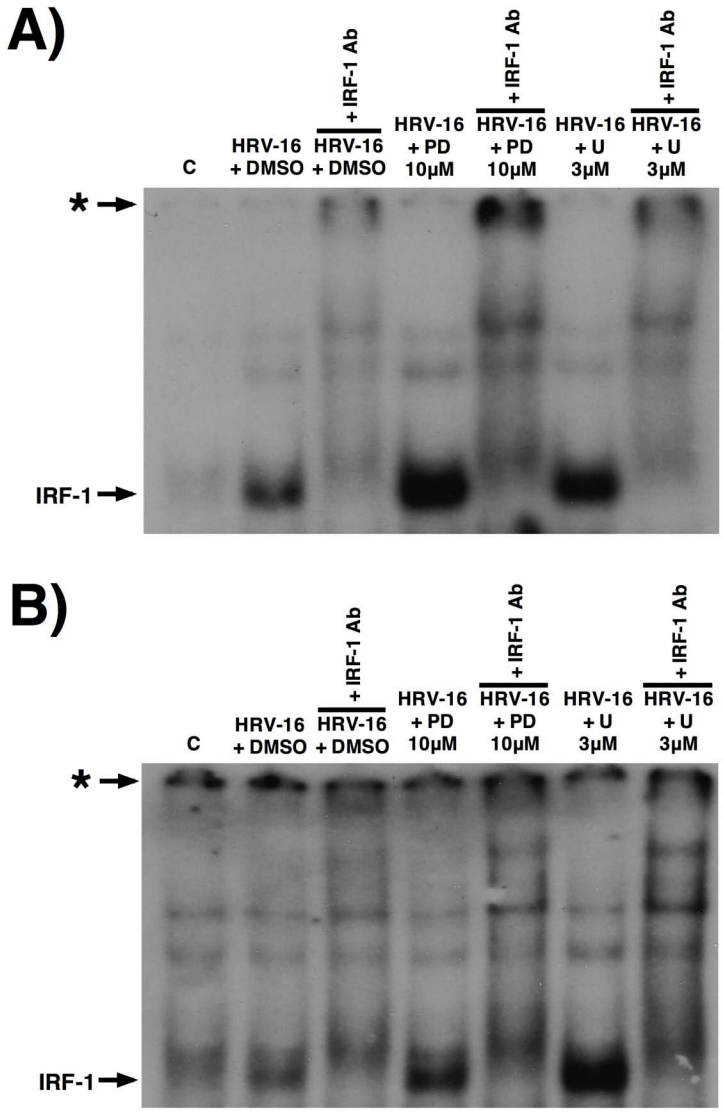

Figure 4.13 – Effects of IRF-1 supershift antibody on enhanced HRV-16-induced IRF-1 binding to CXCL10 ISRE recognition sequence. IRF-1 supershift antibody was added to nuclear extracts from BEAS-2B **(A)** or HBE **(B)** cells pre-incubated with PD98059 (10 μM) or U0126 (3 μM) followed by HRV-16 infection for 6 or 9 h, respectively. Samples were incubated with [γ-^{32}P]-labeled CXCL10-specific ISRE probe and analysed by EMSA. IRF-1 is indicated by arrow and asterisk indicates loading wells. Blots are representative of three separate experiments.

To correlate the results of EMSA analysis with promoter-luciferase data, a mutant ISRE oligonucleotide (see section 2.2.11.3 for details) with mutations similar to those introduced in the ISRE site of the 376-bp construct was created. In BEAS-2B cells, HRV-16-induced complex binding was completely lost with the ISRE mutant oligonucleotide compared to wildtype (Figure 4.12F). Overall, these data show that in airway epithelial cells HRV-16 induces IRF-1 nuclear translocation and/or binding to the ISRE recognition site in the CXCL10 promoter and its interaction with the ISRE is enhanced upon inhibition of the MEK1/2 pathway.

4.4 Discussion

It has been shown that HRV-16-induced CXCL10 expression is regulated at the level of transcription, in part through the actions of NF-κB[143,236]. This chapter further explored the effects of MEK1/2 pathway inhibition on HRV-16-induced CXCL10 expression with specific focus on transcriptional activation. Pharmacologic inhibition of the MEK1/2 pathway with either PD98059 or U0126, in a concentration-dependent manner, enhanced activation of a 972-bp full length CXCL10 promoter-luciferase construct compared to activation by HRV-16 plus DMSO alone. This demonstrated that MEK1/2 pathway inhibition enhances HRV-16-induced CXCL10 expression, at least in part, through transcriptional effects.

The transcription factor binding sites involved in the MEK1/2 pathway-mediated enhancement of CXCL10 transcription were contained within the 376-bp truncated CXCL10 promoter-luciferase construct. Consistent with previous studies[143,236], mutation of either the κB1 or κB2 recognition sites for NF-κB reduced HRV-16-induced promoter

activation, although to variable degrees. Importantly, it was also shown that the ISRE site is also critical for HRV-16-induced CXCL10 promoter activation and the MEK1/2 pathway-mediated enhancement of CXCL10 transcription. The MEK-ERK pathway has been shown to modulate NF-κB-dependent gene expression through alterations in basal transcription factors binding to the TATA box[371], but basal transcription was not altered by virus or inhibitors.

NF-κB did not seem to be involved in the MEK1/2 pathway-mediated down-regulation of HRV-induced CXCL10 expression, as assessed by various approaches. Analysis of the mutated κB1 oligonucleotide sequence determined that the point mutations eliminated the presence of a highly conserved NF-κB consensus binding site compared to the wild-type sequence. Instead, a new consensus sequence specific for octamer binding proteins was formed. This family of transcription factors, specifically Oct4, have been implicated in stem cell pluripotency and mammalian development[422,423], but have not been shown to play a role in virus-induced chemokine expression in airway epithelial cells. Studies with the κB1 and κB2 recognition sequences showed nearly identical trends, including roles in CXCL10 promoter drive by HRV-16 and the lack of any marked changes in NF-κB translocation and/or binding in the presence of MEK1/2 pathway inhibitors. Additionally, HRV-16 did not induce promoter drive of a construct containing tandem copies of mutant κB1 sequences (unpublished observation). Therefore, the formation of the new complex on the mutant κB1 radiolabeled probe is merely due to the chance formation of a new consensus binding site for a protein not involved in the expression or negative regulation of CXCL10 by HRV-16.

Studies using the ISRE recognition sequence found that HRV-16-induced IRF-1 nuclear translocation and/or binding was enhanced upon MEK1/2 pathway inhibition in both BEAS-2B cells and HBE. The similar IRF-1 results in BEAS-2B cells and HBE again suggests the negative regulation of HRV-inducible chemokine expression is a conserved mechanism and is not unique to a certain cell type. Furthermore, the MEK1/2 pathway-mediated enhanced IRF-1 band completely shifted in the presence of IRF-1 antibody, confirming that, indeed, the binding of IRF-1 is enhanced upon MEK1/2 pathway inhibition. Even though the contribution of ISRE to HRV-induced CXCL10 promoter activity required the presence of a functional κB site, the current data confirm that negative regulation of HRV-16-induced CXCL10 expression is solely mediated through the ISRE.

Although HRV-16-induced IRF-1 nuclear translocation and/or binding was enhanced upon MEK1/2 pathway inhibition, a clear difference between BEAS-2B cells and HBE was evident. As previously mentioned, IRF-2 binding was detected in HBE, but not in BEAS-2B cells. Interestingly, the HRV-induced band that is enhanced upon MEK1/2 pathway inhibition contained an IRF-1/IRF-2 heterodimer, thus raising the possibility that IRF-2 binding, in addition to IRF-1, is enhanced at the ISRE reconigition sequence in HBE. Since the band above the enhanced band was found to shift only with IRF-2 antibody, but was not enhanced upon MEK1/2 pathway inhibition, in addition to the observation that the enhanced band is entirely shifted with IRF-1 antibody suggested that IRF-2 binding is not necessarily enhanced like IRF-1. Additionally, ISGF-3 was not detected in BEAS-2B cells, but was evident in HBE using the same ISRE recognition sequence. The transcription factors involved in the positive regulation of HRV-16-

induced CXCL10 expression seem to be divergent in either cell type as evidenced by the supershift experiments, but both cell types share the common observation that MEK1/2 pathway-mediated regulation of IRF-1 interactions with the ISRE is associated with the negative regulation of HRV-16-induced CXCL10 expression.

Although the lowermost band in HBE was enhanced with MEK1/2 pathway inhibition, the identity of this band could not be determined with antibodies against IRF-1, IRF-2, IRF-3, IRF-7, ISGF-3, or STAT1α. It is possible that the lower band is a degraded fragment of IRF-1 as it has been shown that IRF-2, which closely resembles IRF-1, can undergo proteolytic cleavage and still retain promoter binding capacity similar to that of the uncleaved form[424-426]. In this regard, IRF-1 protein is known to undergo 26S proteasome-mediated cleavage[427]. Interestingly, IRF-2 is not present or does not bind ISRE in BEAS-2B cells. Given that the IRF-1 antibody used recognizes the C-terminal domain, while the N-terminal domain is required for DNA binding[428], it is possible that an IRF-1 cleavage product maintains a DNA binding capability, but is not susceptible to supershift due to the loss of the C-terminal epitope.

In summary, the data demonstrate that pharmacologic inhibition of the MEK1/2 pathway enhances HRV-16-induced expression of CXCL10 via effects on transcription. Though transcriptional up-regulation of HRV-16-induced CXCL10 requires both the κB and ISRE sites, the MEK1/2 pathway-mediated negative regulation of HRV-16-induced CXCL10 expression appears only to involve the modification of IRF-1 interactions with the ISRE site found within the CXCL10 promoter and is independent of effects on NF-κB.

Chapter Five: The effects of MEK1 and MEK2 siRNA-mediated knockdown on HRV-16-induced CXCL10 expression in human airway epithelial cells

5.1 Introduction

In the preceding chapters, it was shown that HRV-16-induced CXCL10 expression was enhanced upon pharmacologic inhibition of the MEK1/2 pathway via effects on transcription. This enhancement was associated with altered IRF-1 nuclear translocation and/or binding to the ISRE recognition sequence in the CXCL10 promoter. Importantly, two structurally distinct and specific inhibitors of MEK1/2, PD98059[404] and U0126[342], were used to delineate this mechanism. The level of enhancement using either inhibitor was nearly identical. Though the specificity of PD98059 and U0126 has been extensively characterized[342,404,415], a non-pharmacologic approach targeting the MEK-ERK pathway was considered important to corroborate and extend the observations from the previous chapters. In addition, the relative contribution of MEK1 and/or MEK2 in the negative regulation of CXCL10 could not be definitively assessed using pharmacologic approaches, since both PD98059 and U0126 inhibit MEK1/2 activity, albeit to different degrees[342,404].

First discovered in the nematode *Caenorhabditis elegans*, RNA interference (RNAi) was demonstrated when gene expression was shown to be silenced with the introduction of short double-stranded RNA (dsRNA) into cells[429]. RNAi has now been shown to be an evolutionarily conserved mechanism in eukaryotes that serves to control gene expression by translational silencing and more recently, transcriptional silencing through DNA methylation[430-434]. It has also has been shown to have an important role in

host defense during viral infection[435-438]. The discovery of RNAi is now widely exploited to permit a more in-depth study of cellular processes through the introducton of short interfering RNA (siRNA) duplexes into mammalian cells that silence gene expression by binding to a complementary mRNA sequence[430]. The similarities and differences of RNAi versus pharmacologic inhibition are described in Table 5.1. The validity of this approach has improved since its initial discovery, but concerns remain, such as variable "off-target" effects. It has been shown that siRNA knockdown of a specific target may result in different phenotypic responses between the various siRNAs used[439]. This may be due, in part, to the induction of siRNA-specific transcriptional profiles that create different siRNA-specific cellular environments and may hinder the interpretation of results[440,441]. To improve the validity of siRNA techniques, modifications have been introduced such as changes in siRNA base pair length or removal of 5' phosphates to prevent the activation of dsRNA-induced anti-viral interferon responses via activation of PRRs, including PKR or RIG-I[187,430,442,443].

This chapter focuses on the use of siRNA to confirm the results from Chapters 3 and 4, and to further delineate the role of the MEK-ERK pathway in the negative regulation of HRV-16-induced CXCL10 expression. It was hypothesized that siRNA knockdown of MEK1 and MEK2 would enhance HRV-16-induced expression of CXCL10 and the nuclear translocation and/or binding of IRF-1 to the CXCL10 ISRE promoter site.

Table 5.1 – Comparison of RNAi versus pharmacological inhibitors

	RNAi	**Inhibitors**
Mechanism of action	-mRNA degradation -Inhibition of translation -Epigenetic modification	-Substrate competition -Covalent modification -Ligand competition -Protein conformational changes -Allosteric binding
Cellular Outcome	-Removal of transcript and loss of protein over many hours	-Immediate inhibition of protein active site -Competition with ligand -Conformational changes in protein
Specificity issues	-Sequence homology (sense and antisense) -miRNA mimic or competition -Protein complex disruption -Epigenetic effects -Dosage	-Binding site homology -Dosage
Utility	-Novel target finding -Pathway analysis -Target validation -Therapeutics	-Pathway analysis -Target validation -Therapeutics

5.2 Results

5.2.1 Selective MEK1 siRNA knockdown enhances HRV-16-induced CXCL10 protein production in BEAS-2B cells

Two different siRNA sequences designed to target MEK1 or MEK2 (designated duplex A and duplex B in each case) were used to assess any effect on HRV-16-induced CXCL10 expression. In BEAS-2B cells, preliminary experiments determined that the optimal time for knockdown of MEK1 and MEK2 protein was 72 h post-transfection (data not shown). Furthermore, it was determined that neither the lipid transfection

reagent nor control siRNA altered MEK1 or MEK2 protein levels compared to the medium alone control. Transfection of 30 nM MEK1 duplex A or duplex B siRNA knocked down MEK1 protein levels compared to control siRNA (Figure 5.1A). Using densitometric analysis, the expression of MEK1 protein was significantly ($p < 0.0001$ in both cases) reduced in the presence of both MEK1 duplex A (87.6% ± 1.5% MEK1 knockdown) and duplex B (82.2% ± 0.4% MEK1 knockdown) compared to control siRNA (Figure 5.1B). Surprisingly, MEK1 duplex B significantly ($p < 0.05$) reduced MEK2 protein levels (60.4% ± 24.2% MEK2 knockdown), but MEK1 duplex A did not significantly alter MEK2 protein (20.5% ± 23.9% MEK2 knockdown) compared to control siRNA (Figures 5.1C & D). Transfection of both MEK1 duplexes also significantly ($p < 0.0001$) abrogated MEK1 protein expression (88.8% ± 1.2% MEK1 knockdown) and MEK2 protein expression (44.0% ± 16.6% MEK2 knockdown) compared to control siRNA (Figures 5.1A-D).

As expected, both MEK2 duplex A (95.3% ± 1.1% MEK2 knockdown) and B (95.3% ± 0.9% MEK2 knockdown) significantly ($p < 0.05$) reduced MEK2 protein levels to an identical degree (Figures 5.1C & D). MEK2 protein (93.2% ± 1.8% knockdown) was significantly ($p < 0.0001$) reduced in the presence of both MEK2 duplexes compared to control siRNA. Interestingly, MEK1 protein levels were modestly, but significantly ($p < 0.05$), enhanced with transfection of either MEK2 duplex A to 138.1% ± 18.3% of basal MEK1 expression or duplex B to 129.7% ± 8.6% of basal MEK1 expression compared to control siRNA (Figure 5.1B). When used in combination, the MEK2 siRNA duplexes also enhanced MEK1 protein to 121% ± 1.1% of basal MEK1 expression, but this was

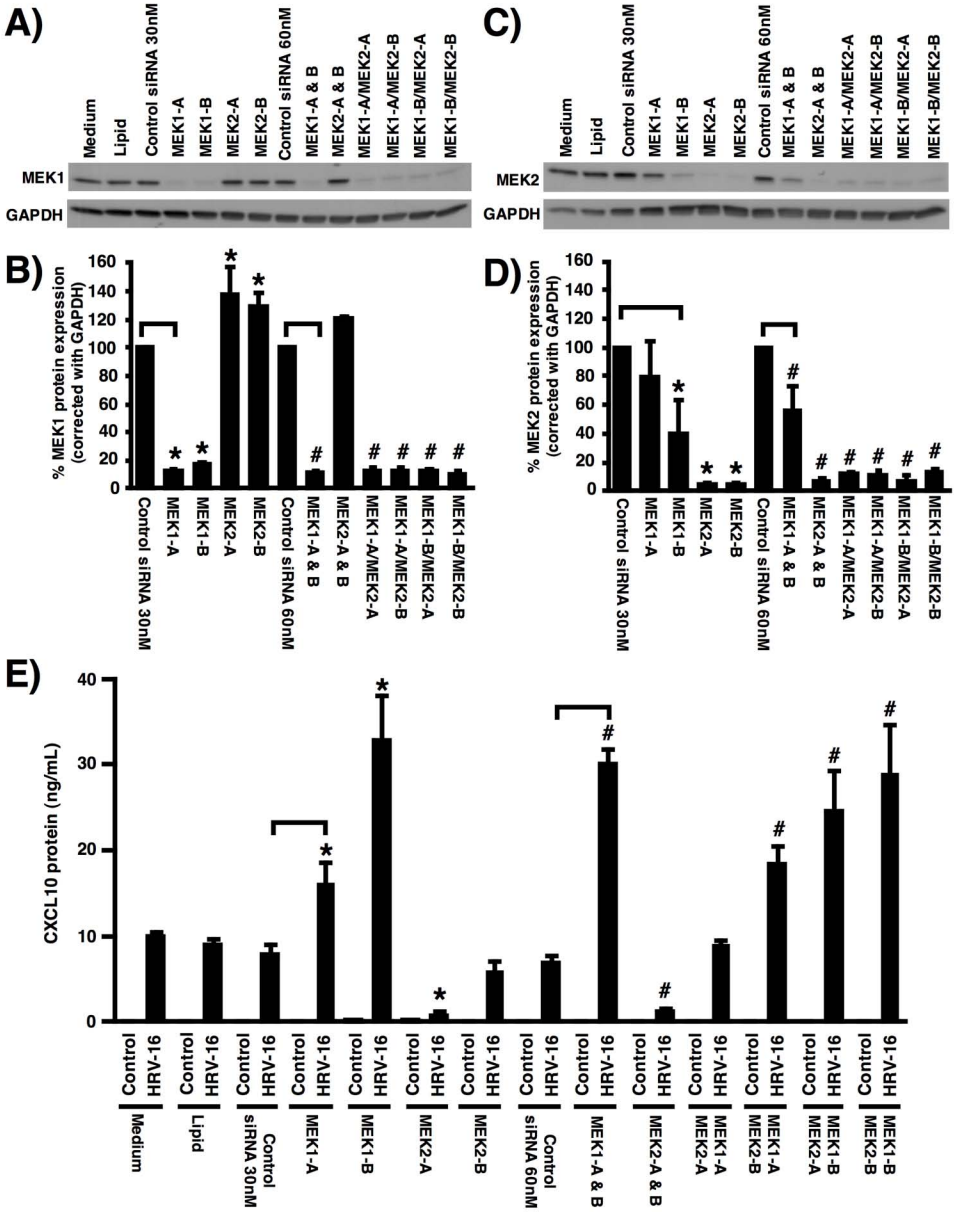

Figure 5.1 – Selective knockdown of MEK1 enhances HRV-16-induced CXCL10 expression in BEAS-2B. The effect of 30 nM MEK1 and MEK2 siRNA duplexes, individually or in combination, on MEK1 **(A)** and MEK2 **(B)** protein expression (72 h post-transfection) was assessed by immunoblotting (n = 3). Densitometric analysis of MEK1 **(C)** and MEK2 **(D)** protein expression compared to control siRNA. **E)** Assessment of HRV-16-induced CXCL10 protein release 24 h post-infection in the presence of MEK siRNA by ELISA (n = 4). Significant differences compared to 30 nM (*) or 60 nM (#) control siRNA were assessed with one way ANOVA followed by Fisher's least significant difference test. Lipid reagent and medium alone were used as

appropriate controls. Immunoblots were stripped and re-probed with GAPDH to ensure equal loading.

not statistically significant. Transfection of each formulation of combinations of MEK1 and MEK2 duplexes significantly (p <0.01 in all cases) reduced both MEK1 and MEK2 protein compared to control siRNA (Figures 5.1A-D). HRV-16-induced CXCL10 protein release was not markedly altered in the presence of either lipid transfection reagent or control siRNA when compared to medium only control. Selective knockdown of MEK1 protein significantly enhanced HRV-16-induced CXCL10 protein production using either MEK1 duplex A (p <0.05), MEK1 duplex B (p <0.0001) or both duplexes combined (p <0.0001) compared to control siRNA (Figure 5.1E). In contrast, HRV-16-induced CXCL10 protein production was significantly reduced in the presence of MEK2 duplex A (p <0.0001) or the combination of both duplexes (p <0.05), but was not altered using MEK2 duplex B alone. Surprisingly, the combination of MEK1 duplex A and MEK2 duplex A did not alter HRV-16-induced CXCL10 protein production compared to control siRNA. All other combinations of MEK1 and MEK2 duplexes, however, significantly (p <0.05 in all cases) enhanced HRV-16-induced CXCL10 protein release (Figure 5.1E). In BEAS-2B cells, the knockdown of MEK1 appears to essentially reproduce the data seen with pharmacologic inhibition of the MEK1/2 pathway, but potential crosstalk between these pathways cannot be ruled out given the effects of MEK1 siRNA on MEK2 expression.

5.2.2 Selective MEK1 siRNA knockdown enhances HRV-16-induced CXCL10 protein production in HBE cells

Having shown that selective knockdown of MEK1 in BEAS-2B cells enhanced HRV-16-induced CXCL10 protein expression, similar experiments using only the MEK1 duplexes were carried out in HBE to confirm this main finding in a more physiologically relevant model. Transfection of MEK1 siRNA resulted in significant (p <0.0001 in all cases) knockdown of MEK1 protein expression using duplex A (84.2% ± 1.1% MEK1 knockdown), duplex B (86.2% ± 3.0% MEK1 knockdown) or both duplexes (82.0% ±0.7% MEK1 knockdown) compared to control siRNA (Figures 5.2A & B). Similar to the results in BEAS-2B cells, MEK2 protein expression was significantly (p <0.0001 in both cases) reduced by MEK1 duplex B (73.1% ± 6.8% MEK2 knockdown) or combination of MEK1 duplexes (75.0% ± 3.5% MEK2 knockdown) compared to control siRNA (Figures 5.2A & B). Transfection of MEK1 duplex A did not markedly alter MEK2 protein expression. Interestingly, the pattern of MEK1 and MEK2 protein knockdown in HBE was very similar to the knockdown seen in BEAS-2B cells.

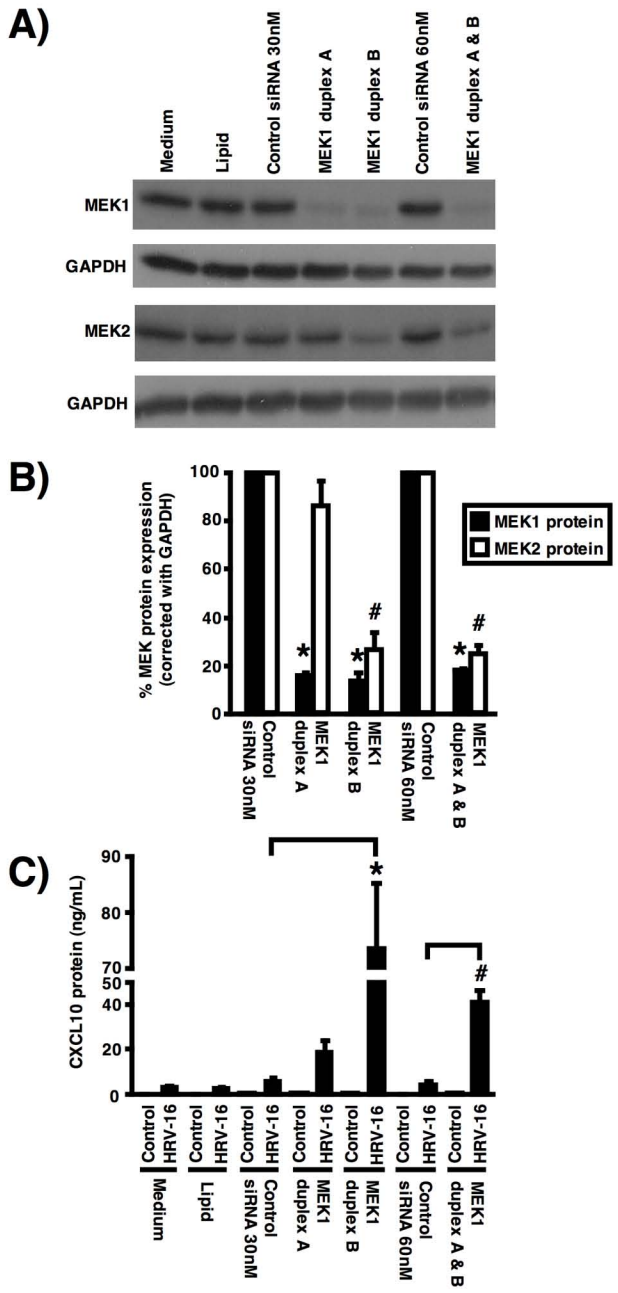

Figure 5.2 – Selective knockdown of MEK1 enhances HRV-16-induced CXCL10 expression in HBE. The effect of 30 nM MEK1 siRNA duplexes, individually or in combination, on MEK1 and MEK2 **(A)** protein expression (72 h post-transfection) was assessed by immunoblotting (n = 4). Densitometric analysis of MEK1 and MEK2 **(B)** protein expression compared to control siRNA. **C)** Assessment of HRV-16-induced CXCL10 protein release 24 h post-infection in the presence of MEK siRNA by ELISA (n = 5). Significant differences compared to 30 nM (*) or 60 nM (#) control siRNA were assessed with one way ANOVA followed by Fisher's least significant difference test.

Lipid reagent and medium alone were used as appropriate controls. Immunoblots were stripped and re-probed with GAPDH to ensure equal loading.

Similar to findings in BEAS-2B cells, MEK1 protein knockdown in HBE resulted in a significant enhancement of HRV-16-induced CXCL10 protein production using MEK1 duplex B (p <0.0001) and the combination of both MEK1 duplexes (p <0.001) compared to control siRNA (Figure 5.2C). Transfection of MEK1 duplex A clearly enhanced HRV-16-induced CXCL10 protein production, but this did not reach statistical significance nor was the degree of enhancement comparable to MEK1 duplex B or the combination of the MEK1 duplexes. Interestingly, the effect of MEK1 and MEK2 protein knockdown showed similar effects on HRV-16-induced CXCL10, therefore, MEK2 siRNA were not used in these experiments. Collectively, these results demonstrate that MEK1 siRNA knockdown of MEK1 protein expression and HRV-16-induced CXCL10 protein production is similarly enhanced with selective MEK1 knockdown in both BEAS-2B cells and HBE.

5.2.3 Knockdown of MEK1 enhances HRV-16-induced IRF-1 binding to CXCL10 ISRE

Having demonstrated that MEK1 knockdown resulted in enhancement of HRV-16-induced CXCL10 expression in both BEAS-2B cells and HBE, studies were performed to evaluate the effects of MEK1 knockdown on IRF-1 nuclear translocation and/or binding to the ISRE recognition sequence from the CXCL10 promoter. Transfection of MEK1 duplex B, enhanced HRV-16-induced IRF-1 binding to CXCL10-specific ISRE radiolabeled probe versus control siRNA in both BEAS-2B cells and HBE

(Figures 5.3A & B). Interestingly, in both BEAS-2B cells and HBE, transfection of MEK1 duplex A, which enhanced CXCL10 production to a lesser extent than MEK1 duplex B (Figure 5.2C) did not enhance the identified IRF-1 band. These results demonstrate that HRV-16-induced IRF-1 binding to the ISRE recognition sequence is enhanced with the reduction of both MEK1 and MEK2 protein by MEK1 duplex B.

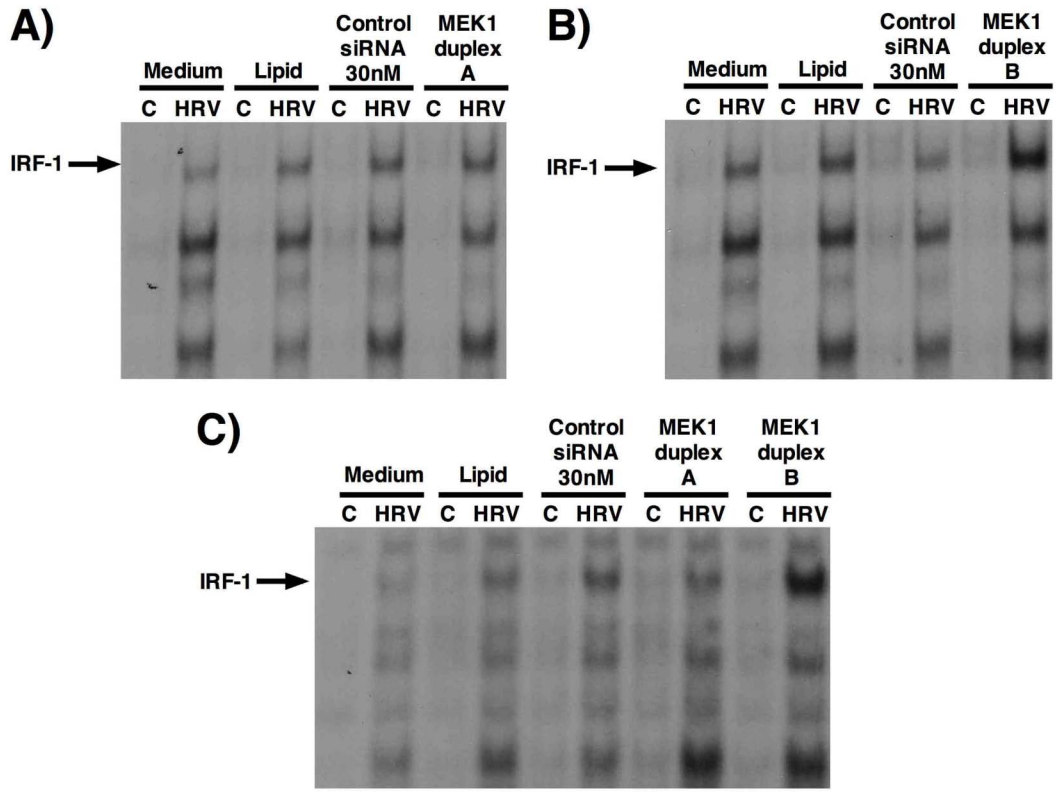

Figure 5.3 – MEK1 siRNA enhances HRV-16-induced IRF-1 binding to CXCL10-specific ISRE in BEAS-2B cells and HBE. Nuclear extracts (2.5 μg) were prepared from BEAS-2B cells (6 h post-infection) with 30 nM control siRNA, MEK1 duplex A **(A)** or duplex B **(B)**. **C)** Similarly, HBE (9 h post-infection) were transfected with 30 nM MEK1 duplex A, duplex B or control siRNA. Samples were incubated with [γ-^{32}P]-labeled CXCL10-specific ISRE, separated on a 6% non-SDS gel and visualized by autoradiography (n = 3 for both cell types). Lipid reagent and medium alone were used as controls. Medium control is abbreviated as C.

5.2.4 MEK1 siRNA does not abrogate HRV-16-induced ERK1/2 phosphorylation

To confirm if MEK1 siRNA-mediated enhancement of CXCL10 expression was associated with a loss of ERK phosphorylation as shown with pharmacologic inhibition, the effect of MEK siRNA on HRV-16-induced ERK1/2 phosphorylation was determined. Surprisingly, transfection of BEAS-2B with MEK1 or MEK2 siRNA did not markedly alter the phosphorylation state of ERK1/2 (1 h post-infection) compared to control siRNA (Figures 5.4A & B).

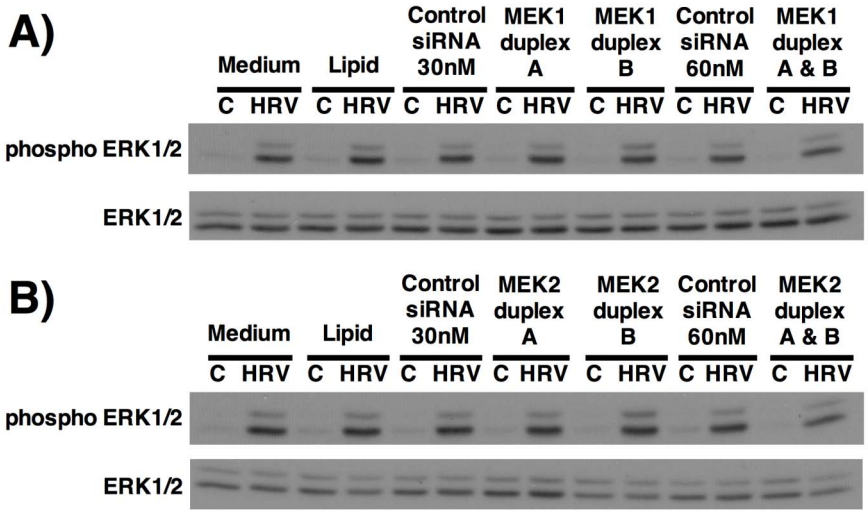

Figure 5.4 – Knockdown of MEK1 or MEK2 protein expression does not abrogate HRV-16-induced ERK1/2 phosphorylation in BEAS-2B cells. The effect of MEK1 **(A)** or MEK2 **(B)** siRNA (72 h post-transfection), individually or in combination, on HRV-16-induced ERK1/2 phosphorylation (1 h post-infection) was assessed by immunoblotting with phospho-specific ERK1/2 antibody (n = 3). Immunoblots were stripped and re-probed with total ERK1/2 antibody to ensure equal loading. Medium control is abbreviated as C.

Moreover, the combination of MEK1 and MEK2 siRNA did not alter HRV-16-induced ERK1/2 phosphorylation 1 h post-infection (Figures 5.5A & B), even though HRV-16-induced CXCL10 protein release at 24 h post-infection was enhanced by the combination of MEK1 and MEK2 siRNA (Figure 5.5C). Given that MEK1/2 pathway-mediated enhancement of HRV-16-induced CXCL10 by PD98059 and U0126 was associated with the inhibition of ERK1, and to some degree ERK2 (Figure 3.4), experiments were performed to assess the effect of these inhibitors in the presence of MEK siRNA to determine if inhibition of HRV-16-induced ERK1/2 phosphorylation could further increase the level of CXCL10 enhancement due to MEK siRNA treatment. In cells transfected with control siRNA, both PD98059 (10 μM) and U0126 (3 μM) inhibited HRV-16-induced ERK1/2 phosphorylation although the effect of U0126 was more pronounced (Figures 5.5A & B). Interestingly, in cells transfected with MEK1 and MEK2 siRNA, subsequent PD98059 treatment consistently did not inhibit phosphorylation of ERK1/2 (Figure 5.5A). In contrast, U0126 almost completely inhibited HRV-16-induced ERK1/2 phosphorylation in both MEK1/2 and control siRNA-transfected cells to near baseline levels (Figure 5.5B). Although treatment with PD98059 in MEK1/2 siRNA-transfected cells did not inhibit ERK1/2 phosphorylation (Figure 5.5A), PD98059 caused a modest further enhancement of HRV-16-induced CXCL10 protein release in MEK1 and MEK2 siRNA-transfected cells, but this did not achieve statistical significance (Figure 5.5C). In addition, U0126 treatment did not further enhance CXCL10 production in MEK1/2 siRNA-transfected cells, despite almost complete inhibition of ERK1/2 phosphorylation (Figure 5.5C). Control experiments confirmed that HRV-16-induced CXCL10 protein release 24 h post-infection was

significantly (p <0.05 in all cases) enhanced by PD98059 and U0126 compared to HRV-16 plus DMSO in cells exposed to transfection medium or lipid transfection reagent (Figure 5.5C). These results suggest that the MEK1-pathway mediated enhancement of HRV-16-induced CXCL10 expression in BEAS-2B cells is independent of ERK1/2 phosphorylation.

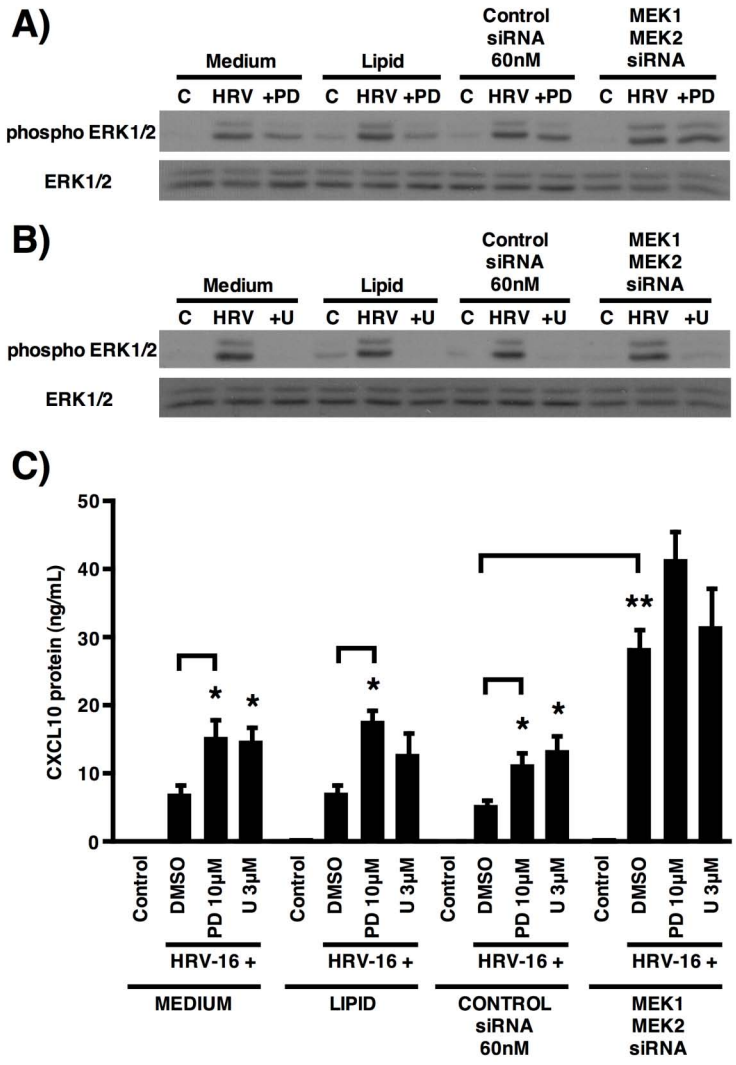

Figure 5.5 – Effect of MEK1/2 pathway inhibitors on HRV-16-induced ERK1/2 phosphorylation in the presence of MEK1 and MEK2 siRNA in BEAS-2B cells. Cells were transfected with 30 nM MEK1 duplex B and MEK2 duplex B siRNA with 72 h recovery followed by pre-incubation with **(A)** PD98059 (10 μM) or **(B)** U0126 (3 μM) and HRV-16 infection for 1 h. Whole cell lysates were assessed for ERK1/2

phosphorylation by immunoblotting (n = 3). **C)** HRV-16-induced CXCL10 protein release in the presence of MEK inhibitors and/or siRNA was assessed from supernatants by ELISA (n = 4). DMSO (0.1% v/v) was used as inhibitor vehicle control. Lipid reagent and medium only were used as appropriate control for siRNA studies. Immunoblots were stripped and re-probed with total ERK1/2 antibody to ensure equal loading. Single asterisk indicates significant difference compared to HRV-16 plus DMSO within each siRNA treatment group using one way ANOVA followed by Fisher's least significant difference test. Double asterisk indicates significant difference of HRV-16 plus DMSO-induced CXCL10 between control siRNA and MEK siRNA treatment groups with unpaired t-test.

5.2.5 ERK1/2 siRNA knockdown enhances HRV-16-induced CXCL10 expression

To further evaluate the role of ERK1/2 in the enhancement of CXCL10 expression, pharmacological inhibitors and siRNA against ERK1 and ERK2 were used. First, two structurally and functionally distinct ERK inhibitors, ERK Inhibitor[407] and FR180204[408], were employed. In BEAS-2B cells, both ERK Inhibitor (10-1 μM) and FR180204 (10-1 μM) had no effect on HRV-16-induced CXCL10 protein release compared to HRV-16 plus DMSO (Figure 5.6A). This result was in contrast to the significant enhancement of HRV-16-induced CXCL10 in the presence of either PD98059 (10 μM) or U0126 (3 μM) in the same experiments. In order to validate the effectiveness of the ERK inhibitors, whole cell lysates from HRV-16-infected cells were assayed for HRV-16-induced phosphorylation of Elk-1, a known downstream target of ERK1/2[444]. ERK Inhibitor I (10-0.3 μM) did not markedly alter HRV-16-induced phosphorylation of Elk-1 (1 h post-infection) at any concentration (Figure 5.6B). Phosphorylation of Elk-1 after HRV-16 infection was clearly reduced by FR180204 (10-0.3 μM) in a concentration-dependent manner. The level of Elk-1 phosphorylation after PD98059 (10 μM) treatment was inhibited to levels comparable to FR180204 at 10 μM. Treatment

with U0126 reduced the levels of phosphorylated Elk-1 to near baseline levels (Figure 5.6B).

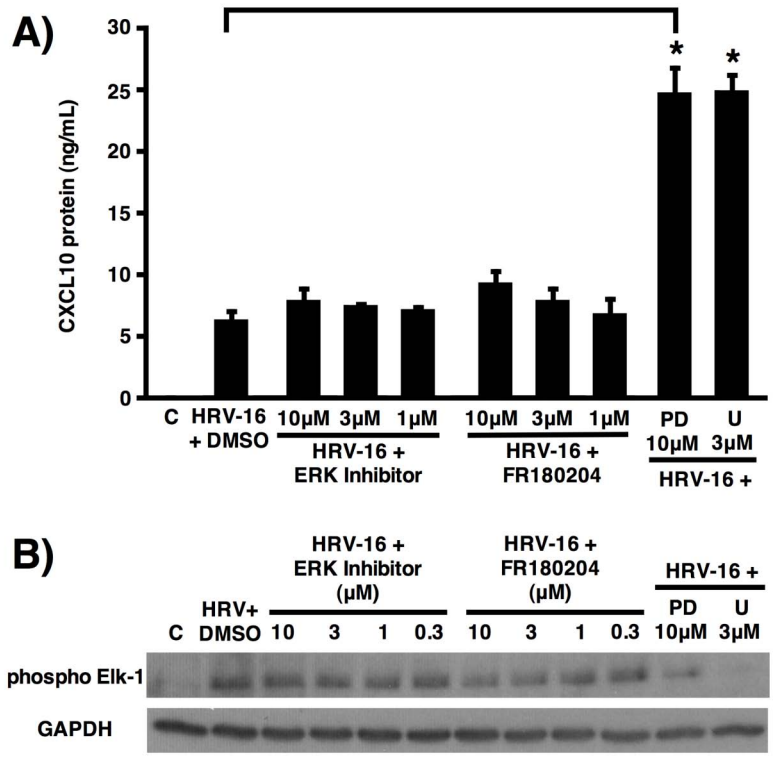

Figure 5.6 – Pharmacologic inhibition of ERK1 and ERK2 does not enhance HRV-16-induced CXCL10 protein expression. BEAS-2B cell were pre-incubated with the ERK inhibitors, ERK Inhibitor (10-1 μM) or FR180204 (10-1 μM) and DMSO (0.1% v/v) for 1 h followed by HRV-16 infection. The MEK1/2 inhibitors, PD98059 (10 μM) and U0126 (3 μM), were used as positive controls. **A)** HRV-16-induced CXCL10 protein release into supernatants 24 h post-infection was assessed by ELISA (n = 4). **B)** Whole cell lysates were assessed for HRV-16-induced Elk-1 phosphorylation 1 h post-infection by immunoblotting (n =3). Immunoblots were stripped and re-probed with GAPDH to ensure equal loading. Significant differences compared to HRV-16 plus DMSO were assessed with one way ANOVA followed by Fisher's least significant difference test.

Further experiments were performed using siRNA designed to target ERK1 and ERK2 to assess any effects on HRV-16-induced CXCL10 expression. In BEAS-2B cells, preliminary experiments determined that the optimal concentration of ERK siRNA was 3 nM and maximal ERK protein knockdown was reached by 72 h post-transfection. Transfection of 3 nM ERK1 siRNA resulted in a significant (p <0.0001 in both cases) knockdown of ERK1 protein with duplex A (96.5% ± 2.3% ERK1 knockdown) and duplex B (98.4% ± 0.8% ERK1 knockdown) compared to 3 nM control siRNA (Figures 5.7A & B). Neither ERK1 siRNA duplex consistently or significantly altered ERK2 protein levels. Surprisingly, HRV-16-induced CXCL10 protein production was significantly (p <0.001) enhanced with ERK1 duplex A, but not duplex B (Figure 5.1C). Transfection of 3 nM ERK2 siRNA resulted in a significant (p <0.0001 in both cases) knockdown of ERK2 protein with both duplex A (90.8% ± 0.8% ERK2 knockdown) or duplex B (92.3% ± 1.9% ERK2 knockdown) compared to control siRNA (Figures 5.7A & B). In the presence of ERK2 duplex B, ERK1 protein expression was modestly, but significantly (p = 0.04), lowered (78.4 ± 11.4% ERK1 knockdown) compared to control siRNA (Figures 5.7A & B). Similar to ERK1 siRNA, ERK2 duplex A, but not duplex B, significantly (p <0.0001) enhanced HRV-16-induced CXCL10 protein production compared to control siRNA (Figure 5.1C). In the presence of both ERK1 duplexes, ERK1 protein levels were significantly (p <0.0001) lowered without effect on ERK2 protein compared to 6 nM control siRNA. This siRNA combination, however, did not result in a change HRV-16-induced CXCL10 protein production compared to control siRNA. In contrast, ERK2 protein levels were significantly reduced (p < 0.0001) in the presence of both ERK2 duplexes without effect on ERK1 protein and this knockdown

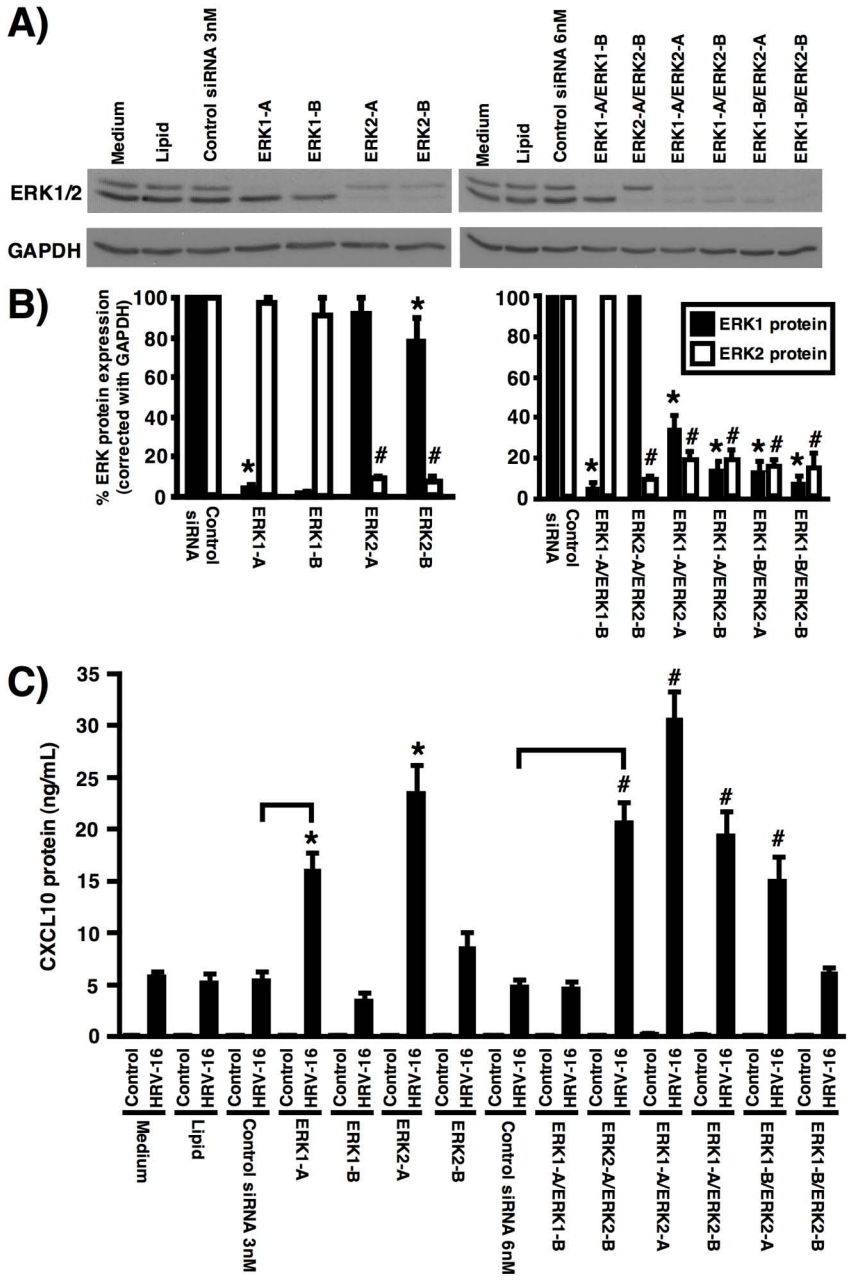

Figure 5.7 – Effect of ERK siRNA on ERK1 and ERK2 protein expression and HRV-16-induced CXCL10 protein expression. BEAS-2B cells were transiently transfected with 3 nM ERK1 or ERK2 siRNA, individually or in combination, followed by 72 h recovery and HRV-16 infection for 24 h. **A)** Whole cell lysates were assessed for ERK1 and ERK2 protein expression by immunoblotting (n = 3). **B)** Densitometric analysis of ERK1 (black) and ERK2 (white) protein expression compared to control siRNA. **C)** Supernatants were assessed for HRV-16-induced CXCL10 protein production by ELISA (n = 4). Significant differences compared to 30 nM (*) or 60 nM (#) control siRNA were assessed with one way ANOVA followed by Fisher's least

significant difference test. Lipid reagent and medium alone were used as appropriate controls. Immunoblots were stripped and re-probed with GAPDH to ensure equal loading.

was associated with a significant (p <0.0001) enhancement of HRV-16-induced CXCL10 protein production (Figures 5.7A-C). All combinations of ERK1 and ERK2 siRNA resulted in a significant (p < 0.0001 in all cases) reduction of both ERK1 and ERK2 protein levels (Figures 5.7A & B). HRV-16-induced CXCL10 protein production was significantly (p <0.001 in all cases) enhanced in the presence of ERK1 and ERK2 duplex combinations except when ERK1 duplexA/ERK2 duplex B or ERK1 duplex B/ERK2 duplex B were combined. None of the ERK siRNA conditions markedly altered MEK1 or MEK2 protein levels, thus confirming that HRV-16-induced CXCL10 enhancement with ERK siRNA was not due to altered MEK1 or MEK2 protein expression (Figures 5.8A and B).

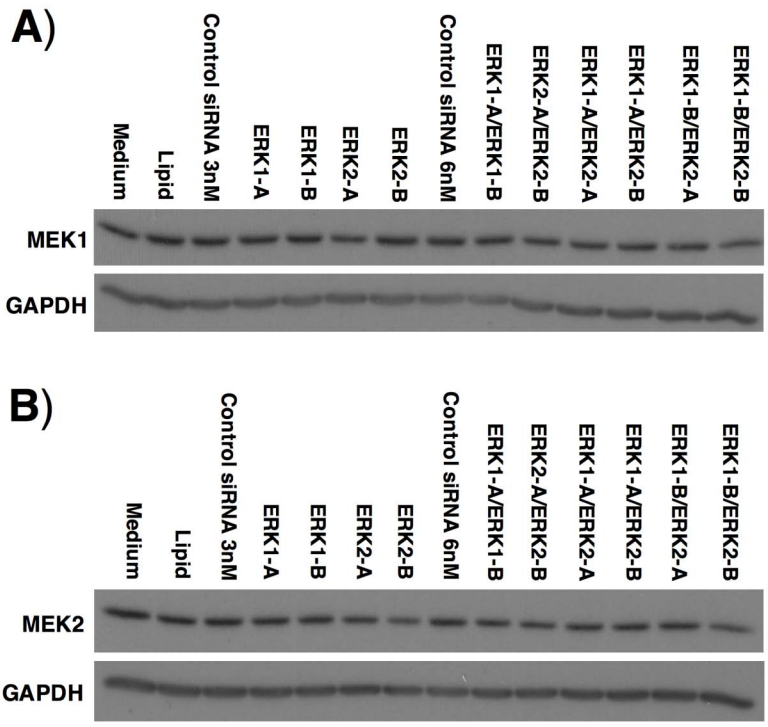

Figure 5.8 – ERK1 and ERK2 siRNA do not markedly alter MEK1 and MEK2 protein expression. BEAS-2B cells were transiently transfected with 3 nM ERK1 or ERK2 siRNA, individually or in combination, followed by 72 h recovery. Whole cell lysates were assessed for MEK1 **(A)** and MEK2 **(B)** protein expression by immunoblotting (n = 2). Immunoblots were stripped and re-probed with GAPDH to ensure equal loading. Control siRNA, lipid reagent, and medium alone were used as appropriate controls.

5.3 Discussion

In Chapter 3, pharmacologic inhibition of the MEK1/2 pathway was shown to enhance HRV-16-induced CXCL10 expression via transcriptional effects. Additionally, MEK1/2 pathway inhibition enhanced HRV-16-induced IRF-1 interactions with the CXCL10 promoter. In order to further delineate the mechanisms underlying the negative regulation of HRV-induced CXCL10 production by the MEK1/2 pathway, siRNA designed to target the MEK and ERK proteins were employed to confirm our earlier

observations and to assess the specific roles of the MEK and ERK proteins, which could not be delineated using pharmacological inhibitors.

As expected, both MEK1 siRNA duplexes substantially reduced MEK1 protein expression compared to control siRNA in both BEAS-2B cells and HBE. Unexpectedly, MEK2 protein expression was greatly reduced in the presence of both MEK1 duplex B and the combination of MEK1 duplexes, but not MEK1 duplex A. Further analysis of the siRNA sequences found that MEK1 duplex B sequence, but not MEK1 duplex A, had a high degree of alignment (21/25 bp) with the MEK2 mRNA sequence. This would explain the reduction of MEK2 protein levels in the presence of MEK1 duplex B, but not duplex A. Unfortunately, the sequences of these commercially available duplexes were not made available until after receipt, thus analysis of siRNA alignment with non-targeting mRNA sequences could not be done prior to experiments. Also, transfection of MEK2 duplexes in BEAS-2B cells reduced MEK2 protein levels, but modestly increased MEK1 protein expression. The nature of this apparent redundancy is unclear and would require study beyond the scope of the current thesis.

Though enhancement of HRV-16-induced CXCL10 expression with both MEK1 duplexes was significant, duplex B resulted in a higher level of enhancement than duplex A. In contrast to MEK1 siRNA, the knockdown of MEK2 protein with either MEK2 duplex did not enhance HRV-16-induced CXCL10 protein production, confirming that MEK2 does not mediate the negative regulation of HRV-16-induced CXCL10 expression. Furthermore, the findings with MEK1 siRNA were confirmed in HBE, a more physiologically relevant and non-transformed cell model. Similar to BEAS-2B cells, the loss of both MEK1 and MEK2 protein maximized the enhancement of CXCL10

compared to the enhancement associated with the loss of only MEK1 protein. Overall, these results suggested that selective knockdown of MEK1 protein results in an enhancement of HRV-16-induced CXCL10 expression, similarly to the MEK1/2 pathway inhibitors. The data also indicate that MEK2 alone does not mediate the enhancement of HRV-16-induced CXCL10 expression. In the current study, the enhancement phenomenon is primarily mediated through a MEK1-dependent pathway, but MEK2 may affect MEK1 function or counteract downstream MEK1-dependent processes.

In Chapter 4, pharmacologic inhibition of the MEK1/2 pathway was shown to enhance HRV-16-induced IRF-1 nuclear translocation and/or binding to the ISRE in the CXCL10 promoter (Figure 4.12). This previous finding was confirmed as we show that MEK1 duplex B, which reduced both MEK1 and MEK2 protein, enhanced HRV-16-induced IRF-1 nuclear translocation and/or binding to the ISRE within the CXCL10 promoter in both BEAS-2B cells and HBE. As shown in Figures 5.1 and 5.2, enhancement of HRV-16-induced CXCL10 expression was maximized with the loss of both MEK1 and MEK2 protein. Interestingly, MEK1 duplex A, which did not alter MEK2 protein levels, also did not enhance HRV-16-induced IRF-1 binding. Therefore, the enhancement of HRV-16-induced IRF-1 binding, similar to the enhancement of CXCL10 expression, may require the knockdown of both MEK1 and MEK2 protein. This again suggests that MEK2 may counter-regulate MEK1. Furthermore, the lack of enhanced HRV-16-induced IRF-1 binding to the CXCL10 ISRE with MEK1 duplex A indicates that CXCL10 enhancement may also be regulated by a mechanism independent of changes in IRF-1 interaction with the CXCL10 promoter. Nonetheless, HRV-16-induced CXCL10 expression is enhanced with the loss of both MEK1 and MEK2 protein

and this is associated with enhanced IRF-1 nuclear translocation and/or binding to the CXCL10 ISRE.

Surprisingly, in the presence of MEK1 and MEK2 duplexes, individually or in combination, HRV-16-induced ERK1 or ERK2 phosphorylation was not markedly altered in contrast to the inhibition seen with PD98059 and U0126. These results were intriguing as the activation of ERK1/2 has been long thought to be a direct result of MEK1/2 activity[327,416]. The lack of effect on ERK1/2 phosphorylation after MEK1 and MEK2 protein knockdown suggested that the remaining MEK1 or MEK2 protein possibly retained the capacity to induce the activation of ERK1/2 after HRV-16 infection to a comparable degree in cells not lacking MEK1 and MEK2. Alternatively, a redundant pathway also capable of inducing ERK1/2 phosphorylation after HRV-16 infection could have compensated for the loss of MEK1 and MEK2 protein. Indeed, it has been reported that constitutive ERK1/2 activation can be MEK1/2-independent, but protein kinase (PKC) and phosphatidyl-3-kinase (PI3K)-dependent[445,446]. Finally, it is possible that the loss of MEK1 and MEK2 protein results in the loss of ERK1/2 feedback regulation that is normally mediated by the MEKs (e.g. phosphatases)[447].

Given that HRV-16-induced CXCL10 expression was enhanced in the presence of continued ERK1/2 phosphorylation indicated that the effects of MEK1 on CXCL10 enhancement were independent of ERK1/2 phosphorylation status. PD98059 consistently had little or no effect on ERK1/2 phosphorylation in MEK1/2 siRNA transfected cells compared with the inhibition seen in control siRNA cells suggesting that PD98059 does indeed specifically target MEK1/2. Interestingly, treatment with U0126 completely inhibited HRV-16-induced ERK1/2 phosphorylation transfected with MEK1

and 2 siRNA similarly to cells transfected with control siRNA. These contradictory observations were troubling as it indicates that the U0126 compound may possibly have off-target effects, as has been reported[448], and reinforces the concept that at least two unique inhibitors be used to confirm any results[449]. Fortunately, in the current epithelial cell models, PD98059 and U0126 both enhance HRV-16-induced CXCL10 expression to near identical degrees, regardless of their effects on downstream kinases, such as ERK1/2, ERK5, or p38 (Chapter 3). Taken further, neither PD98059 nor U0126 could further increase the enhanced levels of HRV-16-induced CXCL10 protein in the presence of MEK1 and MEK2 siRNA, thus implying that the enhancement of HRV-16-induced CXCL10 expression is independent of ERK1/2 phosphorylation status, but dependent on MEK1 function as assessed by MEK1/2 inhibitors and siRNA.

Direct studies on ERK1 and ERK2 showed that pharmacological inhibition of ERK1 and ERK2 did not enhance HRV-16-induced CXCL10 protein production, in contrast to the enhancement seen with PD98059 or U0126 in the same sets of experiments. The phosphorylation of Elk-1, a well-described downstream target of ERK1/2[444], was used to validate the actions of ERK Inhibitor, but did not alter Elk-1 phosphorylation at any of the concentrations used. In contrast, FR180204 inhibited HRV-16-induced Elk-1 phosphorylation in a concentration-dependent manner. This difference can be explained by the fact that FR180204 has been shown to an ATP-competitive inhibitor with near equal affinity for ERK1 and ERK2[408], but ERK Inhibitor is known to only block ERK2 interactions with downstream targets[407]. This indicated that ERK1 may be capable of inducing Elk-1 phosphorylation in a redundant fashion upon the loss of ERK2 function or that ERK2 does not normally phosphorylate Elk-1

after HRV-16 infection in BEAS-2B cells. The addition of PD98059 or U0126 inhibited HRV-16-induced Elk-1 phosphorylation nearly to baseline levels and also resulted in the enhancement of HRV-16-induced CXCL10 expression. The observation that inhibition of Elk-1 phosphorylation by FR180204 in the absence of CXCL10 enhancement implies that ERK1/2 activity is not essential in the MEK1 pathway-dependent enhancement of CXCL10.

The role of ERK1 and ERK2 in the negative regulation of HRV-16-induced CXCL10 expression was further explored using siRNA duplexes designed to target ERK1 and ERK2. Surprisingly, HRV-16-induced CXCL10 protein release was enhanced in the presence of certain ERK1 or ERK2 duplexes, individually or in combination. These contradictory results are difficult to explain and may be due, in part, to the limitations of siRNA, such as off-target effects or induction of siRNA duplex-specific transcriptional profiles[437-439]. As such, further studies are required to ascertain the role of ERK1/2 during the enhancement of HRV-16-induced CXCL10 expression.

In summary, the selective knockdown of MEK1 protein enhances HRV-16-induced CXCL10 expression in both BEAS-2B and HBE, thus confirming the results using inhibitors of the MEK1/2 pathway. The enhancement of CXCL10 expression and enhancement of IRF-1 nuclear translocation and/or binding to the CXCL10 promoter was maximized with the knockdown of both MEK1 and MEK2 protein. The enhancement of CXCL10 was not dependent on the phosphorylation state of ERK1/2 or possibly ERK1/2 activity. These results further underscore that the negative regulation of HRV-16-induced CXCL10 expression occurs, in part, through a MEK1 pathway-dependent manner in human airway epithelial cells.

Chapter Six: Human rhinovirus-induced epithelial production of CXCL10 is dependent upon IRF-1

6.1 Introduction

Data thus far have shown that inhibition or knockdown of the MEK1 pathway enhances both HRV-16-induced CXCL10 expression, and nuclear translocation and/or binding of IRF-1 to the ISRE in the CXCL10 promoter. Although IRF-1 has been associated with HRV-induced production of CXCL10[236,368], no studies have shown a direct role of IRF-1 in HRV-induced gene expression. In this chapter, the role of IRF-1 in HRV-16 induction of CXCL10 expression, and its regulation by the MEK1 pathway, was further explored. It was hypothesized that HRV-16 infection would up-regulate IRF-1 expression and that siRNA knockdown of IRF-1 would result in the inhibition of HRV-16-induced CXCL10 expression. Furthermore, the loss of MEK1 function would directly alter the ability of IRF-1 to mediate the enhancement of CXCL10 expression.

As a member of the IRF transcription factor family (section 1.10.2), IRF-1 expression is induced by RNA viruses[392,450-452], IFN-β[453], IFN-γ[454], EGF[455], and DNA damage[456]. It can be constitutively expressed and is localized mainly in the nucleus[397]. As shown in Table 1.2, IRF-1 has been implicated in a wide variety of processes, such as anti-viral defense, growth arrest, apoptosis, and T_H1 lymphocyte development[377,397,457]. Other IRF-1 targets include, iNOS[458,459] and CCL5[454,460], which have also been shown to be up-regulated by HRV infection. In addition, picornavirus-infected IRF-1 knockout mice show increased mortality and viral titres compared with wildtype mice[400].

6.2 Results

6.2.1 HRV-16 infection of airway epithelial cells increases IRF-1 mRNA and protein

Initial experiments studied the effect of HRV-16 infection on IRF-1 expression in airway epithelial cells. In BEAS-2B cells, IRF-1 mRNA expression was increased in a time-dependent (p <0.05), but transient manner in HRV-16 infected cells. Expression reached a peak at 6 h post-infection (3.9 ± 0.2 fold increase) and decreased to close to basal levels by 24 h (Figure 6.1A). HRV-16 induction of IRF-1 protein followed a similar transient pattern in BEAS-2B cells. Protein expression was evident at 3 h post-infection, reached peak levels by 6-9 h, and was lost by 24 h (Figure 6.1B). In contrast, HRV-16 infection of HBE resulted in a time-dependent (p <0.05) and consistent 2-fold increase in IRF-1 mRNA expression from 6 to 12 h post-infection, with a peak at 24 h (4.7 ± 1.0 fold increase) (Figure 6.1C). IRF-1 protein was evident at 6 h post-infection with continued production at 24 h post-infection (Figure 6.1D). These results demonstrate that IRF-1 mRNA and protein expression is upregulated in response to HRV-16 infection, but there is a difference in the temporal pattern of expression of IRF-1 mRNA and protein in BEAS-2B cells versus HBE.

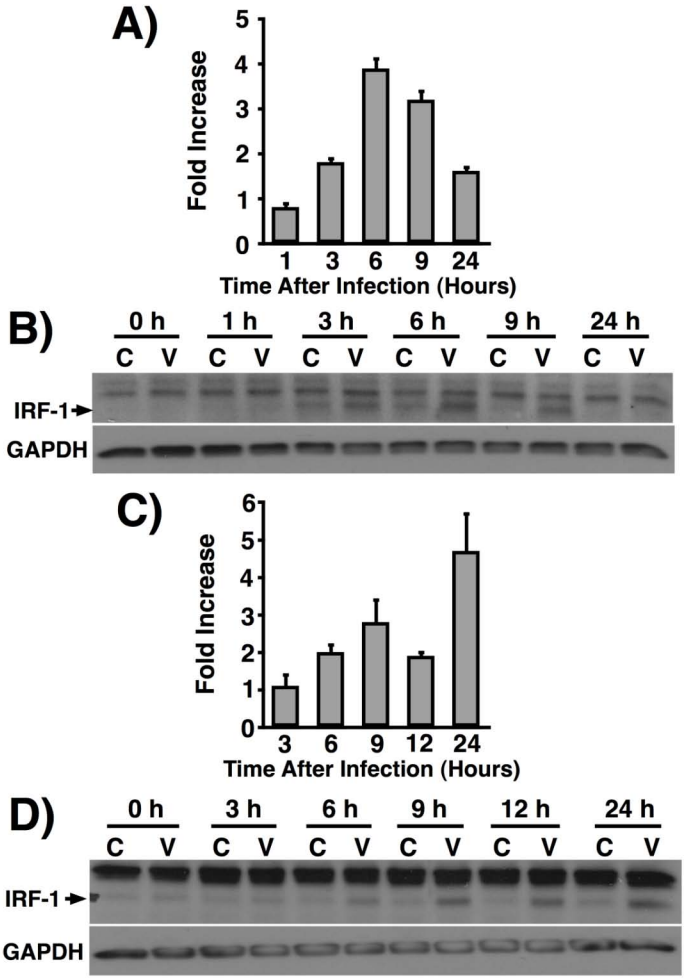

Figure 6.1 – HRV-16 infection induces the expression of IRF-1 mRNA and protein in human airway epithelial cells. Induction of IRF-1 mRNA expression after HRV-16 infection in BEAS- 2B **(A)** and HBE **(C)**. IRF-1 protein production after HRV-16 infection in BEAS-2B **(B)** and HBE **(D)**. IRF-1 mRNA data are expressed as mean fold increase ± SEM (n=3). Significant time-dependent changes in HRV-16-induced IRF-1 mRNA expression were assessed with Kruskal Wallis ANOVA. IRF-1 blots are representative of three separate experiments in each case. GAPDH was used as a control for mRNA and protein experiments. HRV-16 is abbreviated as V, while medium control is abbreviated as C.

6.2.2 IRF-1 siRNA decreases HRV-16-induced CXCL10 protein production

To further establish the functional role of IRF-1 in HRV-16-induced CXCL10 expression, siRNA duplexes specific for IRF-1 (10 nM), together with an appropriate control siRNA (10 nM) were used. It was first established that transfection (72 h post-transfection recovery) with specific siRNAs inhibited HRV-16-induced IRF-1 protein expression at optimal induction times both in BEAS-2B cells (6 h post-infection) and HBE (24 h post-infection). In BEAS-2B cells, HRV-16-induced IRF-1 protein (Figures 6.2A & B) was reduced in the presence of IRF-1 duplex A (65.6% ± 1.2% knockdown; p <0.05) and IRF-1 duplex B (84.3% ± 1.8% knockdown; p <0.05) compared to control siRNA. The reduction of IRF-1 protein in siRNA-treated cells was associated with a marked loss of HRV-16-induced IRF-1 binding to the ISRE sequence from the CXCL10 promoter, as assessed by EMSA (Figure 6.2C). In accord with the greater efficacy of duplex B versus duplex A in reducing IRF-1 levels, duplex B also consistently led to a more pronounced reduction of IRF-1 binding. Consistent with reduced IRF-1 protein and ISRE binding, a significant (p <0.001) abrogation of HRV-16-induced CXCL10 protein expression was observed with both duplexes (Figure 6.2D). Of note, reduction of HRV-16-induced CXCL10 protein production was significantly (p <0.05) greater using duplex B compared to duplex A, which is in agreement with the greater knockdown of IRF-1 protein and IRF-1 binding to CXCL10 ISRE by this duplex.

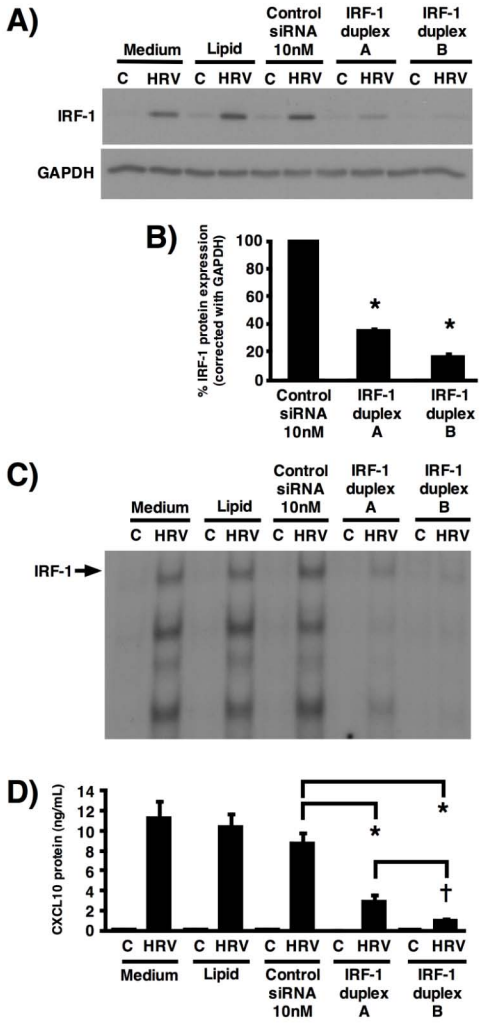

Figure 6.2 – Effect of IRF-1 siRNA on HRV-16-induced IRF-1 protein, CXCL10-specific ISRE binding, and CXCL10 protein production in BEAS-2B cells. IRF-1 siRNA duplex A (10 nM), duplex B (10 nM) or control siRNA (10 nM) were transfected into BEAS-2B and allowed to recover for 72 h followed by HRV-16 infection. **A)** Whole cell lysates were collected 6 h post-infection and assessed for IRF-1 protein knockdown (representative of n = 3). **B)** Densitometric analysis to determine % HRV-16-induced IRF-1 protein expression in the presence of IRF-1 siRNA compared with control siRNA. **C)** Nuclear extracts were prepared 6 h post-infection, incubated with [γ-^{32}P]-labeled CXCL10-specific ISRE probe and analysed by EMSA (representative of n = 3). **D)** Supernatants were collected 24 h post-infection and assayed for CXCL10 protein release using ELISA (n = 4). Data are expressed as mean ± SEM. Single asterisk indicates significant difference compared with HRV-16-induced protein expression in the presence of control siRNA with one-way ANOVA followed by Fisher's least significant difference test. Single dagger indicates significant difference in the levels of HRV-16-induced protein expression between duplex A and duplex B by non-paired t-test. Medium control is abbreviated as C.

Similar to BEAS-2B cells, transfection of HBE (72 h post-transfection recovery) with IRF-1 siRNAs (10 nM) resulted in a reduction of HRV-16-induced IRF-1 protein (24 h post-infection) with duplex B (97% ± 1.8% knockdown; $p < 0.01$) and duplex C (90.5% ± 6.4% knockdown; $p < 0.001$) compared to control siRNA (Figures 6.3A-D). IRF-1 duplex A was ineffective at in HBE, hence a third IRF-1 siRNA (duplex C) was employed to confirm results obtained using duplex B. In EMSA experiments, siRNA treatment with either duplex led to a clear loss of HRV-16-induced IRF-1 binding to the ISRE sequence from the CXCL10 promoter (Figures 6.3E & F). HRV-16-induced CXCL10 protein production also was significantly inhibited ($p < 0.01$) in cells treated with either IRF-1 duplex B or duplex C compared to control siRNA (Figures 6.3G & H). Thus, transfection of BEAS-2B or HBE with IRF-1 specific siRNA resulted in decreased HRV-16-induced IRF-1 protein, IRF-1 binding to CXCL10 ISRE, and CXCL10 protein release, clearly demonstrating the functional importance of IRF-1 in HRV-16-induced CXCL10 expression.

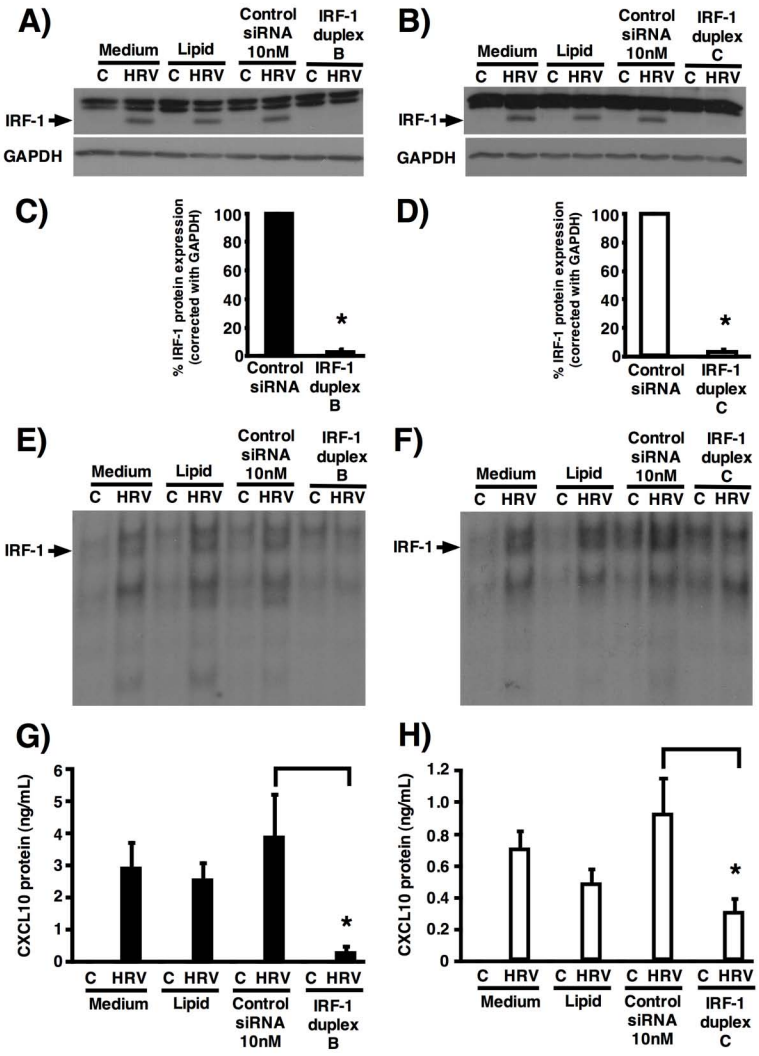

Figure 6.3 - Effect of IRF-1 siRNA on HRV-16-induced IRF-1 protein, CXCL10-specific ISRE binding, and CXCL10 protein production in HBE. IRF-1 siRNA duplex B (10 nM), duplex C (10 nM) or control siRNA (10 nM) were transfected into HBE and allowed to recover for 72 h followed by HRV-16 infection. Whole cell lysates were collected 24 h post-infection and assessed for IRF-1 protein knockdown by IRF-1 duplex B **(A)** or duplex C **(B)** (n = 3). Densitometric analysis to determine % HRV-16-induced IRF-1 protein expression in the presence of IRF-1 duplex B **(C)** or duplex C **(D)** compared with control siRNA. Nuclear extracts from IRF-1 duplex B **(E)** or duplex C **(F)** transfected cells were prepared 9 h post-infection, incubated with CXCL10-specific ISRE probe and analysed by EMSA (n = 3). Supernatants from IRF-1 duplex B **(G)** or duplex C **(H)** transfected cells were collected 24 h post-infection and assayed for CXCL10 protein (n = 4). Data are expressed as mean ± SEM. Single asterisk indicates significant difference of CXCL10 or IRF-1 protein expression with IRF-1 siRNA compared with control siRNA with one-way ANOVA followed by Fisher's least significant difference test or paired t-test, respectively. Medium control (C).

6.2.3 Effect of IRF-1 siRNA on other HRV-inducible chemokines

In Chapter 3, it was shown that inhibition of the MEK1/2 pathway also enhanced HRV-16-induced CCL5 expression. In contrast, HRV-16-induced CXCL8 expression is not enhanced by MEK1/2 pathway inhibition[267]. To further investigate the role of IRF-1 during HRV-induced chemokine expression, the effect of IRF-1 siRNA on HRV-16-induced CCL5 and CXCL8 expression was also evaluated. Transfection of IRF-1 duplex B significantly (p <0.01) abrogated HRV-16-induced CCL5 protein release in BEAS-2B cells (Figure 6.4A). In contrast, IRF-1 duplex B did not significantly alter HRV-16-induced CXCL8 protein release from the same cells (Figure 6.4B). These results suggest that IRF-1 may play a selective role in the expression of a subset of HRV-inducible chemokines.

6.2.4 Effect of MEK1 pathway inhibition or knockdown on HRV-16-induced IRF-1 mRNA and protein expression

We next determined if the enhancement of HRV-16-induced IRF-1 binding seen with pharmacological inhibition of MEK pathway inhibition was related to an increase in IRF-1 mRNA and protein expression. In BEAS-2B cells, MEK pathway inhibition with PD98059 (10 μM) or U0126 (3 μM) significantly (p <0.05) enhanced HRV-16-induced IRF-1 mRNA expression at 6 h post-infection, but did not significantly alter HRV-16-induced IRF-1 protein expression 6 h post-infection (Figures 6.5A & B). In HBE, PD98059 and U0126 also significantly (p <0.05) enhanced HRV-16-induced IRF-1 mRNA at 9 h post-infection (Figure 6.5C). Not only was this enhancement more striking than that seen in BEAS-2B cells, but, in contrast to data from BEAS-2B cells, HRV-16-

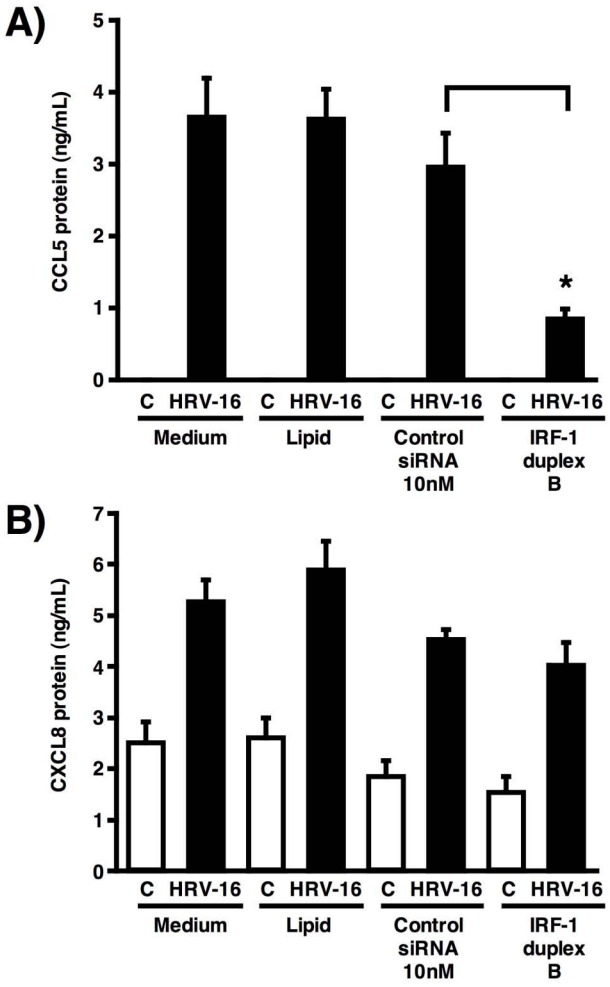

Figure 6.4 – Effect of IRF-1 siRNA on HRV-16-induced CCL5 and CXCL8 protein production in BEAS-2B cells. HRV-16-induced CCL5 **(A)** or CXCL8 **(B)** protein expression (24 post-infection) was assessed from cells transfected with IRF-1 duplex B (10 nM) or control siRNA (10 nM) with ELISA (n = 4). Data are expressed as mean ± SEM. Asterisk indicates significant difference between HRV-16-induced CCL5 protein expression in the presence of IRF-1 siRNA compared with control siRNA with one-way ANOVA followed by Fisher's least significant difference test. Medium control is abbreviated as C.

induced IRF-1 protein in HBE also was clearly enhanced at 9 h post-infection in the presence of either PD98059 or U0126 (Figure 6.5D).

The lack of IRF-1 protein enhancement upon MEK pathway inhibition in BEAS-2B was unexpected, thus we sought to confirm in BEAS-2B cells that enhancement of HRV-16-induced CXCL10 expression could occur in the absence of IRF-1 protein enhancement. Samples assayed for IRF-1 mRNA and protein (Figures 6.5A & B) were from matched experiments and from these samples both PD98059 and U0126 significantly (p <0.01) enhanced HRV-16-induced CXCL10 mRNA expression 6 h post-infection compared to HRV-16 plus DMSO (Figure 6.5E). By contrast, HRV-16-induced IRF-1 protein production was enhanced in the presence of 30 nM MEK1 siRNA (duplex B or duplex A & B) compared to 30 nM control siRNA in BEAS-2B cells (Figure 6.5F). The ability of MEK inhibitors to enhance HRV-16-induced CXCL10 expression in the absence of enhanced IRF-1 protein production, suggest that factors other than IRF-1 protein expression, per se must regulate MEK pathway-mediated effects on HRV-16-induced CXCL10.

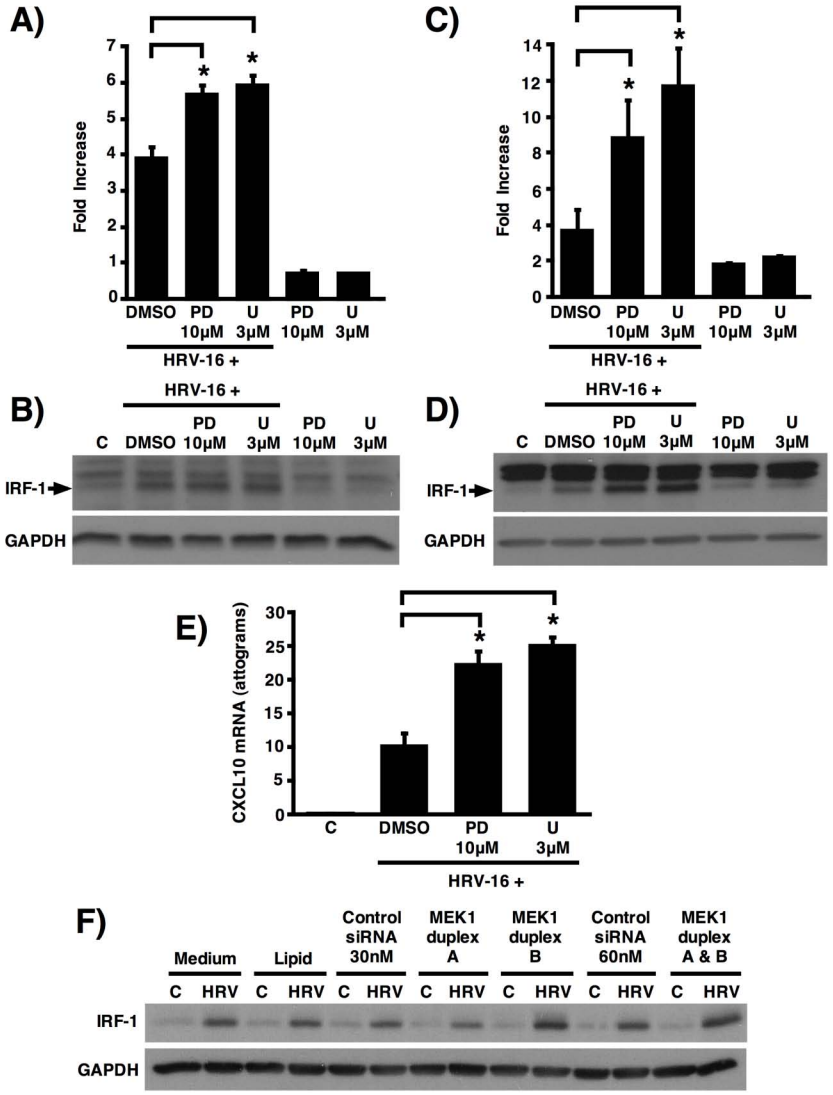

Figure 6.5 – Effect of MEK pathway inhibition or MEK1 knockdown on HRV-16-induced IRF-1 mRNA and protein expression. Cells were pre-incubated with PD98059 (10 μM) or U0126 (3 μM) for 1 h followed by HRV-16 infection. Samples were assessed for either IRF-1 mRNA or protein levels in BEAS-2B **(A & B)** or HBE **(C & D)** at 6 and 9 h post-infection, respectively. **E)** Samples from panel **(A)** were assessed for HRV-16-induced CXCL10 mRNA levels in the presence of PD98059 and U0126. **F)** BEAS-2B cells transfected with MEK1 duplex A and/or duplex B were assessed for HRV-16-induced IRF-1 protein production 6 h post-infection. IRF-1 mRNA data are expressed as mean fold increase ± SEM (n = 6). CXCL10 mRNA data are expressed as mean attograms ± SEM (n = 4). IRF-1 blots are representative of three (MEK1 siRNA) or four (MEK inhibitors) separate experiments. Single asterisk indicates significant difference between HRV-16 plus inhibitor treatment versus HRV-16 plus DMSO by one way ANOVA (CXCL10 mRNA) or Kruskal Wallis ANOVA (IRF-1 mRNA) followed by Fisher's least significant difference test or Wilcoxon matched-pairs signed-rank test.

6.2.5 Effect of IRF-1 knockdown on MEK1 pathway-mediated enhancement of HRV-16-induced CXCL10 production

To definitively establish the link between MEK pathway-induced enhancement of HRV-16-induced CXCL10 expression and the IRF-1 pathway, we examined whether IRF-1 knockdown would affect MEK1 pathway-mediated CXCL10 protein enhancement. To do this, BEAS-2B cells were transfected with 10 nM IRF-1 siRNA (duplex A or duplex B) with 72 h recovery followed by pre-treatment with PD98059 (10 μM) or U0126 (3 μM) for 1 h and HRV-16 infection for 24 h. It should be noted that neither PD98059 nor U0126 alone had any direct effects on CXCL10 production in cells treated with siRNA to IRF-1 but not exposed to HRV-16 (data not shown). Both specific siRNAs significantly (p <0.01) reduced HRV-16-induced CXCL10 protein release compared to control siRNA, although, again, duplex B was more effective (Figure 6.6A). PD98059 and U0126 significantly enhanced HRV-16-induced CXCL10 protein in cells with control siRNA (p <0.001). In cells transfected with control siRNA, PD98059 did not enhance HRV-16-induced IRF-1 protein (Figure 6.6B). Although U0126 caused a slight enhancement of IRF-1 protein, the level of CXCL10 protein enhancement was similar using either inhibitor (Figures 6.6A & B). Significant enhancement (p <0.05) also was still seen in cells transfected with the less effective IRF-1 duplex A. In contrast, in cells transfected with duplex B, neither PD98059 nor U0126 caused any significant enhancement of HRV-16-induced CXCL10 protein production. These results suggest that the almost complete loss of HRV-16-induced IRF-1 expression and binding to the ISRE site seen in cells treated with duplex B prevented the enhancement of HRV-16-induced CXCL10 protein production, further supporting a functional relationship

between IRF-1 activation and the MEK1 pathway-mediated enhancement of HRV-16-induced CXCL10 production.

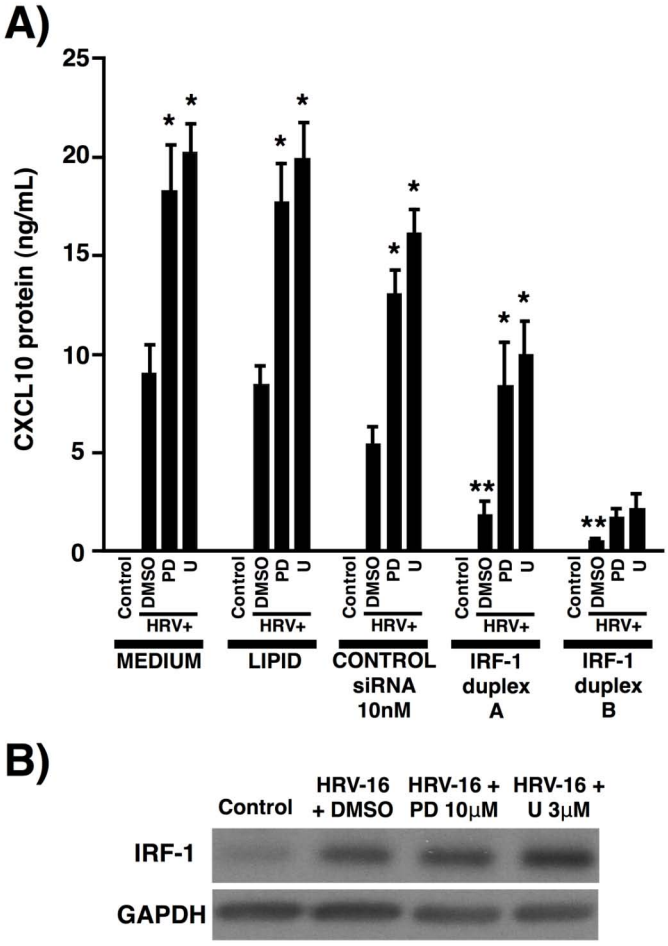

Figure 6.6 - Effect of MEK pathway inhibitors on HRV-16-induced CXCL10 protein in IRF-1 siRNA transfected BEAS-2B cells. A) IRF-1 siRNA duplex A (10 nM), duplex B (10 nM), or control siRNA (10 nM) were transfected into BEAS-2B followed by 1 h pre-incubation with PD98059 (10 μM) or U0126 (3 μM) and HRV-16 infection for 24 h. Supernatants were assessed for HRV-16-induced CXCL10 protein release using ELISA (n = 4). **B)** HRV-16-induced IRF-1 protein production (6 h post-infection) was assessed in cells transfected with 10 nM control siRNA by SDS/PAGE and immunoblotting with IRF-1 antibody (n = 4). Single asterisk indicates significant differences between HRV-16 plus inhibitor treated cells versus HRV-16 plus DMSO within each siRNA treatment group. Double asterisk indicates significant differences between IRF-1 duplexes and control siRNA. Significance was assessed using one way ANOVA followed by Fisher's least significant difference test.

6.2.6 Effect of phosphorylation on HRV-16-induced IRF-1 DNA binding

MEK1/2 pathway inhibition or MEK1 knockdown enhanced HRV-16-induced IRF-1 binding to the CXCL10 promoter with associated enhancement of CXCL10 expression, but in the absence of enhanced IRF-1 protein production in BEAS-2B cells (Figure 6.5B). It was speculated, therefore, that the enhancement of HRV-16-induced IRF-1 binding to the CXCL10 promoter is not necessarily due to increased amounts of IRF-1 protein through modulation of transcription or protein stability, but, rather, modulation of the phosphorylation state of IRF-1, which has been shown to be an important modification in IRF-1 DNA binding and transcriptional activity[461,462]. In BEAS-2B cells, however, the addition of 6.5 Units calf intestinal alkaline phosphatase (CIP) to nuclear extracts did not alter the binding of HRV-16-induced IRF-1 to CXCL10-specific ISRE probe (Figure 6.7). The activity of CIP was confirmed by its ability to dephosphorylate the ISRE radiolabeled probe and inhibition with the addition of EDTA (data not shown).

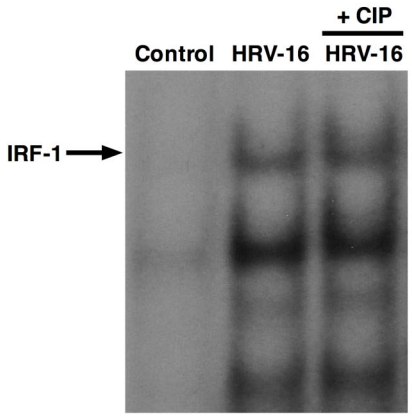

Figure 6.7 - The addition of calf intestinal alkaline phosphatase (CIP) does not alter IRF-1 binding to CXCL10-specific ISRE. Nuclear extracts (2.5 μg) from HRV-16-infected cells (6 h post-infection) were incubated with 6.5 Units of CIP for 15 min at 37^{o}C followed by the addition of 50 mM EDTA to inactivate CIP. EMSA was performed on treated extracts using CXCL10-specific ISRE probe. Data is representative of three separate experiments.

6.3 Discussion

In this chapter, the role of IRF-1 during HRV-16-induced CXCL10 expression and MEK1 pathway-mediated CXCL10 negative regulation is further investigated. It was first established that IRF-1 mRNA and protein are induced, in a time-dependent manner, upon HRV-16 infection of BEAS-2B cells and HBE. Interestingly, in both cell types, there was high basal expression of IRF-1 mRNA (data not shown), but little or no basal expression of IRF-1 protein. Although HRV-16-induced IRF-1 expression was evident in both BEAS-2B cells and HBE, the kinetics of mRNA and protein induction varied between the two cells types. Interestingly the 6 to 9 h peak for both IRF-1 mRNA and protein induction in BEAS-2B cells is consistent with the time of maximum binding of IRF-1 to the ISRE site from the CXCL10 promoter that was previously noted in Chapter 4. Also, at 24 h post-infection, though HRV-16-induced IRF-1 mRNA expression was ~2-fold, there clearly was no detectable IRF-1 protein production in BEAS-2B cells. By contrast, IRF-1 induction in HBE had a delayed onset but was also more sustained, presumably reflecting underlying differences in the two cell types. The presence in both cell types of high basal IRF-1 mRNA together with absolute concordance between HRV-induced increases in IRF-1 mRNA expression and the appearance of IRF-1 protein, suggest that rapid translational control mechanisms are involved in IRF-1 regulation. This would be consistent with other studies also showing

temporal concordance between increases in IRF-1 mRNA and protein expression and binding to promoter recognition sequences[463-465]. In addition, the continued expression of IRF-1 mRNA without corresponding IRF-1 protein in BEAS-2B cells at 24 h may be due to modulation of IRF-1 protein stability[427,466-468]. Finally, it is highly plausible that multiple mechanisms regulate HRV-16-induced IRF-1 expression at the translational and/or post-translational levels and is dependent on the cell type.

Although IRF-1 has been shown to be associated with CXCL10 production induced by several viruses, including measles and influenza[450,451], and we have previously shown that HRV-16 infection of epithelial cells induces the binding of IRF-1 to the ISRE site from the CXCL10 promoter[236], siRNA approaches were utilized to definitively establish a direct involvement of IRF-1 in HRV-16-induced CXCL10 expression. Using two distinct duplexes in each case, it was observed that each siRNA knocked down HRV-16-induced IRF-1 protein expression in both BEAS-2B and HBE, although to a variable degree. Knockdown of IRF-1 using siRNAs led to both decreased HRV-16-induced IRF-1 binding to the ISRE site from the CXCL10 promoter and significantly abrogated HRV-16-induced CXCL10 protein production. The efficacy of each siRNA in affecting HRV-induced CXCL10 promoter activation and protein production was generally in accord with their effectiveness in knocking down IRF-1 levels in the cell type under study. Although IRF-1 siRNA reduced the HRV-16-induced binding of IRF-1 to the CXCL10 recognition sequence, there was also a reduction in the binding of both identified (IRF-2, ISGF-3) and unidentified bands in BEAS-2B cells and HBE. This indicated the other bound proteins required IRF-1 in order to either recognize or bind ISRE. Although IRF-1 duplex A was effective in BEAS-2B cells, it did not

induce effective knockdown in HBE. To confirm the data with duplex B in primary HBE, therefore, we used a third siRNA (duplex C), such that two distinct siRNA duplexes were confirmed the role of IRF-1 in HRV-16-induced CXCL10 in both cell types. The reason for the lack of effect by duplex A is not clear but could relate to differences in processing.

Both CCL5 and CXCL8 have been reported to contain functional ISRE sites in their promoter regions and to bind IRF-1 upon induction by cytokines or pathogens[454,460,469,470]. Interestingly, IRF-1 knockdown reduced HRV-16-induced production of CCL5 protein levels, but not CXCL8 protein from BEAS-2B cells. These data are consistent with earlier observations in Chapter 3 that inhibition of the MEK pathway significantly enhanced HRV-16-induced CCL5, but not CXCL8 production[267]. Thus, a subset of HRV-inducible genes, including CXCL10 and CCL5, are regulated by IRF-1 and, for these genes, the MEK1 pathway negatively regulates IRF-1.

In Chapters 4 and 5, we showed that inhibition or siRNA knockdown of MEK proteins enhanced HRV-16-induced IRF-1 binding to the CXCL10 ISRE recognition sequence in both BEAS-2B cell and HBE. In Chapter 6, we now show that HRV-16-induced IRF-1 mRNA and protein expression is not similarly enhanced in BEAS-2B or HBE upon MEK1/2 pathway inhibition or MEK protein knockdown. Given that HRV-16-induced CXCL10 expression in BEAS-2B cells is enhanced in the apparent absence of enhanced IRF-1 protein levels suggests that changes in HRV-16-induced IRF-1 binding to the CXCL10 may not be due changes in IRF-1 protein levels. This is further supported by the data showing that regardless of cell type or approach to alter MEK pathway function, HRV-16-induced IRF-1 binding is similarly enhanced in each instance.

Therefore, any changes in the level of HRV-16-induced IRF-1 protein in the presence of inhibitors or siRNA may be irrelevant during MEK1 pathway-mediated enhancement of HRV-16-induced production of CXCL10.

When BEAS-2B cells were treated with two different siRNAs against IRF-1 followed by MEK pathway inhibition (PD98059 or U0126) and HRV-16 infection, the results obtained differed with the two siRNAs used but were consistent with their relative effectiveness. Addition of either PD98059 or U0126 to cells transfected with IRF-1 duplex A still caused a marked enhancement. By contrast, in cells transfected with IRF-1 duplex B, neither PD98059 nor U0126 caused a significant enhancement of CXCL10 protein production. These results suggest that a substantial threshold degree of IRF-1 inhibition is required to prevent enhancement of HRV-induced CXCL10 production upon MEK pathway inhibition. When IRF-1 protein is reduced to a sufficient degree, then the MEK1 pathway can no longer adequately modulate IRF-1 to cause enhancement of CXCL10, indicating that IRF-1 is, indeed, a target of the MEK1 pathway and primarily mediates the negative regulation of HRV-induced CXCL10 expression. Although minor differences were seen in control siRNA-transfected cells on HRV-induced IRF-1 protein expression in the presence of U0126 and PD98059, both MEK pathway inhibitors enhanced HRV-16 induced CXCL10 protein production to a comparable degree. This further supports the concept that enhancement of CXCL10 production is not dependent solely on increased IRF-1 expression. Although phosphatase treatment did not alter HRV-16-induced IRF-1 binding to CXCL10 ISRE, it does not rule out the possible role of a post-translational modification of IRF-1 that is modulated by the MEK1 pathway[386,461,462,466]. Given that IRF-1 is known to dimerize[471], it is possible that any

HRV-induced phosphorylation events on IRF-1 are masked, in part, through dimerization, thus the exogenous phosphatase may not have access to these potentially phosphorylated residues.

In summary, the results demonstrate that IRF-1 is induced upon HRV-16 infection of human airway epithelial cells and plays a direct role in HRV-16-induced CXCL10 expression. Inhibitors of the MEK pathway enhanced HRV-16 induced IRF-1 mRNA but have variable effects on IRF-1 protein, depending on the cell type, raising the possibility that post-translational modification of IRF-1 may mediate its ability to bind to CXCL10 ISRE and enhance transcription. Although phosphorylation of IRF-1 does not appear to be essential for binding to the ISRE sequence in the CXCL10 promoter, it is possible that phosphorylation may enhance its transcriptional efficiency. Adequate ablation of IRF-1 protein prevents MEK1-pathway mediated enhancement of HRV-16-induced CXCL10. This is first demonstration of a direct role of HRV-16-induced IRF-1 in CXCL10 expression and its modulation by the MEK1 pathway.

Chapter Seven: General Discussion

While discussion of individual experimental results has been provided within the relevant chapters of this thesis, we will now review major findings to provide an overview of the thesis work and to discuss its implications.

7.1 General rationale

Currently, there is no effective treatment for HRV-induced exacerbations of asthma and COPD[78,472]. In a cohort of mild asthmatics, *Grunberg et al.*[472], found that inhaled corticosteroids were ineffective in reducing the increased airway inflammation following experimental HRV-16 infection. In addition, there have been no studies specifically examining the effects of corticosteroids during virus-induced exacerbations. It is clear, therefore, that elucidating the mechanisms through which HRV-induced exacerbations occurs is crucial to developing any effective treatment. HRV infection of the airway epithelium does not lead to any overt changes in cell integrity or viability, thus increased epithelial production of pro-inflammatory cytokines and chemokines likely contribute to the increased airway inflammation. We have previously shown that infection of human airway epithelial cells with HRV-16 induces both *in vivo* and *in vitro* expression of CXCL10[143,257]. This chemokine serves as a ligand for the CXCR3 receptor and may contribute to the inflammatory response by serving as a chemoattractant for various cells, including activated Type-1 lymphocytes and NK cells[240,241,250]. CXCL10 expression is increased in patients with asthma and COPD, and also has been linked to airway hyperresponsiveness in a murine model of asthma[72,221,253]. In addition, CXCL10

has been proposed to be a novel serum biomarker for HRV-induced exacerbations of asthma[222] and COPD[223], thus it is reasonable to suggest that epithelial cell production of CXCL10 contributes to the pathogenesis of HRV-induced exacerbations of asthma and COPD.

Activation of specific signalling pathways following HRV infection of the airway epithelium is a major mechanism through which chemokine expression is increased. Therefore, the current thesis focuses on specific signalling mechanisms by which HRV-induced CXCL10 expression is increased in airway epithelial cells. Surprisingly, there is limited knowledge on the signalling mechanisms responsible for HRV-induced CXCL10 expression. We, and others, have shown that HRV-16 induces the activation of the major MAPK pathways[262,267,268]. As such, we hypothesized that the MAPK pathways were involved in HRV-16-induced production of CXCL10 in airway epithelial cells.

7.2 MEK1/2 pathway-mediated enhancement of HRV-16-induced CXCL10 expression

In Chapter 3, it was shown that HRV-16 infection activated the four major MAPK pathways, including ERK1/2, ERK5, JNK, and p38 MAPK. In contrast to the other MAPK pathways, the ERK1/2 pathway was chronically active over all times points. The role of the MAPK pathways were further investigated using selective pharmacological inhibitors. They are widely employed to study the contribution of individual signalling pathway during stimulus-induced gene expression by blocking the activity of a specific kinase. It must be noted that results derived from the use of inhibitors must take into

account certain factors, including inhibitor specificity, pathway cross-talk, and redundancy[415].

Surprisingly, inhibition of the MEK1/2 pathway with either PD98059 or U0126, two structurally distinct and well-characterized compounds[342,404], enhanced airway epithelial production of HRV-16-induced CXCL10 mRNA and protein to a similar level. These similar effects were not limited to the BEAS-2B cell line, but were also seen in primary airway epithelial cells, thus confirming the effect in a more physiologically relevant cell type. The enhancement was surprising, given that the MEK1/2 pathway mediates the positive regulation of adenovirus[410] and rabies virus[411] production of CXCL10 expression. However, it has been shown in skin keratinocytes that PD98059 and U0126 enhances TNF-α-induced CXCL10 mRNA expression, in addition to expression of CCL2 and CCL5[473]. Interestingly, these effects were not at the transcriptional level, but rather, via effects on mRNA stability. It is possible, therefore, that in addition to effects on transcription, HRV-16-induced CXCL10 expression is also enhanced through effects on mRNA stability, but this is not addressed in the current thesis. More recently, PD98059 and U0126 has been shown to enhance CXCL10 mRNA after minor HRV group, HRV-1B, infection in BEAS-2B cells[474]. This finding was intriguing as it suggests that the negative regulation of virally-induced CXCL10 via the MEK1/2 pathway is a common event for both major and minor group HRV.

HRV-16-induced CXCL10 expression was also associated with a concentration-dependent abrogation of ERK1 in the presence of PD98059 and U0126. Since the ERK1/2 pathway is important in various cellular processes, including proliferation and differentiation, it is without surprise that other MAPK pathways, such as the ERK5

pathway, function in a redundant manner to replace to the loss of ERK1/2 function[475,476]. This is demonstrated by the fact that both ERK1/2 and ERK5 share a similar phosphorylation consensus site (TEY) and a similar kinase domain[291]. Furthermore, both kinases can phosphorylate common downstream targets[294,477,478]. Finally, PD98059 and U0126 have also been shown to inhibit both the MEK1/2 and MEK5 pathways[294,295]. Given these similarities, it was interesting to find that HRV-16-induced ERK5 did not play a role in the CXCL10 enhancement phenomenon. Although they are considered part of separate pathways, both the p38 and ERK1/2 pathways are capable of cross-talk[373,412,414], but no evidence indicated any p38 MAPK pathway cross-talk and, therefore, did not contribute to the MEK-ERK pathway-mediated down-regulation of CXCL10. Overall, the enhancement of HRV-16-induced CXCL10 expression is mediated through the MEK1/2-ERK pathway and is not due to either compensatory effects or cross-talk with other MAPK pathways.

CXCL10 was chosen as an appropriate model chemokine to study, but it is clear that there are numerous epithelium-derived chemokines[8], many of which are induced by HRV, including CXCL8 and CCL5[267]. In contrast to our previous finding with CXCL8[267], the current thesis demonstrates that HRV-16-induced CCL5 expression is enhanced upon MEK1/2 pathway inhibition. This suggests that a subset of HRV-inducible genes are differentially regulated by the MEK1/2 pathway. Furthermore, the enhancement phenomenon was selective for HRV infection, as demonstrated by the lack of IFN-β-induced CXCL10 enhancement. Furthermore, IFN-β did not induce ERK1/2 phosphorylation, which suggested that enhancement of CXCL10 expression was stimulus-specific and dependent on ERK1/2 phosphorylation. RNA viruses, including

influenza, are known to modulate the MEK1/2 pathway to facilitate their replication in host cells[326]. Interestingly, it was confirmed that HRV replication was not altered by either MEK1/2 pathway inhibitor, thus the changes to HRV-induced CXCL10 expression are not due to changes that increase viral replication and subsequent virion release. This is the first demonstration, to my knowledge, of the selective down-regulation of a subset of HRV-induced chemokines in human airway epithelial cells.

7.3 Effect of the MEK1/2 pathway on CXCL10 transcriptional regulation

We have previously shown that HRV-16-induced CXCL10 expression is mediated, in part, through transcriptional regulation[143,236]. In Chapter 4, this transcriptional effect was confirmed and it was further demonstrated that HRV-16-induced transcription requires a level of co-operation between the ISRE and κB recognition sequences. Interestingly, there is precedent for a similar type of ISRE and κB co-operativity in the regulation of iNOS[459], IFN-β[479], and CCL5[388]. Furthermore, it was confirmed that, indeed, MEK1/2 pathway-mediated enhancement of CXCL10 expression occurs at the level of transcription. Although binding of the NF-κB isoforms p50 and p65 to the CXCL10 κB recognition sequences are required for the up-regulation of CXCL10 expression, neither NF-κB signalling nor nuclear translocation and/or DNA binding was markedly altered by the MEK1/2 pathway. This is in contrast to previous reports that suggest that the MEK1/2 can negatively regulate NF-κB-dependent gene expression through effects on IKK activity, IκBα phosphorylation, and NF-κB nuclear translocation[371,480,481]. This result was surprising given the prominent role of NF-κB in

HRV-induced gene expression[267,359,368,482], but is supported by a study in the A549 alveolar epithelial carcinoma cell line, in which TNF-α or IL-1β-induced NF-κB nuclear translocation or DNA binding is not altered by inhibition of the MEK1/2 pathway[483]. This implies that any negative regulatory effects on the NF-κB pathway are stimulus and/or cell type specific.

In contrast to the lack of effect on NF-κB, pharmacologic inhibition of the MEK1/2 pathway enhanced HRV-16-induced IRF-1 nuclear translocation and/or binding to the CXCL10 ISRE in both BEAS-2B cells and HBE. Furthermore, supershift analysis confirmed that the enhanced IRF-1 band was, indeed, IRF-1 and not a different protein. This finding is consistent with a previous study in which TNF-α-induced CCL5 expression in colonic myofibroblasts is down-regulated through IL-17-induced effects on IRF-1 binding, independent of changes to NF-κB[484]. These data suggest that separate mechanisms may exist to positively and negatively regulate IRF-1 interactions with the CXCL10 promoter. In this regard, we have previously shown HRV-16-induced CXCL10 expression occurs, in part, through NF-κB-mediated modulation of IRF-1 synthesis and binding to CXCL10 ISRE[368]. Since the current thesis demonstrates that the MEK1/2 pathway does not alter NF-κB, it suggests any changes in IRF-1 nuclear translocation and/or binding are not due to MEK1/2 pathway modulation of the NF-κB pathway.

In summary, HRV-16-induced CXCL10 expression is transcriptionally down-regulated via MEK1/2 pathway modulation of IRF-1 interactions with the CXCL10 promoter, independent of effects on NF-κB.

7.4 MEK1 primarily mediates the down-regulation of CXCL10 expression

Although MEK1 and MEK2 share a high level of homology, their functions are not necessarily interachangeable[327,328,416,485]. In a mouse model, loss of MEK1 is embryonic lethal, while loss of MEK2 does affect viability[332]. Other studies have also shown that MEK1 and MEK2 selectively modulate various cellular processes, including cellular proliferation[486,487], cell cycle progression[488], and ERK2 subcellular localization[489]. A previous study has also shown the negative regulation of an anti-viral interferon response to vesicular stomatitis virus (VSV) is selectively mediated through a MEK2-dependent mechanism[490]. Given these functional differences, siRNA approaches were used to confirm a similar selectively, namely, that MEK1 primarily mediated the negative regulation of HRV-16-induced CXCL10 expression through changes in IRF-1 interactions with the CXCL10 promoter. Interestingly, the presence of MEK2 seemed to block the maximal effect of MEK1 on HRV-16-induced CXCL10 expression and IRF-1 interactions with the CXCL10 promoter. In fact, a model of MEK1/MEK2 counter-regulation has recently been proposed in which MEK1 can modulate MEK2 activity[332].

7.4.1 The role of ERK1/2 in HRV-16-induced CXCL10 expression

In Chapter 3, the enhancement of HRV-16-induced CXCL10 expression was shown to be associated with a loss of ERK1 phosphorylation in presence of MEK1/2 pathway inhibitors. In contrast, results from Chapter 5 showed that MEK1 siRNA-mediated enhancement of HRV-16-induced CXCL10 expression was not associated with a loss of ERK1/2 phosphorylation. Moreover, directly pharmacological inhibition of ERK1/2 activity did not result in the enhancement of HRV-induced CXCL10 expression.

Collectively, these data implied that ERK1/2 may not be involved in the enhancement phenomenon. In fact, previous studies have shown various cellular processes can function in a MEK-dependent, but ERK-independent manner, including, mitosis[491], protein phosphorylation[492], differentiation[493], and autophagy[494]. However, this conclusion was brought into doubt with ERK siRNA studies. Although the individual ERK1 and ERK2 siRNA data were inconclusive, 4 of 6 ERK1 and ERK2 siRNA duplex combinations resulted in the enhancement of HRV-16-induced production of CXCL10. Although MEK1 and MEK2 protein expression was not altered, siRNA knockdown of both ERK1 and ERK2, but not individual ERK proteins, in human lung fibroblasts has been shown to alter phosphatase function resulting in increased MEK activity[495]. Alternatively, it is possible that loss of ERK protein results in the breakdown of the MEK-ERK complex, which does not occur with the use of pharmacological inhibitors. The scaffold proteins, MEK partner 1 (MP1) and P14, are known to be central in maintaining the specificity of MEK-ERK signalling and localization at endosomes[496,497], thus it is plausible that a breakdown of the scaffolded MEK-ERK structure may partly explain these contradictory results between pharmacological inhibitors and siRNA. In addition, this may also explain why HRV-16-induced ERK1/2 phosphorylation is not abrogated upon siRNA knockdown of MEK1 and MEK2 protein. It is feasible that the loss of MEK1 and MEK2 protein may perturb cellular signalling pathways, such that ERK1/2 is now free to interact with other kinase(s) that does not normally occur in the presence of the normal MEK-ERK protein complex.

It is apparent that the removal of a protein from a cell using siRNA can result in a different phenotypic response than pharmacological inhibition of a physically intact

protein within the same signalling pathway or protein complex[440,441,498-501]. Given the complexity of signalling pathways, it is without surprise that siRNA and pharmacologic approaches can achieve differing results. These may occur due to changes in pathway redundancy, changes in feedback regulation and protein localization[440,441,498,499]. Any differences seen with siRNA and pharmacological approaches may be the result of a true biologic effect and not due to commonly assumed "off-target" effects[437,438]. Therefore, the current data emphasizes the need for careful interpretation of results obtained using siRNA knockdown versus pharmacologic inhibition.

In summary, siRNA knockdown revealed that MEK1 primarily mediates the negative regulation of HRV-induced CXCL10 expression, but the role of ERK1/2 remains inconclusive and requires further study. Even though certain discrepancies involving ERK1/2 remain unresolved, it is important to note that the same overall effect, namely, MEK1 pathway-mediated enhancement of HRV-16-induced CXCL10 and IRF-1 binding to ISRE, is seen using either siRNA and pharmacological approaches in both BEAS-2B cells and HBE.

7.5 IRF-1 regulation of HRV-induced CXCL10 expression

In Chapter 6, it is demonstrated for the first time that IRF-1 is, indeed, a direct regulator of HRV-16-induced CXCL10 expression. Furthermore, IRF-1 was also shown to regulate HRV-16-induced CCL5, but not CXCL8 expression, thus demonstrating a subset of IRF-1-dependent genes that are also susceptible to MEK pathway-mediated enhancement (Chapter 3). This finding is important as it expands our knowledge of the

transcriptional mechanisms involved in the epithelial expression of many HRV-inducible genes, including CXCL10.

In general, IRF-1 siRNA knockdown reduced HRV-16-induced binding of IRF-1, in addition to both identified (IRF-2 and ISGF-3) and unidentified proteins, to the CXCL10 ISRE recognition sequence. This implied that IRF-1 is mediating the translocation and/or binding of both IRF-2 and ISGF-3 to the CXCL10 ISRE. In this regard, IRF-1 has previously been shown to mediate IRF-2 and IRF8 DNA binding[386,502]. It is possible that the unidentified bands are unrecognized degradation fragments of IRF-1[427]. Although the binding of IRF-2, ISGF-3, and the unidentified protein(s) is increased by HRV-16 infection, and is dependent on the presence of IRF-1, they were not modulated by the MEK1 pathway. Therefore, these proteins do not seem to contribute to the down-regulation of HRV-16-induced CXCL10 expression. Clearly, the regulation of IRF interactions is complex and further studies would be required to investigate the significance of these interactions in the current context.

Although IRF-1 directly regulates HRV-16-induced CXCL10 expression, the current paradigm of virally-induced pro-inflammatory gene expression has implicated IRF-3 as a crucial transcriptional regulator[503]. In this regard, a previous study has shown that HRV-1B-induced epithelial gene expression, including CXCL10, is dependent on IRF-3[175]. Unfortunately, this study is limited by its reliance on only measuring mRNA levels and using a single IRF-3 siRNA duplex. Furthermore, the same group has preliminary data suggesting that the enhancement of HRV-1B-induced CXCL10 mRNA occurs independent of effects on IRF-3 activation[474]. In Chapter 4, an increase in IRF-3 binding to the CXCL10 promoter after HRV-16 infection was not detected, but this does

not exclude a role for IRF-3, as it is possible that DNA binding masked the epitope recognized by the supershift antibody. Alternatively, this discrepancy may be a result of differences between major group and minor group HRV activation of IRF-3, although two recent reports have shown that both major and minor group HRV prevent IRF-3 activation[398,399].

In summary, it is demonstrated for the first time that HRV-induced CXCL10 expression requires IRF-1 binding to the CXCL10 promoter. In addition, the expression of HRV-16-induced CCL5, but not CXCL8, is dependent on HRV-16-induced IRF-1. Coincidentally, both HRV-16-induced CXCL10 and CCL5, but not CXCL8, are regulated, in part, via effects of the MEK1 pathway.

7.6 Modulation of IRF-1 activity

In Chapter 6, it is confirmed that the MEK1 pathway, through an unknown mechanism, is directly altering IRF-1 interactions with the CXCL10 promoter, as a substantial loss of IRF-1 protein prevents the enhancement of HRV-induced CXCL10 expression. In HBE, enhancement of HRV-16-induced IRF-1 binding at the CXCL10 promoter was associated with enhanced HRV-16-induced IRF-1 mRNA and protein. In contrast, further investigation of MEK1 pathway effects on IRF-1 showed the ability of MEK1 pathway blockade to both enhance HRV-16-induced CXCL10 production and IRF-1 binding to the CXCL10 promoter in BEAS-2B cells in the apparent absence of enhanced IRF-1 protein induction. This intriguing observation raises the possibility that the increased binding of IRF-1 in both cell types is mediated via MEK pathway-sensitive post-translational modifications to IRF-1, rather than transcriptional or translational

changes. It is known that IRF-1 is susceptible to phosphorylation, SUMOylation, and ubiquitination[386,452,461-463,466-468]. Of these modifications, SUMOylation and ubiquitination are primarily involved in transcriptional repression of IRF-1 and/or stabilization of IRF-1 protein[463,466-468]. Phosphorylation of IRF-1 has been linked both to binding to ISRE sites and to transcriptional activation[386,461-463]. Unfortunately, the phosphorylation sites on the IRF-1 molecule have not been fully characterized. Accordingly, the effects of overall phosphorylation status on the ability of IRF-1 to bind to the ISRE site in the CXCL10 promoter were examined. Because IRF-1 has been reported to be phosphorylated on both serine and tyrosine residues[462], calf intestinal alkaline phosphatase was used as it dephosphorylates serine, threonine and tyrosine residues. Phosphatase treatment, however, did not alter HRV-16-induced IRF-1 binding to the ISRE sequence from the CXCL10 promoter. While this suggests that phosphorylation is not essential for binding, it does not rule out IRF-1 phosphorylation as an important post-translational modification that alters IRF-1 DNA binding and/or transcriptional efficiency. IRF-1 has been shown to both homo- and heterodimerize[396], in addition to associating with transcriptional co-activators (p300/CBP)[508] and basal transcription proteins (TFIIB)[396,471,502], but it is not known whether this dimerization and co-activator association is a prerequisite for IRF-1 DNA binding. It is plausible that phosphorylation-dependent modification of IRF-1 may be required prior to binding to induce IRF-1 dimerization and association with transcriptional activators to increase IRF-1 transcriptional efficiency. Interestingly, dimerization and subsequent transcriptional activation of the IRF-1-related transcription factors, IRF-3 and IRF-5, is dependent on site-specific phosphorylation[504-506]. Though highly speculative, the MEK1 pathway may

mediate its effects on IRF-1 by modulating phosphatase activity that may target IRF-1. In this regard, a previous study has demonstrated that increased expression of endogenous alkaline phosphatase directly de-phosphorylates IRF-5 resulting in decreased transcriptional activity[506]. Further studies, as discussed in Chapter 8, would be required to determine the phosphorylation status of IRF-1 and to elucidate the potential mechanism through the MEK1 pathway exerts its effects on IRF-1.

7.7 Clinical Implications

7.7.1 Targeting the MEK1 pathway

Inhibition of the MAPK pathways has been suggested to be a potential therapeutic target to reduce chronic inflammation, which is a hallmark of asthma and COPD[260,261]. The development of clinically effective p38 MAPK pathway inhibitors to reduce inflammatory mediator expression is currently being investigated[507]. In addition, several JNK pathway inhibitors are also undergoing preclinical evaluation[289]. Studies on the role of the ERK1/2 pathway have not been as intensive, even though levels of ERK1/2 phosphorylation are increased in airway epithelium of asthmatic subjects and correlate with neutrophil and eosinophil counts in airway tissue[279]. In a murine model of allergic airway inflammation, inhibition of the ERK1/2 pathway with U0126 reduced eosinophilia, mucus production, as well as the release of various pro-inflammatory cytokines and chemokines[343,508]. Furthermore, PD98059 treatment reduced the release of allergen-induced cysteinyl leukotrienes in guinea pig airways[509]. These results all support the paradigm that inhibition of elevated ERK1/2 pathway activity would be clinically beneficial in treating airway inflammation.

Data from the current thesis, in which the MEK1 pathway functions to down-regulate the expression of a subset of HRV-induced chemokines, including CXCL10 and CCL5, is not consistent with the above paradigm. However, it must be noted that these findings were based on allergen, and not HRV, induced airway inflammation. Therefore, it is not clear whether targeting the MEK1 pathway in the airway epithelium following HRV infection is necessarily beneficial or detrimental as a therapeutic target. In an *in vivo* setting, blocking MEK1 pathway function during an HRV-induced exacerbation could be detrimental as it may invariably lead to enhancement of inflammatory cell infiltration and mediator release into the airways based on the variety of cells CXCL10 can act on (section 1.8.2). Alternatively, enhancement of CXCL10 and CCL5 could be beneficial. Both CXCL10 and CCL5 are NK cell chemoattractants and it has been shown that CXCL10 increases NK cytolytic activity[240]. Serving as a major component of the innate immune system, NK cells can induce the apoptosis of virus-infected cells[510]. Therefore, enhancing innate responses through increased NK cell infiltration and cytolytic activity may be beneficial in the clearance of HRV-infected epithelial cells. Further studies both *in vivo* and *in vitro* are required to elucidate the subset of HRV-inducible and IRF-1-dependent genes that are also susceptible to MEK1 pathway modulation. Importantly, the down-regulatory effect of the MEK1 pathway *in vivo* also requires confirmation. Murine models of HRV infection have been studied[511-514], but their relevance to human infection is still not fully understood. Collectively, this thesis can be viewed as a novel, but preliminary evaluation of the endogenous down-regulatory pathways that serve to control HRV-induced and IRF-1-dependent pro-inflammatory gene expression in the airway epithelium. Although any clinical applicability is difficult

to assess at this point, the thesis offers a potential counter-intuitive approach to modulate HRV-induced inflammatory responses.

7.7.2 IRF-1 in asthma and COPD

The role of IRF-1 in asthma and COPD has not been studied in depth. Interestingly, gene association studies have shown that IRF-1 gene polymorphisms are linked to childhood atopic asthma[515,516], but similar studies in a COPD cohort have yet to be carried out. Recently, IRF-1 was proposed to mediate, in part, TNF-α/IFN-γ-induced corticosteroid resistance in airway smooth muscle cells by sequestering the glucocorticoid receptor co-activator, GR-interacting protein-1 (GRIP-1), preventing GR-dependent transcriptional regulation[517,518]. Whether a similar mechanism exists in airway epithelial cells remains unknown at this time. Interestingly, increased levels of IRF-1 protein are detected in the airway epithelium of asthmatic subjects, but not in the epithelium of chronic bronchitis or healthy subjects[519]. Corticosteroid treatment for HRV-induced exacerbations of asthma is largely ineffective and there are no currently commercially available anti-rhinoviral drugs. Therefore, the current finding that HRV-16 increases levels of IRF-1 protein in the airway epithelium, in addition to the previously published finding that IRF-1 protein levels are increased in the epithelium of asthmatics subjects, is an exciting starting point to study the potential of IRF-1 as a therapeutic target to reduce the inflammation associated with HRV-induced exacerbations. It may potentially also help explain why HRV-induced exacerbations of asthma are resistant to GC treatment.

7.8 Conclusions

In summary, I propose a model (Figure 7.1) in which the MEK1 pathway selectively down-regulates HRV-16-induced expression of CXCL10 in airway epithelial cells, in part, through effects on transcription. The mechanism appears to involve modification of IRF-1 interaction with the ISRE found within the CXCL10 promoter. Further investigation of IRF-1 determined that it is induced upon HRV-16 infection and plays a direct role in HRV-16-induced CXCL10 expression. The effects of the MEK1 pathway on HRV-induced CXCL10 are blocked with adequate ablation of IRF-1 protein. Furthermore, the MEK1 pathway may mediate its effect on IRF-1 through a post-translational modification that may alter IRF-1 binding and/or transcriptional efficiency. Although phosphorylation of IRF-1 does not appear to be essential for binding to the ISRE sequence in the CXCL10 promoter, it is possible that phosphorylation may enhance transcriptional efficiency of IRF-1. To my knowledge, this is the first description of the negative regulation of HRV-induced chemokine expression in airway epithelial cells via MEK1 pathway effects on IRF-1. This indicates that the MEK1 pathway may have anti-inflammatory and protective roles during HRV infections. A better understanding of the mechanisms underlying MEK1 pathway-mediated down-regulation of IRF-1-dependent gene expression may help elucidate potentially novel therapeutic targets to combat HRV-induced exacerbations of asthma and COPD.

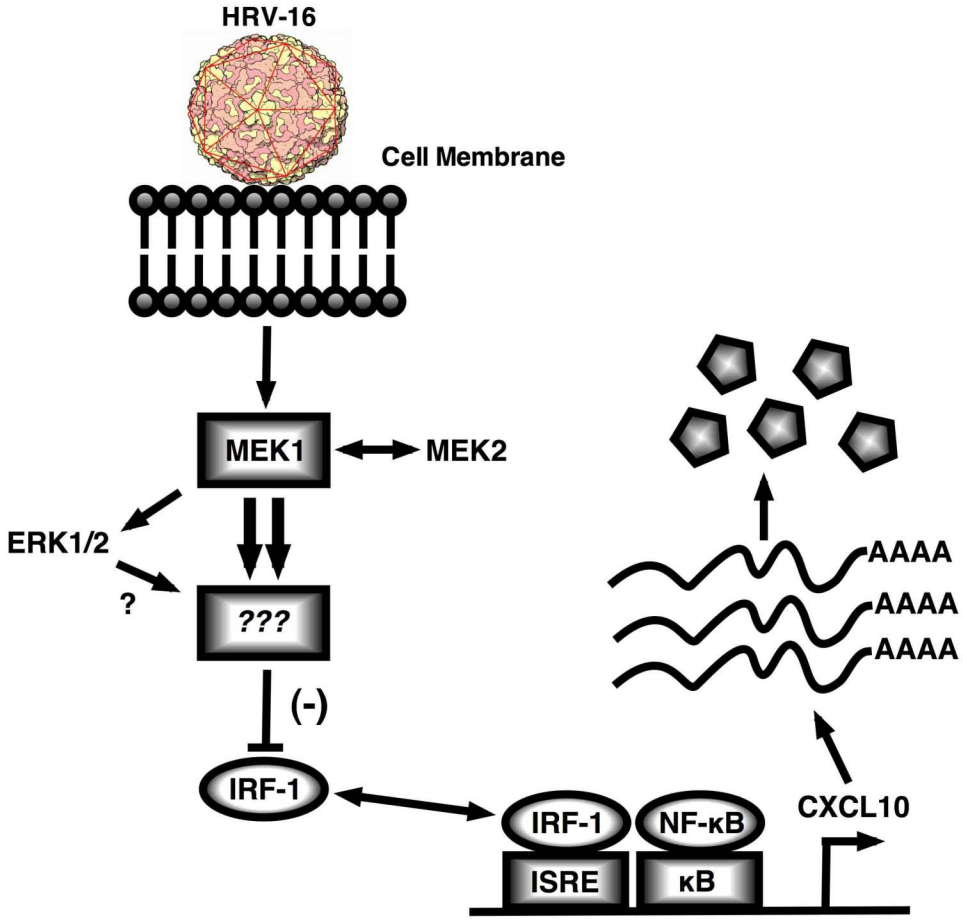

Figure 7.1 – Proposed model of the selective down-regulation of HRV-16-induced CXCL10 expression in human airway epithelial cells. HRV infection of airway epithelial cells induces CXCL10 expression through increased binding of NF-κB and IRF-1 to specific recognition sequences found within the CXCL10 promoter. HRV-16 infection also activates the MEK1/2-ERK1/2 pathway and loss of MEK1 function through pharmacologic inhibition or siRNA knockdown enhances HRV-16-induced CXCL10 transcription, in an NF-κB-independent manner, via effects on IRF-1 interactions at the ISRE within the CXCL10 promoter. Loss of MEK2 protein maximizes CXCL10 enhancement through an unknown mechanism. The role of ERK1/2 in this process is also uncertain. Finally, MEK1 pathway alteration of IRF-1 interactions with ISRE may be mediated through a post-translational modification, such as phosphorylation, which may modulate IRF-1 transcriptional efficiency to down-regulate HRV-induced CXCL10 transcription.

Chapter Eight: Future Studies

The data presented in this thesis highlights several areas for further investigation.

8.1 Chapter 3

In Chapter 3, HRV-16 infection of the BEAS-2B cells was shown to induce the activation of various MAPK pathways, including ERK1/2, ERK5, p38, and JNK MAPK. Compared with the other pathways, ERK1/2 was chronically phosphorylated in response to HRV-16 infection. Future studies would confirm if a similar chronic activation of ERK1/2 is seen in primary airway epithelial cells. Furthermore, given that ERK1/2 is chronically active it would also be of interest to determine the temporal kinetics of MEK1/2 activation in response to HRV infection.

Pharmacologic inhibition of the MEK1/2 pathway was shown to enhance both HRV-16-induced CXCL10 and CCL5 expression, but not CXCL8 expression[267], indicating that not all HRV-inducible chemokines are susceptible to MEK1/2 pathway-mediated negative regulation. As such, it would be important to perform a larger characterization of HRV-inducible genes that are or are not susceptible to MEK1/2 pathway-mediated regulation.

All of the studies in the current thesis have used HRV serotype 16, a member of the major group HRV, which account for the majority of HRVs (> 90) and utilize the surface expressed ICAM-1 receptor for cell entry. The effect of minor group HRV, which use LDLR for cell entry, would also be assessed confirm that the MEK1-mediated

enhancement of CXCL10 is common to both groups of HRV and not associated with only ICAM-1 usage.

Finally, since HRV infections are strongly associated with exacerbations of asthma and COPD[88,520], it would be of interest to perform similar experiments in airway epithelial cells from individuals with either airway disease to confirm whether the enhancement phenotype persists.

8.2 Chapter 4

In Chapter 4, MEK1/2 pathway inhibition was shown to enhance IRF-1 binding to the CXCL10 ISRE recognition sequence. Changes in IRF-1 binding were demonstrated using EMSA, but a limitation of this *in vitro* technique is that binding is assessed using a short synthetic nucleotide sequence and does not account for binding that may be dependent on a larger sequence context or chromatin structure. Future studies would confirm the enhancement of IRF-1 binding using the chromatin immunoprecipitation (ChIP) technique. In contrast to EMSA, this *in vivo* approach permits the study of transcription factor binding to specific promoter sites on endogenous DNA, thus addressing some of the limitations associated with EMSAs.

The studies in this chapter solely focused on transcriptional effects, but effects on CXCL10 mRNA stability could also occur given that changes in transcription and mRNA stability are not necessarily mutually exclusive. Changes to steady state levels of CXCL10 mRNA levels occur over an extended period[143], thus actinomycin D pulse-chase experiments would not be feasible given the high level of cytotoxicity associated with lengthy exposure to BEAS-2B cells. An alternative method to study changes in mRNA

stability is through the use of a plasmid containing the normally stable rabbit β-globin gene, but with its 3'UTR sequence replaced by the 3'UTR sequence of CXCL10. Changes in rabbit β-globin-CXCL10 3'UTR mRNA stability in the presence of HRV-16 with or without MEK1/2 pathway inhibitors over various time points would be assessed by RT-PCR.

8.3 Chapter 5

In Chapter 5, the combined siRNA knockdown of both ERK1 and ERK2 protein consistently enhanced HRV-16-induced CXCL10 expression with the majority of ERK siRNA combinations. The enhancement of HRV-induced CXCL10 following ERK1 and ERK2 knockdown may be due to alterations in MEK1/2 activity[495], therefore the any changes in MEK1/2 activation could be assessed.

8.4 Chapter 6

The studies performed in Chapter 6 demonstrated that CXCL10 expression is regulated by IRF-1. Even though the addition of an exogenous phosphatase to nuclear extracts did not alter HRV-induced IRF-1 binding to the CXCL10 ISRE recognition sequence, this result does not exclude phosphorylation as an important post-translational modification of IRF-1. Assessment of any IRF-1 post-translational modificiation after HRV infection with and without loss of MEK1 function could be initially assessed by 2D-gel electrophoresis. If changes are detected then experiments could be carried out by over-expressing tagged wildtype IRF-1 protein in HRV-infected airway epithelial cells with or without MEK1/2 inhibitors, immunoprecipating the overexpressed IRF-1 protein

and immunoblotting with pan phospho-Serine as various serine residues in the C-terminal portion of IRF-1 are necessary for IRF-1 binding and transcriptional activity[462]. This would crudely determine whether overall phosphorylation of IRF-1 is increased by HRV infection and if loss of MEK1 function alters the overall phosphorylation state of IRF-1. One approach to demonstrate the formation of IRF-1 dimers is through the over-expression of recombinant IRF-1 protein with different protein tags (e.g. FLAG and HA) in HRV-infected airway epithelial cells. Immunoprecipitation of FLAG-tagged IRF-1 from whole cell lysates followed by immunoblotting for HA could demonstrate the formation of IRF-1 dimers.

As mentioned in Chapter 7, IRF-1 protein levels are increased in asthmatic airway epithelial cells compared with healthy subjects[519] and IRF-1 may also play a role in airway smooth muscle steroid dysfunction[518], thus it would be interesting to assess if a similar phenomenon of IRF-1-mediated steroid dysfunction exists in epithelial cells.

Overall, the focus of any future studies would be to assess both HRV-induced IRF-1-dependent and MEK1 pathway susceptible genes in the airway epithelium. These studies would further delineate the molecular mechanisms by which HRV-induced gene expression is down-regulated. Finally, it would be interesting to correlate the current findings in epithelial cells from patients with asthma and COPD.

References

1. Donnelly, L.E. The Epithelium as a Target. in *The Pulmonary Epithelium in Health and Disease* (ed. Proud, D.) 57-74 (John Wiley and Sons, West Sussex, 2008).
2. Thurlbeck, W.M. The lung: structure, function and disease. Miscellany. *Monogr Pathol* **19**, 287-315 (1978).
3. Chang, M., Shih, L., and Wu, R. Pulmonary Epithelium: Cell Types and Functions. in *The Pulmonary Epithelium in Health and Disease* (ed. Proud, D.) 2-26 (John Wiley and Sons, West Sussex, 2008).
4. Breeze, R.G. & Wheeldon, E.B. The cells of the pulmonary airways. *Am Rev Respir Dis* **116**, 705-777 (1977).
5. Young, B., Lowe, J., Stevens, A. & Heath, J. *Wheater's Functional HIstology: A Text and Color Atlas*, (Elsevier Science, Philadelphia, 2006).
6. Nettesheim, P., Jetten, A.M., Inayama, Y., Brody, A.R., George, M.A., Gilmore, L.B., Gray, T. & Hook, G.E. Pathways of differentiation of airway epithelial cells. *Environ Health Perspect* **85**, 317-329 (1990).
7. Griffiths, M.J., Bonnet, D. & Janes, S.M. Stem cells of the alveolar epithelium. *Lancet* **366**, 249-260 (2005).
8. Proud, D. Biology of Epithelial Cells. in *Middleton's Allergy: Principles and Practice*, Vol. 1 (ed. Adkinson, N., Busse, W., Bochner, B., Holgate, S., Lemankse, R., and Simons, F.) 373-387 (Mosby, Philadelphia, 2009).
9. Knight, D.A. & Holgate, S.T. The airway epithelium: structural and functional properties in health and disease. *Respirology* **8**, 432-446 (2003).
10. Holgate, S.T. Epithelium dysfunction in asthma. *J Allergy Clin Immunol* **120**, 1233-1244; quiz 1245-1236 (2007).
11. Busse, W.W. & Lemanske, R.F., Jr. Asthma. *N Engl J Med* **344**, 350-362 (2001).
12. Bateman, E.D., Hurd, S.S., Barnes, P.J., Bousquet, J., Drazen, J.M., FitzGerald, M., Gibson, P., Ohta, K., O'Byrne, P., Pedersen, S.E., Pizzichini, E., Sullivan, S.D., Wenzel, S.E. & Zar, H.J. Global strategy for asthma management and prevention: GINA executive summary. *Eur Respir J* **31**, 143-178 (2008).
13. Senthilselvan, A. Prevalence of physician-diagnosed asthma in Saskatchewan, 1981 to 1990. *Chest* **114**, 388-392 (1998).
14. Mao, Y., Semenciw, R., Morrison, H., MacWilliam, L., Davies, J. & Wigle, D. Increased rates of illness and death from asthma in Canada. *CMAJ* **137**, 620-624 (1987).
15. DeMeo, D., and Weiss, S. Epidemiology. in *Asthma and COPD* (ed. Barnes, P.J., Drazen, J.M., Rennard, S., Thomson, N.C.) 7-18 (Academic Press, London, 2002).
16. Hoskins, G., McCowan, C., Neville, R.G., Thomas, G.E., Smith, B. & Silverman, S. Risk factors and costs associated with an asthma attack. *Thorax* **55**, 19-24 (2000).
17. Krahn, M.D., Berka, C., Langlois, P. & Detsky, A.S. Direct and indirect costs of asthma in Canada, 1990. *CMAJ* **154**, 821-831 (1996).

18. Burrows, B., Martinez, F.D., Halonen, M., Barbee, R.A. & Cline, M.G. Association of asthma with serum IgE levels and skin-test reactivity to allergens. *N Engl J Med* **320**, 271-277 (1989).
19. Jackson, D.J., Gangnon, R.E., Evans, M.D., Roberg, K.A., Anderson, E.L., Pappas, T.E., Printz, M.C., Lee, W.M., Shult, P.A., Reisdorf, E., Carlson-Dakes, K.T., Salazar, L.P., DaSilva, D.F., Tisler, C.J., Gern, J.E. & Lemanske, R.F., Jr. Wheezing rhinovirus illnesses in early life predict asthma development in high-risk children. *Am J Respir Crit Care Med* **178**, 667-672 (2008).
20. Larche, M., Robinson, D.S. & Kay, A.B. The role of T lymphocytes in the pathogenesis of asthma. *J Allergy Clin Immunol* **111**, 450-463; quiz 464 (2003).
21. Horn, B.R., Robin, E.D., Theodore, J. & Van Kessel, A. Total eosinophil counts in the management of bronchial asthma. *N Engl J Med* **292**, 1152-1155 (1975).
22. Frigas, E., Loegering, D.A. & Gleich, G.J. Cytotoxic effects of the guinea pig eosinophil major basic protein on tracheal epithelium. *Lab Invest* **42**, 35-43 (1980).
23. Hamid, Q. & Tulic, M. Immunobiology of asthma. *Annu Rev Physiol* **71**, 489-507 (2009).
24. Hartl, D., Koller, B., Mehlhorn, A.T., Reinhardt, D., Nicolai, T., Schendel, D.J., Griese, M. & Krauss-Etschmann, S. Quantitative and functional impairment of pulmonary CD4+CD25hi regulatory T cells in pediatric asthma. *J Allergy Clin Immunol* **119**, 1258-1266 (2007).
25. Robinson, D.S. Regulatory T cells and asthma. *Clin Exp Allergy* **39**, 1314-1323 (2009).
26. Lisbonne, M., Diem, S., de Castro Keller, A., Lefort, J., Araujo, L.M., Hachem, P., Fourneau, J.M., Sidobre, S., Kronenberg, M., Taniguchi, M., Van Endert, P., Dy, M., Askenase, P., Russo, M., Vargaftig, B.B., Herbelin, A. & Leite-de-Moraes, M.C. Cutting edge: invariant V alpha 14 NKT cells are required for allergen-induced airway inflammation and hyperreactivity in an experimental asthma model. *J Immunol* **171**, 1637-1641 (2003).
27. Akbari, O., Faul, J.L., Hoyte, E.G., Berry, G.J., Wahlstrom, J., Kronenberg, M., DeKruyff, R.H. & Umetsu, D.T. CD4+ invariant T-cell-receptor+ natural killer T cells in bronchial asthma. *N Engl J Med* **354**, 1117-1129 (2006).
28. Vijayanand, P., Seumois, G., Pickard, C., Powell, R.M., Angco, G., Sammut, D., Gadola, S.D., Friedmann, P.S. & Djukanovic, R. Invariant natural killer T cells in asthma and chronic obstructive pulmonary disease. *N Engl J Med* **356**, 1410-1422 (2007).
29. Alcorn, J.F., Christopher R. Crowe, & Kolls, a.J.K. TH17 Cells in Asthma and COPD. *Annual Reviews of Physiology* **72**, 14.11-14.22 (2010).
30. Bergeron, C. & Boulet, L.P. Structural changes in airway diseases: characteristics, mechanisms, consequences, and pharmacologic modulation. *Chest* **129**, 1068-1087 (2006).
31. Laitinen, L.A., Heino, M., Laitinen, A., Kava, T. & Haahtela, T. Damage of the airway epithelium and bronchial reactivity in patients with asthma. *Am Rev Respir Dis* **131**, 599-606 (1985).

32. Jeffery, P.K. Structural and inflammatory changes in COPD: a comparison with asthma. *Thorax* **53**, 129-136 (1998).
33. Ordonez, C.L. & Fahy, J.V. Epithelial desquamation in asthma. *Am J Respir Crit Care Med* **164**, 1997 (2001).
34. Rickard, K.A., Taylor, J. & Rennard, S.I. Observations of development of resistance to detachment of cultured bovine bronchial epithelial cells in response to protease treatment. *Am J Respir Cell Mol Biol* **6**, 414-420 (1992).
35. Winther, B., Gwaltney, J.M. & Hendley, J.O. Respiratory virus infection of monolayer cultures of human nasal epithelial cells. *Am Rev Respir Dis* **141**, 839-845 (1990).
36. Ordonez, C., Ferrando, R., Hyde, D.M., Wong, H.H. & Fahy, J.V. Epithelial desquamation in asthma: artifact or pathology? *Am J Respir Crit Care Med* **162**, 2324-2329 (2000).
37. Roche, W.R., Beasley, R., Williams, J.H. & Holgate, S.T. Subepithelial fibrosis in the bronchi of asthmatics. *Lancet* **1**, 520-524 (1989).
38. Laitinen, A., Altraja, A., Kampe, M., Linden, M., Virtanen, I. & Laitinen, L.A. Tenascin is increased in airway basement membrane of asthmatics and decreased by an inhaled steroid. *Am J Respir Crit Care Med* **156**, 951-958 (1997).
39. Willis, B.C. & Borok, Z. TGF-beta-induced EMT: mechanisms and implications for fibrotic lung disease. *Am J Physiol Lung Cell Mol Physiol* **293**, L525-534 (2007).
40. Hackett, T.L., Warner, S.M., Stefanowicz, D., Shaheen, F., Pechkovsky, D.V., Murray, L.A., Argentieri, R., Kicic, A., Stick, S.M., Bai, T.R. & Knight, D.A. Induction of epithelial-mesenchymal transition in primary airway epithelial cells from patients with asthma by transforming growth factor-beta1. *Am J Respir Crit Care Med* **180**, 122-133 (2009).
41. Mannino, D.M. & Buist, A.S. Global burden of COPD: risk factors, prevalence, and future trends. *Lancet* **370**, 765-773 (2007).
42. Rabe, K.F., Hurd, S., Anzueto, A., Barnes, P.J., Buist, S.A., Calverley, P., Fukuchi, Y., Jenkins, C., Rodriguez-Roisin, R., van Weel, C. & Zielinski, J. Global strategy for the diagnosis, management, and prevention of chronic obstructive pulmonary disease: GOLD executive summary. *Am J Respir Crit Care Med* **176**, 532-555 (2007).
43. Mannino, D.M., Doherty, D.E. & Sonia Buist, A. Global Initiative on Obstructive Lung Disease (GOLD) classification of lung disease and mortality: findings from the Atherosclerosis Risk in Communities (ARIC) study. *Respir Med* **100**, 115-122 (2006).
44. Lopez, A.D. & Murray, C.C. The global burden of disease, 1990-2020. *Nat Med* **4**, 1241-1243 (1998).
45. Chapman, K.R. Chronic obstructive pulmonary disease: are women more susceptible than men? *Clin Chest Med* **25**, 331-341 (2004).
46. McFarlane, N., Goldstein, R. Life and Breath: Respiratory Disease in Canada. (ed. Canada, P.H.A.o.) 51-62 (Minister of Health, Ottawa, 2007).

47. Franklin, W., Lowell, F.C., Michelson, A.L. & Schiller, I.W. Chronic obstructive pulmonary emphysema; a disease of smokers. *Ann Intern Med* **45**, 268-274 (1956).
48. Rennard, S.I. & Vestbo, J. COPD: the dangerous underestimate of 15%. *Lancet* **367**, 1216-1219 (2006).
49. Smith, C.A. & Harrison, D.J. Association between polymorphism in gene for microsomal epoxide hydrolase and susceptibility to emphysema. *Lancet* **350**, 630-633 (1997).
50. Wu, L., Chau, J., Young, R.P., Pokorny, V., Mills, G.D., Hopkins, R., McLean, L. & Black, P.N. Transforming growth factor-beta1 genotype and susceptibility to chronic obstructive pulmonary disease. *Thorax* **59**, 126-129 (2004).
51. Stoller, J.K. & Aboussouan, L.S. Alpha1-antitrypsin deficiency. *Lancet* **365**, 2225-2236 (2005).
52. Hnizdo, E., Sullivan, P.A., Bang, K.M. & Wagner, G. Association between chronic obstructive pulmonary disease and employment by industry and occupation in the US population: a study of data from the Third National Health and Nutrition Examination Survey. *Am J Epidemiol* **156**, 738-746 (2002).
53. Orozco-Levi, M., Garcia-Aymerich, J., Villar, J., Ramirez-Sarmiento, A., Anto, J.M. & Gea, J. Wood smoke exposure and risk of chronic obstructive pulmonary disease. *Eur Respir J* **27**, 542-546 (2006).
54. Barnes, P.J. *Chronic Obstructive Pulmonary Disease : Cellular and Molecular Mechanisms*, (Taylor and Francis Group, Boca Raton, 2005).
55. Barnes, P.J. Genetics and pulmonary medicine. 9. Molecular genetics of chronic obstructive pulmonary disease. *Thorax* **54**, 245-252 (1999).
56. Meshi, B., Vitalis, T.Z., Ionescu, D., Elliott, W.M., Liu, C., Wang, X.D., Hayashi, S. & Hogg, J.C. Emphysematous lung destruction by cigarette smoke. The effects of latent adenoviral infection on the lung inflammatory response. *Am J Respir Cell Mol Biol* **26**, 52-57 (2002).
57. Matthews, J.G., Ito, K., Barnes, P.J. & Adcock, I.M. Defective glucocorticoid receptor nuclear translocation and altered histone acetylation patterns in glucocorticoid-resistant patients. *J Allergy Clin Immunol* **113**, 1100-1108 (2004).
58. Marwick, J.A., Ito, K., Adcock, I.M. & Kirkham, P.A. Oxidative stress and steroid resistance in asthma and COPD: pharmacological manipulation of HDAC-2 as a therapeutic strategy. *Expert Opin Ther Targets* **11**, 745-755 (2007).
59. Cosio, M.G. Autoimmunity, T-cells and STAT-4 in the pathogenesis of chronic obstructive pulmonary disease. *Eur Respir J* **24**, 3-5 (2004).
60. Cosio, M.G., Saetta, M. & Agusti, A. Immunologic aspects of chronic obstructive pulmonary disease. *N Engl J Med* **360**, 2445-2454 (2009).
61. Hogg, J.C. Pathophysiology of airflow limitation in chronic obstructive pulmonary disease. *Lancet* **364**, 709-721 (2004).
62. Hogg, J.C., Chu, F., Utokaparch, S., Woods, R., Elliott, W.M., Buzatu, L., Cherniack, R.M., Rogers, R.M., Sciurba, F.C., Coxson, H.O. & Pare, P.D. The nature of small-airway obstruction in chronic obstructive pulmonary disease. *N Engl J Med* **350**, 2645-2653 (2004).

63. Lacoste, J.Y., Bousquet, J., Chanez, P., Van Vyve, T., Simony-Lafontaine, J., Lequeu, N., Vic, P., Enander, I., Godard, P. & Michel, F.B. Eosinophilic and neutrophilic inflammation in asthma, chronic bronchitis, and chronic obstructive pulmonary disease. *J Allergy Clin Immunol* **92**, 537-548 (1993).
64. Keatings, V.M., Collins, P.D., Scott, D.M. & Barnes, P.J. Differences in interleukin-8 and tumor necrosis factor-alpha in induced sputum from patients with chronic obstructive pulmonary disease or asthma. *Am J Respir Crit Care Med* **153**, 530-534 (1996).
65. Stockley, R.A. Neutrophils and the pathogenesis of COPD. *Chest* **121**, 151S-155S (2002).
66. Finkelstein, R., Fraser, R.S., Ghezzo, H. & Cosio, M.G. Alveolar inflammation and its relation to emphysema in smokers. *Am J Respir Crit Care Med* **152**, 1666-1672 (1995).
67. Di Stefano, A., Capelli, A., Lusuardi, M., Balbo, P., Vecchio, C., Maestrelli, P., Mapp, C.E., Fabbri, L.M., Donner, C.F. & Saetta, M. Severity of airflow limitation is associated with severity of airway inflammation in smokers. *Am J Respir Crit Care Med* **158**, 1277-1285 (1998).
68. Retamales, I., Elliott, W.M., Meshi, B., Coxson, H.O., Pare, P.D., Sciurba, F.C., Rogers, R.M., Hayashi, S. & Hogg, J.C. Amplification of inflammation in emphysema and its association with latent adenoviral infection. *Am J Respir Crit Care Med* **164**, 469-473 (2001).
69. Song, W., Zhao, J. & Li, Z. Interleukin-6 in bronchoalveolar lavage fluid from patients with COPD. *Chin Med J (Engl)* **114**, 1140-1142 (2001).
70. Kharitonov, S.A. & Barnes, P.J. Exhaled markers of pulmonary disease. *Am J Respir Crit Care Med* **163**, 1693-1722 (2001).
71. Kanazawa, H., Shiraishi, S., Hirata, K. & Yoshikawa, J. Imbalance between levels of nitrogen oxides and peroxynitrite inhibitory activity in chronic obstructive pulmonary disease. *Thorax* **58**, 106-109 (2003).
72. Saetta, M., Mariani, M., Panina-Bordignon, P., Turato, G., Buonsanti, C., Baraldo, S., Bellettato, C.M., Papi, A., Corbetta, L., Zuin, R., Sinigaglia, F. & Fabbri, L.M. Increased expression of the chemokine receptor CXCR3 and its ligand CXCL10 in peripheral airways of smokers with chronic obstructive pulmonary disease. *Am J Respir Crit Care Med* **165**, 1404-1409 (2002).
73. Traves, S.L., Culpitt, S.V., Russell, R.E., Barnes, P.J. & Donnelly, L.E. Increased levels of the chemokines GROalpha and MCP-1 in sputum samples from patients with COPD. *Thorax* **57**, 590-595 (2002).
74. Grumelli, S., Corry, D.B., Song, L.Z., Song, L., Green, L., Huh, J., Hacken, J., Espada, R., Bag, R., Lewis, D.E. & Kheradmand, F. An immune basis for lung parenchymal destruction in chronic obstructive pulmonary disease and emphysema. *PLoS Med* **1**, e8 (2004).
75. Smyth, L.J., Starkey, C., Vestbo, J. & Singh, D. CD4-regulatory cells in COPD patients. *Chest* **132**, 156-163 (2007).
76. Barnes, P.J. Immunology of asthma and chronic obstructive pulmonary disease. *Nat Rev Immunol* **8**, 183-192 (2008).

77. Rodriguez-Roisin, R. Toward a consensus definition for COPD exacerbations. *Chest* **117**, 398S-401S (2000).
78. Traves, S.L. & Proud, D. Viral-associated exacerbations of asthma and COPD. *Curr Opin Pharmacol* **7**, 252-258 (2007).
79. Pauwels, R.A., Buist, A.S., Calverley, P.M., Jenkins, C.R. & Hurd, S.S. Global strategy for the diagnosis, management, and prevention of chronic obstructive pulmonary disease. NHLBI/WHO Global Initiative for Chronic Obstructive Lung Disease (GOLD) Workshop summary. *Am J Respir Crit Care Med* **163**, 1256-1276 (2001).
80. Spencer, S., Calverley, P.M., Sherwood Burge, P. & Jones, P.W. Health status deterioration in patients with chronic obstructive pulmonary disease. *Am J Respir Crit Care Med* **163**, 122-128 (2001).
81. Heymann, P.W., Carper, H.T., Murphy, D.D., Platts-Mills, T.A., Patrie, J., McLaughlin, A.P., Erwin, E.A., Shaker, M.S., Hellems, M., Peerzada, J., Hayden, F.G., Hatley, T.K. & Chamberlain, R. Viral infections in relation to age, atopy, and season of admission among children hospitalized for wheezing. *J Allergy Clin Immunol* **114**, 239-247 (2004).
82. Kling, S., Donninger, H., Williams, Z., Vermeulen, J., Weinberg, E., Latiff, K., Ghildyal, R. & Bardin, P. Persistence of rhinovirus RNA after asthma exacerbation in children. *Clin Exp Allergy* **35**, 672-678 (2005).
83. Mallia, P. & Johnston, S.L. How viral infections cause exacerbation of airway diseases. *Chest* **130**, 1203-1210 (2006).
84. Murray, C.S., Poletti, G., Kebadze, T., Morris, J., Woodcock, A., Johnston, S.L. & Custovic, A. Study of modifiable risk factors for asthma exacerbations: virus infection and allergen exposure increase the risk of asthma hospital admissions in children. *Thorax* **61**, 376-382 (2006).
85. Nicholson, K.G., Kent, J. & Ireland, D.C. Respiratory viruses and exacerbations of asthma in adults. *BMJ* **307**, 982-986 (1993).
86. Dales, R.E., Schweitzer, I., Toogood, J.H., Drouin, M., Yang, W., Dolovich, J. & Boulet, J. Respiratory infections and the autumn increase in asthma morbidity. *Eur Respir J* **9**, 72-77 (1996).
87. Johnston, S.L., Pattemore, P.K., Sanderson, G., Smith, S., Campbell, M.J., Josephs, L.K., Cunningham, A., Robinson, B.S., Myint, S.H., Ward, M.E., Tyrrell, D.A. & Holgate, S.T. The relationship between upper respiratory infections and hospital admissions for asthma: a time-trend analysis. *Am J Respir Crit Care Med* **154**, 654-660 (1996).
88. Johnston, S.L., Pattemore, P.K., Sanderson, G., Smith, S., Lampe, F., Josephs, L., Symington, P., O'Toole, S., Myint, S.H., Tyrrell, D.A. & et al. Community study of role of viral infections in exacerbations of asthma in 9-11 year old children. *BMJ* **310**, 1225-1229 (1995).
89. Seemungal, T., Harper-Owen, R., Bhowmik, A., Moric, I., Sanderson, G., Message, S., Maccallum, P., Meade, T.W., Jeffries, D.J., Johnston, S.L. & Wedzicha, J.A. Respiratory viruses, symptoms, and inflammatory markers in acute exacerbations and stable chronic obstructive pulmonary disease. *Am J Respir Crit Care Med* **164**, 1618-1623 (2001).

90. Papi, A., Bellettato, C.M., Braccioni, F., Romagnoli, M., Casolari, P., Caramori, G., Fabbri, L.M. & Johnston, S.L. Infections and airway inflammation in chronic obstructive pulmonary disease severe exacerbations. *Am J Respir Crit Care Med* **173**, 1114-1121 (2006).
91. van den Hoogen, B.G., van Doornum, G.J., Fockens, J.C., Cornelissen, J.J., Beyer, W.E., de Groot, R., Osterhaus, A.D. & Fouchier, R.A. Prevalence and clinical symptoms of human metapneumovirus infection in hospitalized patients. *J Infect Dis* **188**, 1571-1577 (2003).
92. Pelon, W., Mogabgab, W.J., Phillips, I.A. & Pierce, W.E. A cytopathogenic agent isolated from naval recruits with mild respiratory illnesses. *Proc Soc Exp Biol Med* **94**, 262-267 (1957).
93. Andrewes, C.H. Rhinoviruses and common colds. *Annu Rev Med* **17**, 361-370 (1966).
94. Blomqvist, S., Roivainen, M., Puhakka, T., Kleemola, M. & Hovi, T. Virological and serological analysis of rhinovirus infections during the first two years of life in a cohort of children. *J Med Virol* **66**, 263-268 (2002).
95. Savolainen-Kopra, C., Blomqvist, S., Kilpi, T., Roivainen, M. & Hovi, T. Novel species of human rhinoviruses in acute otitis media. *Pediatr Infect Dis J* **28**, 59-61 (2009).
96. Turner, B.W., Cail, W.S., Hendley, J.O., Hayden, F.G., Doyle, W.J., Sorrentino, J.V. & Gwaltney, J.M., Jr. Physiologic abnormalities in the paranasal sinuses during experimental rhinovirus colds. *J Allergy Clin Immunol* **90**, 474-478 (1992).
97. Monto, A.S. The seasonality of rhinovirus infections and its implications for clinical recognition. *Clin Ther* **24**, 1987-1997 (2002).
98. Arruda, E., Pitkaranta, A., Witek, T.J., Jr., Doyle, C.A. & Hayden, F.G. Frequency and natural history of rhinovirus infections in adults during autumn. *J Clin Microbiol* **35**, 2864-2868 (1997).
99. Sears, M.R. & Johnston, N.W. Understanding the September asthma epidemic. *J Allergy Clin Immunol* **120**, 526-529 (2007).
100. Donaldson, G.C. & Wedzicha, J.A. COPD exacerbations .1: Epidemiology. *Thorax* **61**, 164-168 (2006).
101. Rollinger, J.M. & Schmidtke, M. The human rhinovirus: human-pathological impact, mechanisms of antirhinoviral agents, and strategies for their discovery. *Med Res Rev* (2009).
102. Lau, S.K., Yip, C.C., Tsoi, H.W., Lee, R.A., So, L.Y., Lau, Y.L., Chan, K.H., Woo, P.C. & Yuen, K.Y. Clinical features and complete genome characterization of a distinct human rhinovirus (HRV) genetic cluster, probably representing a previously undetected HRV species, HRV-C, associated with acute respiratory illness in children. *J Clin Microbiol* **45**, 3655-3664 (2007).
103. Palmenberg, A.C., Spiro, D., Kuzmickas, R., Wang, S., Djikeng, A., Rathe, J.A., Fraser-Liggett, C.M. & Liggett, S.B. Sequencing and analyses of all known human rhinovirus genomes reveal structure and evolution. *Science* **324**, 55-59 (2009).
104. Rossmann, M.G., Arnold, E., Erickson, J.W., Frankenberger, E.A., Griffith, J.P., Hecht, H.J., Johnson, J.E., Kamer, G., Luo, M., Mosser, A.G. & et al. Structure of

a human common cold virus and functional relationship to other picornaviruses. *Nature* **317**, 145-153 (1985).
105. Staunton, D.E., Merluzzi, V.J., Rothlein, R., Barton, R., Marlin, S.D. & Springer, T.A. A cell adhesion molecule, ICAM-1, is the major surface receptor for rhinoviruses. *Cell* **56**, 849-853 (1989).
106. Hofer, F., Gruenberger, M., Kowalski, H., Machat, H., Huettinger, M., Kuechler, E. & Blaas, D. Members of the low density lipoprotein receptor family mediate cell entry of a minor-group common cold virus. *Proc Natl Acad Sci U S A* **91**, 1839-1842 (1994).
107. Uncapher, C.R., DeWitt, C.M. & Colonno, R.J. The major and minor group receptor families contain all but one human rhinovirus serotype. *Virology* **180**, 814-817 (1991).
108. Vlasak, M., Goesler, I. & Blaas, D. Human rhinovirus type 89 variants use heparan sulfate proteoglycan for cell attachment. *J Virol* **79**, 5963-5970 (2005).
109. Khan, A.G., Pichler, J., Rosemann, A. & Blaas, D. Human rhinovirus type 54 infection via heparan sulfate is less efficient and strictly dependent on low endosomal pH. *J Virol* **81**, 4625-4632 (2007).
110. Marlin, S.D. & Springer, T.A. Purified intercellular adhesion molecule-1 (ICAM-1) is a ligand for lymphocyte function-associated antigen 1 (LFA-1). *Cell* **51**, 813-819 (1987).
111. Staunton, D.E., Dustin, M.L., Erickson, H.P. & Springer, T.A. The arrangement of the immunoglobulin-like domains of ICAM-1 and the binding sites for LFA-1 and rhinovirus. *Cell* **61**, 243-254 (1990).
112. Staunton, D.E., Gaur, A., Chan, P.Y. & Springer, T.A. Internalization of a major group human rhinovirus does not require cytoplasmic or transmembrane domains of ICAM-1. *J Immunol* **148**, 3271-3274 (1992).
113. Oliveira, M.A., Zhao, R., Lee, W.M., Kremer, M.J., Minor, I., Rueckert, R.R., Diana, G.D., Pevear, D.C., Dutko, F.J., McKinlay, M.A. & et al. The structure of human rhinovirus 16. *Structure* **1**, 51-68 (1993).
114. Hewat, E.A., Neumann, E., Conway, J.F., Moser, R., Ronacher, B., Marlovits, T.C. & Blaas, D. The cellular receptor to human rhinovirus 2 binds around the 5-fold axis and not in the canyon: a structural view. *EMBO J* **19**, 6317-6325 (2000).
115. DeTulleo, L. & Kirchhausen, T. The clathrin endocytic pathway in viral infection. *EMBO J* **17**, 4585-4593 (1998).
116. Snyers, L., Zwickl, H. & Blaas, D. Human rhinovirus type 2 is internalized by clathrin-mediated endocytosis. *J Virol* **77**, 5360-5369 (2003).
117. Bayer, N., Prchla, E., Schwab, M., Blaas, D. & Fuchs, R. Human rhinovirus HRV14 uncoats from early endosomes in the presence of bafilomycin. *FEBS Lett* **463**, 175-178 (1999).
118. Dreschers, S., Franz, P., Dumitru, C., Wilker, B., Jahnke, K. & Gulbins, E. Infections with human rhinovirus induce the formation of distinct functional membrane domains. *Cell Physiol Biochem* **20**, 241-254 (2007).
119. Rueckert, R.R. *Picornaviridae*: The Viruses and Their Replication. in *Fields Virology*, Vol. 1 (ed. Fields, B.) 609-655 (Lipincott-Raven, New York, 1996).

120. Arnold, E. & Rossmann, M.G. The use of molecular-replacement phases for the refinement of the human rhinovirus 14 structure. *Acta Crystallogr A* **44 (Pt 3)**, 270-282 (1988).
121. Sommergruber, W., Zorn, M., Blaas, D., Fessl, F., Volkmann, P., Maurer-Fogy, I., Pallai, P., Merluzzi, V., Matteo, M., Skern, T. & et al. Polypeptide 2A of human rhinovirus type 2: identification as a protease and characterization by mutational analysis. *Virology* **169**, 68-77 (1989).
122. Knott, J.A., Orr, D.C., Montgomery, D.S., Sullivan, C.A. & Weston, A. The expression and purification of human rhinovirus protease 3C. *Eur J Biochem* **182**, 547-555 (1989).
123. Clark, M.E., Lieberman, P.M., Berk, A.J. & Dasgupta, A. Direct cleavage of human TATA-binding protein by poliovirus protease 3C in vivo and in vitro. *Mol Cell Biol* **13**, 1232-1237 (1993).
124. Amineva, S.P., Aminev, A.G., Palmenberg, A.C. & Gern, J.E. Rhinovirus 3C protease precursors 3CD and 3CD' localize to the nuclei of infected cells. *J Gen Virol* **85**, 2969-2979 (2004).
125. Haghighat, A., Svitkin, Y., Novoa, I., Kuechler, E., Skern, T. & Sonenberg, N. The eIF4G-eIF4E complex is the target for direct cleavage by the rhinovirus 2A proteinase. *J Virol* **70**, 8444-8450 (1996).
126. Lee, W.M., Monroe, S.S. & Rueckert, R.R. Role of maturation cleavage in infectivity of picornaviruses: activation of an infectosome. *J Virol* **67**, 2110-2122 (1993).
127. Deszcz, L., Gaudernak, E., Kuechler, E. & Seipelt, J. Apoptotic events induced by human rhinovirus infection. *J Gen Virol* **86**, 1379-1389 (2005).
128. Taylor, M.P., Burgon, T.B., Kirkegaard, K. & Jackson, W.T. Role of microtubules in extracellular release of poliovirus. *J Virol* **83**, 6599-6609 (2009).
129. Turner, R.B., Hendley, J.O. & Gwaltney, J.M., Jr. Shedding of infected ciliated epithelial cells in rhinovirus colds. *J Infect Dis* **145**, 849-853 (1982).
130. Bardin, P.G., Johnston, S.L., Sanderson, G., Robinson, B.S., Pickett, M.A., Fraenkel, D.J. & Holgate, S.T. Detection of rhinovirus infection of the nasal mucosa by oligonucleotide in situ hybridization. *Am J Respir Cell Mol Biol* **10**, 207-213 (1994).
131. Winther, B., Gwaltney, J.M., Jr., Mygind, N., Turner, R.B. & Hendley, J.O. Sites of rhinovirus recovery after point inoculation of the upper airway. *JAMA* **256**, 1763-1767 (1986).
132. Harris, J.M., 2nd & Gwaltney, J.M., Jr. Incubation periods of experimental rhinovirus infection and illness. *Clin Infect Dis* **23**, 1287-1290 (1996).
133. McFadden, E.R., Jr., Pichurko, B.M., Bowman, H.F., Ingenito, E., Burns, S., Dowling, N. & Solway, J. Thermal mapping of the airways in humans. *J Appl Physiol* **58**, 564-570 (1985).
134. Arruda, E., Boyle, T.R., Winther, B., Pevear, D.C., Gwaltney, J.M., Jr. & Hayden, F.G. Localization of human rhinovirus replication in the upper respiratory tract by in situ hybridization. *J Infect Dis* **171**, 1329-1333 (1995).

135. Gern, J.E., Galagan, D.M., Jarjour, N.N., Dick, E.C. & Busse, W.W. Detection of rhinovirus RNA in lower airway cells during experimentally induced infection. *Am J Respir Crit Care Med* **155**, 1159-1161 (1997).
136. Papadopoulos, N.G., Bates, P.J., Bardin, P.G., Papi, A., Leir, S.H., Fraenkel, D.J., Meyer, J., Lackie, P.M., Sanderson, G., Holgate, S.T. & Johnston, S.L. Rhinoviruses infect the lower airways. *J Infect Dis* **181**, 1875-1884 (2000).
137. Mosser, A.G., Vrtis, R., Burchell, L., Lee, W.M., Dick, C.R., Weisshaar, E., Bock, D., Swenson, C.A., Cornwell, R.D., Meyer, K.C., Jarjour, N.N., Busse, W.W. & Gern, J.E. Quantitative and qualitative analysis of rhinovirus infection in bronchial tissues. *Am J Respir Crit Care Med* **171**, 645-651 (2005).
138. Kaiser, L., Aubert, J.D., Pache, J.C., Deffernez, C., Rochat, T., Garbino, J., Wunderli, W., Meylan, P., Yerly, S., Perrin, L., Letovanec, I., Nicod, L., Tapparel, C. & Soccal, P.M. Chronic rhinoviral infection in lung transplant recipients. *Am J Respir Crit Care Med* **174**, 1392-1399 (2006).
139. Mosser, A.G., Brockman-Schneider, R., Amineva, S., Burchell, L., Sedgwick, J.B., Busse, W.W. & Gern, J.E. Similar frequency of rhinovirus-infectible cells in upper and lower airway epithelium. *J Infect Dis* **185**, 734-743 (2002).
140. Winther, B., Brofeldt, S., Christensen, B. & Mygind, N. Light and scanning electron microscopy of nasal biopsy material from patients with naturally acquired common colds. *Acta Otolaryngol* **97**, 309-318 (1984).
141. Subauste, M.C., Jacoby, D.B., Richards, S.M. & Proud, D. Infection of a human respiratory epithelial cell line with rhinovirus. Induction of cytokine release and modulation of susceptibility to infection by cytokine exposure. *J Clin Invest* **96**, 549-557 (1995).
142. Turner, R.B., Weingand, K.W., Yeh, C.H. & Leedy, D.W. Association between interleukin-8 concentration in nasal secretions and severity of symptoms of experimental rhinovirus colds. *Clin Infect Dis* **26**, 840-846 (1998).
143. Spurrell, J.C., Wiehler, S., Zaheer, R.S., Sanders, S.P. & Proud, D. Human airway epithelial cells produce IP-10 (CXCL10) in vitro and in vivo upon rhinovirus infection. *Am J Physiol Lung Cell Mol Physiol* **289**, L85-95 (2005).
144. Bossios, A., Psarras, S., Gourgiotis, D., Skevaki, C.L., Constantopoulos, A.G., Saxoni-Papageorgiou, P. & Papadopoulos, N.G. Rhinovirus infection induces cytotoxicity and delays wound healing in bronchial epithelial cells. *Respir Res* **6**, 114 (2005).
145. Wark, P.A., Grissell, T., Davies, B., See, H. & Gibson, P.G. Diversity in the bronchial epithelial cell response to infection with different rhinovirus strains. *Respirology* **14**, 180-186 (2009).
146. Lopez-Souza, N., Dolganov, G., Dubin, R., Sachs, L.A., Sassina, L., Sporer, H., Yagi, S., Schnurr, D., Boushey, H.A. & Widdicombe, J.H. Resistance of differentiated human airway epithelium to infection by rhinovirus. *Am J Physiol Lung Cell Mol Physiol* **286**, L373-381 (2004).
147. Jakiela, B., Brockman-Schneider, R., Amineva, S., Lee, W.M. & Gern, J.E. Basal cells of differentiated bronchial epithelium are more susceptible to rhinovirus infection. *Am J Respir Cell Mol Biol* **38**, 517-523 (2008).

148. Terajima, M., Yamaya, M., Sekizawa, K., Okinaga, S., Suzuki, T., Yamada, N., Nakayama, K., Ohrui, T., Oshima, T., Numazaki, Y. & Sasaki, H. Rhinovirus infection of primary cultures of human tracheal epithelium: role of ICAM-1 and IL-1beta. *Am J Physiol* **273**, L749-759 (1997).
149. Kim, J., Sanders, S.P., Siekierski, E.S., Casolaro, V. & Proud, D. Role of NF-kappa B in cytokine production induced from human airway epithelial cells by rhinovirus infection. *J Immunol* **165**, 3384-3392 (2000).
150. Zhu, Z., Tang, W., Gwaltney, J.M., Jr., Wu, Y. & Elias, J.A. Rhinovirus stimulation of interleukin-8 in vivo and in vitro: role of NF-kappaB. *Am J Physiol* **273**, L814-824 (1997).
151. Schroth, M.K., Grimm, E., Frindt, P., Galagan, D.M., Konno, S.I., Love, R. & Gern, J.E. Rhinovirus replication causes RANTES production in primary bronchial epithelial cells. *Am J Respir Cell Mol Biol* **20**, 1220-1228 (1999).
152. Papadopoulos, N.G., Papi, A., Meyer, J., Stanciu, L.A., Salvi, S., Holgate, S.T. & Johnston, S.L. Rhinovirus infection up-regulates eotaxin and eotaxin-2 expression in bronchial epithelial cells. *Clin Exp Allergy* **31**, 1060-1066 (2001).
153. Couch, R.B. Rhinoviruses. in *Fields' Virology*, Vol. 1 (ed. Fields, B.) 713-730 (Lippincott-Raven, Philadelphia, 1996).
154. Cate, T.R., Rossen, R.D., Douglas, R.G., Jr., Butler, W.T. & Couch, R.B. The role of nasal secretion and serum antibody in the rhinovirus common cold. *Am J Epidemiol* **84**, 352-363 (1966).
155. Barclay, W.S., al-Nakib, W., Higgins, P.G. & Tyrrell, D.A. The time course of the humoral immune response to rhinovirus infection. *Epidemiol Infect* **103**, 659-669 (1989).
156. Kirchberger, S., Majdic, O. & Stockl, J. Modulation of the immune system by human rhinoviruses. *Int Arch Allergy Immunol* **142**, 1-10 (2007).
157. Gern, J.E., Dick, E.C., Kelly, E.A., Vrtis, R. & Klein, B. Rhinovirus-specific T cells recognize both shared and serotype-restricted viral epitopes. *J Infect Dis* **175**, 1108-1114 (1997).
158. Wimalasundera, S.S., Katz, D.R. & Chain, B.M. Characterization of the T cell response to human rhinovirus in children: implications for understanding the immunopathology of the common cold. *J Infect Dis* **176**, 755-759 (1997).
159. Kirchberger, S., Majdic, O., Steinberger, P., Bluml, S., Pfistershammer, K., Zlabinger, G., Deszcz, L., Kuechler, E., Knapp, W. & Stockl, J. Human rhinoviruses inhibit the accessory function of dendritic cells by inducing sialoadhesin and B7-H1 expression. *J Immunol* **175**, 1145-1152 (2005).
160. Seyerl, M., Kirchberger, S., Majdic, O., Seipelt, J., Jindra, C., Schrauf, C. & Stockl, J. Human rhinoviruses induce IL-35-producing Treg via induction of B7-H1 (CD274) and sialoadhesin (CD169) on DC. *Eur J Immunol* (2009).
161. Rate, A.a.U., J. The Epithelium and Immunoregulation. in *The Pulmonary Epithelium in Health and Disease* (ed. Proud, D.) 201-224 (John Wiley and Sons, West Sussex, 2009).
162. Kato, A., Favoreto, S., Jr., Avila, P.C. & Schleimer, R.P. TLR3- and Th2 cytokine-dependent production of thymic stromal lymphopoietin in human airway epithelial cells. *J Immunol* **179**, 1080-1087 (2007).

163. Reche, P.A., Soumelis, V., Gorman, D.M., Clifford, T., Liu, M., Travis, M., Zurawski, S.M., Johnston, J., Liu, Y.J., Spits, H., de Waal Malefyt, R., Kastelein, R.A. & Bazan, J.F. Human thymic stromal lymphopoietin preferentially stimulates myeloid cells. *J Immunol* **167**, 336-343 (2001).
164. Liu, Y.J., Soumelis, V., Watanabe, N., Ito, T., Wang, Y.H., Malefyt Rde, W., Omori, M., Zhou, B. & Ziegler, S.F. TSLP: an epithelial cell cytokine that regulates T cell differentiation by conditioning dendritic cell maturation. *Annu Rev Immunol* **25**, 193-219 (2007).
165. Papi, A., Stanciu, L.A., Papadopoulos, N.G., Teran, L.M., Holgate, S.T. & Johnston, S.L. Rhinovirus infection induces major histocompatibility complex class I and costimulatory molecule upregulation on respiratory epithelial cells. *J Infect Dis* **181**, 1780-1784 (2000).
166. Kim, J., Myers, A.C., Chen, L., Pardoll, D.M., Truong-Tran, Q.A., Lane, A.P., McDyer, J.F., Fortuno, L. & Schleimer, R.P. Constitutive and inducible expression of b7 family of ligands by human airway epithelial cells. *Am J Respir Cell Mol Biol* **33**, 280-289 (2005).
167. Heinecke, L., Proud, D., Sanders, S., Schleimer, R.P. & Kim, J. Induction of B7-H1 and B7-DC expression on airway epithelial cells by the Toll-like receptor 3 agonist double-stranded RNA and human rhinovirus infection: In vivo and in vitro studies. *J Allergy Clin Immunol* **121**, 1155-1160 (2008).
168. Salik, E., Tyorkin, M., Mohan, S., George, I., Becker, K., Oei, E., Kalb, T. & Sperber, K. Antigen trafficking and accessory cell function in respiratory epithelial cells. *Am J Respir Cell Mol Biol* **21**, 365-379 (1999).
169. Kalb, T.H., Chuang, M.T., Marom, Z. & Mayer, L. Evidence for accessory cell function by class II MHC antigen-expressing airway epithelial cells. *Am J Respir Cell Mol Biol* **4**, 320-329 (1991).
170. Nakhaei, P., Genin, P., Civas, A. & Hiscott, J. RIG-I-like receptors: sensing and responding to RNA virus infection. *Semin Immunol* **21**, 215-222 (2009).
171. Takeuchi, O. & Akira, S. Innate immunity to virus infection. *Immunol Rev* **227**, 75-86 (2009).
172. Muir, A., Soong, G., Sokol, S., Reddy, B., Gomez, M.I., Van Heeckeren, A. & Prince, A. Toll-like receptors in normal and cystic fibrosis airway epithelial cells. *Am J Respir Cell Mol Biol* **30**, 777-783 (2004).
173. Guillot, L., Le Goffic, R., Bloch, S., Escriou, N., Akira, S., Chignard, M. & Si-Tahar, M. Involvement of toll-like receptor 3 in the immune response of lung epithelial cells to double-stranded RNA and influenza A virus. *J Biol Chem* **280**, 5571-5580 (2005).
174. Sajjan, U.S., Jia, Y., Newcomb, D.C., Bentley, J.K., Lukacs, N.W., LiPuma, J.J. & Hershenson, M.B. H. influenzae potentiates airway epithelial cell responses to rhinovirus by increasing ICAM-1 and TLR3 expression. *FASEB J* **20**, 2121-2123 (2006).
175. Wang, Q., Nagarkar, D.R., Bowman, E.R., Schneider, D., Gosangi, B., Lei, J., Zhao, Y., McHenry, C.L., Burgens, R.V., Miller, D.J., Sajjan, U. & Hershenson, M.B. Role of double-stranded RNA pattern recognition receptors in rhinovirus-induced airway epithelial cell responses. *J Immunol* **183**, 6989-6997 (2009).

176. Matsukura, S., Kokubu, F., Kurokawa, M., Kawaguchi, M., Ieki, K., Kuga, H., Odaka, M., Suzuki, S., Watanabe, S., Homma, T., Takeuchi, H., Nohtomi, K. & Adachi, M. Role of RIG-I, MDA-5, and PKR on the expression of inflammatory chemokines induced by synthetic dsRNA in airway epithelial cells. *Int Arch Allergy Immunol* **143 Suppl 1**, 80-83 (2007).
177. Yoneyama, M., Kikuchi, M., Natsukawa, T., Shinobu, N., Imaizumi, T., Miyagishi, M., Taira, K., Akira, S. & Fujita, T. The RNA helicase RIG-I has an essential function in double-stranded RNA-induced innate antiviral responses. *Nat Immunol* **5**, 730-737 (2004).
178. Muruve, D.A., Petrilli, V., Zaiss, A.K., White, L.R., Clark, S.A., Ross, P.J., Parks, R.J. & Tschopp, J. The inflammasome recognizes cytosolic microbial and host DNA and triggers an innate immune response. *Nature* **452**, 103-107 (2008).
179. Drygin, D., Koo, S., Perera, R., Barone, S. & Bennett, C.F. Induction of toll-like receptors and NALP/PAN/PYPAF family members by modified oligonucleotides in lung epithelial carcinoma cells. *Oligonucleotides* **15**, 105-118 (2005).
180. Abraham, N., Stojdl, D.F., Duncan, P.I., Methot, N., Ishii, T., Dube, M., Vanderhyden, B.C., Atkins, H.L., Gray, D.A., McBurney, M.W., Koromilas, A.E., Brown, E.G., Sonenberg, N. & Bell, J.C. Characterization of transgenic mice with targeted disruption of the catalytic domain of the double-stranded RNA-dependent protein kinase, PKR. *J Biol Chem* **274**, 5953-5962 (1999).
181. Gern, J.E., French, D.A., Grindle, K.A., Brockman-Schneider, R.A., Konno, S. & Busse, W.W. Double-stranded RNA induces the synthesis of specific chemokines by bronchial epithelial cells. *Am J Respir Cell Mol Biol* **28**, 731-737 (2003).
182. Edwards, M.R., Hewson, C.A., Laza-Stanca, V., Lau, H.T., Mukaida, N., Hershenson, M.B. & Johnston, S.L. Protein kinase R, IkappaB kinase-beta and NF-kappaB are required for human rhinovirus induced pro-inflammatory cytokine production in bronchial epithelial cells. *Mol Immunol* **44**, 1587-1597 (2007).
183. Zhang, P. & Samuel, C.E. Induction of protein kinase PKR-dependent activation of interferon regulatory factor 3 by vaccinia virus occurs through adapter IPS-1 signaling. *J Biol Chem* **283**, 34580-34587 (2008).
184. de Bouteiller, O., Merck, E., Hasan, U.A., Hubac, S., Benguigui, B., Trinchieri, G., Bates, E.E. & Caux, C. Recognition of double-stranded RNA by human toll-like receptor 3 and downstream receptor signaling requires multimerization and an acidic pH. *J Biol Chem* **280**, 38133-38145 (2005).
185. Liu, L., Botos, I., Wang, Y., Leonard, J.N., Shiloach, J., Segal, D.M. & Davies, D.R. Structural basis of toll-like receptor 3 signaling with double-stranded RNA. *Science* **320**, 379-381 (2008).
186. Kato, H., Takeuchi, O., Mikamo-Satoh, E., Hirai, R., Kawai, T., Matsushita, K., Hiiragi, A., Dermody, T.S., Fujita, T. & Akira, S. Length-dependent recognition of double-stranded ribonucleic acids by retinoic acid-inducible gene-I and melanoma differentiation-associated gene 5. *J Exp Med* **205**, 1601-1610 (2008).
187. Pichlmair, A., Schulz, O., Tan, C.P., Naslund, T.I., Liljestrom, P., Weber, F. & Reis e Sousa, C. RIG-I-mediated antiviral responses to single-stranded RNA bearing 5'-phosphates. *Science* **314**, 997-1001 (2006).

188. DeWitte-Orr, S.J., Mehta, D.R., Collins, S.E., Suthar, M.S., Gale, M., Jr. & Mossman, K.L. Long double-stranded RNA induces an antiviral response independent of IFN regulatory factor 3, IFN-beta promoter stimulator 1, and IFN. *J Immunol* **183**, 6545-6553 (2009).
189. Kato, H., Sato, S., Yoneyama, M., Yamamoto, M., Uematsu, S., Matsui, K., Tsujimura, T., Takeda, K., Fujita, T., Takeuchi, O. & Akira, S. Cell type-specific involvement of RIG-I in antiviral response. *Immunity* **23**, 19-28 (2005).
190. Edelmann, K.H., Richardson-Burns, S., Alexopoulou, L., Tyler, K.L., Flavell, R.A. & Oldstone, M.B. Does Toll-like receptor 3 play a biological role in virus infections? *Virology* **322**, 231-238 (2004).
191. Hemmi, H., Takeuchi, O., Sato, S., Yamamoto, M., Kaisho, T., Sanjo, H., Kawai, T., Hoshino, K., Takeda, K. & Akira, S. The roles of two IkappaB kinase-related kinases in lipopolysaccharide and double stranded RNA signaling and viral infection. *J Exp Med* **199**, 1641-1650 (2004).
192. Kato, H., Takeuchi, O., Sato, S., Yoneyama, M., Yamamoto, M., Matsui, K., Uematsu, S., Jung, A., Kawai, T., Ishii, K.J., Yamaguchi, O., Otsu, K., Tsujimura, T., Koh, C.S., Reis e Sousa, C., Matsuura, Y., Fujita, T. & Akira, S. Differential roles of MDA5 and RIG-I helicases in the recognition of RNA viruses. *Nature* **441**, 101-105 (2006).
193. Gitlin, L., Barchet, W., Gilfillan, S., Cella, M., Beutler, B., Flavell, R.A., Diamond, M.S. & Colonna, M. Essential role of mda-5 in type I IFN responses to polyriboinosinic:polyribocytidylic acid and encephalomyocarditis picornavirus. *Proc Natl Acad Sci U S A* **103**, 8459-8464 (2006).
194. Hewson, C.A., Jardine, A., Edwards, M.R., Laza-Stanca, V. & Johnston, S.L. Toll-like receptor 3 is induced by and mediates antiviral activity against rhinovirus infection of human bronchial epithelial cells. *J Virol* **79**, 12273-12279 (2005).
195. Yamamoto, M., Sato, S., Hemmi, H., Hoshino, K., Kaisho, T., Sanjo, H., Takeuchi, O., Sugiyama, M., Okabe, M., Takeda, K. & Akira, S. Role of adaptor TRIF in the MyD88-independent toll-like receptor signaling pathway. *Science* **301**, 640-643 (2003).
196. Kawai, T., Takahashi, K., Sato, S., Coban, C., Kumar, H., Kato, H., Ishii, K.J., Takeuchi, O. & Akira, S. IPS-1, an adaptor triggering RIG-I- and Mda5-mediated type I interferon induction. *Nat Immunol* **6**, 981-988 (2005).
197. Seth, R.B., Sun, L., Ea, C.K. & Chen, Z.J. Identification and characterization of MAVS, a mitochondrial antiviral signaling protein that activates NF-kappaB and IRF 3. *Cell* **122**, 669-682 (2005).
198. Xu, L.G., Wang, Y.Y., Han, K.J., Li, L.Y., Zhai, Z. & Shu, H.B. VISA is an adapter protein required for virus-triggered IFN-beta signaling. *Mol Cell* **19**, 727-740 (2005).
199. Meylan, E., Curran, J., Hofmann, K., Moradpour, D., Binder, M., Bartenschlager, R. & Tschopp, J. Cardif is an adaptor protein in the RIG-I antiviral pathway and is targeted by hepatitis C virus. *Nature* **437**, 1167-1172 (2005).
200. Li, X., Massa, P.E., Hanidu, A., Peet, G.W., Aro, P., Savitt, A., Mische, S., Li, J. & Marcu, K.B. IKKalpha, IKKbeta, and NEMO/IKKgamma are each required for

the NF-kappa B-mediated inflammatory response program. *J Biol Chem* **277**, 45129-45140 (2002).

201. Hacker, H. & Karin, M. Regulation and function of IKK and IKK-related kinases. *Sci STKE* **2006**, re13 (2006).
202. Fitzgerald, K.A., McWhirter, S.M., Faia, K.L., Rowe, D.C., Latz, E., Golenbock, D.T., Coyle, A.J., Liao, S.M. & Maniatis, T. IKKepsilon and TBK1 are essential components of the IRF3 signaling pathway. *Nat Immunol* **4**, 491-496 (2003).
203. Zhao, T., Yang, L., Sun, Q., Arguello, M., Ballard, D.W., Hiscott, J. & Lin, R. The NEMO adaptor bridges the nuclear factor-kappaB and interferon regulatory factor signaling pathways. *Nat Immunol* **8**, 592-600 (2007).
204. McWhirter, S.M., Fitzgerald, K.A., Rosains, J., Rowe, D.C., Golenbock, D.T. & Maniatis, T. IFN-regulatory factor 3-dependent gene expression is defective in Tbk1-deficient mouse embryonic fibroblasts. *Proc Natl Acad Sci U S A* **101**, 233-238 (2004).
205. Melchjorsen, J. & Paludan, S.R. Induction of RANTES/CCL5 by herpes simplex virus is regulated by nuclear factor kappa B and interferon regulatory factor 3. *J Gen Virol* **84**, 2491-2495 (2003).
206. Bisset, L.R. & Schmid-Grendelmeier, P. Chemokines and their receptors in the pathogenesis of allergic asthma: progress and perspective. *Curr Opin Pulm Med* **11**, 35-42 (2005).
207. Barnes, P.J. Inflammatory Mediators. in *Chronic Obstructive Pulmonary Disease: Cellular and Molecular Mechanisms*, Vol. 198 (ed. Barnes, P.J.) 258-262 (Taylor & Francis Group, Boca Raton, 2005).
208. Kallal, L.E. & Lukacs, N.W. The role of chemokines in virus-associated asthma exacerbations. *Curr Allergy Asthma Rep* **8**, 443-450 (2008).
209. Mikhak, Z.a.A.L. Chemokines in Cell Movement and Allergic Inflammation. in *Middleton's Allergy: Principles and Practice*, Vol. 1 (ed. Adkinson, N., Busse, W., Bochner, B., Holgate, S., Lemankse, R., and Simons, F.) 181-202 (Mosby Elsevier, Philadelphia, 2009).
210. Thelen, M., Peveri, P., Kernen, P., von Tscharner, V., Walz, A. & Baggiolini, M. Mechanism of neutrophil activation by NAF, a novel monocyte-derived peptide agonist. *FASEB J* **2**, 2702-2706 (1988).
211. Walz, A., Burgener, R., Car, B., Baggiolini, M., Kunkel, S.L. & Strieter, R.M. Structure and neutrophil-activating properties of a novel inflammatory peptide (ENA-78) with homology to interleukin 8. *J Exp Med* **174**, 1355-1362 (1991).
212. Luster, A.D., Unkeless, J.C. & Ravetch, J.V. Gamma-interferon transcriptionally regulates an early-response gene containing homology to platelet proteins. *Nature* **315**, 672-676 (1985).
213. Liao, F., Rabin, R.L., Yannelli, J.R., Koniaris, L.G., Vanguri, P. & Farber, J.M. Human Mig chemokine: biochemical and functional characterization. *J Exp Med* **182**, 1301-1314 (1995).
214. Cole, K.E., Strick, C.A., Paradis, T.J., Ogborne, K.T., Loetscher, M., Gladue, R.P., Lin, W., Boyd, J.G., Moser, B., Wood, D.E., Sahagan, B.G. & Neote, K. Interferon-inducible T cell alpha chemoattractant (I-TAC): a novel non-ELR CXC

chemokine with potent activity on activated T cells through selective high affinity binding to CXCR3. *J Exp Med* **187**, 2009-2021 (1998).
215. Schall, T.J., Bacon, K., Toy, K.J. & Goeddel, D.V. Selective attraction of monocytes and T lymphocytes of the memory phenotype by cytokine RANTES. *Nature* **347**, 669-671 (1990).
216. Imai, T., Yoshida, T., Baba, M., Nishimura, M., Kakizaki, M. & Yoshie, O. Molecular cloning of a novel T cell-directed CC chemokine expressed in thymus by signal sequence trap using Epstein-Barr virus vector. *J Biol Chem* **271**, 21514-21521 (1996).
217. Ponath, P.D., Qin, S., Ringler, D.J., Clark-Lewis, I., Wang, J., Kassam, N., Smith, H., Shi, X., Gonzalo, J.A., Newman, W., Gutierrez-Ramos, J.C. & Mackay, C.R. Cloning of the human eosinophil chemoattractant, eotaxin. Expression, receptor binding, and functional properties suggest a mechanism for the selective recruitment of eosinophils. *J Clin Invest* **97**, 604-612 (1996).
218. Houck, J.C. & Chang, C.M. The purification and characterization of a lymphokine chemotactic for lymphocytes--lymphotactin. *Inflammation* **2**, 105-113 (1977).
219. Yoshida, T., Imai, T., Kakizaki, M., Nishimura, M. & Yoshie, O. Molecular cloning of a novel C or gamma type chemokine, SCM-1. *FEBS Lett* **360**, 155-159 (1995).
220. Bazan, J.F., Bacon, K.B., Hardiman, G., Wang, W., Soo, K., Rossi, D., Greaves, D.R., Zlotnik, A. & Schall, T.J. A new class of membrane-bound chemokine with a CX3C motif. *Nature* **385**, 640-644 (1997).
221. Miotto, D., Christodoulopoulos, P., Olivenstein, R., Taha, R., Cameron, L., Tsicopoulos, A., Tonnel, A.B., Fahy, O., Lafitte, J.J., Luster, A.D., Wallaert, B., Mapp, C.E. & Hamid, Q. Expression of IFN-gamma-inducible protein; monocyte chemotactic proteins 1, 3, and 4; and eotaxin in TH1- and TH2-mediated lung diseases. *J Allergy Clin Immunol* **107**, 664-670 (2001).
222. Wark, P.A., Bucchieri, F., Johnston, S.L., Gibson, P.G., Hamilton, L., Mimica, J., Zummo, G., Holgate, S.T., Attia, J., Thakkinstian, A. & Davies, D.E. IFN-gamma-induced protein 10 is a novel biomarker of rhinovirus-induced asthma exacerbations. *J Allergy Clin Immunol* **120**, 586-593 (2007).
223. Quint, J.K., Donaldson, G.C., Goldring, J.J., Baghai-Ravary, R., Hurst, J.R. & Wedzicha, J.A. Serum IP-10 as a biomarker of human rhinovirus infection at exacerbation of COPD. *Chest* (2009).
224. Neville, L.F., Mathiak, G. & Bagasra, O. The immunobiology of interferon-gamma inducible protein 10 kD (IP-10): a novel, pleiotropic member of the C-X-C chemokine superfamily. *Cytokine Growth Factor Rev* **8**, 207-219 (1997).
225. Angiolillo, A.L., Sgadari, C., Taub, D.D., Liao, F., Farber, J.M., Maheshwari, S., Kleinman, H.K., Reaman, G.H. & Tosato, G. Human interferon-inducible protein 10 is a potent inhibitor of angiogenesis in vivo. *J Exp Med* **182**, 155-162 (1995).
226. Luster, A.D. & Leder, P. IP-10, a -C-X-C- chemokine, elicits a potent thymus-dependent antitumor response in vivo. *J Exp Med* **178**, 1057-1065 (1993).

227. Cole, A.M., Ganz, T., Liese, A.M., Burdick, M.D., Liu, L. & Strieter, R.M. Cutting edge: IFN-inducible ELR- CXC chemokines display defensin-like antimicrobial activity. *J Immunol* **167**, 623-627 (2001).
228. Sauty, A., Dziejman, M., Taha, R.A., Iarossi, A.S., Neote, K., Garcia-Zepeda, E.A., Hamid, Q. & Luster, A.D. The T cell-specific CXC chemokines IP-10, Mig, and I-TAC are expressed by activated human bronchial epithelial cells. *J Immunol* **162**, 3549-3558 (1999).
229. Sheikh, A.M., Ochi, H., Manabe, A. & Masuda, J. Lysophosphatidylcholine posttranscriptionally inhibits interferon-gamma-induced IP-10, Mig and I-Tac expression in endothelial cells. *Cardiovasc Res* **65**, 263-271 (2005).
230. Bedard, P.A. & Golds, E.E. Cytokine-induced expression of mRNAs for chemotactic factors in human synovial cells and fibroblasts. *J Cell Physiol* **154**, 433-441 (1993).
231. Gattass, C.R., King, L.B., Luster, A.D. & Ashwell, J.D. Constitutive expression of interferon gamma-inducible protein 10 in lymphoid organs and inducible expression in T cells and thymocytes. *J Exp Med* **179**, 1373-1378 (1994).
232. Qi, X.F., Kim, D.H., Yoon, Y.S., Jin, D., Huang, X.Z., Li, J.H., Deung, Y.K. & Lee, K.J. Essential involvement of cross-talk between IFN-gamma and TNF-alpha in CXCL10 production in human THP-1 monocytes. *J Cell Physiol* **220**, 690-697 (2009).
233. Tamassia, N., Calzetti, F., Ear, T., Cloutier, A., Gasperini, S., Bazzoni, F., McDonald, P.P. & Cassatella, M.A. Molecular mechanisms underlying the synergistic induction of CXCL10 by LPS and IFN-gamma in human neutrophils. *Eur J Immunol* **37**, 2627-2634 (2007).
234. Hua, L.L. & Lee, S.C. Distinct patterns of stimulus-inducible chemokine mRNA accumulation in human fetal astrocytes and microglia. *Glia* **30**, 74-81 (2000).
235. Tannenbaum, C.S., Wicker, N., Armstrong, D., Tubbs, R., Finke, J., Bukowski, R.M. & Hamilton, T.A. Cytokine and chemokine expression in tumors of mice receiving systemic therapy with IL-12. *J Immunol* **156**, 693-699 (1996).
236. Koetzler, R., Zaheer, R.S., Wiehler, S., Holden, N.S., Giembycz, M.A. & Proud, D. Nitric oxide inhibits human rhinovirus-induced transcriptional activation of CXCL10 in airway epithelial cells. *J Allergy Clin Immunol* **123**, 201-208 e209 (2009).
237. Karakurum, M., Shreeniwas, R., Chen, J., Pinsky, D., Yan, S.D., Anderson, M., Sunouchi, K., Major, J., Hamilton, T., Kuwabara, K. & et al. Hypoxic induction of interleukin-8 gene expression in human endothelial cells. *J Clin Invest* **93**, 1564-1570 (1994).
238. Monick, M.M., Powers, L.S., Hassan, I., Groskreutz, D., Yarovinsky, T.O., Barrett, C.W., Castilow, E.M., Tifrea, D., Varga, S.M. & Hunninghake, G.W. Respiratory syncytial virus synergizes with Th2 cytokines to induce optimal levels of TARC/CCL17. *J Immunol* **179**, 1648-1658 (2007).
239. Larner, A.C., Petricoin, E.F., Nakagawa, Y. & Finbloom, D.S. IL-4 attenuates the transcriptional activation of both IFN-alpha and IFN-gamma-induced cellular gene expression in monocytes and monocytic cell lines. *J Immunol* **150**, 1944-1950 (1993).

240. Taub, D.D., Sayers, T.J., Carter, C.R. & Ortaldo, J.R. Alpha and beta chemokines induce NK cell migration and enhance NK-mediated cytolysis. *J Immunol* **155**, 3877-3888 (1995).
241. Taub, D.D., Lloyd, A.R., Conlon, K., Wang, J.M., Ortaldo, J.R., Harada, A., Matsushima, K., Kelvin, D.J. & Oppenheim, J.J. Recombinant human interferon-inducible protein 10 is a chemoattractant for human monocytes and T lymphocytes and promotes T cell adhesion to endothelial cells. *J Exp Med* **177**, 1809-1814 (1993).
242. Taub, D.D., Longo, D.L. & Murphy, W.J. Human interferon-inducible protein-10 induces mononuclear cell infiltration in mice and promotes the migration of human T lymphocytes into the peripheral tissues and human peripheral blood lymphocytes-SCID mice. *Blood* **87**, 1423-1431 (1996).
243. Thomas, S.Y., Hou, R., Boyson, J.E., Means, T.K., Hess, C., Olson, D.P., Strominger, J.L., Brenner, M.B., Gumperz, J.E., Wilson, S.B. & Luster, A.D. CD1d-restricted NKT cells express a chemokine receptor profile indicative of Th1-type inflammatory homing cells. *J Immunol* **171**, 2571-2580 (2003).
244. Garcia-Lopez, M.A., Sanchez-Madrid, F., Rodriguez-Frade, J.M., Mellado, M., Acevedo, A., Garcia, M.I., Albar, J.P., Martinez, C. & Marazuela, M. CXCR3 chemokine receptor distribution in normal and inflamed tissues: expression on activated lymphocytes, endothelial cells, and dendritic cells. *Lab Invest* **81**, 409-418 (2001).
245. Jinquan, T., Jing, C., Jacobi, H.H., Reimert, C.M., Millner, A., Quan, S., Hansen, J.B., Dissing, S., Malling, H.J., Skov, P.S. & Poulsen, L.K. CXCR3 expression and activation of eosinophils: role of IFN-gamma-inducible protein-10 and monokine induced by IFN-gamma. *J Immunol* **165**, 1548-1556 (2000).
246. Brightling, C.E., Kaur, D., Berger, P., Morgan, A.J., Wardlaw, A.J. & Bradding, P. Differential expression of CCR3 and CXCR3 by human lung and bone marrow-derived mast cells: implications for tissue mast cell migration. *J Leukoc Biol* **77**, 759-766 (2005).
247. Kelsen, S.G., Aksoy, M.O., Yang, Y., Shahabuddin, S., Litvin, J., Safadi, F. & Rogers, T.J. The chemokine receptor CXCR3 and its splice variant are expressed in human airway epithelial cells. *Am J Physiol Lung Cell Mol Physiol* **287**, L584-591 (2004).
248. Bonecchi, R., Bianchi, G., Bordignon, P.P., D'Ambrosio, D., Lang, R., Borsatti, A., Sozzani, S., Allavena, P., Gray, P.A., Mantovani, A. & Sinigaglia, F. Differential expression of chemokine receptors and chemotactic responsiveness of type 1 T helper cells (Th1s) and Th2s. *J Exp Med* **187**, 129-134 (1998).
249. Yamamoto, J., Adachi, Y., Onoue, Y., Adachi, Y.S., Okabe, Y., Itazawa, T., Toyoda, M., Seki, T., Morohashi, M., Matsushima, K. & Miyawaki, T. Differential expression of the chemokine receptors by the Th1- and Th2-type effector populations within circulating CD4+ T cells. *J Leukoc Biol* **68**, 568-574 (2000).
250. Loetscher, M., Gerber, B., Loetscher, P., Jones, S.A., Piali, L., Clark-Lewis, I., Baggiolini, M. & Moser, B. Chemokine receptor specific for IP10 and mig:

structure, function, and expression in activated T-lymphocytes. *J Exp Med* **184**, 963-969 (1996).
251. Lasagni, L., Francalanci, M., Annunziato, F., Lazzeri, E., Giannini, S., Cosmi, L., Sagrinati, C., Mazzinghi, B., Orlando, C., Maggi, E., Marra, F., Romagnani, S., Serio, M. & Romagnani, P. An alternatively spliced variant of CXCR3 mediates the inhibition of endothelial cell growth induced by IP-10, Mig, and I-TAC, and acts as functional receptor for platelet factor 4. *J Exp Med* **197**, 1537-1549 (2003).
252. Costa, C., Rufino, R., Traves, S.L., Lapa, E.S.J.R., Barnes, P.J. & Donnelly, L.E. CXCR3 and CCR5 chemokines in induced sputum from patients with COPD. *Chest* **133**, 26-33 (2008).
253. Medoff, B.D., Sauty, A., Tager, A.M., Maclean, J.A., Smith, R.N., Mathew, A., Dufour, J.H. & Luster, A.D. IFN-gamma-inducible protein 10 (CXCL10) contributes to airway hyperreactivity and airway inflammation in a mouse model of asthma. *J Immunol* **168**, 5278-5286 (2002).
254. Thomas, M.S., Kunkel, S.L. & Lukacs, N.W. Differential role of IFN-gamma-inducible protein 10 kDa in a cockroach antigen-induced model of allergic airway hyperreactivity: systemic versus local effects. *J Immunol* **169**, 7045-7053 (2002).
255. Bochner, B.S., Hudson, S.A., Xiao, H.Q. & Liu, M.C. Release of both CCR4-active and CXCR3-active chemokines during human allergic pulmonary late-phase reactions. *J Allergy Clin Immunol* **112**, 930-934 (2003).
256. Dufour, J.H., Dziejman, M., Liu, M.T., Leung, J.H., Lane, T.E. & Luster, A.D. IFN-gamma-inducible protein 10 (IP-10; CXCL10)-deficient mice reveal a role for IP-10 in effector T cell generation and trafficking. *J Immunol* **168**, 3195-3204 (2002).
257. Proud, D., Turner, R.B., Winther, B., Wiehler, S., Tiesman, J.P., Reichling, T.D., Juhlin, K.D., Fulmer, A.W., Ho, B.Y., Walanski, A.A., Poore, C.L., Mizoguchi, H., Jump, L., Moore, M.L., Zukowski, C.K. & Clymer, J.W. Gene expression profiles during in vivo human rhinovirus infection: insights into the host response. *Am J Respir Crit Care Med* **178**, 962-968 (2008).
258. Bertics, P., Koziol, C. & Wiepz, G. Signal Transduction. in *Middleton's Allergy: Principles and Practice*, Vol. 1 (ed. Adkinson, N., Busse, W., Bochner, B., Holgate, S., Lemankse, R., and Simons, F.) 128-147 (Mosby Elsevier, Philadelphia, 2009).
259. Liu, Y., Shepherd, E.G. & Nelin, L.D. MAPK phosphatases--regulating the immune response. *Nat Rev Immunol* **7**, 202-212 (2007).
260. Adcock, I.M., Caramori, G. & Chung, K.F. New targets for drug development in asthma. *Lancet* **372**, 1073-1087 (2008).
261. Barnes, P.J. Frontrunners in novel pharmacotherapy of COPD. *Curr Opin Pharmacol* **8**, 300-307 (2008).
262. Wang, X., Lau, C., Wiehler, S., Pow, A., Mazzulli, T., Gutierrez, C., Proud, D. & Chow, C.W. Syk is downstream of intercellular adhesion molecule-1 and mediates human rhinovirus activation of p38 MAPK in airway epithelial cells. *J Immunol* **177**, 6859-6870 (2006).

263. Lau, C., Wang, X., Song, L., North, M., Wiehler, S., Proud, D. & Chow, C.W. Syk associates with clathrin and mediates phosphatidylinositol 3-kinase activation during human rhinovirus internalization. *J Immunol* **180**, 870-880 (2008).
264. Bentley, J.K., Newcomb, D.C., Goldsmith, A.M., Jia, Y., Sajjan, U.S. & Hershenson, M.B. Rhinovirus activates interleukin-8 expression via a Src/p110beta phosphatidylinositol 3-kinase/Akt pathway in human airway epithelial cells. *J Virol* **81**, 1186-1194 (2007).
265. Newcomb, D.C., Sajjan, U., Nanua, S., Jia, Y., Goldsmith, A.M., Bentley, J.K. & Hershenson, M.B. Phosphatidylinositol 3-kinase is required for rhinovirus-induced airway epithelial cell interleukin-8 expression. *J Biol Chem* **280**, 36952-36961 (2005).
266. Griego, S.D., Weston, C.B., Adams, J.L., Tal-Singer, R. & Dillon, S.B. Role of p38 mitogen-activated protein kinase in rhinovirus-induced cytokine production by bronchial epithelial cells. *J Immunol* **165**, 5211-5220 (2000).
267. Wiehler, S. & Proud, D. Interleukin-17A modulates human airway epithelial responses to human rhinovirus infection. *Am J Physiol Lung Cell Mol Physiol* **293**, L505-515 (2007).
268. Leigh, R., Oyelusi, W., Wiehler, S., Koetzler, R., Zaheer, R.S., Newton, R. & Proud, D. Human rhinovirus infection enhances airway epithelial cell production of growth factors involved in airway remodeling. *J Allergy Clin Immunol* **121**, 1238-1245 e1234 (2008).
269. Rubinfeld, H. & Seger, R. The ERK Cascade As a Prototype of MAPK Signaling Pathways. in *MAPK Signaling Protocols* (ed. Seger, R.) 1-28 (Humana Press, Totowa, 2004).
270. Pearson, G., Robinson, F., Beers Gibson, T., Xu, B.E., Karandikar, M., Berman, K. & Cobb, M.H. Mitogen-activated protein (MAP) kinase pathways: regulation and physiological functions. *Endocr Rev* **22**, 153-183 (2001).
271. Chen, Z., Gibson, T.B., Robinson, F., Silvestro, L., Pearson, G., Xu, B., Wright, A., Vanderbilt, C. & Cobb, M.H. MAP kinases. *Chem Rev* **101**, 2449-2476 (2001).
272. Chang, L. & Karin, M. Mammalian MAP kinase signalling cascades. *Nature* **410**, 37-40 (2001).
273. Shaul, Y.D. & Seger, R. The MEK/ERK cascade: from signaling specificity to diverse functions. *Biochim Biophys Acta* **1773**, 1213-1226 (2007).
274. Lee, J.C., Laydon, J.T., McDonnell, P.C., Gallagher, T.F., Kumar, S., Green, D., McNulty, D., Blumenthal, M.J., Heys, J.R., Landvatter, S.W. & et al. A protein kinase involved in the regulation of inflammatory cytokine biosynthesis. *Nature* **372**, 739-746 (1994).
275. Derijard, B., Raingeaud, J., Barrett, T., Wu, I.H., Han, J., Ulevitch, R.J. & Davis, R.J. Independent human MAP-kinase signal transduction pathways defined by MEK and MKK isoforms. *Science* **267**, 682-685 (1995).
276. Stein, B., Brady, H., Yang, M.X., Young, D.B. & Barbosa, M.S. Cloning and characterization of MEK6, a novel member of the mitogen-activated protein kinase kinase cascade. *J Biol Chem* **271**, 11427-11433 (1996).

277. McLaughlin, M.M., Kumar, S., McDonnell, P.C., Van Horn, S., Lee, J.C., Livi, G.P. & Young, P.R. Identification of mitogen-activated protein (MAP) kinase-activated protein kinase-3, a novel substrate of CSBP p38 MAP kinase. *J Biol Chem* **271**, 8488-8492 (1996).
278. Ono, K. & Han, J. The p38 signal transduction pathway: activation and function. *Cell Signal* **12**, 1-13 (2000).
279. Liu, W., Liang, Q., Balzar, S., Wenzel, S., Gorska, M. & Alam, R. Cell-specific activation profile of extracellular signal-regulated kinase 1/2, Jun N-terminal kinase, and p38 mitogen-activated protein kinases in asthmatic airways. *J Allergy Clin Immunol* **121**, 893-902 e892 (2008).
280. Rincon, M., Enslen, H., Raingeaud, J., Recht, M., Zapton, T., Su, M.S., Penix, L.A., Davis, R.J. & Flavell, R.A. Interferon-gamma expression by Th1 effector T cells mediated by the p38 MAP kinase signaling pathway. *EMBO J* **17**, 2817-2829 (1998).
281. Undevia, N.S., Dorscheid, D.R., Marroquin, B.A., Gugliotta, W.L., Tse, R. & White, S.R. Smad and p38-MAPK signaling mediates apoptotic effects of transforming growth factor-beta1 in human airway epithelial cells. *Am J Physiol Lung Cell Mol Physiol* **287**, L515-524 (2004).
282. Kampen, G.T., Stafford, S., Adachi, T., Jinquan, T., Quan, S., Grant, J.A., Skov, P.S., Poulsen, L.K. & Alam, R. Eotaxin induces degranulation and chemotaxis of eosinophils through the activation of ERK2 and p38 mitogen-activated protein kinases. *Blood* **95**, 1911-1917 (2000).
283. Pelaia, G., Cuda, G., Vatrella, A., Gallelli, L., Caraglia, M., Marra, M., Abbruzzese, A., Caputi, M., Maselli, R., Costanzo, F.S. & Marsico, S.A. Mitogen-activated protein kinases and asthma. *J Cell Physiol* **202**, 642-653 (2005).
284. Newton, R. & Holden, N. Inhibitors of p38 mitogen-activated protein kinase: potential as anti-inflammatory agents in asthma? *BioDrugs* **17**, 113-129 (2003).
285. Yang, D.D., Kuan, C.Y., Whitmarsh, A.J., Rincon, M., Zheng, T.S., Davis, R.J., Rakic, P. & Flavell, R.A. Absence of excitotoxicity-induced apoptosis in the hippocampus of mice lacking the Jnk3 gene. *Nature* **389**, 865-870 (1997).
286. Gupta, S., Barrett, T., Whitmarsh, A.J., Cavanagh, J., Sluss, H.K., Derijard, B. & Davis, R.J. Selective interaction of JNK protein kinase isoforms with transcription factors. *EMBO J* **15**, 2760-2770 (1996).
287. Dong, C., Yang, D.D., Wysk, M., Whitmarsh, A.J., Davis, R.J. & Flavell, R.A. Defective T cell differentiation in the absence of Jnk1. *Science* **282**, 2092-2095 (1998).
288. Hashimoto, S., Gon, Y., Takeshita, I., Matsumoto, K., Maruoka, S. & Horie, T. Transforming growth Factor-beta1 induces phenotypic modulation of human lung fibroblasts to myofibroblast through a c-Jun-NH2-terminal kinase-dependent pathway. *Am J Respir Crit Care Med* **163**, 152-157 (2001).
289. Nath, P., Eynott, P., Leung, S.Y., Adcock, I.M., Bennett, B.L. & Chung, K.F. Potential role of c-Jun NH2-terminal kinase in allergic airway inflammation and remodelling: effects of SP600125. *Eur J Pharmacol* **506**, 273-283 (2005).

290. Eynott, P.R., Nath, P., Leung, S.Y., Adcock, I.M., Bennett, B.L. & Chung, K.F. Allergen-induced inflammation and airway epithelial and smooth muscle cell proliferation: role of Jun N-terminal kinase. *Br J Pharmacol* **140**, 1373-1380 (2003).
291. Nishimoto, S. & Nishida, E. MAPK signalling: ERK5 versus ERK1/2. *EMBO Rep* **7**, 782-786 (2006).
292. Lee, J.D., Ulevitch, R.J. & Han, J. Primary structure of BMK1: a new mammalian map kinase. *Biochem Biophys Res Commun* **213**, 715-724 (1995).
293. Zhou, G., Bao, Z.Q. & Dixon, J.E. Components of a new human protein kinase signal transduction pathway. *J Biol Chem* **270**, 12665-12669 (1995).
294. Kamakura, S., Moriguchi, T. & Nishida, E. Activation of the protein kinase ERK5/BMK1 by receptor tyrosine kinases. Identification and characterization of a signaling pathway to the nucleus. *J Biol Chem* **274**, 26563-26571 (1999).
295. Mody, N., Leitch, J., Armstrong, C., Dixon, J. & Cohen, P. Effects of MAP kinase cascade inhibitors on the MKK5/ERK5 pathway. *FEBS Lett* **502**, 21-24 (2001).
296. Kasler, H.G., Victoria, J., Duramad, O. & Winoto, A. ERK5 is a novel type of mitogen-activated protein kinase containing a transcriptional activation domain. *Mol Cell Biol* **20**, 8382-8389 (2000).
297. Ray, L.B. & Sturgill, T.W. Rapid stimulation by insulin of a serine/threonine kinase in 3T3-L1 adipocytes that phosphorylates microtubule-associated protein 2 in vitro. *Proc Natl Acad Sci U S A* **84**, 1502-1506 (1987).
298. Boulton, T.G., Yancopoulos, G.D., Gregory, J.S., Slaughter, C., Moomaw, C., Hsu, J. & Cobb, M.H. An insulin-stimulated protein kinase similar to yeast kinases involved in cell cycle control. *Science* **249**, 64-67 (1990).
299. Boulton, T.G., Nye, S.H., Robbins, D.J., Ip, N.Y., Radziejewska, E., Morgenbesser, S.D., DePinho, R.A., Panayotatos, N., Cobb, M.H. & Yancopoulos, G.D. ERKs: a family of protein-serine/threonine kinases that are activated and tyrosine phosphorylated in response to insulin and NGF. *Cell* **65**, 663-675 (1991).
300. Yung, Y., Yao, Z., Hanoch, T. & Seger, R. ERK1b, a 46-kDa ERK isoform that is differentially regulated by MEK. *J Biol Chem* **275**, 15799-15808 (2000).
301. Gonzalez, F.A., Raden, D.L., Rigby, M.R. & Davis, R.J. Heterogeneous expression of four MAP kinase isoforms in human tissues. *FEBS Lett* **304**, 170-178 (1992).
302. Payne, D.M., Rossomando, A.J., Martino, P., Erickson, A.K., Her, J.H., Shabanowitz, J., Hunt, D.F., Weber, M.J. & Sturgill, T.W. Identification of the regulatory phosphorylation sites in pp42/mitogen-activated protein kinase (MAP kinase). *EMBO J* **10**, 885-892 (1991).
303. Seger, R., Ahn, N.G., Posada, J., Munar, E.S., Jensen, A.M., Cooper, J.A., Cobb, M.H. & Krebs, E.G. Purification and characterization of mitogen-activated protein kinase activator(s) from epidermal growth factor-stimulated A431 cells. *J Biol Chem* **267**, 14373-14381 (1992).

304. Adachi, M., Fukuda, M. & Nishida, E. Two co-existing mechanisms for nuclear import of MAP kinase: passive diffusion of a monomer and active transport of a dimer. *EMBO J* **18**, 5347-5358 (1999).
305. Matsubayashi, Y., Fukuda, M. & Nishida, E. Evidence for existence of a nuclear pore complex-mediated, cytosol-independent pathway of nuclear translocation of ERK MAP kinase in permeabilized cells. *J Biol Chem* **276**, 41755-41760 (2001).
306. Gille, H., Sharrocks, A.D. & Shaw, P.E. Phosphorylation of transcription factor p62TCF by MAP kinase stimulates ternary complex formation at c-fos promoter. *Nature* **358**, 414-417 (1992).
307. Murphy, L.O., Smith, S., Chen, R.H., Fingar, D.C. & Blenis, J. Molecular interpretation of ERK signal duration by immediate early gene products. *Nat Cell Biol* **4**, 556-564 (2002).
308. Milne, D.M., Campbell, D.G., Caudwell, F.B. & Meek, D.W. Phosphorylation of the tumor suppressor protein p53 by mitogen-activated protein kinases. *J Biol Chem* **269**, 9253-9260 (1994).
309. Yang, B.S., Hauser, C.A., Henkel, G., Colman, M.S., Van Beveren, C., Stacey, K.J., Hume, D.A., Maki, R.A. & Ostrowski, M.C. Ras-mediated phosphorylation of a conserved threonine residue enhances the transactivation activities of c-Ets1 and c-Ets2. *Mol Cell Biol* **16**, 538-547 (1996).
310. Pircher, T.J., Petersen, H., Gustafsson, J.A. & Haldosen, L.A. Extracellular signal-regulated kinase (ERK) interacts with signal transducer and activator of transcription (STAT) 5a. *Mol Endocrinol* **13**, 555-565 (1999).
311. Sturgill, T.W., Ray, L.B., Erikson, E. & Maller, J.L. Insulin-stimulated MAP-2 kinase phosphorylates and activates ribosomal protein S6 kinase II. *Nature* **334**, 715-718 (1988).
312. Alessi, D.R., Gomez, N., Moorhead, G., Lewis, T., Keyse, S.M. & Cohen, P. Inactivation of p42 MAP kinase by protein phosphatase 2A and a protein tyrosine phosphatase, but not CL100, in various cell lines. *Curr Biol* **5**, 283-295 (1995).
313. Pulido, R., Zuniga, A. & Ullrich, A. PTP-SL and STEP protein tyrosine phosphatases regulate the activation of the extracellular signal-regulated kinases ERK1 and ERK2 by association through a kinase interaction motif. *EMBO J* **17**, 7337-7350 (1998).
314. Sun, H., Charles, C.H., Lau, L.F. & Tonks, N.K. MKP-1 (3CH134), an immediate early gene product, is a dual specificity phosphatase that dephosphorylates MAP kinase in vivo. *Cell* **75**, 487-493 (1993).
315. Liu, X., Yan, S., Zhou, T., Terada, Y. & Erikson, R.L. The MAP kinase pathway is required for entry into mitosis and cell survival. *Oncogene* **23**, 763-776 (2004).
316. Lloyd, A.C. Distinct functions for ERKs? *J Biol* **5**, 13 (2006).
317. Vantaggiato, C., Formentini, I., Bondanza, A., Bonini, C., Naldini, L. & Brambilla, R. ERK1 and ERK2 mitogen-activated protein kinases affect Ras-dependent cell signaling differentially. *J Biol* **5**, 14 (2006).
318. Pages, G., Guerin, S., Grall, D., Bonino, F., Smith, A., Anjuere, F., Auberger, P. & Pouyssegur, J. Defective thymocyte maturation in p44 MAP kinase (Erk 1) knockout mice. *Science* **286**, 1374-1377 (1999).

319. Saba-El-Leil, M.K., Vella, F.D., Vernay, B., Voisin, L., Chen, L., Labrecque, N., Ang, S.L. & Meloche, S. An essential function of the mitogen-activated protein kinase Erk2 in mouse trophoblast development. *EMBO Rep* **4**, 964-968 (2003).
320. Yamashita, M., Kimura, M., Kubo, M., Shimizu, C., Tada, T., Perlmutter, R.M. & Nakayama, T. T cell antigen receptor-mediated activation of the Ras/mitogen-activated protein kinase pathway controls interleukin 4 receptor function and type-2 helper T cell differentiation. *Proc Natl Acad Sci U S A* **96**, 1024-1029 (1999).
321. Ramakrishnan, M., Musa, N.L., Li, J., Liu, P.T., Pestell, R.G. & Hershenson, M.B. Catalytic activation of extracellular signal-regulated kinases induces cyclin D1 expression in primary tracheal myocytes. *Am J Respir Cell Mol Biol* **18**, 736-740 (1998).
322. Gerthoffer, W.T. & Singer, C.A. MAPK regulation of gene expression in airway smooth muscle. *Respir Physiol Neurobiol* **137**, 237-250 (2003).
323. Hellermann, G.R., Nagy, S.B., Kong, X., Lockey, R.F. & Mohapatra, S.S. Mechanism of cigarette smoke condensate-induced acute inflammatory response in human bronchial epithelial cells. *Respir Res* **3**, 22 (2002).
324. Petecchia, L., Sabatini, F., Varesio, L., Camoirano, A., Usai, C., Pezzolo, A. & Rossi, G.A. Bronchial airway epithelial cell damage following exposure to cigarette smoke includes disassembly of tight junction components mediated by the extracellular signal-regulated kinase 1/2 pathway. *Chest* **135**, 1502-1512 (2009).
325. Serikov, V.B., Choi, H., Chmiel, K.J., Wu, R. & Widdicombe, J.H. Activation of extracellular regulated kinases is required for the increase in airway epithelial permeability during leukocyte transmigration. *Am J Respir Cell Mol Biol* **30**, 261-270 (2004).
326. Pleschka, S. RNA viruses and the mitogenic Raf/MEK/ERK signal transduction cascade. *Biol Chem* **389**, 1273-1282 (2008).
327. Crews, C.M., Alessandrini, A. & Erikson, R.L. The primary structure of MEK, a protein kinase that phosphorylates the ERK gene product. *Science* **258**, 478-480 (1992).
328. Zheng, C.F. & Guan, K.L. Properties of MEKs, the kinases that phosphorylate and activate the extracellular signal-regulated kinases. *J Biol Chem* **268**, 23933-23939 (1993).
329. Alessi, D.R., Saito, Y., Campbell, D.G., Cohen, P., Sithanandam, G., Rapp, U., Ashworth, A., Marshall, C.J. & Cowley, S. Identification of the sites in MAP kinase kinase-1 phosphorylated by p74raf-1. *EMBO J* **13**, 1610-1619 (1994).
330. Brunet, A., Pages, G. & Pouyssegur, J. Growth factor-stimulated MAP kinase induces rapid retrophosphorylation and inhibition of MAP kinase kinase (MEK1). *FEBS Lett* **346**, 299-303 (1994).
331. Nantel, A., Mohammad-Ali, K., Sherk, J., Posner, B.I. & Thomas, D.Y. Interaction of the Grb10 adapter protein with the Raf1 and MEK1 kinases. *J Biol Chem* **273**, 10475-10484 (1998).
332. Catalanotti, F., Reyes, G., Jesenberger, V., Galabova-Kovacs, G., de Matos Simoes, R., Carugo, O. & Baccarini, M. A Mek1-Mek2 heterodimer determines

the strength and duration of the Erk signal. *Nat Struct Mol Biol* **16**, 294-303 (2009).
333. Sontag, E., Fedorov, S., Kamibayashi, C., Robbins, D., Cobb, M. & Mumby, M. The interaction of SV40 small tumor antigen with protein phosphatase 2A stimulates the map kinase pathway and induces cell proliferation. *Cell* **75**, 887-897 (1993).
334. Yu, W., Fantl, W.J., Harrowe, G. & Williams, L.T. Regulation of the MAP kinase pathway by mammalian Ksr through direct interaction with MEK and ERK. *Curr Biol* **8**, 56-64 (1998).
335. Tohgo, A., Pierce, K.L., Choy, E.W., Lefkowitz, R.J. & Luttrell, L.M. beta-Arrestin scaffolding of the ERK cascade enhances cytosolic ERK activity but inhibits ERK-mediated transcription following angiotensin AT1a receptor stimulation. *J Biol Chem* **277**, 9429-9436 (2002).
336. Schaeffer, H.J., Catling, A.D., Eblen, S.T., Collier, L.S., Krauss, A. & Weber, M.J. MP1: a MEK binding partner that enhances enzymatic activation of the MAP kinase cascade. *Science* **281**, 1668-1671 (1998).
337. Fukuda, M., Gotoh, I., Gotoh, Y. & Nishida, E. Cytoplasmic localization of mitogen-activated protein kinase kinase directed by its NH2-terminal, leucine-rich short amino acid sequence, which acts as a nuclear export signal. *J Biol Chem* **271**, 20024-20028 (1996).
338. Giroux, S., Tremblay, M., Bernard, D., Cardin-Girard, J.F., Aubry, S., Larouche, L., Rousseau, S., Huot, J., Landry, J., Jeannotte, L. & Charron, J. Embryonic death of Mek1-deficient mice reveals a role for this kinase in angiogenesis in the labyrinthine region of the placenta. *Curr Biol* **9**, 369-372 (1999).
339. Belanger, L.F., Roy, S., Tremblay, M., Brott, B., Steff, A.M., Mourad, W., Hugo, P., Erikson, R. & Charron, J. Mek2 is dispensable for mouse growth and development. *Mol Cell Biol* **23**, 4778-4787 (2003).
340. Jelinek, T., Catling, A.D., Reuter, C.W., Moodie, S.A., Wolfman, A. & Weber, M.J. RAS and RAF-1 form a signalling complex with MEK-1 but not MEK-2. *Mol Cell Biol* **14**, 8212-8218 (1994).
341. Wu, X., Noh, S.J., Zhou, G., Dixon, J.E. & Guan, K.L. Selective activation of MEK1 but not MEK2 by A-Raf from epidermal growth factor-stimulated Hela cells. *J Biol Chem* **271**, 3265-3271 (1996).
342. Favata, M.F., Horiuchi, K.Y., Manos, E.J., Daulerio, A.J., Stradley, D.A., Feeser, W.S., Van Dyk, D.E., Pitts, W.J., Earl, R.A., Hobbs, F., Copeland, R.A., Magolda, R.L., Scherle, P.A. & Trzaskos, J.M. Identification of a novel inhibitor of mitogen-activated protein kinase kinase. *J Biol Chem* **273**, 18623-18632 (1998).
343. Duan, W., Chan, J.H., Wong, C.H., Leung, B.P. & Wong, W.S. Anti-inflammatory effects of mitogen-activated protein kinase kinase inhibitor U0126 in an asthma mouse model. *J Immunol* **172**, 7053-7059 (2004).
344. Brivanlou, A.H. & Darnell, J.E., Jr. Signal transduction and the control of gene expression. *Science* **295**, 813-818 (2002).
345. Medzhitov, R. & Horng, T. Transcriptional control of the inflammatory response. *Nat Rev Immunol* **9**, 692-703 (2009).

346. Edwards, M.R., Bartlett, N.W., Clarke, D., Birrell, M., Belvisi, M. & Johnston, S.L. Targeting the NF-kappaB pathway in asthma and chronic obstructive pulmonary disease. *Pharmacol Ther* **121**, 1-13 (2009).
347. Vallabhapurapu, S. & Karin, M. Regulation and function of NF-kappaB transcription factors in the immune system. *Annu Rev Immunol* **27**, 693-733 (2009).
348. Hart, L.A., Krishnan, V.L., Adcock, I.M., Barnes, P.J. & Chung, K.F. Activation and localization of transcription factor, nuclear factor-kappaB, in asthma. *Am J Respir Crit Care Med* **158**, 1585-1592 (1998).
349. Zhao, S., Qi, Y., Liu, X., Jiang, Q., Liu, S., Jiang, Y. & Jiang, Z. Activation of NF-kappa B in bronchial epithelial cells from children with asthma. *Chin Med J (Engl)* **114**, 909-911 (2001).
350. Di Stefano, A., Caramori, G., Oates, T., Capelli, A., Lusuardi, M., Gnemmi, I., Ioli, F., Chung, K.F., Donner, C.F., Barnes, P.J. & Adcock, I.M. Increased expression of nuclear factor-kappaB in bronchial biopsies from smokers and patients with COPD. *Eur Respir J* **20**, 556-563 (2002).
351. Haddad, J.J. Nuclear factor (NF)-kappa B blockade attenuates but does not abrogate LPS-mediated interleukin (IL)-1 beta biosynthesis in alveolar epithelial cells. *Biochem Biophys Res Commun* **293**, 252-257 (2002).
352. Das, J., Chen, C.H., Yang, L., Cohn, L., Ray, P. & Ray, A. A critical role for NF-kappa B in GATA3 expression and TH2 differentiation in allergic airway inflammation. *Nat Immunol* **2**, 45-50 (2001).
353. Laza-Stanca, V., Stanciu, L.A., Message, S.D., Edwards, M.R., Gern, J.E. & Johnston, S.L. Rhinovirus replication in human macrophages induces NF-kappaB-dependent tumor necrosis factor alpha production. *J Virol* **80**, 8248-8258 (2006).
354. Thomas, L.H., Friedland, J.S., Sharland, M. & Becker, S. Respiratory syncytial virus-induced RANTES production from human bronchial epithelial cells is dependent on nuclear factor-kappa B nuclear binding and is inhibited by adenovirus-mediated expression of inhibitor of kappa B alpha. *J Immunol* **161**, 1007-1016 (1998).
355. Yang, L., Cohn, L., Zhang, D.H., Homer, R., Ray, A. & Ray, P. Essential role of nuclear factor kappaB in the induction of eosinophilia in allergic airway inflammation. *J Exp Med* **188**, 1739-1750 (1998).
356. Papi, A. & Johnston, S.L. Rhinovirus infection induces expression of its own receptor intercellular adhesion molecule 1 (ICAM-1) via increased NF-kappaB-mediated transcription. *J Biol Chem* **274**, 9707-9720 (1999).
357. Oomizu, S., Yanase, Y., Suzuki, H., Kameyoshi, Y. & Hide, M. Fucoidan prevents C epsilon germline transcription and NFkappaB p52 translocation for IgE production in B cells. *Biochem Biophys Res Commun* **350**, 501-507 (2006).
358. Li, Y.H., Yan, Z.Q., Brauner, A. & Tullus, K. Activation of macrophage nuclear factor-kappa B and induction of inducible nitric oxide synthase by LPS. *Respir Res* **3**, 23 (2002).

359. Tacon, C.E., Wiehler, S., Holden, N.S., Newton, R., Proud, D. & Leigh, R. Human Rhinovirus Infection Upregulates MMP-9 Production in Airway Epithelial Cells via NF-{kappa}B. *Am J Respir Cell Mol Biol* (2009).
360. Baeuerle, P.A. & Baltimore, D. I kappa B: a specific inhibitor of the NF-kappa B transcription factor. *Science* **242**, 540-546 (1988).
361. Li, Z.W., Chu, W., Hu, Y., Delhase, M., Deerinck, T., Ellisman, M., Johnson, R. & Karin, M. The IKKbeta subunit of IkappaB kinase (IKK) is essential for nuclear factor kappaB activation and prevention of apoptosis. *J Exp Med* **189**, 1839-1845 (1999).
362. Chen, Z., Hagler, J., Palombella, V.J., Melandri, F., Scherer, D., Ballard, D. & Maniatis, T. Signal-induced site-specific phosphorylation targets I kappa B alpha to the ubiquitin-proteasome pathway. *Genes Dev* **9**, 1586-1597 (1995).
363. Zandi, E., Rothwarf, D.M., Delhase, M., Hayakawa, M. & Karin, M. The IkappaB kinase complex (IKK) contains two kinase subunits, IKKalpha and IKKbeta, necessary for IkappaB phosphorylation and NF-kappaB activation. *Cell* **91**, 243-252 (1997).
364. Yamaoka, S., Courtois, G., Bessia, C., Whiteside, S.T., Weil, R., Agou, F., Kirk, H.E., Kay, R.J. & Israel, A. Complementation cloning of NEMO, a component of the IkappaB kinase complex essential for NF-kappaB activation. *Cell* **93**, 1231-1240 (1998).
365. Mattioli, I., Geng, H., Sebald, A., Hodel, M., Bucher, C., Kracht, M. & Schmitz, M.L. Inducible phosphorylation of NF-kappa B p65 at serine 468 by T cell costimulation is mediated by IKK epsilon. *J Biol Chem* **281**, 6175-6183 (2006).
366. Harris, J., Oliere, S., Sharma, S., Sun, Q., Lin, R., Hiscott, J. & Grandvaux, N. Nuclear accumulation of cRel following C-terminal phosphorylation by TBK1/IKK epsilon. *J Immunol* **177**, 2527-2535 (2006).
367. Hiscott, J. Convergence of the NF-kappaB and IRF pathways in the regulation of the innate antiviral response. *Cytokine Growth Factor Rev* **18**, 483-490 (2007).
368. Koetzler, R., Zaheer, R.S., Newton, R. & Proud, D. Nitric oxide inhibits IFN regulatory factor 1 and nuclear factor-kappaB pathways in rhinovirus-infected epithelial cells. *J Allergy Clin Immunol* **124**, 551-557 (2009).
369. Beyaert, R., Cuenda, A., Vanden Berghe, W., Plaisance, S., Lee, J.C., Haegeman, G., Cohen, P. & Fiers, W. The p38/RK mitogen-activated protein kinase pathway regulates interleukin-6 synthesis response to tumor necrosis factor. *EMBO J* **15**, 1914-1923 (1996).
370. Vanden Berghe, W., Plaisance, S., Boone, E., De Bosscher, K., Schmitz, M.L., Fiers, W. & Haegeman, G. p38 and extracellular signal-regulated kinase mitogen-activated protein kinase pathways are required for nuclear factor-kappaB p65 transactivation mediated by tumor necrosis factor. *J Biol Chem* **273**, 3285-3290 (1998).
371. Carter, A.B. & Hunninghake, G.W. A constitutive active MEK --> ERK pathway negatively regulates NF-kappa B-dependent gene expression by modulating TATA-binding protein phosphorylation. *J Biol Chem* **275**, 27858-27864 (2000).

372. Chen, B.C. & Lin, W.W. PKC- and ERK-dependent activation of I kappa B kinase by lipopolysaccharide in macrophages: enhancement by P2Y receptor-mediated CaMK activation. *Br J Pharmacol* **134**, 1055-1065 (2001).
373. Birkenkamp, K.U., Tuyt, L.M., Lummen, C., Wierenga, A.T., Kruijer, W. & Vellenga, E. The p38 MAP kinase inhibitor SB203580 enhances nuclear factor-kappa B transcriptional activity by a non-specific effect upon the ERK pathway. *Br J Pharmacol* **131**, 99-107 (2000).
374. Saccani, S., Pantano, S. & Natoli, G. p38-Dependent marking of inflammatory genes for increased NF-kappa B recruitment. *Nat Immunol* **3**, 69-75 (2002).
375. Vermeulen, L., De Wilde, G., Van Damme, P., Vanden Berghe, W. & Haegeman, G. Transcriptional activation of the NF-kappaB p65 subunit by mitogen- and stress-activated protein kinase-1 (MSK1). *EMBO J* **22**, 1313-1324 (2003).
376. Honda, K. & Taniguchi, T. IRFs: master regulators of signalling by Toll-like receptors and cytosolic pattern-recognition receptors. *Nat Rev Immunol* **6**, 644-658 (2006).
377. Tamura, T., Yanai, H., Savitsky, D. & Taniguchi, T. The IRF family transcription factors in immunity and oncogenesis. *Annu Rev Immunol* **26**, 535-584 (2008).
378. Takaoka, A., Tamura, T. & Taniguchi, T. Interferon regulatory factor family of transcription factors and regulation of oncogenesis. *Cancer Sci* **99**, 467-478 (2008).
379. Bazer, F.W., Spencer, T.E. & Ott, T.L. Interferon tau: a novel pregnancy recognition signal. *Am J Reprod Immunol* **37**, 412-420 (1997).
380. Ozato, K., Tailor, P. & Kubota, T. The interferon regulatory factor family in host defense: mechanism of action. *J Biol Chem* **282**, 20065-20069 (2007).
381. Nehyba, J., Hrdlickova, R., Burnside, J. & Bose, H.R., Jr. A novel interferon regulatory factor (IRF), IRF-10, has a unique role in immune defense and is induced by the v-Rel oncoprotein. *Mol Cell Biol* **22**, 3942-3957 (2002).
382. Uegaki, K., Shirakawa, M., Harada, H., Taniguchi, T. & Kyogoku, Y. Secondary structure and folding topology of the DNA binding domain of interferon regulatory factor 2, as revealed by NMR spectroscopy. *FEBS Lett* **359**, 184-188 (1995).
383. Fujii, Y., Shimizu, T., Kusumoto, M., Kyogoku, Y., Taniguchi, T. & Hakoshima, T. Crystal structure of an IRF-DNA complex reveals novel DNA recognition and cooperative binding to a tandem repeat of core sequences. *EMBO J* **18**, 5028-5041 (1999).
384. Bluyssen, H.A. & Levy, D.E. Stat2 is a transcriptional activator that requires sequence-specific contacts provided by stat1 and p48 for stable interaction with DNA. *J Biol Chem* **272**, 4600-4605 (1997).
385. Liu, J. & Ma, X. Interferon regulatory factor 8 regulates RANTES gene transcription in cooperation with interferon regulatory factor-1, NF-kappaB, and PU.1. *J Biol Chem* **281**, 19188-19195 (2006).
386. Sharf, R., Meraro, D., Azriel, A., Thornton, A.M., Ozato, K., Petricoin, E.F., Larner, A.C., Schaper, F., Hauser, H. & Levi, B.Z. Phosphorylation events modulate the ability of interferon consensus sequence binding protein to interact

with interferon regulatory factors and to bind DNA. *J Biol Chem* **272**, 9785-9792 (1997).
387. Weisz, A., Marx, P., Sharf, R., Appella, E., Driggers, P.H., Ozato, K. & Levi, B.Z. Human interferon consensus sequence binding protein is a negative regulator of enhancer elements common to interferon-inducible genes. *J Biol Chem* **267**, 25589-25596 (1992).
388. Genin, P., Algarte, M., Roof, P., Lin, R. & Hiscott, J. Regulation of RANTES chemokine gene expression requires cooperativity between NF-kappa B and IFN-regulatory factor transcription factors. *J Immunol* **164**, 5352-5361 (2000).
389. Wietek, C., Miggin, S.M., Jefferies, C.A. & O'Neill, L.A. Interferon regulatory factor-3-mediated activation of the interferon-sensitive response element by Toll-like receptor (TLR) 4 but not TLR3 requires the p65 subunit of NF-kappa. *J Biol Chem* **278**, 50923-50931 (2003).
390. Leung, T.H., Hoffmann, A. & Baltimore, D. One nucleotide in a kappaB site can determine cofactor specificity for NF-kappaB dimers. *Cell* **118**, 453-464 (2004).
391. Chae, M., Kim, K., Park, S.M., Jang, I.S., Seo, T., Kim, D.M., Kim, I.C., Lee, J.H. & Park, J. IRF-2 regulates NF-kappaB activity by modulating the subcellular localization of NF-kappaB. *Biochem Biophys Res Commun* **370**, 519-524 (2008).
392. Sgarbanti, M., Remoli, A.L., Marsili, G., Ridolfi, B., Borsetti, A., Perrotti, E., Orsatti, R., Ilari, R., Sernicola, L., Stellacci, E., Ensoli, B. & Battistini, A. IRF-1 is required for full NF-kappaB transcriptional activity at the human immunodeficiency virus type 1 long terminal repeat enhancer. *J Virol* **82**, 3632-3641 (2008).
393. Nehyba, J., Hrdlickova, R. & Bose, H.R., Jr. Dynamic evolution of immune system regulators: The history of the interferon regulatory factor (IRF) family. *Mol Biol Evol* (2009).
394. Marsili, G., Remoli, A.L., Sgarbanti, M. & Battistini, A. Role of acetylases and deacetylase inhibitors in IRF-1-mediated HIV-1 long terminal repeat transcription. *Ann N Y Acad Sci* **1030**, 636-643 (2004).
395. Masumi, A., Wang, I.M., Lefebvre, B., Yang, X.J., Nakatani, Y. & Ozato, K. The histone acetylase PCAF is a phorbol-ester-inducible coactivator of the IRF family that confers enhanced interferon responsiveness. *Mol Cell Biol* **19**, 1810-1820 (1999).
396. Wang, I.M., Blanco, J.C., Tsai, S.Y., Tsai, M.J. & Ozato, K. Interferon regulatory factors and TFIIB cooperatively regulate interferon-responsive promoter activity in vivo and in vitro. *Mol Cell Biol* **16**, 6313-6324 (1996).
397. Kroger, A., Koster, M., Schroeder, K., Hauser, H. & Mueller, P.P. Activities of IRF-1. *J Interferon Cytokine Res* **22**, 5-14 (2002).
398. Kotla, S., Peng, T., Bumgarner, R.E. & Gustin, K.E. Attenuation of the type I interferon response in cells infected with human rhinovirus. *Virology* **374**, 399-410 (2008).
399. Drahos, J. & Racaniello, V.R. Cleavage of IPS-1 in cells infected with human rhinovirus. *J Virol* (2009).
400. Kimura, T., Nakayama, K., Penninger, J., Kitagawa, M., Harada, H., Matsuyama, T., Tanaka, N., Kamijo, R., Vilcek, J., Mak, T.W. & et al. Involvement of the

IRF-1 transcription factor in antiviral responses to interferons. *Science* **264**, 1921-1924 (1994).
401. Reed, L.a.M., H. A simple method of estimating fifty percent endpoints. *The American Journal of Hygiene* **27**, 493-497 (1938).
402. Reddel, R.R., Ke, Y., Gerwin, B.I., McMenamin, M.G., Lechner, J.F., Su, R.T., Brash, D.E., Park, J.B., Rhim, J.S. & Harris, C.C. Transformation of human bronchial epithelial cells by infection with SV40 or adenovirus-12 SV40 hybrid virus, or transfection via strontium phosphate coprecipitation with a plasmid containing SV40 early region genes. *Cancer Res* **48**, 1904-1909 (1988).
403. Churchill, L., Chilton, F.H., Resau, J.H., Bascom, R., Hubbard, W.C. & Proud, D. Cyclooxygenase metabolism of endogenous arachidonic acid by cultured human tracheal epithelial cells. *Am Rev Respir Dis* **140**, 449-459 (1989).
404. Dudley, D.T., Pang, L., Decker, S.J., Bridges, A.J. & Saltiel, A.R. A synthetic inhibitor of the mitogen-activated protein kinase cascade. *Proc Natl Acad Sci U S A* **92**, 7686-7689 (1995).
405. Cuenda, A., Rouse, J., Doza, Y.N., Meier, R., Cohen, P., Gallagher, T.F., Young, P.R. & Lee, J.C. SB 203580 is a specific inhibitor of a MAP kinase homologue which is stimulated by cellular stresses and interleukin-1. *FEBS Lett* **364**, 229-233 (1995).
406. Bennett, B.L., Sasaki, D.T., Murray, B.W., O'Leary, E.C., Sakata, S.T., Xu, W., Leisten, J.C., Motiwala, A., Pierce, S., Satoh, Y., Bhagwat, S.S., Manning, A.M. & Anderson, D.W. SP600125, an anthrapyrazolone inhibitor of Jun N-terminal kinase. *Proc Natl Acad Sci U S A* **98**, 13681-13686 (2001).
407. Hancock, C.N., Macias, A., Lee, E.K., Yu, S.Y., Mackerell, A.D., Jr. & Shapiro, P. Identification of novel extracellular signal-regulated kinase docking domain inhibitors. *J Med Chem* **48**, 4586-4595 (2005).
408. Ohori, M., Kinoshita, T., Okubo, M., Sato, K., Yamazaki, A., Arakawa, H., Nishimura, S., Inamura, N., Nakajima, H., Neya, M., Miyake, H. & Fujii, T. Identification of a selective ERK inhibitor and structural determination of the inhibitor-ERK2 complex. *Biochem Biophys Res Commun* **336**, 357-363 (2005).
409. Sanders, S.P., Siekierski, E.S., Richards, S.M., Porter, J.D., Imani, F. & Proud, D. Rhinovirus infection induces expression of type 2 nitric oxide synthase in human respiratory epithelial cells in vitro and in vivo. *J Allergy Clin Immunol* **107**, 235-243 (2001).
410. Tibbles, L.A., Spurrell, J.C., Bowen, G.P., Liu, Q., Lam, M., Zaiss, A.K., Robbins, S.M., Hollenberg, M.D., Wickham, T.J. & Muruve, D.A. Activation of p38 and ERK signaling during adenovirus vector cell entry lead to expression of the C-X-C chemokine IP-10. *J Virol* **76**, 1559-1568 (2002).
411. Nakamichi, K., Inoue, S., Takasaki, T., Morimoto, K. & Kurane, I. Rabies virus stimulates nitric oxide production and CXC chemokine ligand 10 expression in macrophages through activation of extracellular signal-regulated kinases 1 and 2. *J Virol* **78**, 9376-9388 (2004).
412. Aguirre-Ghiso, J.A., Estrada, Y., Liu, D. & Ossowski, L. ERK(MAPK) activity as a determinant of tumor growth and dormancy; regulation by p38(SAPK). *Cancer Res* **63**, 1684-1695 (2003).

413. Lewthwaite, J.C., Bastow, E.R., Lamb, K.J., Blenis, J., Wheeler-Jones, C.P. & Pitsillides, A.A. A specific mechanomodulatory role for p38 MAPK in embryonic joint articular surface cell MEK-ERK pathway regulation. *J Biol Chem* **281**, 11011-11018 (2006).
414. Estrada, Y., Dong, J. & Ossowski, L. Positive crosstalk between ERK and p38 in melanoma stimulates migration and in vivo proliferation. *Pigment Cell Melanoma Res* **22**, 66-76 (2009).
415. Bain, J., Plater, L., Elliott, M., Shpiro, N., Hastie, C.J., McLauchlan, H., Klevernic, I., Arthur, J.S., Alessi, D.R. & Cohen, P. The selectivity of protein kinase inhibitors: a further update. *Biochem J* **408**, 297-315 (2007).
416. Zheng, C.F. & Guan, K.L. Cloning and characterization of two distinct human extracellular signal-regulated kinase activator kinases, MEK1 and MEK2. *J Biol Chem* **268**, 11435-11439 (1993).
417. Fuda, N.J., Ardehali, M.B. & Lis, J.T. Defining mechanisms that regulate RNA polymerase II transcription in vivo. *Nature* **461**, 186-192 (2009).
418. Nicolas, F.E., Lopez-Gomollon, S., Lopez-Martinez, A.F. & Dalmay, T. RNA silencing: Recent developments on miRNAs. *Recent Pat DNA Gene Seq* **3**, 77-87 (2009).
419. Houseley, J. & Tollervey, D. The many pathways of RNA degradation. *Cell* **136**, 763-776 (2009).
420. Li, Q. & Verma, I.M. NF-kappaB regulation in the immune system. *Nat Rev Immunol* **2**, 725-734 (2002).
421. Cheng, G., Nazar, A.S., Shin, H.S., Vanguri, P. & Shin, M.L. IP-10 gene transcription by virus in astrocytes requires cooperation of ISRE with adjacent kappaB site but not IRF-1 or viral transcription. *J Interferon Cytokine Res* **18**, 987-997 (1998).
422. Pesce, M. & Scholer, H.R. Oct-4: gatekeeper in the beginnings of mammalian development. *Stem Cells* **19**, 271-278 (2001).
423. Pan, G.J., Chang, Z.Y., Scholer, H.R. & Pei, D. Stem cell pluripotency and transcription factor Oct4. *Cell Res* **12**, 321-329 (2002).
424. Palombella, V.J. & Maniatis, T. Inducible processing of interferon regulatory factor-2. *Mol Cell Biol* **12**, 3325-3336 (1992).
425. Cohen, L. & Hiscott, J. Characterization of TH3, an induction-specific protein interacting with the interferon beta promoter. *Virology* **191**, 589-599 (1992).
426. Whiteside, S.T., King, P. & Goodbourn, S. A truncated form of the IRF-2 transcription factor has the properties of a postinduction repressor of interferon-beta gene expression. *J Biol Chem* **269**, 27059-27065 (1994).
427. Pion, E., Narayan, V., Eckert, M. & Ball, K.L. Role of the IRF-1 enhancer domain in signalling polyubiquitination and degradation. *Cell Signal* **21**, 1479-1487 (2009).
428. Schaper, F., Kirchhoff, S., Posern, G., Koster, M., Oumard, A., Sharf, R., Levi, B.Z. & Hauser, H. Functional domains of interferon regulatory factor I (IRF-1). *Biochem J* **335 (Pt 1)**, 147-157 (1998).

429. Fire, A., Xu, S., Montgomery, M.K., Kostas, S.A., Driver, S.E. & Mello, C.C. Potent and specific genetic interference by double-stranded RNA in Caenorhabditis elegans. *Nature* **391**, 806-811 (1998).
430. Elbashir, S.M., Harborth, J., Lendeckel, W., Yalcin, A., Weber, K. & Tuschl, T. Duplexes of 21-nucleotide RNAs mediate RNA interference in cultured mammalian cells. *Nature* **411**, 494-498 (2001).
431. Morris, K.V., Chan, S.W., Jacobsen, S.E. & Looney, D.J. Small interfering RNA-induced transcriptional gene silencing in human cells. *Science* **305**, 1289-1292 (2004).
432. Kawasaki, H. & Taira, K. Induction of DNA methylation and gene silencing by short interfering RNAs in human cells. *Nature* **431**, 211-217 (2004).
433. Weinberg, M.S., Villeneuve, L.M., Ehsani, A., Amarzguioui, M., Aagaard, L., Chen, Z.X., Riggs, A.D., Rossi, J.J. & Morris, K.V. The antisense strand of small interfering RNAs directs histone methylation and transcriptional gene silencing in human cells. *RNA* **12**, 256-262 (2006).
434. Kim, D.H., Villeneuve, L.M., Morris, K.V. & Rossi, J.J. Argonaute-1 directs siRNA-mediated transcriptional gene silencing in human cells. *Nat Struct Mol Biol* **13**, 793-797 (2006).
435. Gitlin, L., Karelsky, S. & Andino, R. Short interfering RNA confers intracellular antiviral immunity in human cells. *Nature* **418**, 430-434 (2002).
436. Bucher, E., Hemmes, H., de Haan, P., Goldbach, R. & Prins, M. The influenza A virus NS1 protein binds small interfering RNAs and suppresses RNA silencing in plants. *J Gen Virol* **85**, 983-991 (2004).
437. Lecellier, C.H., Dunoyer, P., Arar, K., Lehmann-Che, J., Eyquem, S., Himber, C., Saib, A. & Voinnet, O. A cellular microRNA mediates antiviral defense in human cells. *Science* **308**, 557-560 (2005).
438. Gitlin, L., Stone, J.K. & Andino, R. Poliovirus escape from RNA interference: short interfering RNA-target recognition and implications for therapeutic approaches. *J Virol* **79**, 1027-1035 (2005).
439. Scacheri, P.C., Rozenblatt-Rosen, O., Caplen, N.J., Wolfsberg, T.G., Umayam, L., Lee, J.C., Hughes, C.M., Shanmugam, K.S., Bhattacharjee, A., Meyerson, M. & Collins, F.S. Short interfering RNAs can induce unexpected and divergent changes in the levels of untargeted proteins in mammalian cells. *Proc Natl Acad Sci U S A* **101**, 1892-1897 (2004).
440. Vankoningsloo, S., de Longueville, F., Evrard, S., Rahier, P., Houbion, A., Fattaccioli, A., Gastellier, M., Remacle, J., Raes, M., Renard, P. & Arnould, T. Gene expression silencing with 'specific' small interfering RNA goes beyond specificity - a study of key parameters to take into account in the onset of small interfering RNA off-target effects. *FEBS J* **275**, 2738-2753 (2008).
441. Jackson, A.L., Bartz, S.R., Schelter, J., Kobayashi, S.V., Burchard, J., Mao, M., Li, B., Cavet, G. & Linsley, P.S. Expression profiling reveals off-target gene regulation by RNAi. *Nat Biotechnol* **21**, 635-637 (2003).
442. Sledz, C.A., Holko, M., de Veer, M.J., Silverman, R.H. & Williams, B.R. Activation of the interferon system by short-interfering RNAs. *Nat Cell Biol* **5**, 834-839 (2003).

443. Elbashir, S.M., Lendeckel, W. & Tuschl, T. RNA interference is mediated by 21- and 22-nucleotide RNAs. *Genes Dev* **15**, 188-200 (2001).
444. Gille, H., Kortenjann, M., Thomae, O., Moomaw, C., Slaughter, C., Cobb, M.H. & Shaw, P.E. ERK phosphorylation potentiates Elk-1-mediated ternary complex formation and transactivation. *EMBO J* **14**, 951-962 (1995).
445. Barry, O.P., Mullan, B., Sheehan, D., Kazanietz, M.G., Shanahan, F., Collins, J.K. & O'Sullivan, G.C. Constitutive ERK1/2 activation in esophagogastric rib bone marrow micrometastatic cells is MEK-independent. *J Biol Chem* **276**, 15537-15546 (2001).
446. Grammer, T.C. & Blenis, J. Evidence for MEK-independent pathways regulating the prolonged activation of the ERK-MAP kinases. *Oncogene* **14**, 1635-1642 (1997).
447. Pouyssegur, J., Volmat, V. & Lenormand, P. Fidelity and spatio-temporal control in MAP kinase (ERKs) signalling. *Biochem Pharmacol* **64**, 755-763 (2002).
448. Quan, H., Liu, H., Li, C. & Lou, L. 1,4-Diamino-2,3-dicyano-1,4-bis(methylthio)butadiene (U0126) enhances the cytotoxicity of combretastatin A4 independently of mitogen-activated protein kinase kinase. *J Pharmacol Exp Ther* **330**, 326-333 (2009).
449. Dokladda, K., Green, K.A., Pan, D.A. & Hardie, D.G. PD98059 and U0126 activate AMP-activated protein kinase by increasing the cellular AMP:ATP ratio and not via inhibition of the MAP kinase pathway. *FEBS Lett* **579**, 236-240 (2005).
450. Nazar, A.S., Cheng, G., Shin, H.S., Brothers, P.N., Dhib-Jalbut, S., Shin, M.L. & Vanguri, P. Induction of IP-10 chemokine promoter by measles virus: comparison with interferon-gamma shows the use of the same response element but with differential DNA-protein binding profiles. *J Neuroimmunol* **77**, 116-127 (1997).
451. Veckman, V., Osterlund, P., Fagerlund, R., Melen, K., Matikainen, S. & Julkunen, I. TNF-alpha and IFN-alpha enhance influenza-A-virus-induced chemokine gene expression in human A549 lung epithelial cells. *Virology* **345**, 96-104 (2006).
452. Lallemand, C., Blanchard, B., Palmieri, M., Lebon, P., May, E. & Tovey, M.G. Single-stranded RNA viruses inactivate the transcriptional activity of p53 but induce NOXA-dependent apoptosis via post-translational modifications of IRF-1, IRF-3 and CREB. *Oncogene* **26**, 328-338 (2007).
453. Bauvois, B., Nguyen, J., Tang, R., Billard, C. & Kolb, J.P. Types I and II interferons upregulate the costimulatory CD80 molecule in monocytes via interferon regulatory factor-1. *Biochem Pharmacol* (2009).
454. Liu, J., Guan, X. & Ma, X. Interferon regulatory factor 1 is an essential and direct transcriptional activator for interferon {gamma}-induced RANTES/CCl5 expression in macrophages. *J Biol Chem* **280**, 24347-24355 (2005).
455. Andersen, P., Pedersen, M.W., Woetmann, A., Villingshoj, M., Stockhausen, M.T., Odum, N. & Poulsen, H.S. EGFR induces expression of IRF-1 via STAT1 and STAT3 activation leading to growth arrest of human cancer cells. *Int J Cancer* **122**, 342-349 (2008).

456. Pamment, J., Ramsay, E., Kelleher, M., Dornan, D. & Ball, K.L. Regulation of the IRF-1 tumour modifier during the response to genotoxic stress involves an ATM-dependent signalling pathway. *Oncogene* **21**, 7776-7785 (2002).
457. Kano, S., Sato, K., Morishita, Y., Vollstedt, S., Kim, S., Bishop, K., Honda, K., Kubo, M. & Taniguchi, T. The contribution of transcription factor IRF1 to the interferon-gamma-interleukin 12 signaling axis and TH1 versus TH-17 differentiation of CD4+ T cells. *Nat Immunol* **9**, 34-41 (2008).
458. Kamijo, R., Harada, H., Matsuyama, T., Bosland, M., Gerecitano, J., Shapiro, D., Le, J., Koh, S.I., Kimura, T., Green, S.J. & et al. Requirement for transcription factor IRF-1 in NO synthase induction in macrophages. *Science* **263**, 1612-1615 (1994).
459. Saura, M., Zaragoza, C., Bao, C., McMillan, A. & Lowenstein, C.J. Interaction of interferon regulatory factor-1 and nuclear factor kappaB during activation of inducible nitric oxide synthase transcription. *J Mol Biol* **289**, 459-471 (1999).
460. Lee, A.H., Hong, J.H. & Seo, Y.S. Tumour necrosis factor-alpha and interferon-gamma synergistically activate the RANTES promoter through nuclear factor kappaB and interferon regulatory factor 1 (IRF-1) transcription factors. *Biochem J* **350 Pt 1**, 131-138 (2000).
461. Pine, R., Decker, T., Kessler, D.S., Levy, D.E. & Darnell, J.E., Jr. Purification and cloning of interferon-stimulated gene factor 2 (ISGF2): ISGF2 (IRF-1) can bind to the promoters of both beta interferon- and interferon-stimulated genes but is not a primary transcriptional activator of either. *Mol Cell Biol* **10**, 2448-2457 (1990).
462. Lin, R. & Hiscott, J. A role for casein kinase II phosphorylation in the regulation of IRF-1 transcriptional activity. *Mol Cell Biochem* **191**, 169-180 (1999).
463. Watanabe, N., Sakakibara, J., Hovanessian, A.G., Taniguchi, T. & Fujita, T. Activation of IFN-beta element by IRF-1 requires a posttranslational event in addition to IRF-1 synthesis. *Nucleic Acids Res* **19**, 4421-4428 (1991).
464. Fujita, T., Reis, L.F., Watanabe, N., Kimura, Y., Taniguchi, T. & Vilcek, J. Induction of the transcription factor IRF-1 and interferon-beta mRNAs by cytokines and activators of second-messenger pathways. *Proc Natl Acad Sci U S A* **86**, 9936-9940 (1989).
465. Harada, H., Fujita, T., Miyamoto, M., Kimura, Y., Maruyama, M., Furia, A., Miyata, T. & Taniguchi, T. Structurally similar but functionally distinct factors, IRF-1 and IRF-2, bind to the same regulatory elements of IFN and IFN-inducible genes. *Cell* **58**, 729-739 (1989).
466. Park, J., Kim, K., Lee, E.J., Seo, Y.J., Lim, S.N., Park, K., Rho, S.B., Lee, S.H. & Lee, J.H. Elevated level of SUMOylated IRF-1 in tumor cells interferes with IRF-1-mediated apoptosis. *Proc Natl Acad Sci U S A* **104**, 17028-17033 (2007).
467. Nakagawa, K. & Yokosawa, H. PIAS3 induces SUMO-1 modification and transcriptional repression of IRF-1. *FEBS Lett* **530**, 204-208 (2002).
468. Nakagawa, K. & Yokosawa, H. Degradation of transcription factor IRF-1 by the ubiquitin-proteasome pathway. The C-terminal region governs the protein stability. *Eur J Biochem* **267**, 1680-1686 (2000).

469. Castro, S.M., Kolli, D., Guerrero-Plata, A., Garofalo, R.P. & Casola, A. Cigarette smoke condensate enhances respiratory syncytial virus-induced chemokine release by modulating NF-kappa B and interferon regulatory factor activation. *Toxicol Sci* **106**, 509-518 (2008).
470. Yamaoka, Y., Kudo, T., Lu, H., Casola, A., Brasier, A.R. & Graham, D.Y. Role of interferon-stimulated responsive element-like element in interleukin-8 promoter in Helicobacter pylori infection. *Gastroenterology* **126**, 1030-1043 (2004).
471. Kirchhoff, S., Schaper, F., Oumard, A. & Hauser, H. In vivo formation of IRF-1 homodimers. *Biochimie* **80**, 659-664 (1998).
472. Grunberg, K., Sharon, R.F., Sont, J.K., In 't Veen, J.C., Van Schadewijk, W.A., De Klerk, E.P., Dick, C.R., Van Krieken, J.H. & Sterk, P.J. Rhinovirus-induced airway inflammation in asthma: effect of treatment with inhaled corticosteroids before and during experimental infection. *Am J Respir Crit Care Med* **164**, 1816-1822 (2001).
473. Pastore, S., Mascia, F., Mariotti, F., Dattilo, C., Mariani, V. & Girolomoni, G. ERK1/2 regulates epidermal chemokine expression and skin inflammation. *J Immunol* **174**, 5047-5056 (2005).
474. Wang, Q., Brown, E.R., Nagarkar, D.R., Zhao, Y., McHenry, C., Sajjan, U. & Hershenson, M.B. Differential Regulation of Rhinovirus−Induced Airway Epithelial Responses by ERK and JNK. *American Journal of Respiratory and Critical Care Medicine* **179**, A5164
(2009).
475. Hayashi, M., Tapping, R.I., Chao, T.H., Lo, J.F., King, C.C., Yang, Y. & Lee, J.D. BMK1 mediates growth factor-induced cell proliferation through direct cellular activation of serum and glucocorticoid-inducible kinase. *J Biol Chem* **276**, 8631-8634 (2001).
476. Kato, Y., Tapping, R.I., Huang, S., Watson, M.H., Ulevitch, R.J. & Lee, J.D. Bmk1/Erk5 is required for cell proliferation induced by epidermal growth factor. *Nature* **395**, 713-716 (1998).
477. Pearson, G., English, J.M., White, M.A. & Cobb, M.H. ERK5 and ERK2 cooperate to regulate NF-kappaB and cell transformation. *J Biol Chem* **276**, 7927-7931 (2001).
478. English, J.M., Pearson, G., Baer, R. & Cobb, M.H. Identification of substrates and regulators of the mitogen-activated protein kinase ERK5 using chimeric protein kinases. *J Biol Chem* **273**, 3854-3860 (1998).
479. Hiscott, J., Pitha, P., Genin, P., Nguyen, H., Heylbroeck, C., Mamane, Y., Algarte, M. & Lin, R. Triggering the interferon response: the role of IRF-3 transcription factor. *J Interferon Cytokine Res* **19**, 1-13 (1999).
480. Shibuya, Y., Hirasawa, N., Sakai, T., Togashi, Y., Muramatsu, R., Ishii, K., Yamashita, M., Takayanagi, M. & Ohuchi, K. Negative regulation of the protein kinase C activator-induced ICAM-1 expression in the human bronchial epithelial cell line NCI-H292 by p44/42 mitogen-activated protein kinase. *Life Sci* **75**, 435-446 (2004).

481. Maeng, Y.S., Min, J.K., Kim, J.H., Yamagishi, A., Mochizuki, N., Kwon, J.Y., Park, Y.W., Kim, Y.M. & Kwon, Y.G. ERK is an anti-inflammatory signal that suppresses expression of NF-kappaB-dependent inflammatory genes by inhibiting IKK activity in endothelial cells. *Cell Signal* **18**, 994-1005 (2006).
482. Proud, D., Sanders, S.P. & Wiehler, S. Human rhinovirus infection induces airway epithelial cell production of human beta-defensin 2 both in vitro and in vivo. *J Immunol* **172**, 4637-4645 (2004).
483. Holden, N.S., Catley, M.C., Cambridge, L.M., Barnes, P.J. & Newton, R. ICAM-1 expression is highly NF-kappaB-dependent in A549 cells. No role for ERK and p38 MAPK. *Eur J Biochem* **271**, 785-791 (2004).
484. Andoh, A., Fujino, S., Bamba, S., Araki, Y., Okuno, T., Bamba, T. & Fujiyama, Y. IL-17 selectively down-regulates TNF-alpha-induced RANTES gene expression in human colonic subepithelial myofibroblasts. *J Immunol* **169**, 1683-1687 (2002).
485. Ohren, J.F., Chen, H., Pavlovsky, A., Whitehead, C., Zhang, E., Kuffa, P., Yan, C., McConnell, P., Spessard, C., Banotai, C., Mueller, W.T., Delaney, A., Omer, C., Sebolt-Leopold, J., Dudley, D.T., Leung, I.K., Flamme, C., Warmus, J., Kaufman, M., Barrett, S., Tecle, H. & Hasemann, C.A. Structures of human MAP kinase kinase 1 (MEK1) and MEK2 describe novel noncompetitive kinase inhibition. *Nat Struct Mol Biol* **11**, 1192-1197 (2004).
486. Gailhouste, L., Ezan, F., Bessard, A., Fremin, C., Rageul, J., Langouet, S. & Baffet, G. RNAi-mediated MEK1 knock-down prevents ERK1/2 activation and abolishes human hepatocarcinoma growth in vitro and in vivo. *Int J Cancer* (2009).
487. Scholl, F.A., Dumesic, P.A., Barragan, D.I., Harada, K., Charron, J. & Khavari, P.A. Selective role for Mek1 but not Mek2 in the induction of epidermal neoplasia. *Cancer Res* **69**, 3772-3778 (2009).
488. Ussar, S. & Voss, T. MEK1 and MEK2, different regulators of the G1/S transition. *J Biol Chem* **279**, 43861-43869 (2004).
489. Skarpen, E., Flinder, L.I., Rosseland, C.M., Orstavik, S., Wierod, L., Oksvold, M.P., Skalhegg, B.S. & Huitfeldt, H.S. MEK1 and MEK2 regulate distinct functions by sorting ERK2 to different intracellular compartments. *FASEB J* **22**, 466-476 (2008).
490. Battcock, S.M., Collier, T.W., Zu, D. & Hirasawa, K. Negative regulation of the alpha interferon-induced antiviral response by the Ras/Raf/MEK pathway. *J Virol* **80**, 4422-4430 (2006).
491. Colanzi, A., Deerinck, T.J., Ellisman, M.H. & Malhotra, V. A specific activation of the mitogen-activated protein kinase kinase 1 (MEK1) is required for Golgi fragmentation during mitosis. *J Cell Biol* **149**, 331-339 (2000).
492. Holt, K.H., Kasson, B.G. & Pessin, J.E. Insulin stimulation of a MEK-dependent but ERK-independent SOS protein kinase. *Mol Cell Biol* **16**, 577-583 (1996).
493. Jo, C., Jang, B.G. & Jo, S.A. MEK1 plays contrary stage-specific roles in skeletal myogenic differentiation. *Cell Signal* **21**, 1910-1917 (2009).

494. Wang, J., Whiteman, M.W., Lian, H., Wang, G., Singh, A., Huang, D. & Denmark, T. A non-canonical MEK/ERK signaling pathway regulates autophagy via regulating Beclin 1. *J Biol Chem* **284**, 21412-21424 (2009).
495. Bae, D. & Ceryak, S. Raf-independent, PP2A-dependent MEK activation in response to ERK silencing. *Biochem Biophys Res Commun* **385**, 523-527 (2009).
496. Teis, D., Wunderlich, W. & Huber, L.A. Localization of the MP1-MAPK scaffold complex to endosomes is mediated by p14 and required for signal transduction. *Dev Cell* **3**, 803-814 (2002).
497. Brahma, A. & Dalby, K.N. Regulation of protein phosphorylation within the MKK1-ERK2 complex by MP1 and the MP1*P14 heterodimer. *Arch Biochem Biophys* **460**, 85-91 (2007).
498. Weiss, W.A., Taylor, S.S. & Shokat, K.M. Recognizing and exploiting differences between RNAi and small-molecule inhibitors. *Nat Chem Biol* **3**, 739-744 (2007).
499. Fitzgerald, K. RNAi versus small molecules: different mechanisms and specificities can lead to different outcomes. *Curr Opin Drug Discov Devel* **8**, 557-566 (2005).
500. Ditchfield, C., Johnson, V.L., Tighe, A., Ellston, R., Haworth, C., Johnson, T., Mortlock, A., Keen, N. & Taylor, S.S. Aurora B couples chromosome alignment with anaphase by targeting BubR1, Mad2, and Cenp-E to kinetochores. *J Cell Biol* **161**, 267-280 (2003).
501. An, H.J., Cho, N.H., Yang, H.S., Kwak, K.B., Kim, N.K., Oh, D.Y., Lee, S.W., Kim, H.O. & Koh, J.J. Targeted RNA interference of phosphatidylinositol 3-kinase p110-beta induces apoptosis and proliferation arrest in endometrial carcinoma cells. *J Pathol* **212**, 161-169 (2007).
502. Bovolenta, C., Driggers, P.H., Marks, M.S., Medin, J.A., Politis, A.D., Vogel, S.N., Levy, D.E., Sakaguchi, K., Appella, E., Coligan, J.E. & et al. Molecular interactions between interferon consensus sequence binding protein and members of the interferon regulatory factor family. *Proc Natl Acad Sci U S A* **91**, 5046-5050 (1994).
503. Hiscott, J. Triggering the innate antiviral response through IRF-3 activation. *J Biol Chem* **282**, 15325-15329 (2007).
504. Lin, R., Heylbroeck, C., Pitha, P.M. & Hiscott, J. Virus-dependent phosphorylation of the IRF-3 transcription factor regulates nuclear translocation, transactivation potential, and proteasome-mediated degradation. *Mol Cell Biol* **18**, 2986-2996 (1998).
505. Chen, W., Lam, S.S., Srinath, H., Jiang, Z., Correia, J.J., Schiffer, C.A., Fitzgerald, K.A., Lin, K. & Royer, W.E., Jr. Insights into interferon regulatory factor activation from the crystal structure of dimeric IRF5. *Nat Struct Mol Biol* **15**, 1213-1220 (2008).
506. Balkhi, M.Y., Fitzgerald, K.A. & Pitha, P.M. IKKalpha negatively regulates IRF5 function in a MyD88-TRAF6 pathway. *Cell Signal* (2009).
507. Smith, S.J., Fenwick, P.S., Nicholson, A.G., Kirschenbaum, F., Finney-Hayward, T.K., Higgins, L.S., Giembycz, M.A., Barnes, P.J. & Donnelly, L.E. Inhibitory

effect of p38 mitogen-activated protein kinase inhibitors on cytokine release from human macrophages. *Br J Pharmacol* **149**, 393-404 (2006).
508. Chialda, L., Zhang, M., Brune, K. & Pahl, A. Inhibitors of mitogen-activated protein kinases differentially regulate costimulated T cell cytokine production and mouse airway eosinophilia. *Respir Res* **6**, 36 (2005).
509. Tsang, F., Koh, A.H., Ting, W.L., Wong, P.T. & Wong, W.S. Effects of mitogen-activated protein kinase kinase inhibitor PD 098059 on antigen challenge of guinea-pig airways in vitro. *Br J Pharmacol* **125**, 61-68 (1998).
510. Culley, F.J. Natural killer cells in infection and inflammation of the lung. *Immunology* **128**, 151-163 (2009).
511. Bartlett, N.W., Walton, R.P., Edwards, M.R., Aniscenko, J., Caramori, G., Zhu, J., Glanville, N., Choy, K.J., Jourdan, P., Burnet, J., Tuthill, T.J., Pedrick, M.S., Hurle, M.J., Plumpton, C., Sharp, N.A., Bussell, J.N., Swallow, D.M., Schwarze, J., Guy, B., Almond, J.W., Jeffery, P.K., Lloyd, C.M., Papi, A., Killington, R.A., Rowlands, D.J., Blair, E.D., Clarke, N.J. & Johnston, S.L. Mouse models of rhinovirus-induced disease and exacerbation of allergic airway inflammation. *Nat Med* **14**, 199-204 (2008).
512. Newcomb, D.C., Sajjan, U.S., Nagarkar, D.R., Wang, Q., Nanua, S., Zhou, Y., McHenry, C.L., Hennrick, K.T., Tsai, W.C., Bentley, J.K., Lukacs, N.W., Johnston, S.L. & Hershenson, M.B. Human rhinovirus 1B exposure induces phosphatidylinositol 3-kinase-dependent airway inflammation in mice. *Am J Respir Crit Care Med* **177**, 1111-1121 (2008).
513. Sajjan, U., Ganesan, S., Comstock, A.T., Shim, J., Wang, Q., Nagarkar, D.R., Zhao, Y., Goldsmith, A.M., Sonstein, J., Linn, M.J., Curtis, J.L. & Hershenson, M.B. Elastase- and LPS-exposed mice display altered responses to rhinovirus infection. *Am J Physiol Lung Cell Mol Physiol* **297**, L931-944 (2009).
514. Nagarkar, D.R., Wang, Q., Shim, J., Zhao, Y., Tsai, W.C., Lukacs, N.W., Sajjan, U. & Hershenson, M.B. CXCR2 is required for neutrophilic airway inflammation and hyperresponsiveness in a mouse model of human rhinovirus infection. *J Immunol* **183**, 6698-6707 (2009).
515. Wang, T.N., Chu, Y.T., Chen, W.Y., Feng, W.W., Shih, N.H., Hsiang, C.H. & Ko, Y.C. Association of interferon-gamma and interferon regulatory factor 1 polymorphisms with asthma in a family-based association study in Taiwan. *Clin Exp Allergy* **36**, 1147-1152 (2006).
516. Schedel, M., Pinto, L.A., Schaub, B., Rosenstiel, P., Cherkasov, D., Cameron, L., Klopp, N., Illig, T., Vogelberg, C., Weiland, S.K., von Mutius, E., Lohoff, M. & Kabesch, M. IRF-1 gene variations influence IgE regulation and atopy. *Am J Respir Crit Care Med* **177**, 613-621 (2008).
517. Tliba, O., Damera, G., Banerjee, A., Gu, S., Baidouri, H., Keslacy, S. & Amrani, Y. Cytokines induce an early steroid resistance in airway smooth muscle cells: novel role of interferon regulatory factor-1. *Am J Respir Cell Mol Biol* **38**, 463-472 (2008).
518. Bhandare, R., Damera, G., Banerjee, A., Flammer, J.R., Keslacy, S., Rogatsky, I., Panettieri, R.A., Amrani, Y. & Tliba, O. Glucocorticoid receptor interacting

protein-1 restores glucocorticoid responsiveness in steroid-resistant airway structural cells. *Am J Respir Cell Mol Biol* **42**, 9-15 (2010).

519. Sampath, D., Castro, M., Look, D.C. & Holtzman, M.J. Constitutive activation of an epithelial signal transducer and activator of transcription (STAT) pathway in asthma. *J Clin Invest* **103**, 1353-1361 (1999).
520. Rohde, G., Wiethege, A., Borg, I., Kauth, M., Bauer, T.T., Gillissen, A., Bufe, A. & Schultze-Werninghaus, G. Respiratory viruses in exacerbations of chronic obstructive pulmonary disease requiring hospitalisation: a case-control study. *Thorax* **58**, 37-42 (2003).

APPENDIX A: PUBLICATION LIST

First author publications

Zaheer, R. S., and D. Proud. 2009. Human Rhinovirus-induced Epithelial Production of CXCL10 is Dependent upon IFN Regulatory Factor-1. *Am J Respir Cell Mol Biol*. Epub date: 2009/11/03

As primary author, I am responsible for all of the experiments carried out. The manuscript was written in conjunction with Dr. David Proud.

Zaheer, R. S., R. Koetzler, N. S. Holden, S. Wiehler, and D. Proud. 2009. Selective transcriptional down-regulation of human rhinovirus-induced production of CXCL10 from airway epithelial cells via the MEK1 pathway. *J Immunol* 182:4854-4864

As primary author, I am responsible for the majority of the experiments carried out. The manuscript was written in conjunction with Dr. David Proud. Shahina Wiehler generated initial wild-type full length and truncated CXCL10 promoter constructs. EMSA and tandem repeat promoter-luciferase experiments were carried out in conjunction with Dr. Rommy Koetzler. Dr. Neil Holden provided the EMSA protocol and helped during pilot experiments.

Co-author publications

Koetzler, R., R. S. Zaheer, R. Newton, and D. Proud. 2009. Nitric oxide inhibits IFN regulatory factor 1 and nuclear factor-kappaB pathways in rhinovirus-infected epithelial cells. *J Allergy Clin Immunol* 124:551-557.

As a co-author, my contribution included the initial characterization of HRV-induced IRF-1 mRNA and protein in airway epithelial cells.

Koetzler, R., R. S. Zaheer, S. Wiehler, N. S. Holden, M. A. Giembycz, and D. Proud. 2009. Nitric oxide inhibits human rhinovirus-induced transcriptional activation of CXCL10 in airway epithelial cells. *J Allergy Clin Immunol* 123:201-208 e209.

As a co-author, my contribution included the generation of mutant promoter-luciferase constructs and EMSA studies.

Leigh, R., W. Oyelusi, S. Wiehler, R. Koetzler, R. S. Zaheer, R. Newton, and D. Proud. 2008. Human rhinovirus infection enhances airway epithelial cell production of growth factors involved in airway remodeling. *J Allergy Clin Immunol* 121:1238-1245 e1234.

As a co-author, my contribution involved experiments studying the MAPK pathways during HRV-induced VEGF expression.

Spurrell, J. C., S. Wiehler, R. S. Zaheer, S. P. Sanders, and D. Proud. 2005. Human airway epithelial cells produce IP-10 (CXCL10) in vitro and in vivo upon rhinovirus infection. *Am J Physiol Lung Cell Mol Physiol* 289:L85-95.

As a co-author, my contribution involved performing experiments during manuscript revisions mandated by peer reviewers.